Impact of environmental drivers and phytoplankton diversity on the dimethylsulfoniopropionate (DMSP) and dimethylsulfoxide (DMSO) cell quotas: laboratory experiments and natural variability.

Thesis submitted by Colin ROYER
in fulfilment of the requirements of the PhD Degree in Agronomic Sciences and Bioengineering (ULB and ULiège)
Academic year 2020-2021

Supervisors: Professor Nathalie GYPENS (Université libre de Bruxelles)
Ecology of Aquatic Systems

and Professor Alberto V. BORGES (Université de Liège)
Chemical Oceanography Unit

Impact of environmental drivers and phytoplankton diversity on the dimethylsulfoniopropionate (DMSP) and dimethylsulfoxide (DMSO) cell quotas: laboratory experiments and natural variability.

Thesis jury:

François Fripiat (Université Libre de Bruxelles, Chair)
Nathalie Gypens (Université Libre de Bruxelles, Secretary)
Alberto V. Borges (Université de Liège)
Pierre Cardol (Université de Liège)
Stéphane Roberty (Université de Liège)
Michel Lavoie (Bureau Veritas Canada)

Remerciements

Il est difficile de se rendre compte du chemin parcouru en quatre années, chemin si long et si court à la fois. Les personnes rencontrées sur le parcours sont nombreuses et je devrais toutes les remercier pour leur aide, même involontaire ou inconsciente, qui m'a permis de finaliser ce travail. Mes premiers remerciements vont bien entendu à mes professeurs Nathalie Gypens et Alberto V. Borges pour leur soutien et leur enseignement. Le rire de Nathalie qui s'entend à travers les couloirs nous a manqué pendant cette année de confinement. Il y a sans aucun doute Willy Champenois, Bruno Delille, Jonathan Richir, et Fleur Roland du laboratoire d'Océanographie chimique (ULiège) pour leur aide au bon fonctionnement du chromatographe ; Jonas Mortelmans (VLIZ) pour l'organisation des campagnes en mer ; Pierre Cardol pour l'accès aux infrastructures du laboratoire de Génétique et Physiologie des Microalgues (ULiège) ; le laboratoire d'InBios (ULiège) pour les analyses de stress oxydatif ; ou encore le laboratoire d'Ecologie des Systèmes Aquatiques où l'ambiance et les rigolades permettent de relativiser toute mauvaise journée. Il est certain que nous nous inscrirons l'année prochaine au prochain tournoi basque de Bollo. Je tiens à remercier particulièrement cette nouvelle amitié avec Jon Lapeyra, à travers lequel nos deux projets respectifs sont devenus une co-motivation, et une source d'ennui profonde pour nos amis lors de nos conversations professionnelles, un verre à la main. J'aimerais également remercier Adriana Anzil pour nos discussions, nos ragots, et son aide précieuse. Par la même occasion, je remercie Marc Commarieu avec qui nous nous retrouvions à 7h pour profiter de l'air frais du matin à Liège. L'aide et l'optimisme de Stéphane Roberty m'a quant à lui permis de clôturer cette thèse avec le sourire et avec le sentiment d'un travail accompli. Comment finaliser un tel projet si ce n'est accompagné de SupraVida, des BlackGoozes et de l'EntrePotes qui m'ont supporté pendant ces années, ces trajets à Liège interminables, et qui ont fait semblant de m'écouter leur expliquer le sujet, ne sachant toujours pas aujourd'hui ce que je fais réellement. L'ouverture éphémère de *notre* bar m'a permis de passer malgré tout un agréable été. Nos récents diners clandestins du mercredi soir ont été d'ailleurs une bouffée de bien-être ces derniers mois. J'aimerais également remercier Antoinette, pour notre tendresse et notre amour passé, qui m'a suivi et amené à évoluer émotionnellement. Une nouvelle étape de vie s'offre à nous. Enfin, il y a ma famille, toujours présente, toujours derrière moi pour me soutenir et me porter, à profiter de mon horaire variable pour aller manger le midi ensemble, qui me donne et m'enivre d'énergie. Ma dernière phrase sera portée vers ma sœur, une personne qui mérite un bonheur démesuré, par ce qu'elle offre sentimentalement, par sa surexcitation, et son optimisme. Cette dernière année, par son caractère unique et rebondissant, par la rédaction et la finalisation de ce projet, par la situation sanitaire et anxiogène, nous a permis à tous de grandir, parfois par la force des choses. Laissons donc maintenant de la place au vide que puisse venir l'extraordinaire.

Abstract

In the last two decades, particular interest has been given to the cycle of dimethylsulfide (DMS), a climate active gas, and its precursors the dimethylsulfoniopropionate (DMSP) and the dimethylsulfoxide (DMSO). DMS is involved in the Earth's radiation budget while the DMS(P,O) are produced by a wide variety of micro- and macroalgae, corals, bacteria, or angiosperms in response to diverse environmental stresses. Several functions have been suggested for these sulfur compounds such as antioxidants, cryoprotectants, overflow mechanisms, osmolytes, zooplankton deterrents or signalling compounds.

This research aims at improving the knowledge about the antioxidant role of DMS(P,O) within three major phytoplankton groups: diatom (i.e. *Skeletonema costatum*), Prymnesiophyceae (i.e. *Phaeocystis globosa*) and dinoflagellate (i.e. *Heterocapsa triquetra*). The experimental results demonstrate that cellular DMS(P,O) have the ability to lower cellular reactive oxygen species concentrations produced during high-light and chemically-induced oxidative stresses; thus supporting the antioxidant function. However, the initial DMS(P,O) concentrations of each species are not informative of their ability to tolerate a further oxidative stress, and their concentrations do not increase in high-light grown cells. The DMS(P,O) may then act as antioxidants without being part of the antioxidant response of the cell. We recommend analysing more constituents of the antioxidant system (i.e. enzymes, carotenoids, redox buffer) along with DMS(P,O) by-products and DMSP-lyase activity to better understand the cellular function of DMSP.

Field measurements in the North Sea, including the Belgian Coastal Zone (BCZ) and the Northern North Sea (NNS), bring additional information on the DMS(P,O) variations. While abiotic parameters (nutrients, temperature, and incident light) influence the Chlorophyll-*a* (Chl-*a*) concentrations in the BCZ, this impact is not reflected in the DMS(P,O) concentrations. The latter depend on the succession of low- and high-DMSP producing species (i.e. diatoms and *Phaeocystis*, respectively). In the NNS in August, no distinct pattern can be drawn for the DMS(P,O) evolution regarding the phytoplankton diversity or abiotic parameters. Investigated by correlations between DMS(P,O), photoprotective pigments and incident light, the antioxidant function is not observed for this short-term period of sampling in a temperate sea. Based on Chl-*a* linear regressions, DMS(P,O) concentrations are successfully estimated with two distinct relationships for diatoms and Prymnesiophyceae in the BCZ. However, this estimation lacks accuracy in the NNS due to the mixed phytoplankton community observed. Further work will provide a better understanding about the antioxidant function – especially on the field – and its association with the phytoplankton diversity in temperate regions such as the North Sea.

Résumé

Un intérêt grandissant est né ces deux dernières décennies pour le cycle du dimethylsulfide (DMS) et ses précurseurs le dimethylsulfoniopropionate (DMSP) et le dimethylsulfoxide (DMSO). Le DMS est impliqué dans le budget radiatif terrestre alors que les DMS(P,O) sont produits par une grande variété de macro et microalgues, coraux, bactéries et certains angiospermes pour répondre aux pressions environnementales. Plusieurs fonctions physiologiques leur ont été attribuées avec entre autres des rôles d'antioxydants, de cryoprotecteurs, ou encore d'osmolytes.

Cette recherche a pour but d'améliorer les connaissances à propos du rôle antioxydant du DMS(P,O) au sein de trois groupes phytoplanctoniques majeurs : les diatomées (e.g. *Skeletonema costatum*), les Prymnesiophyceae (e.g. *Phaeocystis globosa*) et les dinoflagellés (e.g. *Heterocapsa triquetra*). Les résultats expérimentaux ont mis en évidence que les DMS(P,O) ont la capacité de réduire les concentrations en dérivés réactifs de l'oxygène produits lors de stress lumineux ou chimiques, supportant ainsi leur rôle d'antioxydants. Cependant, les concentrations initiales en DMS(P,O) de chaque espèce n'informent pas sur leur capacité à résister à un stress ultérieur et n'augmentent pas lors de stress lumineux à long terme. Les DMS(P,O) peuvent jouer le rôle d'antioxydants sans pour autant faire partie de la réponse antioxydante de la cellule. Nous suggérons dès lors d'analyser l'ensemble du système antioxydant (e.g. enzymes, caroténoïdes, tampon redox) de même que les sous-produits d'oxydation du DMS(P,O) et l'activité DMSP-lyase pour mieux comprendre la fonction cellulaire jouée par le DMSP.

Des mesures de terrain en Mer du Nord, incluant la Zone Côtière Belge (ZCB) et le Nord de la Mer du Nord (NMN), apportent un regard supplémentaire sur les variations du DMS(P,O). Alors que les paramètres abiotiques (nutriments, température et lumière incidente) influencent la concentration en Chlorophylle-*a* (Chl-*a*) en ZCB, cet impact ne se reflète pas dans les concentrations en DMS(P,O). Ces dernières sont déterminées par la succession de faibles et forts producteurs de DMSP (diatomées et *Phaeocystis*, respectivement). Au mois d'août en NMN, aucun pattern n'a pu être identifié quant à l'évolution du DMS(P,O) par rapport à la diversité phytoplanctonique et les paramètres abiotiques. Etudiée grâce aux corrélations entre le DMS(P,O), les pigments photoprotecteurs et la lumière incidente, la fonction antioxydante n'a pas été observée pour cette courte période d'échantillonnage en mer tempérée. Basés sur les régressions linéaires avec la Chl-*a,* les DMS(P,O) ont été estimés avec succès en ZCB avec deux relations distinctes pour les diatomées et les Prymnesiophyceae. Cependant, cette estimation n'a pas été satisfaisante pour la NMN en raison d'une communauté phytoplanctonique mixte. Des recherches supplémentaires permettront de mieux comprendre la fonction antioxydante – en particulier sur le terrain – et son lien avec la diversité phytoplanctonique des régions tempérées comme la Mer du Nord.

Table of content

Table of figures

List of Tables

List of abbreviations

3-MPA	3-mercaptopropionate
Amplex Red	10-acetyl-3,7-dihydroxyphenoxazine
APX	Ascorbate peroxidase
AT	2-oxoglutarate-dependent aminotransferase
BCZ	Belgian coastal zone
CAT	Catalase
CCN	Cloud condensation nuclei
CDN	Cloud droplet number
Chl	Chlorophyll
CLAW	Hypothesis postulated by Charlson, Lovelock, Andreae and Warren in 1987
Cys	Cysteine
cytb559	Cytochrome b559
DCMU	3-(3,4-dichlorophenyl)-1,1-dimethylurea
DDx	Diadinoxanthin
DECARB	Oxidative Decarboxylase
DLA	DMSP-Lyase activity
DMS	Dimethylsulfide
DMS(O)	Dimethylsulfide and dimethylsulfoxide
DMS(P)	Dimethylsulfide and dimethylsulfoniopropionate
DMS(P,O)	Dimethylsulfoniopropionate and dimethylsulfoxide
DMSHB	4-dimethylsulfonio-2-hydroxy-butyrate
DMSO	Dimethylsulfoxide
$DMSO_2$	Dimethylsulfone
$DMSO_d$	Dissolved dimethylsulfoxide
$DMSP_d$	Dissolved dimethylsulfoniopropionate
$DMSO_p$	Particulate dimethylsulfoxide
$DMSP_p$	Particulate dimethylsulfoniopropionate
DMSOP	Dimethylsulfoxonium propionate
DMSP	Dimethylsulfoniopropionate
DTX	Diatoxanthin
F_m	Maximal fluorescence of dark-adapted sample
Fuco	Fucoxanthin
F_v/F_m	Maximum photochemical quantum yield of photosystem II
GBT	Glycine betaine
GPX	Glutathione peroxidase
GSH	Glutathione
H_2DCFDA	5-(and-6)-carboxy-2',7'-dichlorodihydrofluorescein diacetate
HL	High-Light
LHC	Light harvesting complex
LHP	Light harvesting pigment
LPO	Lipid peroxidation
MeOH	Methanol
MeSH	Methanethiol
Met	Methionine
MPPA	3-methiolpropionate

MSA	Methane sulfonate
MSB	Menadone Sodium Bisulfite
MSNA	Methylsulfinic acid
MTHB	4-methylthio-2-hydroxybutyrate
MTOB	4-methylthio-2oxobutyrate
NADPH	Nicotinamide adenine dinucleotide phosphate
NNS	Northern North Sea
NPQ	Non-photochemical quenching
OEC	Oxygen-evolving complex
OTU	Operational taxonomic unit
PAR	Photosynthetically active radiation
PQ	Photochemical quenching
PS	Photosystem
PSU	Photosynthetic unit
RC	Reaction centre
REDOX	NADPH-linked reductase
ROS	Reactive Oxygen Species
SAMmt	S-adenosylmethionine-dependent methyltransferase
SNS	Southern North Sea
SOD	Superoxide dismutase
SPM	Suspended particulate matter
SRD	Solar radiation dose
SSS	Sea-surface salinity
SST	Sea-surface temperature
TpMMT	MTHB-methyltransferase
UV	Ultraviolet
Φ_{PSII}	Effective photochemical quantum yield of photosystem II

Chapter I – Introduction

"Human beings are now carrying out a large-scale geophysical experiment of a kind that could not have happened in the past nor be reproduced in the future."

- Roger Revelle and Hans Suess (1957)

1 CLAW hypothesis and its potential climate regulation

In 1974, one of the greatest theories of symbiosis was advanced by James Lovelock and Lynn Margulis as the Gaia hypothesis. They claimed that mutual benefits occur between communities of organisms and their respective environments (Lovelock and Margulis, 1974). The definition of Gaia is: "*a complex entity involving the Earth's biosphere, atmosphere, oceans, and soil, the totality constituting a feedback or cybernetic system which seeks an optimal physical and chemical environment for life on this planet"* (Lovelock and Margulis, 1974). They considered that all living organisms constituting the biosphere can act as a single entity to regulate chemical composition, surface pH and possibly also the climate. In other words, this suggests that our remarkably stable climate and atmospheric composition on Earth is the result of active intervention by lifeforms (Ayers and Cainey, 2007). This Gaia hypothesis has led to extrapolation, interpolation and is under debate on how forms of biological homeostasis are maintained, or not, on this planet (Johnston et al., 2008). Of course, this theory needs some hard data to support it.

In 1972, Lovelock et al. discovered the dimethylsulfide (DMS) as the predominant form of sulfur emitted from the ocean to the atmosphere and thence to the land via precipitation. This provides the critical missing link in the global sulfur cycle. Before this revelation in 1972, hydrogen sulfide (H_2S) was considered to be the key component in this cycle. And yet, attempts to detect H_2S have always failed, and the ocean surface waters are much too oxidising to permit its existence at the concentrations needed for the equilibrium of the sulfur cycle (Lovelock et al., 1972; Yoch et al., 2002). A decade later, the discovery of DMS led to the CLAW hypothesis, an acronym for the surnames of the four authors of the paper. It was proposed as follows: the rate of DMS emissions have a homeostasis effect on global cloud cover, and hence on climate (Charlson et al., 1987; Johnston et al., 2008) (Fig. 1-1). The CLAW hypothesis was thus the perfect example of the Gaia hypothesis described previously.

The CLAW hypothesis originates from Shaw (1983): atmospheric oxidation of sulfur gases produces aerosols that might affect the climate by influencing the radiation balance. From there, three discoveries allowed the possibility to quantify this theory and bring the CLAW hypothesis to light: (1) a wide range of phytoplankton produces DMS which escapes into the atmosphere where it reacts with hydroxyl radicals to form sulfate and methane sulfonate (MSA) aerosols; (2) these sulfate aerosols are present everywhere in the marine atmospheric boundary layer; (3) the same sulfate aerosols act as cloud-condensation nuclei (CCN) in the marine environment.

CCN are microscopic particles less than 300 nm that concentrate water vapor droplets to form clouds. CCN can affect the amount of solar radiation reaching the Earth's surface by altering cloud droplets, their number, concentration, and size, and, as a result, the cloud reflectivity or albedo (Twomey, 1974; Galí et al., 2018). The albedo can be defined as the fraction of incident light from the sun which is reflected back into space by the Earth. The light not reflected is absorbed by the atmosphere, oceans and land maintaining the climate and making the Earth habitable (Twomey, 1974).

As it is schematised on the Fig. 1-1, due to the increase of anthropogenic greenhouse gases such as methane (CH_4) and carbon dioxide (CO_2), the Earth's temperature is increasing. Under warming conditions, the phytoplankton growth rate is enhanced, producing higher levels of biogenic DMS precursors: dimethylsulfoniopropionate (DMSP) and dimethylsulfoxide (DMSO) (here after DMS(P,O)). The DMS flux from the oceans to the atmosphere would therefore increase. Once in the atmosphere, the oxidation of DMS would act as CCN through the sulfate formation and thus, cut off the level of solar radiation. This would, in turn, drop the temperature, and could result in changes in the speciation and abundance of phytoplankton producing DMS, completing a biosphere-mediated negative feedback loop (Fig. 1-2a) (Charlson et al., 1987; Johnston et al., 2008; Quinn and Bates, 2011). Feedbacks are processes that amplify or dampen the effect of a forcing (Carslaw et al., 2010). The original authors even suggested that this feedback loop could be exploited to counteract the effect of increasing atmospheric CO_2, alleviating the effect of global warming (Green and Hatton, 2014).

Nevertheless, after almost three decades of research for evidence of a biological regulation of climate through marine sulfur emissions, several arguments must be reviewed. The first is the apparent altruism of algal populations, as this prior homeostasis regulation will benefit all the plankton as well as the entire biosphere (Dawkins, 1982 in Simó, 2001; Brimblecombe, 2014). To overcome this evolutionary feasibility, Hamilton and Lenton (1998) suggest that the local biogenic CCN releases heat energy of phase change, inducing an increase of local air movements and promoting the aerial dispersion of the DMS-producer phytoplankton cells. However, DMS emissions also occur with non-blooming events and mixed assemblages of phytoplankton species, dispersing cells of competitors as well (Simó, 2001). The evolutionary view of DMS production is outlying since phytoplankton do not produce DMS directly, seen as by- or waste products of its main precursor DMSP (Simó, 2001).

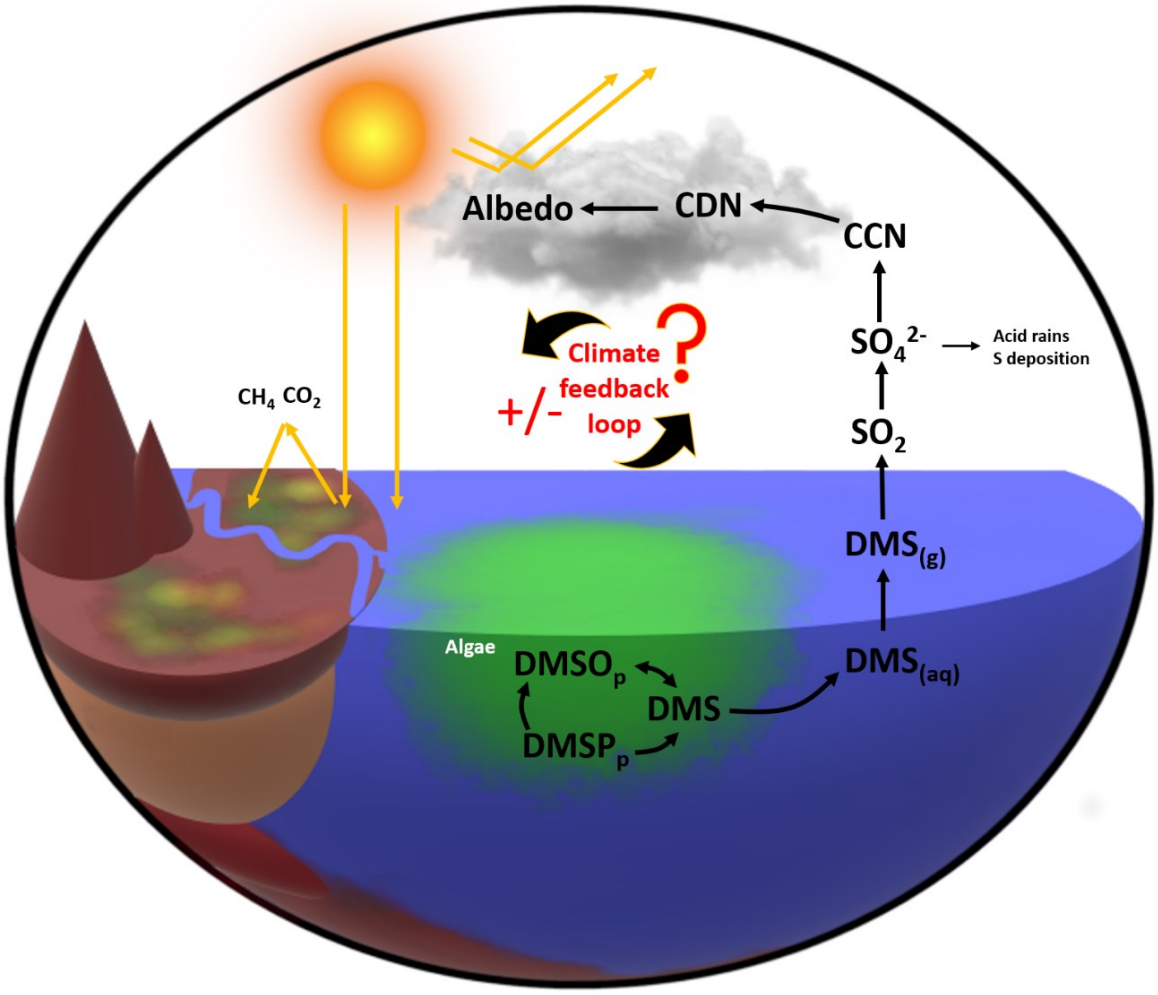

Figure 1-1 : Schematic illustration of the hypothetical influence on the climate system of the DMS(P,O) (inspired by Charlson et al., 1987; Quinn and Bates, 2011; Wittek, 2019). The increase of ocean temperature due to anthropogenic emissions (CO_2 and CH_4) would enhance the biogenic DMS(P,O) production, leading to the increase of DMS emissions to the atmosphere. Its further oxidation into SO_2 and SO_4^{2-} (non-seasalt-SO_4^{2-}) would increase the cloud condensation nuclei (CCN) and then the cloud droplet number (CDN) concentrations. This latter promote the increase the cloud reflectivity or albedo. This would, in turn, cut off the solar radiation to the earth surface, decreasing the light and energy inputs to the ecosystem. Questions remain regarding the positive or negative feedback loop. The SO_4^{2-} would also participate to the wet and dry sulfur deposition and acidic rain.

The second argument to be reviewed deals with the three points evoked in the preceding CLAW hypothesis: (1) that DMS is a significant source of CCN; (2) that variations in CCN concentrations derived from DMS would alter the cloud albedo; and (3) that a change in cloud albedo, surface temperature and/or solar radiation will lead to a change in DMS production (Quinn and Bates, 2011). Actually, step 1 can be discussed from three key perspectives:

(1) There is strong evidence between seasonal DMS, sulfate aerosols and CCN but the chemical composition and the sensitivity of CCN to changes in DMS emissions have to be considered (Quinn and Bates, 2011 and citations therein). As a matter of fact, the link between DMS and CCN in the atmosphere is yet to be clearly identified as only 0.07% of total CCN is induced by an increase of 1% of DMS flux for the Southern Hemisphere.

This sensitivity drops to 0.02% for the Northern Hemisphere (Woodhouse et al., 2010). In fact, the CCN sensitivity can vary by a factor of 20 between marine regions (Woodhouse et al., 2013).

(2) These low sensitivity results are due to the abundance of CCN derived from non-DMS sources and anthropogenic emissions (Woodhouse et al., 2010; Quinn and Bates, 2011). Actually, sea-salts and organic materials can also act as generators of CCN after their expulsion in the atmosphere by wind or wave-movement (Carslaw et al. 2010), with sea-salts making up a large portion of CCN creation (Carslaw et al., 2010; Quinn and Bates, 2011). If these particles are already sufficiently large to serve as CCN, the addition of DMS-derived sulfur to the particle will not increase the number of CCN (Quinn and Bates, 2011).

(3) DMS emissions vary between marine regions due to wind speed and phytoplankton distribution, and do not always cause a correlated increase in CCN (Woodhouse et al., 2010; 2013). The oxidant concentration for the further DMS oxidation strongly affects the potential of the DMS to make new aerosols (Woodhouse et al., 2010). The formation of sulfate aerosols due to DMS oxidation can also be involved in acid rains or sulfur deposition (Woodhouse et al., 2013).

Moreover, the cloud formation and resulting albedo in the second step are complex. Charlson et al. (1987) estimated that a 30% increase of CCN in the atmosphere could increase the planetary albedo, reducing the Earth's surface temperature by 1.3°C (Fig. 1-2a). Regarding the previous statement made by Woodhouse et al. (2010), this hypothesis assumes an increase of about 300% in DMS emissions. In addition, aerosols can affect cloud microphysics (droplet size or number concentration) but also macrophysics such as cloud abundance, fraction, size, albedo, and lifetime (Small et al., 2009; Galí et al., 2018). For instance, the increase in CCN concentration could have a contrary effect, accelerating the evaporation of droplets in clouds, leading to their fractionation, and thereby decreasing the albedo (Small et al., 2009).

Regarding the final step, studies focusing on the climate change show that the impacts of solar irradiance, temperature or atmospheric CO_2 seem to be reduced on the DMS emission by oceanic areas (Gunson et al., 2006; Vallina and Simó, 2007). The effect of the global warming scenario on the global annual mean DMS flux is similar of the interannual variability of wind speed, with negligible consequences on CCN concentrations (Woodhouse et al., 2010).

Nevertheless, field studies have demonstrated that DMS emission is linked to solar radiation in the upper sea layer (Toole and Siegel, 2004; Vallina and Simó, 2007), supporting the CLAW hypothesis. As a matter of fact, an important effect of climate change and global warming is ocean stratification modification (Bopp et al., 2003; Kloster et al., 2007). This leads to the phytoplankton lying closely to the sea surface and where they receive higher doses of radiation that induce higher DMS emissions (Sunda et al., 2002; Vallina and Simó, 2007).

In addition, the warming-induced ocean stratification occurs mainly in the upper 200 m of the ocean with an increase by 1% per decade since 1960 (Li et al., 2020) reducing the nutrient supply from deeper waters, the growth of phytoplankton (Behrenfeld et al., 2006), and hence possibly the DMS emissions (Fig. 1-2b). Changing temperatures and the stratification process could lead to variations in the composition and structure of phytoplankton (Bopp et al., 2003) from low- to high-DMS producers, or inversely, having a small or large effect on DMS emissions (Fig. 1-2b) (Bopp et al., 2003; Kloster et al., 2007). The effect of climate change with the increase in anthropogenic CO_2 emissions also leads to ocean acidification that might result in negative correlation with DMS emissions (Hussherr et al., 2017; Archer et al., 2013; 2018; Jian et al., 2019). Furthermore, the eutrophication of the natural environment with the increased delivery of nutrients from rivers to coastal waters leads to a general increase of primary production but also a modification in the phytoplankton community and structure (Cloern, 2001). This eutrophication disturbance of marine ecosystems can counter the effect of ocean acidification in some case (Gypens and Borges, 2014). Changes in the composition of phytoplankton due to changes in ocean abiotic parameters have the potential to strongly affect oceanic DMS emissions, phytoplankton community, marine aerosol chemistry and CCN concentrations (Wang et al., 2018a;b).

Finally, it has been suggested to withdraw the CLAW hypothesis in the modern-day climate since the previous arguments demonstrated: (1) the significance of non-DMS sources of CCN and the low sensitivity of CCN; (2) the lack of evidence for a DMS-controlled marine biota-climate feedback; and (3) the low sensitivity of modelization between changes and responses at each step of the CLAW process, as well as under global warming scenario (Quinn and Bates, 2011; Woodhouse et al., 2013). Prediction of responses of climate-relevant aerosol particles to variation in DMS emissions requires the understanding of atmospheric chemistry, aerosols microphysics and composition, microbial DMS production and its oxidation (Carslaw et al., 2010). This retirement suggestion is only due to a deeper appreciation of the complexity of

biogeochemistry and climate physics compared to when the hypothesis was first announced (Quinn and Bates, 2011; Green and Hatton, 2014).

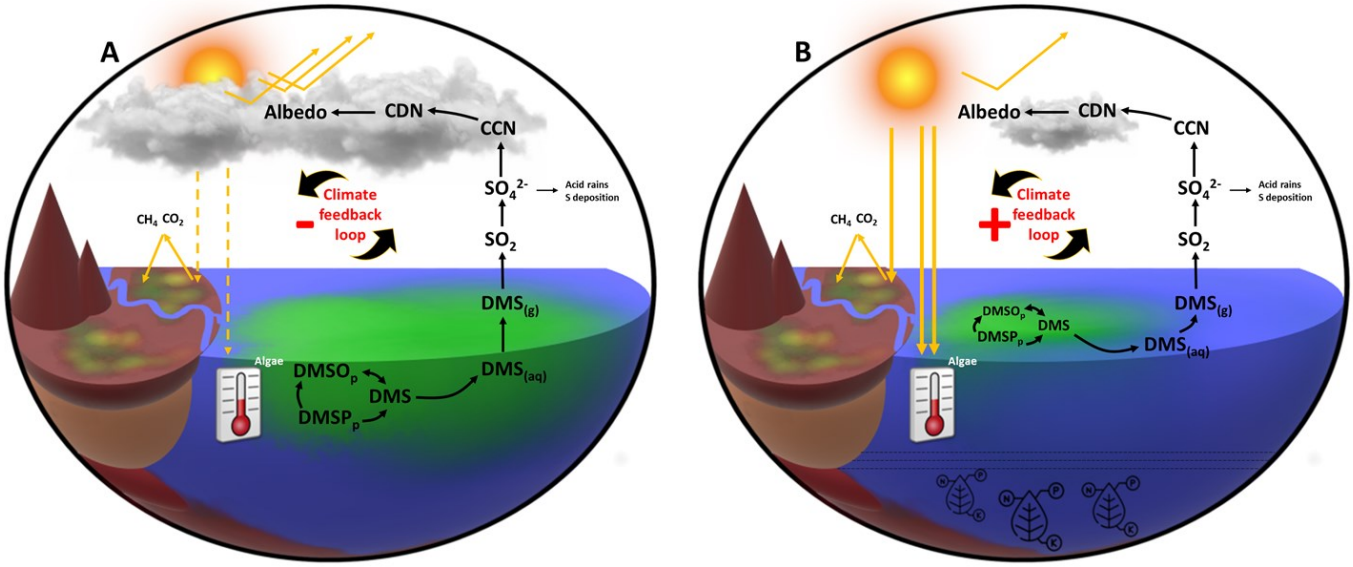

Figure 1-2: Schematic illustration of the hypothetical influence on the climate system of the DMS(P,O) with (A) the negative climate feedback loop and (B) the positive climate feedback loop discussed in this section.

Based on the recent scientific progress, the hypothesis need to be modified by considering that (1) the DMS is not the major source of the CCN, (2) the DMSP has shown to have several hypothetical roles and its response to environmental stress depends on the phytoplankton species, (3) the DMS emissions depend mainly on the microbial activity and (4) the DMSO is a sink of DMS in the water column (Green and Hatton, 2014).

Nevertheless, atmospheric studies and modelling have shown examples whereby marine DMS controls aerosol particle formation (Galí et al., 2018 and citations therein). The Arctic has for instance been identified as a potential area where the number of CCN could be impacted by the biogenic DMS production (Leaitch et al., 2013; Chang et al., 2018). In summer, this region is isolated from important aerosols sources (i.e. anthropogenic pollutants) by the Arctic front (Law et al., 2014) allowing the formation of new CCN particles instead of the aggregation on pre-existing particles. Hence, the CCN formation in the Arctic atmosphere can be enhanced by algal spring blooms and could have a local and seasonal impact on climate (Vallina and Simó, 2007; Levasseur, 2013). Furthermore, it is likely that different responses may function together or in different regions or seasons, complicating the verification of the CLAW hypothesis (Boyd, 2002). The uncertainty of the model simulations, their complexity and the DMS emissions data used add another problem in quantifying and understanding the CLAW hypothesis and the

indirect effect of global aerosols (Woodhouse et al., 2010, Carslaw et al., 2013; Wang et al., 2018b).

In other words, the influence of marine DMS on cloud albedo cannot be rule out (Green and Hatton, 2014) and thus remains in the spotlight (Brooks and Thornton, 2018) even if a "seasonal CLAW" hypothesis in remote marine atmospheres is more conceivable (Vallina and Simó, 2007; Levasseur, 2013). Given the potential significant impact of this climate active gas, the understanding of the production and cycling of DMS is important in light of the continuing issue of global climate change (Green and Hatton, 2014). Finally, in order to understand how any climate feedback loop (positive or negative) between the phytoplankton community and the atmosphere might operate, it is essential to clarify the biological role of the precursors DMS(P,O) within the phytoplankton cells (Ayers and Cainey, 2007).

2 The sulfur cycle

Before explaining the hypothetical physiological roles of DMS(P,O) to better comprehend the DMS cycle, a review of the sulfur cycle is needed since the DMS was found to be the missing link between the hydrosphere, biosphere, atmosphere, and lithosphere (Lovelock, 1972). In fact, sulfur represents one of the most important elements as it is present in the amino acids (methionine (Met) and cysteine (Cys)) and enzymes (CoA) that are needed to sustain life (Brimblecombe, 2014). Most sulfur at Earth's surface is present as sulfate (SO_4^{2-}) since it is thermodynamically stable in the presence of oxygen (Charlson et al., 1987; Takahashi et al., 2011).

2.1 Atmosphere

Volatile sulfur compounds are the precursors of SO_4^{2-} in the atmosphere. The SO_4^{2-} (and SO_2) emissions can produce aerosols that can alter the amount of solar radiation reaching the Earth's surface both directly by scattering solar energy and indirectly by acting as CCN (Chin and Jacob, 1996; Gondwe et al., 2003; Kloster et al., 2007; Carslaw et al., 2010; Wang et al., 2018a). These sulfur precursors are produced through biogenic and anthropogenic processes (Fig. 1-3).

Anthropogenic sulfur emissions result from the combustion of fossil fuels and biomass, oil refining, and smelting of ores; all emitting SO_2 (Chin and Jacob, 1996). These emissions account for almost ~70% of the total sulfur emissions to the atmosphere with 60 – 100 Tg S yr^{-1} (Fig. 1-3) (Chin and Jacob, 1996; Gondwe et al., 2003). Once in the atmosphere, they will react quickly with hydroxyl radicals (OH·) to form SO_4^{2-} (Chin and Jacob, 1996). Another

significant non-biological but natural flux is the emission of SO_2 and H_2S by volcanoes and fumaroles. This process represents between 7 to 20% of the total natural flux of gaseous sulfur to the atmosphere with 4 – 16 Tg S yr^{-1} during non-eruptive events (Fig. 1-3) (Chin and Jacob, 1996; Halmer et al., 2002; Gondwe et al., 2003).

The biogenic sulfur emissions (~23%) (Chin and Jacob, 1996) including H_2S, DMS, carbonyl sulfide (OCS) or carbon disulfide (CS_2) represent more than 60% of natural emissions. DMS dominates the biogenic sulfur emissions (> 90%) in which the production from the oceans are the main sources (95%) to the atmosphere since vegetation and soil are only of minor importance (0.3 Tg S yr^{-1}) (Pham et al., 1995; Kettle and Andreae, 2000;). The marine microbial food web is currently emitting some 28.1 Tg S yr^{-1} (17.6 – 34.4 Tg S yr^{-1}) (Fig. 1-3) (Lana et al., 2011; Wang et al., 2015; Galí et al., 2018).

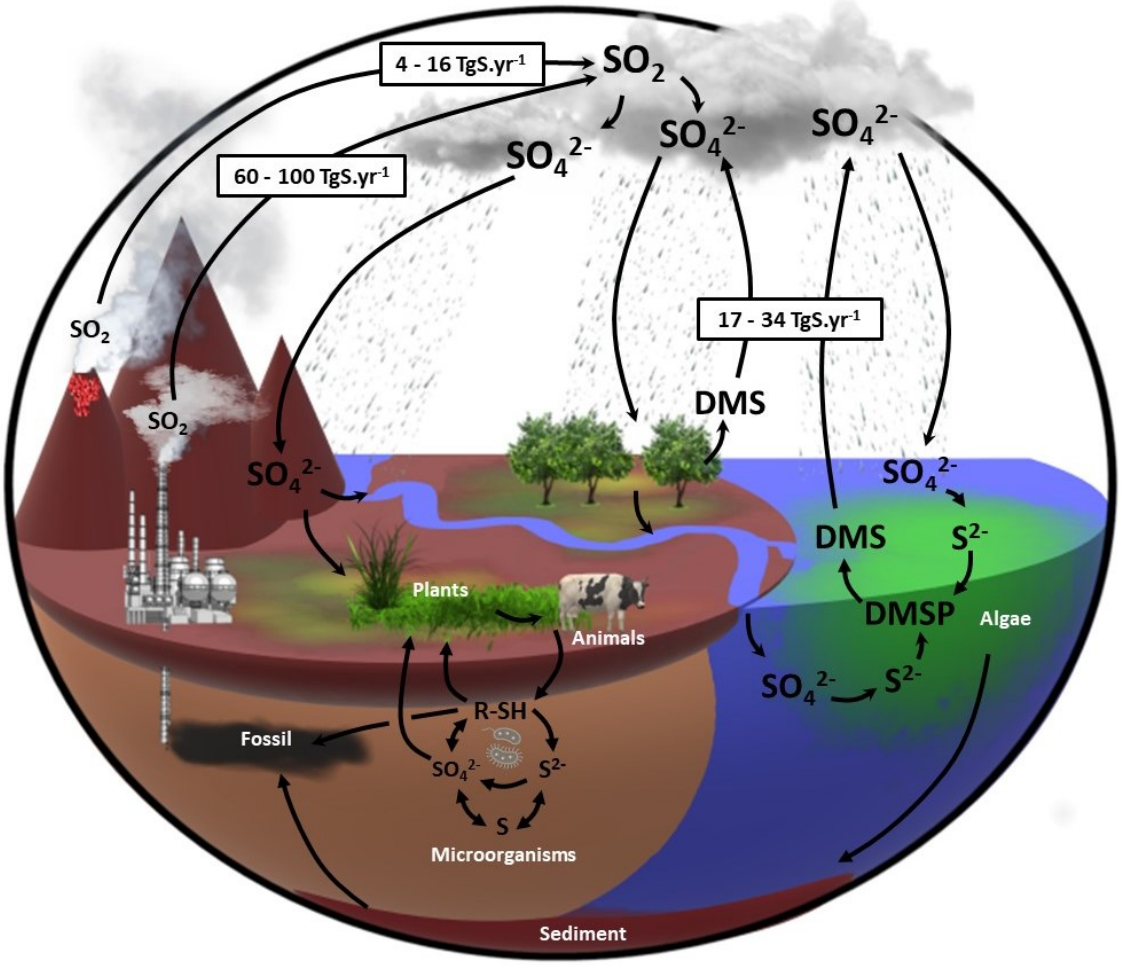

Figure 1-3: Global geochemical sulfur cycle including the anthropogenic, volcanic, and biogenic emissions. The biogenic cycle involves the plants, animals, microorganisms (aerobic and anaerobic) and algae. R-SH represents the organic sulfur. The emission fluxes of volatile sulfur compounds emitted from land and ocean are reported in Tg of sulfur per year. Schematic representation based on Takahashi et al. (2011), Brimblecombe (2014) and Wittek (2019).

This estimation is 17% higher than the previous estimation made by Kettle and Andreae (2000), thanks to the 3-fold increase in the number of field measurements and their spatial and temporal coverage (Lana et al., 2011). DMS emissions will thus depend on this complex web of processes including bacterial consumption and production, zooplankton grazing, viral activity, sea-to-air ventilation, photolysis, and vertical mixing (Simó, 2001 and citations therein).

Once in the atmosphere, the DMS oxidation can follow two pathways. At low temperature and reacting with OH· or bromide acid, the first pathway produces DMSO, dimethylsulfone ($DMSO_2$), methane sulphinic acid (MSNA) and methane sulfonate (MSA). The second pathway produces SO_2, SO_4^{2-} and MSA at higher temperature and when it reacts with nitrate, ozone, chloride or OH· (von Glasow and Crutzen 2004). It is suggested that 18 to 43% of global atmospheric sulfate aerosol is derived from DMS (Gondwe et al., 2003). In the troposphere, the SO_4^{2-} and SO_2 can condensate to form aerosols or nucleate to form new sulfuric acid particles (Pham et al., 1995). The oxidation of SO_2 to SO_4^{2-} is nevertheless highly complex and occurs via different mechanisms (Cainey and Harvey, 2002).

Under atmospheric conditions, sulfate aerosols are the only final product of DMS oxidation that increase the number of CCN while other sulfur products (DMSO, $DMSO_2$, MSNA and MSA) only impact the CCN size by condensing on existing particles (von Glasow and Crutzen 2004). In addition, SO_2 will react preferentially on the surface of pre-existing aerosols (i.e. sea salts), increasing the CCN size rather than its concentration in number (Cainey and Harvey, 2002). This has an impact of the cloud albedo, lifetime, and precipitations. For example, an increase of CCN number would decrease the droplet's size, leading to less precipitations, higher cloud lifetime and, as a result, an increase of its reflectivity (Albrecht, 1989; Stevens and Feingold, 2009). The inhibition of precipitation might further change the heat and water distribution in the atmosphere and thereby modify the Earth's hydrological cycle (Charlson et al., 1992). When the size of the droplets is too small, it can also lead to cloud fractionation due to evaporation which in turn reduces the resulting albedo (Zuidema et al., 2008; Small et al., 2009). DMSO, $DMSO_2$, MSNA and MSA are involved in the CCN size and increase in the mass of the droplets that will reduce the cloud lifetime due to precipitations and consequently the resulting albedo (von Glasow and Crutzen 2004). These elements can be added to the above previously explained complexity regarding the CCN, the sulfate aerosols, the DMS and CLAW hypothesis.

Furthermore, the DMS following the first pathway in the atmosphere can also lead to the formation of reactive halogens (Br^- or Cl^-) contributing to the ozone destruction. In addition,

the production of sulfate aerosols also have an influence on the pH of precipitations leading to acidic rains. These can induce damages to natural ecosystems: deterioration of the boreal forest, damage to crops, ocean acidification, increased alteration of the rocks impacting the biogeochemical cycle (Schindler, 1988; Amiotte Suchet et al., 1995; Brimblecombe, 2014; Huang et al. 2015). The Northern hemisphere sulfur cycle is largely influenced by anthropogenic processes that lead to the previous damage to the ecosystem, associated with a cooling effect in regions of high emissions (Liss et al., 1997; Ayers and Cainey, 2007). This previous acidification, amplified by the continuous anthropogenic CO_2 emissions in the troposphere and the resulting increase in dissolved CO_2 in the oceans (Stocker et al., 2013), have been shown to have repercussions on DMS, DMSP and DMSO concentrations by various effect on biogeochemical processes and ecosystems (Riebesell et al., 2009; Hoegh-Guldberg & Bruno, 2010; Zindler-Schlundt et al., 2016).

Finally, the short residence time of anthropogenic sulfur in the atmosphere compared with DMS that needs to be oxidized before it can be removed, and volcanic emissions that are injected at high altitude, mean that the majority of the sulfur in the global atmosphere comes from biogenic sources (Chin and Jacob, 1996; Liss et al. 1997).

2.2 Lithosphere – Hydrosphere – Biosphere

The inputs from the atmosphere to the lithosphere include wet (precipitations) and dry deposits of SO_2, SO_4^{2-} and OCS. The SO_4^{2-} included in precipitation can also leach from land into ocean. Conversely, the erosion of rocks containing sulfur (gypsum or pyrite) lead to a flux from the lithosphere to the atmosphere (Brimblecombe, 2014). The biosphere is characterized by organism waste (feces, dead organisms or leaves) inputs to the lithosphere while the anthropogenic additions reside in fertilisers and manure (Havlin et al., 2013). Human activities such as burning high sulfur coal contribute largely to SO_2 emissions from the lithosphere to the atmosphere (Brimblecombe, 2014).

Within the organisms, two options can be used to reduce sulfate: the dissimilatory pathway which is restricted to sulfate-reducing bacteria in anaerobic environments; and the assimilatory pathway which produces a large variety of organosulfur compounds such as Cys or Met, and are also present in membrane sulfolipids, cell walls, hormones, vitamins, and cofactors (Charlson et al., 1987; Takahashi et al., 2011). The interactions between these three spheres can be considered in the following ways (Takahashi et al., 2011; Brimblecombe, 2014 and citations therein):

- Plants can not only take up SO_4^{2-} or other sulfur organic compounds from the soil through their roots (active transport) but also SO_2 from the atmosphere through their stomata. In addition, lichen and leafy vegetation remove OCS from the atmosphere. Some plants and lichens can produce the volatile DMS, H_2S or other organosulfides through sulfate assimilation (Andreae and Jaeschke 1992; Gries et al., 1994).
- Bacteria can assimilate the sulfate in organic sulfur molecules; drive the pool of sulfur through mineralisation in sulfide S^{2-}; or through the dissimilative oxido-reduction between SO_4^{2-} and S^{2-}. Bacterial processes can also lead to the production of H_2S to the atmosphere (Havlin et al., 2013).

The last compartment that was not detailed previously was the hydrosphere. The concentration of SO_4^{2-} in the oceans reaches 28 mmol L^{-1} while in freshwater it does not exceed 1 mmol L^{-1} (Holmer and Storkholm 2001; Giordano et al. 2005). Its incorporation, reduction, and transformation are well described in the following sections with an emphasis on the DMS(P,O) cycle.

3 The biogeochemical cycle of DMS

As it was suggested previously, DMS is ubiquitous in the biosphere including vascular plants, lichens, corals, algae and even bacteria. It is also the principal biogenic fraction of the sulfur emissions from the ocean to the atmosphere. However, DMS is due to two biogenic precursors that are DMSP and DMSO. These three sulfur molecules (Fig. 1-4) are part of an important biological cycle.

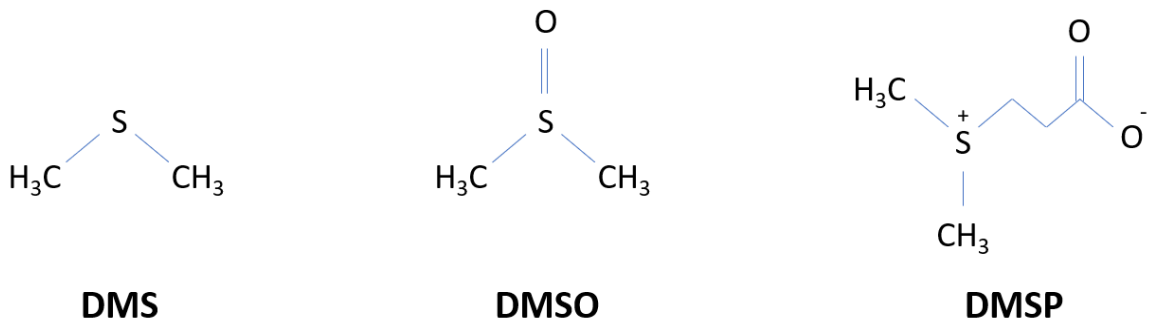

Figure 1-4: DMS, DMSP and DMSO skeletal and chemical formula

The latter transform the uptake of SO_4^{2-} in DMSP that will react inside phytoplankton cells to produce DMSO and DMS. Once in the water column, these DMS(P,O) interact with the bacterioplankton leading to a loop closure. DMSP represents a significant fraction of organic sulfur in marine particles and it is a major sulfur carrier throughout the marine food web (Simó,

2001). DMSP is contributing not only to the cycling of sulfur via its link with DMS, but also to the microbial food web through the supply of carbon and sulfur to marine bacteria (Kiene and Linn, 2000).

3.1 DMSP and CH_4

Before explaining the DMS(P,O) biosynthesis and their hypothetical role within the phytoplankton cell, we have to briefly introduce the possible link between methylated molecules such as DMSP and the production of CH_4. The latter is the second most important anthropogenic greenhouse gas (GHG) after CO_2. The production in the open ocean is weak (< 2 Tg yr^{-1}) compared to other natural (~220 Tg yr^{-1}) or anthropogenic (~350 Tg yr^{-1}) sources (Saunois et al., 2016). CH_4 emissions from coastal waters are more important (~10 Tg yr^{-1}) and result from the methanogenesis occurring in the sediments sustained by high organic matter deposition, natural gas seeps, mud volcanoes or CH_4 hydrates (Borges et al., 2019 and citations therein). Methanogenesis is widely thought to be a product of anaerobic process inhibited or outcompeted by the presence of oxygen and sulfate (Liu and Whitman, 2008; Thauer et al., 2008). Yet, high-sulfate and fully oxygenated surface waters have supersaturated CH_4 concentrations with respect to atmospheric concentrations. The origin of this CH_4 remains elusive and is referred as the "marine CH_4 paradox" (Kiene, 1991; Reeburgh, 2007). The CH_4 sursaturation in the upper surface layer is not coming from the deeper waters and the sediments, neither from the littoral (Damm et al., 2010; Zindler et al., 2013). It involves probably several processes different from an ecosystem to another and might implicate (Dang and Li, 2018):

1. the DMSP or other compounds such as methylphosphonate (MPn) as substrates for the aerobic methylotroph methanogenesis (Karl et al., 2008);

2. the production of CH_4 by the phytoplankton itself (i.e. *Emiliania Huxleyi*) involving the bicarbonate and methionine as carbon precursors in oxic conditions (Lenhart et al., 2016)

3. the methanogenesis in the guts of some species of copepods, or indirect contribution to CH_4 production through release of CH_4 precursors into the surrounding water, followed by microbial degradation (Stawiarski et al., 2019)

4. the possible anaerobic conditions within a methanogenic bacteria (Damm et al., 2015).

The methanogenesis normally requires anaerobic environment but a CH_4 production pathway from methylated substrate such as MPn, DMSP, DMS, MeSH or MMPA (Sowers and Ferry, 1983; Welsh, 2000; Damm et al., 2010; Zindler et al., 2013) was suggested in aerobic conditions (Karl et al., 2008). The methylotroph methanogenesis is realized by some methanogenic coccoid (Oremland et al., 1989) and some *Alphaproteobacteria* (i.e. *Rhodobacteraceae*), *Gammaproteobacteria* (i.e. *Methylophaga sp.;* Neufeld et al., 2008; *Pseudomonas sp.*; Repeta et al., 2016). The nutrient limitation in oligotrophic waters (P limitation) coupled with the presence of DMS(P) or MPn as substrate would regulate the CH_4 production (Karl et al., 2008). In the central Artic Ocean, the N depletion seems to be a requirement for the aerobic CH_4 production, whereas the P excess is used by the bacteria as P source, and DMSP and its degradation products as C source (Damm et al., 2010; Damm et al., 2015). Furthermore, Karl et al. (2008) suggest that nitrogen fixation, promoting further phosphate limitation in the ecosystem, may also enhance both MPn utilization and aerobic methane production. The aerobic methanogenesis seems to occur in the semi-labile dissolved organic matter phosphonates, releasing CH_4 thanks to a multi-enzyme complex (C-P lyase pathway) (Repeta et al., 2016). In addition, a second potent GHG, nitrous oxide (N_2O), may be produced through bacterial nitrification due to the excess of NH_4 produced by the nitrogen fixation (Karl et al., 2008). The GHG production (N_2O and CH_4) due to the previous processes may accelerate the global warming, the thermal stratification of the ocean, expanded the phosphate-limited, nitrogen-fixation-favourable marine habitats (Karl, 2007; Polovina et al., 2008), and accelerating the aerobic methane production scenario, the greenhouse warming and the ecological consequences (Karl et al., 2008).

3.2 The bacteria and algal biosynthesis of DMS(P,O)

DMS(P,O) are produced by a wide variety of marine phytoplankton, macroalgae, angiosperms and corals (Keller et al., 1989; Stefels, 2000; Simó and Vila-Costa, 2006; Hatton and Wilson, 2007; Raina et al., 2013; Borges and Champenois, 2017; McParland and Levine, 2019). A review of the low- and high-DMSP producing species within the eukaryote and prokaryote phylogeny is presented in the figure 1-5 and was assessed using previously published studies (McParland and Levine, 2019).

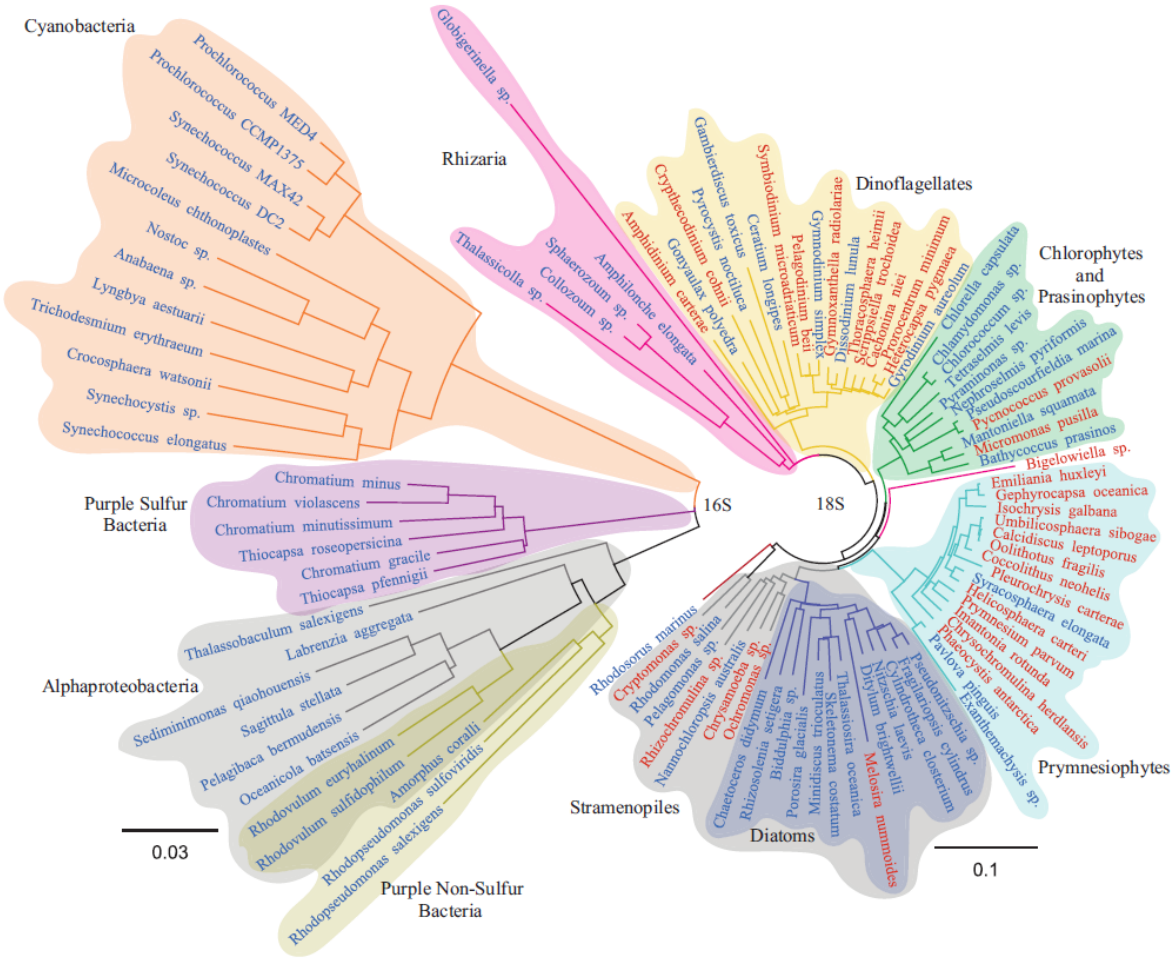

Figure 1-5: Tree of representative prokaryotic (left) and eukaryotic (right) DMSP producers built with 16S and 18S phylogeny. The prokaryotic producers are grouped by functional groups, while the eukaryotic producers are grouped by the major eukaryotic supergroups. Blue text represents low-DMSP producers (intracellular DMSP < 50 mM) and red text represents high-DMSP producers (intracellular DMSP > 50 mM) (McParland and Levine, 2019).

The first complete biosynthesis pathway for the DMSP was described for the green macroalgae *Ulva intestinalis* (Gage et al., 1997; Summers et al., 1998). A review from the different pathway production is presented at the figure 1-6. We focused on the phytoplankton pathway production that can be defined as follows (Bullock et al., 2017):

1) Transamination from methionine to unstable acid: 4-methylthio-2oxobutyrate (MTOB)
2) MTOB is enzymatically reduced to 4-methylthio-2-hydroxybutyrate (MTHB)
3) MTHB is S-methylated in 4-dimethylsulfonio-2-hydroxy-butyrate (DMSHB)
4) DMSHB is oxidatively decarboxylated in DMSP.

The key intermediate of DMSHB was also identified in three other phytoplankton species: the Prymnesiophyceae *Emiliania huxleyi,* the diatom *Melosira nummuloides*, and the prasinophyte *Tetraselmis sp.* (Gage et al., 1997). The same pathway might then operate in other algal species. Microalgae sequentially utilize (1) 2-oxoglutarate-dependent aminotransferase (AT), (2)

NADPH-linked reductase (REDOX), (3) S-adenosylmethionine-dependent methyltransferase (SAMmt) and (4) oxidative Decarboxylase (DECARB) (Gage et al., 1997; Summers et al., 1998). For the dinoflagellates, an alternative pathway has been proposed starting with a Met decarboxylase, and presumably followed by aminotransferase and methyltransferase steps (Kitaguchi et al., 1999). Lyon et al. (2011) identified proteins and possible genes that would be affected to the four enzyme classes needed for the first pathway. These genes need to be confirmed since they are not always detected with similar experiments (Kettles et al., 2014). Moreover, DMSP production seems to be localised in the chloroplast (Trossat et al., 1998; Raina et al., 2017). Using radiotracer ^{34}S, Raina et al. (2017) follow the incorporation of SO_4^{2-} and show an accumulation of DMSP in the vacuoles and cytoplasm as well as the chloroplast. These findings could also confirm the hypothetical role of an osmoregulator, and antioxidant discussed further (Raina et al., 2017).

It was thought that only eukaryotes produce significant amounts of DMSP but Curson et al. (2017) demonstrated that many marine heterotrophic bacteria also produce DMSP. They identified the DMSP gene *dsyB*, which encodes the methyltransferase enzyme needed for the third step of the previously described pathway (Curson et al., 2017). Curson et al. (2018) also identified homologues to this bacterial gene *dsyB*, so-called *DSYB*, in the genome or proteome of most Prymnesiophyceae, dinoflagellates, prymnesiophytes, some corals and about 20% of diatoms and Ochrophyta. However, Kageyama et al. (2018) identified the gene coding for the MTHB-methyltransferase, called *TpMMT*, of the third step in the DMSP biosynthesis in *T. pseudonana.* They did not find homologous genes in other organisms nor with *DSYB*, suggesting it might be difficult to discover the MTHB gene by the sequence homology (Kageyama et al., 2018). Recently, high concentrations of DMS(P) were found in various sediment, from saltmarsh ponds, estuaries, or deep ocean, resulting mainly from bacteria production. Approximatively 1 x 10^8 bacteria g^{-1} of surface marine sediment are predicted to produce DMSP, and their contribution has to be included in future models of DMSP production (Williams et al., 2019).

Even if questions remain regarding the direct and the exact localization of DMSO production, it is in fact generally assumed that its production results from the oxidation of DMSP and DMS by ROS such as $OH\cdot$ or $^1O_2$ (Scaduto, 1995; Lee and De Mora, 1999; Sunda et al., 2002; Spiese et al., 2009). DMSO concentrations within phytoplankton can approach those of DMSP, making DMSO a quantitatively important pool of methylated sulfur compounds (Simó et al., 1998; Simó et al., 2000; Hatton and Wilson, 2007; Zindler et al., 2013).

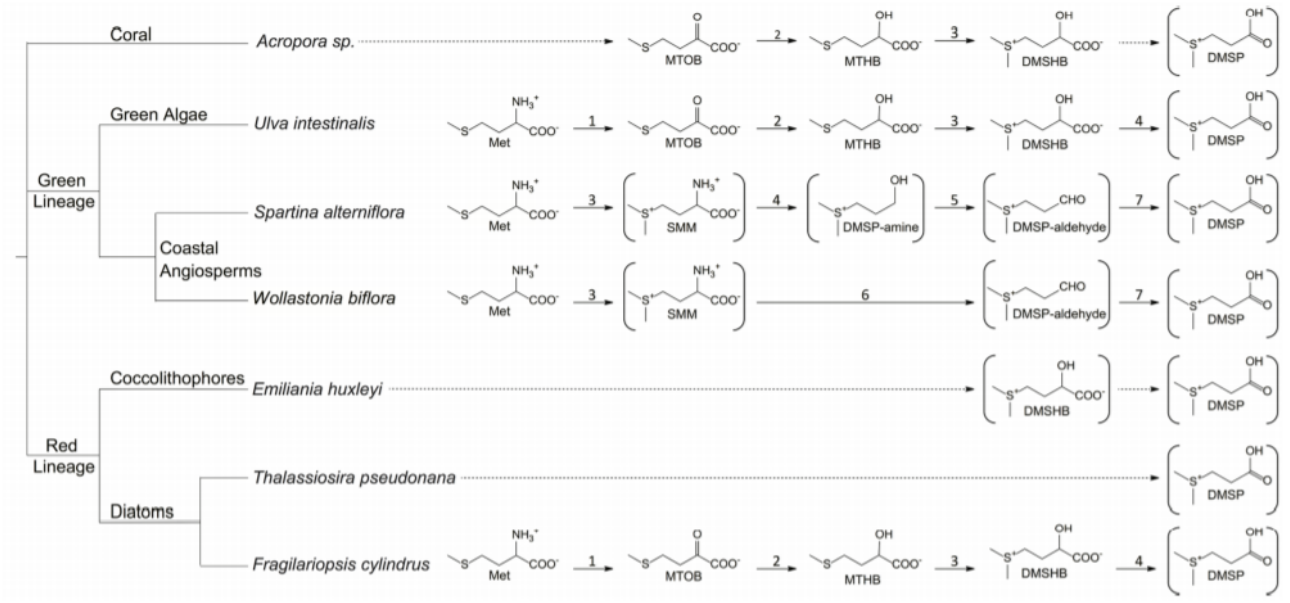

Figure 1-6: DMSP biosynthetic pathways reviewed from Bullock et al. (2017). The structures in brackets have been verified and complete arrows are identified or predicted based on the observed intermediates. 1, aminotransferase; 2, NADPH-reductase; 3, methyltransferase; 4, decarboxylase; 5, oxidase; 6, decarboxylase/transaminase; 7, dehydrogenase. MTOB, 4-methylthio-2-oxobutyrate; MTHB, 4-methylthio-2-hydroxybutyrate; DMSHB, 4-dimethylsulfonio-2-hydroxybutyrate; SMM, S-methyl-L-methionine.

More recently, a new molecule called dimethylsulfoxonium propionate (DMSOP) was found in the dinoflagellates *P. minimum,* the Prymnesiophyceae *P. parvum, I. galbana* and *E. huxleyi*, the diatom *S. costatum* as well as in some bacteria (Thume et al., 2018). They suggest that DMSOP might be produced directly by the phytoplankton or bacteria, and/or result from the oxidation of DMSP. They also concluded that DMSOP might be contributing to the DMSO pool through bacterial degradation. More research needs to be conducted to refine the metabolic pathway of DMS, DMSP, DMSO and DMSOP production as well as their interaction with the bacterioplankton.

From the perspective of an ecosystem, the composition of seawater species is the factor that affects community-DMSP production the most (Stefels et al., 2007). Keller et al. (1989) conclude that the dinoflagellates and the Prymnesiophyceae are high-DMSP-producers while the diatoms and some Chrysophyceae are low-DMSP producers.

3.3 The physiological roles of DMS(P,O)

DMSP, and to a lesser extent DMSO, perform several important physiological and ecological functions which benefit the phytoplankton producer (Simó, 2001). These benefits might have led to the evolutionary selection of DMSP synthesis in many phytoplankton species (Caldeira, 1989). However, these hypothetical functions are not fully understood. As we will see further, intracellular, or particulate DMS(P,O) ($DMS(P,O)_p$), might act as osmolytes, cryoprotectants,

signalling molecules, overflow mechanisms, zooplankton deterrents, or antioxidants. The unifying aspect of these hypotheses is that the $DMSP_p$ synthesis will be upregulated under different types of cellular stress such as changes in osmotic pressure, decrease in external temperature, or increase in reactive oxygen species (McParland and Levine, 2019). Hence, the DMS(P,O) concentration in the ocean would be partially dependent on the environmental conditions as well as the diversity of phytoplankton (Masotti et al., 2010).

3.3.1 Osmoprotectant

Phytoplankton might experience high or changing salinities in their environment due to evaporation, moving of water masses or input of freshwaters, rainfalls, and ice melting. They have to be able to adjust to these conditions of low or changing water potential (osmotic pressure) (van Bergeijk et al., 2003). Phytoplankton cells must be able to change their osmotic pressure to avoid turgidity, when salinity decreases, or plasmolysis, when salinity increases (Durack, 2015). In other words, cells must try to recover their original volume (Stefels, 2000). The adjustment of organic and inorganic solutes in response to changes in salinity is well known as a fundamental mechanism in salinity tolerance (Kirst, 1989). Andreae (1986) first suggests that DMSP might be used as a compatible solute. This latter term means that the molecule has a protecting/stabilizing effect on the metabolic pathway and membrane-dependent processes against adverse effects of high salt concentration (Karsten et al., 1992).

The DMSP structure is similar to the osmoregulatory compound glycine betaine (GBT), which has nitrogen as its central atom in contrast of the sulfur in DMSP. The algae could thus switch between the synthesis and accumulation of GBT, under N repletion, and DMSP, under N deficiency (Liss et al., 1997). Regarding the evolutionary adaptation, this function may have represented an adaptative advantage in N-limited oceans (Falkowski et al., 1998). This would also explain the taxonomic patterns observed: most diatoms evolved in more replete N conditions (i.e. early spring), synthetizing less DMSP per cell volume; conversely the small Prymnesiophyceae or dinoflagellates are typical of more N-deficient conditions and therefore produce more DMSP. The exception to this hypothetical rule is the Prymnesiophyceae *Phaeocystis sp.* which forms extensive algal bloom in high-nitrate but silicate-deficient conditions (Simó, 2001). DMSP accumulation in response to elevated salinity has been observed in diatoms, Prymnesiophyceae and dinoflagellates (Dickson and Kirst, 1986; Karsten et al., 1992; Yang et al., 2011; Zhuang et al., 2011; Kettles et al., 2014; Speeckaert et al., 2019; Wittek et al., 2020).

In addition, GBT has the potential of buoyancy role in some large phytoplankton species while DMSP is heavier than GBT (Boyd and Gradmann, 2002). Since GBT can be replaced by DMSP under nutrient limitation, this has led to the possible DMSP-ballast role to regulate the sinking or rising rates of phytoplankton (Lavoie et al., 2015). The synthesis of DMSP might help the cells to escape the low nutrients (N and Fe) and high irradiance environment in order to sink down to nutrient-rich areas in the euphotic zone (Raven and Waite, 2004; Lavoie et al., 2015).

3.3.2 Cryoprotectant

The first suggestion of the cryoprotectant role was made by Karsten et al. (1990) since they discovered DMSP in polar algae. Adjustment of internal DMSP concentration was observed in Prymnesiophyceae (i.e. *E. huxleyi* (van Rijssel and Gieskes, 2002) and in green macroalgae (Karsten et al., 1990; Sheets and Rhodes, 1996) at low temperatures. DMSP might be part of the cryoprotection system synthetized by algae within other molecules such as heat and cold-shock proteins, exopolysaccharides, polyunsaturated fatty acids, or crystallisation inhibitors (Wittek et al., 2020 and citations therein). The DMSO cryoprotectant function has been suggested through *in vitro* experiment (Liss et al., 1997) but the concentrations observed in ice algae seem to be too low to decrease the freezing point in the algal cells (Lee et al., 2001).

3.3.3 Antigrazing compound

The phytoplankton cells are under the pressure of grazing from the zooplankton. This selection pressure has led to the development of toxins produced by marine microalgae as a chemical defence (Strom et al., 2003a). Shifting the grazing pressure to other prey species also reduces the competition for nutrients (Wolfe et al., 1997). Among these defences, the degradation of DMSP by the enzyme DMSP lyase (DL) produce acrylate that has antimicrobial activity, and thus potential repulsive property. This might be significant in the shaping of the evolutionary photosynthetic lineage (Takahashi et al., 2011 and citations therein). It has been shown that zooplankton grazers will prefer species with low DL activity (Wolfe et al., 1997) to avoid a decrease in their feeding rates (Strom et al., 2003a). This hypothesis has evolved as it has been actually observed that the DMSP itself (naturally produced or by addition in laboratory cultures) decreases microalgae grazing (Strom et al., 2003b; Fredrickson and Storm, 2008) and not the DMS or acrylate (Strom et al., 2003b). DMSP might therefore be a repulsive signal for the predator (Strom et al., 2003b). However, the addition of DMSP in a natural environment has no effect on grazing rates (Fredrickson and Storm, 2008). As a matter of fact, recent studies have led to the same conclusions by supporting a non-repulsive effect or even a potential

chemoattraction between DMSP and grazers (Seymour et al., 2010; Archer et al., 2011; Simó et al., 2018). Seymour et al. (2010) suggested that the saturation of the system with DMSP addition obscured the microscale chemical signature of phytoplankton cells, masking their position, and thus reducing the zooplankton grazing rates.

3.3.4 Infochemical

Even if the DMSP antigrazing compound in marine microorganisms is unclear (*cf. 3.3.3*), DMSP represents directly or indirectly (by DMS) a foraging cue for some motile strain of phytoplankton, heterotrophic bacteria, bacterivore and herbivore zooplankton, sea urchins, coral reef fish, some seabirds, penguins, whale sharks and harbour seals (Seymour et al., 2010; Nevitt, 2011; Savoca and Nevitt, 2014 and citations therein). Savoca and Nevitt (2014) even present the hypothesis of a tritrophic interaction between DMS release, stimulated by zooplankton grazing, and the attraction of seabirds specializing on primary consumers that will reduce predatory pressure and enhance phytoplankton growth through iron recycling and defecation.

3.3.5 Overflow mechanisms

DMSP might also be produced to dissipate an excess of energy, carbon or sulfur as well as regulate cellular nitrogen (Bullock et al., 2017). Algal cells might induce DMSP biosynthesis as well as enzymatic lysis to DMS to discard unneeded fixed carbon and/or reduced sulfur when their incorporation is higher than the assimilation of other nutrients such as nitrogen (Stefels and van Leeuwe, 1998; Stefels, 2000). Under nutrient limitation, this energy and carbon dissipation leads to the regeneration of intracellular nitrogen from Met, which can in turn be used for synthesis of other amino acids (Stefels, 2000). A putative DMSP overflow mechanism could provide a sink for unneeded photosynthetic products (NADPH and ATP) during periods of low cell biosynthesis and growth, helping to prevent overreduction of the photosynthetic apparatus and decreasing a potential oxidative stress (Darroch et al., 2015). In other words, the benefits are ultimately the continuation of the metabolic machinery (Stefels et al., 2007).

3.3.6 Antioxidant

Since the antioxidant function is the main subject of this thesis, it will be largely described in section 6.

4 The fate of DMS(P,O)

We distinguish the particulate ($DMS(P,O)_p$) and the dissolved ($DMS(P,O)_d$) DMS(P,O). The first one occurs within the phytoplankton cell while the other takes place in the water column. As it was mentioned previously, the biosynthesis of $DMSP_p$ begins always with Met (Gage et al., 1997; Summers et al., 1998). The latter is synthetized from the uptake of dissolved SO_4^{2-}, and its further reduction, incorporation, and methylation (Takahashi et al., 2011) (Fig. 1-7). The DMS(P,O) cell quota within the phytoplankton depend on the initial DMS(P,O) concentrations characterizing the low- or high-DMSP producing species (Keller et al., 1989). The cellular concentration variations between the sulfur compounds will then be influenced by the environmental stress that may occur in natural environment. These interactions were explained previously within the physiological roles of $DMS(P,O)_p$ (*cf. 3.2*).

4.1 The fate of DMS(P,O) in a marine environment

The DMS, DMSP and DMSO could be release into the marine environment by several processes (exsudation, senescence, viral attack, or grazing; Fig. 1-7) that can impact, or not, the integrity of the cell. For instance, the algal senescence or the lysis resulting from grazing will lead to the death of cells: programmed in the first case, or because of the zooplankton in the second case. The programmed cell death could be induced by viral attack, by environmental conditions, or by ROS production resulting of oxidative stress (*cf. 4.4*) (Hill et al., 1998; Bidle and Falkowski 2004). Zooplankton grazing will increase the $DMSP_d$ pool when the algae is not entirely consumed in the first place (sloppy feeding), or subsequentially by faecal pellets (Fig. 1-7) (Tang and Simó, 2003). The latter could then sediment or be degraded in deep water (Kwint et al., 1996; Brimblecombe, 2014). Export rates were estimated to be between 0.1% and 16.6% d^{-1} in coastal waters and between 0.03% and 0.74% d^{-1} in the open ocean (Stefels et al., 2007). Viral lysis release the entire $DMSP_p$ content of the algal, increasing the $DMSP_d$ pool, and making it available for bacterial breakdown and potentially contributing to its DMS conversion (Hill et al., 1998).

Zooplankton could use some $DMSP_p$ as a source of carbon or sulfur (Archer et al., 2001), since 24-70% of the ingested prey DMSP can be retained in the grazer (50-60%, Belviso et al., 1990; 24-70%, Wolfe and Sherr, 1994; 33%, Simó et al., 2002; 32-44%, Tang and Simó, 2003). By retaining the ingested DMSP in its biomass, the grazer transfers DMSP further up in the food chain (Tang and Simó, 2003). However, it is assumed that ~70% of the ingested DMSP is released as DMSP in faecal pellets, $DMSP_d$, DMS and acrylate or alternative by-products of

digestion (Fig. 1-7) (Archer et al., 2001; Stefels et al., 2007). The viral lysis or zooplankton grazing could also act as pathways for DMSP cleavage to DMS and acrylate, by mixing the DMSP lyases with its substrate during the physical degradation (Fig. 1-7) (Malin et al., 1993; Wolfe and Steinke, 1996; Evan et al., 2007; Simó et al., 2018). They hypothesized that DMSP and DL are physically compartmentalized in the cell (Wolfe and Steinke, 1996). The microbial activity in the intestinal tract of the zooplankton and in faecal pellets may also be responsible for DMS production (Stefels et al., 2007). Active exudation is also present in algae but is species-specific and can be affected by abiotic parameters such as salinity, temperature, or nutrient limitation (Fig. 1-7) (Stefels et al., 2007).

The main difference for the DMS and DMSO (DMS(O)) is their chemical properties that allow passive diffusion across membranes (Fig. 1-7) (Jacob and Wood, 1967; Hatton and Wilson, 2007; Lavoie et al., 2016; Spiese et al., 2016). If we consider that the DMS(O) are produced inside the chloroplast due to DMSP oxidation, DMS(O) diffusion has to be conducted across several layers of membrane from the thylakoids to the outer cell membrane (Lavoie et al., 2016). DMSO is also produced by the photochemical oxidation of DMS (Fig. 1-7) (Brimblecombe and Shooter, 1986). Unlike DMS(P) which are essentially confined to the euphotic zone of oceans, DMSO might stay at high levels in deep oceans (Hatton et al., 1998).

Once in the marine environment, $DMSP_d$ has a chemical half-life of 8 years (Dacey and Blough, 1987) resulting in high abiotic stability under natural conditions. Most of its removal then results from enzymatic processes (Stefels et al., 2007). $DMSP_d$ could be taken up by algae that are, or not, DMSP producers (Fig. 1-7) (Kiene et al., 2000; van Bergeijk et al., 2003; Spielmeyer et al. 2011; Ruiz-Gonzalez et al. 2012; Lavoie et al., 2018; Petrou and Nielsen, 2018). Non-DMSP producing species may form a considerable sink for $DMSP_d$, reducing $DMSP_d$ availability for other organisms and influencing the turnover of DMSP in the ocean (Lavoie et al., 2018; Petrou and Nielsen, 2018). Some motile phytoplankton can even actively seek out localized $DMSP_d$ using its chemoattraction (Seymour et al., 2010). The $DMSP_d$ can also be incorporated (~15%; Kiene and Linn, 2000) into bacteria as osmolyte, cryoprotectant, or antioxidant (Karsten et al., 1996; Simó et al., 2002; Lesser, 2006; Salgado et al., 2014). In addition, the chemoattraction described previously seems to be present for some motile bacteria strains (Seymour et al., 2010). Since Curson et al. (2017) discovered that bacteria can directly produce DMSP, their death might induce an increase of the $DMSP_d$ pool as well. The

$DMS(P,O)_d$ could also be reduced, oxidised, or enzymatically cleaved by both bacterial and algal processes (Fig. 1-7), leading to the formation of $DMS_{(aq)}$.

Algal enzymatic cleavage includes DMSP-lyase that converts DMSP into DMS and acrylate (Yoch, 2002; Stefels et al., 2007; Mohapatra et al., 2014), and DMSO reductase for DMSO to DMS (Spiese et al., 2009). Studies reported significant DL activity within phytoplankton blooms and among individuals including some Prymnesiophyceae (i.e. *Phaeocystis sp.*) and dinoflagellates (i.e. *Heterocapsa triquetra*) (Stefels and Dijkhuizen, 1996; Niki et al, 2000; Yoch, 2002; Caruana and Malin, 2014). The responsible gene – *Alma1* – has been recently discovered in Prymnesiophyceae *E. huxleyi*. Sequence searches suggest that this gene is the first characterized member of an entire family of DL present in a wide variety of algae (i.e. dinoflagellates and Prymnesiophyceae) (Alcolombri et al., 2015). It has been suggested that all algal species could reduce DMSO to DMS, even species that are non-DMS(P,O) producers (Spiese et al., 2009). This idea proposes a possible uptake of $DMSO_d$ as it is for $DMSP_d$.

The availability of DMSP in the water column will exert the greatest influence on overall microbial consumption of $DMSP_d$ (Lizotte et al., 2012). As a matter of fact, $DMSP_d$ concentration could support 1 – 13% of the bacterial carbon and sulfur demand in surface waters (Kiene, 1996; Kiene et al. 1999; Kiene and Linn, 2000) with the main pathway as follows (Stefels et al., 2007): (1) demethylation producing 3-methiolpropionate (MMPA), (2) demethiolation leading to methanethiol (MeSH), (3) demethylation to produce H_2S (Fig. 1-7). It is likely that about 90% of DMSP in seawater is converted into methanethiol (Kiene and Linn, 2000). The genes DmdA, DmdB, DmdC and DmdD are responsible for the DMSP demethylation pathway (Bullock et al., 2017). This pathway is found in many marine bacteria, notably the clade *Pelagibacter* and *Roseabacter* (Curson et al., 2011). MMPA could also be demethylated in 3-mercaptopropionate (MPA) and then degraded in H_2S and acrylate in anaerobic conditions (Kiene and Taylor, 1988; Taylor and Visscher, 1996). In addition, bacteria could cleave $DMSP_d$ into DMS and acrylate thanks to DL in aerobic conditions (Yoch, 2002). The cleavage pathway is considered as an important source of DMS (Curson et al., 2011). There are actually six different genes with a cupin motif coding for this cleavage pathway (DddP, DddW, DddY, DddQ, DddL and DddK) (Curson et al., 2011; Bullock et al., 2017). Two other DMSP cleavage enzymes have been identified to date, including DddD belonging to the CoA transferase family and DddP of the metallopeptidase family (Alcolombri et al., 2015).

The bacteria will prefer the first demethylation/demethiolation over the lyase pathway when $DMSP_d$ concentrations are low. This pathway leads to higher energy production and it is a relative economic way to assimilate reduced sulfur (Kiene et al. 2000; Welsh 2000), accounting for ~75% of $DMSP_d$ degradation (Kiene and Linn, 2000). When this concentration is higher, the bacteria will cleave the $DMSP_d$ not assimilated in DMS. The DMS can then be also taken up by bacteria but acrylate might be used instead, leaving the DMS untouched (Yoch et al., 2002). However, factors controlling the bacterial degradation of DMSP to DMS versus methanethiol (demethylation/demethiolation) are not well understood and depend on the local phytoplankton bloom, its stage of development, the $DMSP_p$ produced, the microbial species associated with the bloom as well as environmental factors such as the salinity (Yoch et al., 2002; Stefels et al., 2007; Salgado et al., 2014). External DMSP concentration seems to dictate the relative expression of the two pathways, but only at high concentrations (> 1µmol L^{-1} for the demethylation; > 35 nmol L^{-1} for the cleavage) characterizing the vicinity of phytoplankton cells (Gao et al., 2020). Kiene et al. (2000) stipulated that it is the bacterial sulfur demand relative to the $DMSP_d$ availability that will lead to one or another pathway (i.e. if the sulfur demand is low due to nutrient or high light stress, the demethylation pathway will be minor and DMS yield will increase). This hypothesis is supported by field measurements in North Sea where both phytoplankton and microzooplankton herbivory have a considerable impact on the productivity and competitiveness of $DMSP_d$- and DMS-consuming bacterioplankton (Archer et al., 2002). Enhancement of solar radiation exposure has been suggested for example to cause the inhibition of bacterial S demand thus potentially affecting bacterial clades that consume DMS (Slezak et al., 2001; Toole et al., 2006). Thus, the efficiency of bacterial conversion of DMSP into DMS may vary from 2 to 100% depending on the nutrient status of bacteria and the quantity and quality of the pool of dissolved organic matter (Kiene et al., 2000). Recently, it has been suggested that bacteria express both pathways simultaneously, but only modulate the ratio between the cleavage and the demethylation according to DMSP concentration (Gao et al., 2020). Field measurements from various oceanic and coastal areas gave an average of 10-12% for the $DMSP_d$ consumed and cleaved by bacteria into volatile DMS (Kiene and Linn, 2000; Vila-Costa et al., 2008; Lizotte et al., 2012).

$DMSO_d$ concentration in seawater can exceed those of DMS and, in some cases, those of $DMSP_d$ (Hatton et al., 1998; Simó et al., 1997). $DMSO_d$ can be produce from the transformation of DMS via both photolysis and biological consumption (del Valle et al., 2009). The DMSP cleavage pathway, producing DMS and acrylate, and its further catabolism within the cell,

produces DMSO and MeSH. Two enzymes have been identified for this catabolism (Tmm for DMSO and DmoA for MeSH). Because acrylate is toxic to bacteria, further detoxification is required, and structures of three enzymes have been resolved recently (PrpE, AcuI and AcuH) (Wang et al., 2017; Chen and Schäfer, 2019).

DMSO production from DMS photolysis are known to vary substantially from 14% in the Equatorial Pacific Ocean (Kieber et al., 1996), 22-99% in the northern North Sea (Hatton, 2002) and 33-45% for the Southern Ocean (Toole et al., 2004). DMSO production can also be stimulated by physiological stress, as a part of a cellular antioxidant system in phytoplankton (Sunda et al., 2002 – *See 5.4*). Finally, some bacteria such as Roseobacter are also involved in the reduction of $DMSO_d$ to DMS (Spiese et al. 2009; Bullock et al., 2017).

4.2 The fate of DMS

Once in the water column, DMS will be removed by biotic and abiotic processes (Galí et al., 2018). The percentage of each process in the DMS fate is still under debate but the resulting volatilisation mainly depends on bacterial processes and photooxidation. The DMS flux between seawater and the atmosphere is controlled by its difference in concentration with the oversaturation of the upper-mixed layer compared to the atmosphere (Liss et al., 1997; Galí et al., 2018), and by the magnitude of the DMS transfer velocity across the air-sea interface (Bopp et al., 2003). The last term is depending on the sea-surface temperature and wind velocity (Wanninkhof, 1992). DMS emissions, depending on their precursors DMS(P,O) produced by the bacterio-phytoplankton, will thus vary considerably in response to phenology and ecological succession of microbial species, which in turn depend on physical forcing factors such as light, sea-surface temperature, or nutrient supply (Archer et al., 2002; Bopp et al., 2003; Archer et al., 2004; Lizotte et al., 2012; Galí and Simó, 2015). Toole and Siegel (2004) postulate that there are two distinct DMS regimes: (1) a stress-forced regime controlled by environmental stress that might enhance DMS production (see after "*DMS summer paradox*"); and (2) a bloom-forced regime whereby phytoplankton bloom dictates the DMS stock, occurring in regions characterized by monospecific blooms of DMSP-producing species such as *Phaeocystis* in the North Sea.

It has been calculated that 90% of dissolved DMS is consumed by bacterial oxidation and UV-driven photolysis (Fig. 1-7). The remaining 10% is emitted to the atmosphere (Galí and Simó, 2015) (Fig. 1-7). This percentage can vary considerably between 1% and 40% and is correlated to the mixed layer depth (Simó and Pedrós-Alió, 1999). Estimations from Moran et al. (2012)

calculated this volatilisation at about 5%, the photooxidation to DMSO at about 10%, and the bacterial uptake at some 85% (Fig. 1-7). This latter can reach up to 98% of the DMS removal in subsurface layer. As a matter of fact, the dominance of biological processes appeared to moderate the impact of environmental forcing factors on DMS concentrations in the surface layer (Archer et al., 2002).

The photooxidation occurred under UV/Visible wavelengths (Hatton, 2002) and the reaction rate varied with DMS concentration (Brimblecombe and Shooter, 1986). The DMS photolysis does not always result in DMSO production. When it is the case, there is still a possible return to DMS thanks to the reduction pathway (Stefels et al., 2007). It has been shown that 14% and ~37% of the DMS was converted to DMSO by photooxidation in Pacific waters and in the northern North Sea, respectively (Kieber et al., 1996; Hatton, 2002). Toole and Siegel (2004) estimated that 77% of the DMS variability was explained by the UV radiation dose in the Sargasso Sea.

Vila-Costa et al. (2006) estimated that around 70% of the 85% bacterial DMS uptake is metabolized by bacteria in DMSO by DMS dehydrogenase. Only 3% are incorporated in macromolecules while between 13 and 28% are converted into sulfate. The route to sulfate is characterized by the conversion of DMS by monooxygenase and methyltransferase in MeSH and formaldehyde (De Bont et al. 1981; Borodina et al. 2002) whereby the bacteria used this DMS as a source of carbon and sulfur (Fuse et al. 2000; Endoh et al. 2003). However, the significance of bacterial DMS consumption also depends on the strength of other competing loss processes (Stefels et al., 2007). For instance, Simó and Pedrós-Alió (1999) illustrated in the subpolar North Atlantic that: (1) the photooxidation process to DMSO would be dominant under clear skies and when the water column is stratified (Simó and Pedrós-Alió, 1999) since the photooxidation under full light conditions can be responsible of 37% of DMS loss (Hatton, 2002); (2) bacterial consumption is most important when the weather is cloudy and/or when the water column is mixed to a greater depth; and (3) the bacterial consumption is equivalent to the loss due to sea-to-air flux transfer.

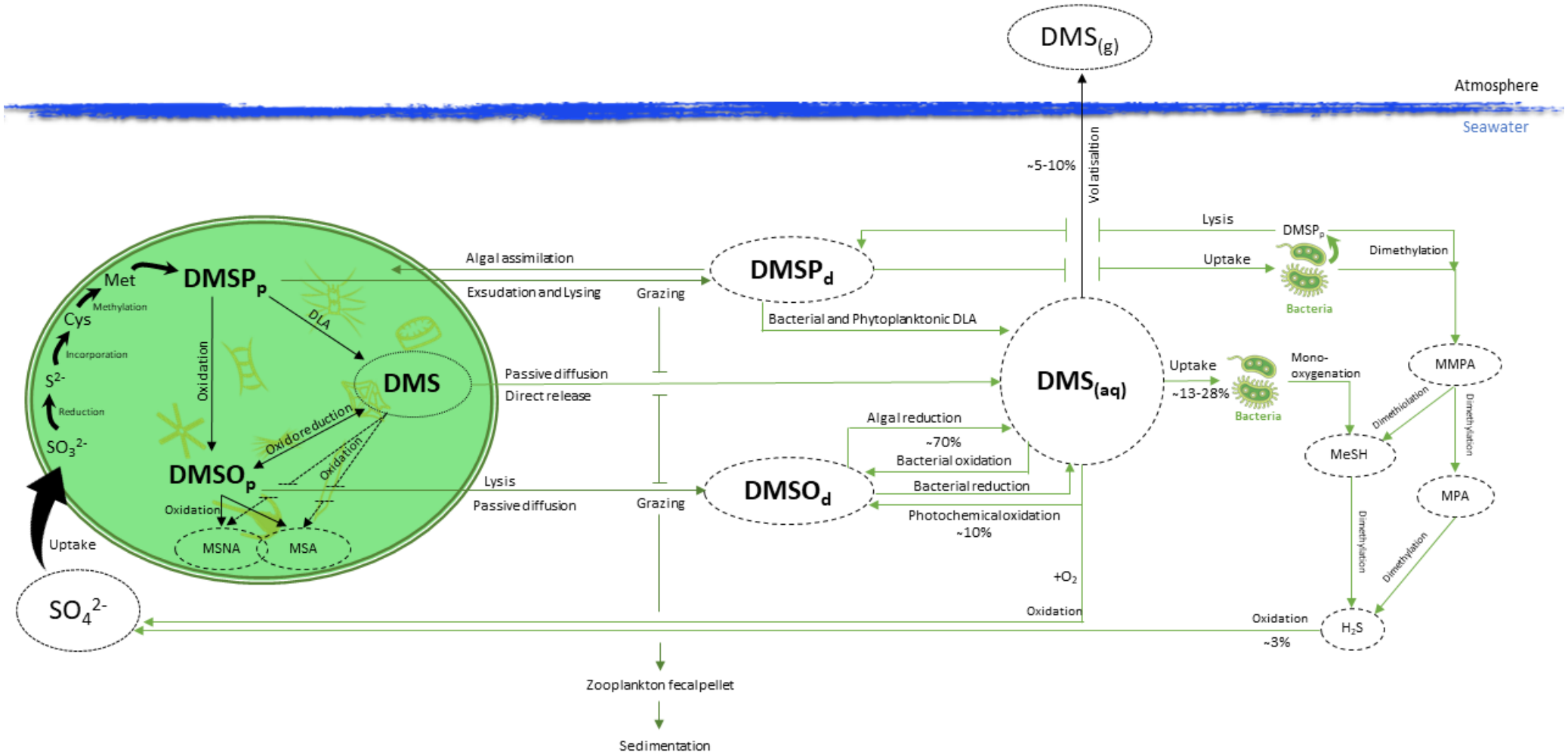

Figure 1-7: Biogeochemical DMS cycle in the marine environment adapted from Stefels (2000), Sunda et al. (2002), Yoch et al. (2002), Stefels et al. (2007), Spiese et al. (2009), Lyon et al. (2016), Curson et al. (2017) and Giordano and Prioretti (2016). Algal and bacteria are schematically represented. The process transforming the Methionine (Met) in DMSP involves transamination, reduction, methylation, and decarboxylation. DLA represents DMSP-lyase activity; Cys = Cysteine; MSA = methane sulfonate ; MSNA = methane sulfinic acid ; MMPA = methylmercaptopropionate; MeSH = methanethiol; MPA = mercaptopropionate. The percentage represents the fate of the DMS in the marine environment, are approximative and based on Vila-Costa et al. (2006), Kloster et al. (2007), Moran et al. (2012) and Galí and Simó (2015).

5 The antioxidant system

Light, temperature, and nutrient availability can be highly dynamic for aquatic and photosynthetic organisms such as microalgae. The conditions change on a spatial and temporal scale. Within these limits, the rate of light absorption has to be adjusted to meet cellular demands, which in turn depends on the nutritional status of the cell (Goss and Jacob, 2010). Nutrient status can change on timescales of days to seasons whereas changes in light availability over several orders of magnitude can occur on much shorter timescales, from seconds to hours and days (Litchman and Klausmeier, 2001; Müller et al., 2001; Jahns and Holzwarth, 2012; Erickson et al., 2015). The fluctuation of cloud formations, surface wave focusing, or vertical mixing can affect the way phytoplankton experience light intensity from complete darkness to around 2000 µmol quanta $m^{-2}s^{-1}$, both temporally and spatially throughout the day (Goss and Jacob, 2010; Huot and Babin, 2010; Ruban et al., 2012; Erickson et al., 2015).

Photosynthetic organisms have elaborated mechanisms to increase the light capture for photosynthesis when light is low; or to protect against oxidative damage caused by excess of light (Niyogi, 2017). Phytoplankton have developed three processes: adaptation, acclimation, and regulation (Huot and Babin, 2010 and citations therein). Photoadaptation includes genetic responses to adapt the organism to particular photic environments (i.e. near the surface or at depth). When the organism is experiencing a cloudy day, or light field variations, the species, adapted for this given environment, may need to change its macromolecular composition (i.e. add or remove pigments) to improve its growth or reduce the damage: it is called the photoacclimation. The latter is a phenotypic modification which involves adjustments of light and dark reactions to harvest the light (i.e. changes in the size of the PSII antennae, the size, or the number of the reaction centres, decrease in the photosynthetic pigments such as chlorophyll content (Fernandes, 2012 and citations therein)). Finally, when the cell is photoadapted to its environment, photoacclimated to its light field variations, it may need to rapidly modify its photosynthetic efficiency due to rapid changes in light fields – this is termed photoregulation. The difference with photoacclimation is that photoregulation does not require *de novo* synthesis or breakdown of molecules (Huot and Babin, 2010). On the other hand, photoprotection is normally used to describe all the mechanisms protecting the cells from photodamage including thermal dissipation (i.e. carotenoids) (Fernandes, 2012).

5.1 ROS production

With the evolution of processes such as photosynthesis or respiration, it has been established that all oxygen-metabolizing organisms produce reactive oxygen species (ROS). ROS are a group of free radicals, reactive molecules, and ions derived from molecular oxygen (O_2; Sharma et al., 2012). In natural waters, ROS are present everywhere though at very low concentrations (10^{-18} – 10^{-6} mol L^{-1}) and with a short-life span (µs-days) (Diaz and Plummer, 2018). This ROS production, within the cell, might be harmful if it is not controlled but can also, in many normal cellular functions, play a role as cellular transducer or messenger (Apel and Hirt, 2004; Lesser, 2006; Diaz and Plummer, 2018). Recently, biological ROS production might also promote growth and survival with some examples in plants, fungi, seaweeds, white blood cells, corals, or sea urchins (Apel and Hirt, 2004; Diaz and Plummer, 2018 and citations therein). Regarding phytoplankton, extracellular ROS production is implicated in the toxicity, the growth, and the iron acquisition of *Chattonella marina* while other species generate extracellular ROS for yet unknown reason (Diaz and Plummer, 2018 and citations therein). This production occurs at several major sites such as chloroplasts, mitochondria, peroxisomes, cell surfaces and the cell free environment (Apel and Hirt, 2004; Diaz and Plummer, 2018). Hereafter, only the ROS production occurring in the chloroplasts will be discussed. Light-driven processes included within the chloroplast are comprised of both energy transfer and electron transport and are then accompanied by the formation of ROS (Pospíšil, 2016).

The first pathway initiating the ROS cascade production is the leakage of electron to molecular oxygen at the acceptor site of the photosystem I (PSI) (or photosystem II (PSII)) providing the formation of the reductant superoxide radicals ($O_2^{\cdot-}$) (Fig. 1-8) (Jahns and Holzwarth, 2012). The latter could be transformed spontaneously or enzymatically to hydrogen peroxide (H_2O_2) and subsequently reduced to OH· via the Haber-Weiss/Fenton reaction in the presence of a transition metal (Mallick and Mohn, 2000; Pospíšil, 2016). ROS production in the PSII occurs due to the oxygen-evolving complex (OEC) (Fig. 1-8) or the cytochrome b559 (*cytb559*), even if this production seems to be minor compared to the PSI (Liu et al., 2004; Pospíšil, 2014). The second pathway involves the energy transfer from excited chlorophyll to molecular oxygen leading to the formation of singlet oxygen ($^1O_2^*$) (Fig. 1-8) (Jahns and Holzwarth, 2012; Pospíšil, 2016). At physiological pH, H_2O_2 might diffuse readily across membranes while the $O_2^{\cdot-}$, with a much shorter life span (~µs), does not (Lesser, 2006; Karuppanapandian et al., 2011; Sharma et al., 2012). The common feature among the different ROS is their capacity to cause

oxidative damage to deoxyribonucleic acid (DNA), lipids and proteins (Apel and Hirt, 2004; Lesser, 2006).

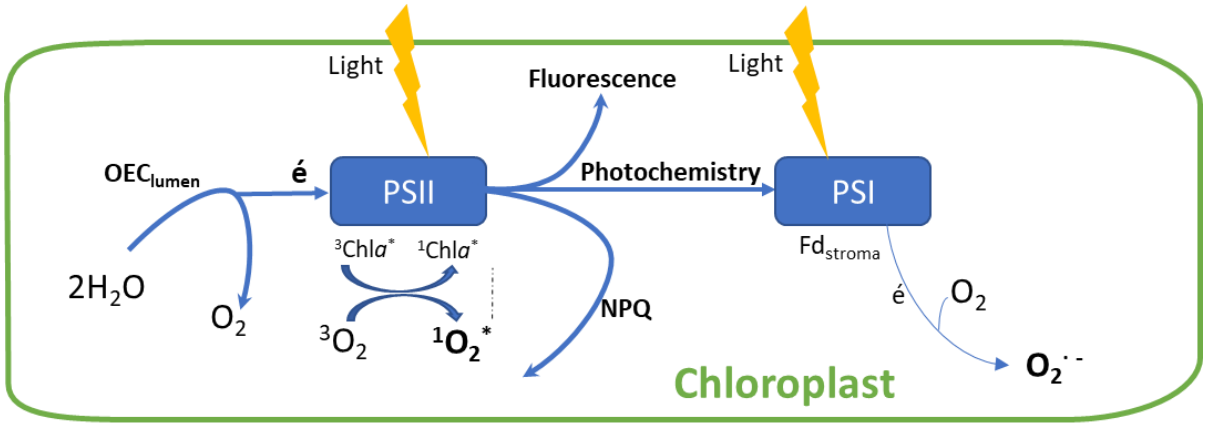

Figure 1-8: Schematic representation of the initiation of ROS production with the leakage of electron to molecular oxygen at the acceptor site of the photosystem I (PSI) (or photosystem II (PSII)) providing the formation of the superoxide radicals ($O_2^{\cdot-}$). ROS production in the PSII occurs due to the oxygen-evolving complex (OEC) or the cytochrome b559 (*cytb559*). The second pathway involves the energy transfer from excited chlorophyll to molecular oxygen leading to the formation of singlet oxygen ($^1O_2^*$). Figure based on Liu et al. (2004), Jahns and Holzwarth (2012), Pospíšil (2014) and Pospíšil (2016).

These cytotoxic properties lead to the evolution of enzymatic and non-enzymatic scavenging systems existing to decrease ROS formation or detoxicate previously formed ROS (Jahns and Holzwarth, 2012) under various and adverse environmental conditions (nutrient limitation, temperature, salinity, CO_2 limitation, UV-radiation, drought, or high light) or biotic stress such as pathogens, bacteria, or fungi (Foyer et al., 1997; Apel and Hirt, 2004; Pospíšil, 2016). The oxidative stress is so-called when the rate of ROS production exceeds the cell's ability to scavenge and convert them into non-reactive species (Apel and Hirt, 2004). Any process that restricts the metabolic efficiency and the flow of excitation energy or electrons within the photosynthetic apparatus will increase ROS production and thereby the oxidative stress within the cell (Bucciarelli and Sunda, 2003). We thus can define an antioxidant as "*any substance that, when present at low concentrations compared with those of an oxidizable substrate, significantly delays or prevents oxidation of that substrate"* (Halliwell, 1995).

5.2 High light forcing

Light-driven photosynthetic electron transport leads to the continuous production of oxygen and simultaneously its removal from the chloroplast through reduction and assimilation (Apel and Hirt, 2004). Light energy is absorbed by the photosystems and three competing pathways dominate (Fig. 1-8): (1) photochemistry (including the photosynthetic electron transfer); (2) fluorescence emission or (3) thermal dissipation (known as non-photochemical quenching) (Müller et al., 2001; Baker, 2008; Cosgrove and Borowitzka, 2010).

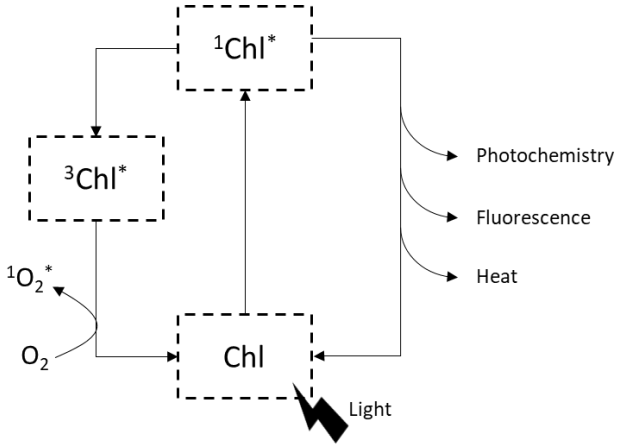

Figure 1-9: Schematic representation based on Müller et al. (2001) of the possible fate of excited Chl. When the Chl absorbs light, it becomes excited from its ground state (Chl) to the singlet excited state ($^1Chl^*$). This excited state can be used for the photosynthetic reactions (photochemistry), can be relaxed by emitting light (fluorescence) or can be de-excite by dissipating heat (non-photochemical quenching).When the photosynthetic capacity is overwhelmed, the excited state can produce the triplet excited state ($^3Chl^*$) which in turn is able to produce singlet oxygen ($^1O_2{}^*$).

When this light energy exceeds the photosynthetic capacity or the CO_2 assimilation, overreduction of the electron transport chain inactivates the PSII (Apel and Hirt, 2004) and limitation in the energy transfer and electron transport generate ROS (Pospíšil, 2016). This energy limitation occurs when light energy is not fully absorbed by the chlorophyll at the reaction centre of the PSII antennae. This provides the conditions needed for the formation of the deleterious triplet chlorophyll ($^3Chl^*$) from the singlet chlorophyll ($^1Chl^*$) (Fig. 1-9) (Müller et al., 2001; Pospíšil, 2016). To prevent this, the chlorophyll is coupled with carotenoids. In the PSII antennae, the carotenoids are mainly composed by xanthophyll that might prevent the formation of this triplet by the quenching of singlet chlorophyll to heat as well as indirectly by the rearrangement of the light harvesting complex (LHC) proteins (Krieger-Liszkay, 2004; Ruban et al., 2012). When this scavenging system is not sufficient, energy from the conversion in triplet chlorophyll is transferred to O_2 forming the singlet oxygen $^1O_2{}^*$ (Fig. 1-9) (Krieger-Liszkay, 2004; Ruban et al., 2012; Erickson et al., 2015; Pospíšil, 2016). With this limitation on the electron transport at the PSII, the cascade electron transfer needed for further oxidation is blocked. Under this condition and at the PSI, the Mehler reaction leads to electron leakage from ferredoxin (Fd) to O_2 forming $O_2^{\cdot-}$ (Apel and Hirt, 2004; Sharma et al., 2012; Pospíšil, 2016). $O_2^{\cdot-}$ is spontaneously and enzymatically dismutated to H_2O_2 by the superoxide dismutase (SOD) (Fig. 1-10) (Apel and Hirt, 2004; Pospíšil, 2016). The $O_2^{\cdot-}$ is eliminated inside the thylakoid membrane by the intrinsic superoxide oxidoreductase activity of the *cytb*$_{559}$. When the $O_2^{\cdot-}$ diffused out of the membrane, it is the ferredoxin SOD (FdSOD) attached to the stroma side of the thylakoid membrane that dismutates it to H_2O_2 (Pospíšil, 2016). The incomplete H_2O oxidation with the limitation of electron transport also results in the H_2O_2 production. The

hydrogen peroxide is normally eliminated properly into H_2O by catalase or peroxidase enzymes (Fig. 1-10) (Ascorbate peroxidase (APX) – Catalase (CAT) – Glutathione peroxidase (GPX)) (Asada, 2006). Otherwise, the H_2O_2 is the precursor of OH· formed by the Haber-Weiss/Fenton reactions catalysed by iron (Fe), manganese (Mn), or copper (Cu) (Fig. 1-10) (Apel and Hirt, 2004; Pospíšil, 2016).

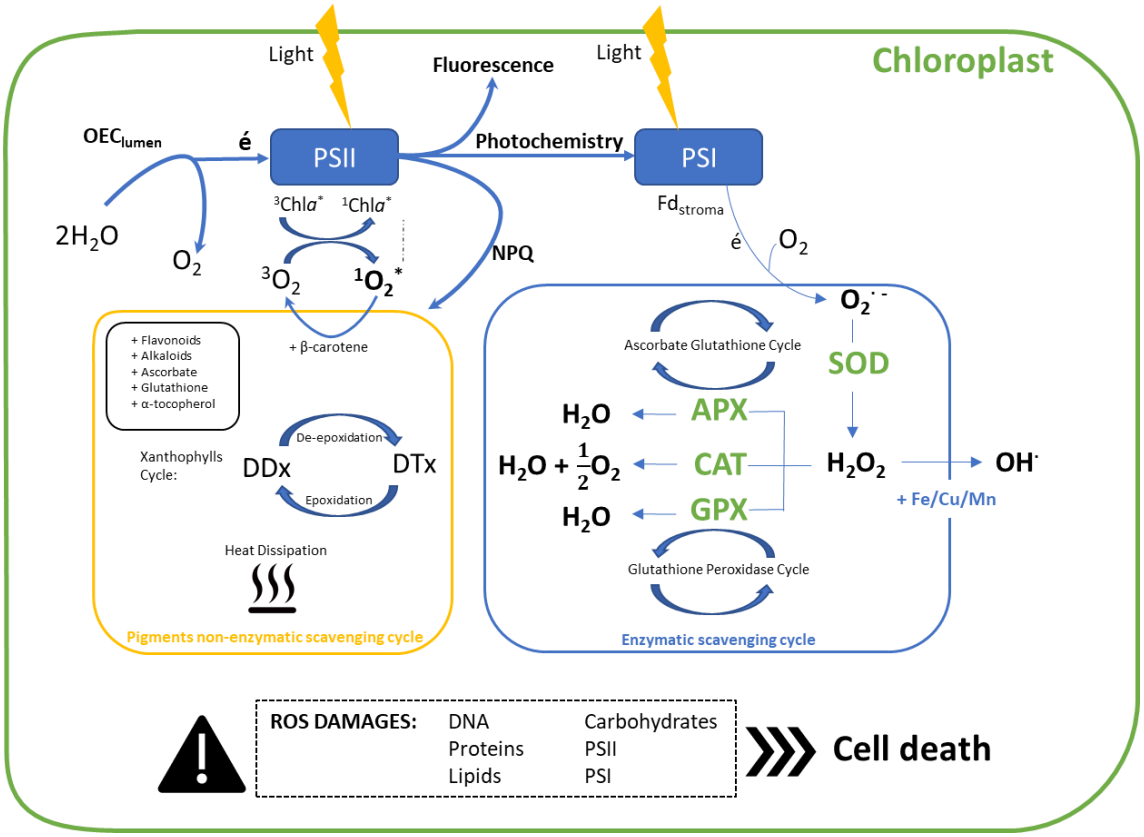

Figure 1-10: Schematic representation based on Asada (2006), Apel and Hirt (2004), Sharma et al. (2012), Pospíšil (2016) of the enzymatic and non-enzymatic system involved in the scavenging of ROS previously produced. The pigment non-enzymatic cycle is schematic and involved various pigments with their own recycling cycle. The non-enzymatic system also involves small molecules such as the DMS(P,O) cycle explained further.

Besides the enzymatic antioxidants described previously, non-enzymatic antioxidants include major cellular redox buffers ascorbate and glutathione (GSH), as well as α-tocopherol, flavonoids, alkaloids, and carotenoids (Fig. 1-10) (Dummermuth et al., 2003; Lesser, 2006). The latter has two functions regarding the photosynthetic system within the cell : (1) with the absorption of light energy and its transfer to chlorophyll molecules to be used in photochemical reactions and (2) the photoprotection of reaction centres and pigment-protein antennae (Ston and Kosakowska, 2000; Telfer, 2002; Strychar and Sammarco, 2011 and citations therein). β-carotene, a carotenoid pigment, operate at PSI and PSII, scavenging predominantly the $^1O_2{}^*$ while the xanthophylls, already cited previously, operate within the PSII (Govindjee and Govindjee, 1974). Short-term acclimation mechanisms include photochemical quenching (PQ) related to fraction of open (oxidised) reactions centres in PSII (Genty et al., 1989) and non-

photochemical quenching (NPQ) of chlorophyll fluorescence related to photoprotective carotenoids, the distribution of excitation energy between the two photosystems, and damages and repairs of PSII (Falkowski and Chen, 2003). NPQ is the most important system for a sudden increase in high light (HL) and can be measured by the decrease in the Chl-*a* fluorescence intensity (Müller et al., 2001). Photoprotective dissipation is also attributed to rapid modifications within the LHC of PSII, leading to non-photochemical Chl-*a* fluorescence quenching (Lavaud et al., 2004). Due to this excess light, the carotenoids play a central role in the deactivation of excited molecules $^{3}Chl^{*}$ and $^{1}O_{2}^{*}$ at PSII, and the reduction of ROS formation due to the thermal dissipation of excess light energy at the level of $^{1}Chl^{*}$ (Jahns and Holzwarth, 2012). Harmful excess energy is dissipated as heat radiation, the deactivation of $^{1}O_{2}^{*}$ is provided by β-carotene (Telfer, 2002) (or α-tocopherol (Krieger-Liszkay, 2004)) and NPQ is modulated by the de-epoxidation of the xanthophylls (Fig. 1-10) (Lavaud et al., 2004; Huot and Babin, 2010; Jahns and Holzwarth, 2012). The main xanthophyll cycle in the diatoms and most eukaryotic algae (Müller et al., 2001; Goss and Jacob, 2010) include the diadinoxanthin (DDx), with low light energy transfer efficiency, that can be converted to diatoxanthin (DTx) under conditions of HL (Fig. 1-10) (Brunet et al., 2011). The reaction is reversed under low light intensities or in darkness (Goss and Jacob, 2010).

In long-term acclimation responses, the cell can adjust the amount and ratio of light harvesting pigments (LHPs: Chl-*c* and Fucoxanthin (Fuco)) and alter the size of the photosynthetic unit (PSU), changing the maximum photosynthetic capacity of the organism (Nymark et al., 2009). At HL, acclimated-cells generally have low LHP content and high amounts of photoprotective carotenoids (Nymark et al., 2009 and citations therein). Other small molecules have been described as antioxidants such as uric acid or DMS (Lesser, 2006) with a hypothetical cascade chain reaction beginning with DMSP and DMSO (Sunda et al., 2002).

5.3 Cascade chain reaction with DMS(P,O)

The first hypothetical link between DMSP and light intensity or day length was addressed by Karsten et al. (1990). They investigated the DMSP cellular content of five benthic Chlorophyceae for one year at three different light intensities under day length conditions of their natural habitat. They observed higher DMSP concentration under long day conditions and higher light intensity. Matrai et al. (1995) also observed that the DMS(P):Chl-*a* ratio by *Phaeocystis sp.* showed a hyperbolic response to irradiance.

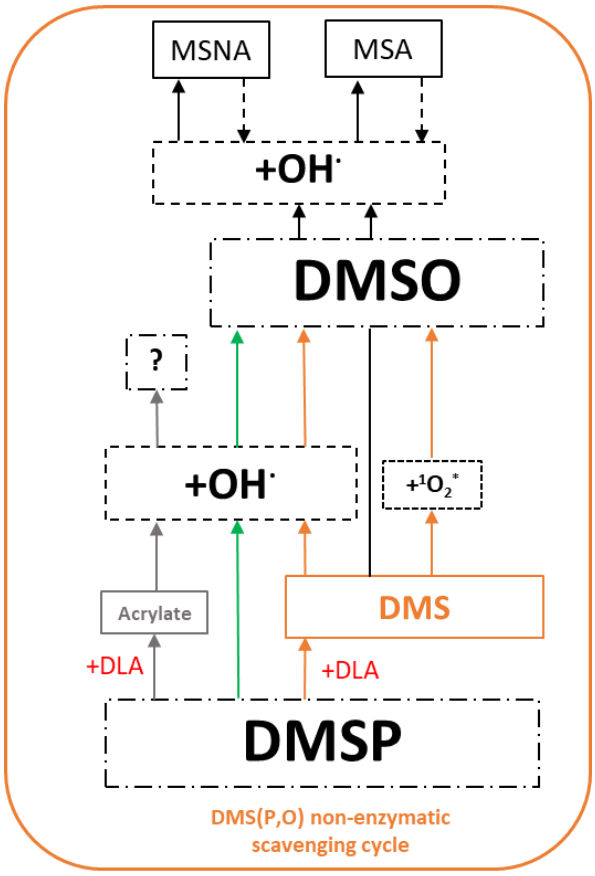

Figure 1-11: Schematic representation based on Sunda et al. (2002) and Spiese et al. (2009) of the reactions involving dimethylsulfide (DMS), dimethylsulfoniopropionate (DMSP) and dimethylsulfoxide (DMSO) and its breakdown products acrylate, methane sulfonate (MSA) and methane sulfinic acid (MSNA), thanks to the DMSP-lyase activity (DLA) or reactive oxygen species such as singlet oxygen ($^1O_2$), hydroxyl radical (OH·). The colour of each arrow follows each potential pathway.

More recently, Sunda et al. (2002) have shown that DMSP might react with the hydroxyl radical (OH·), scavenging one of the most reactive ROS. This reaction leads to the production of DMS and acrylate, more effective for scavenging ROS, as are the DMS oxidation products DMSO and MSNA (Fig. 1-11) (Scaduto, 1995; Sunda et al., 2002). Taken together, these molecules might be even more effective of scavenging OH· than the well-known ascorbate or glutathione (Sunda et al., 2002). Moreover, the DMSP might be lysed to DMS and acrylate thanks to DL activity (Fig. 1-11) (Sunda et al., 2002) present in the Prymnesiophyceae and dinoflagellates, high-DMSP producers (Keller et al., 1989). DMS can also react with singlet oxygen (Wilkinson et al., 1995) to form DMSO (Fig. 1-11). DMSP and acrylate cannot diffuse across membranes since they are charged at physiological pH while DMS does. This difference in diffusion properties can improve the antioxidant system in both aqueous and lipid membranes phases within the cell (Sunda et al., 2002). If DMS does not react with ROS, the remaining DMS will diffuse across the membrane while the DMSO, produced from the OH· oxidation of DMS or DMSP (Fig. 1-11), is more hydrophilic and will accumulate at high cellular concentrations (Simó et al., 1998, 2000). These observations were experimented with *Emiliania huxleyi* and

Thalassiosira pseudonana under CO_2 and Fe limitation, UV-radiation, Cu^{2+} and H_2O_2 exposures (see Sunda et al., 2002 for more information). Bucciarelli and Sunda (2003) experienced a similar upregulation in cellular DMSP of *T. pseudonana* under NO_3, PO_4, $Si(OH)_4$ and CO_2 limitation. An increase in the DMSP to carbon ratio under Fe limitation was also observed in the Antarctic Prymnesiophyceae *Phaeocystis sp.* (Stefels and van Leeuwe, 1998). Micro- and macroalgae have experienced an increase in their DMSP content when exposed to high light and UV irradiances (Karsten et al., 1992; Stefels and van Leeuwe, 1998; Darroch et al., 2015). The exogenous addition of DMSP and acrylate on plant leaves also protects them of oxidative damage (Husband et al., 2012). The DMS(P,O) antioxidant hypothesis is in line with their production site located in the chloroplast (Trossat et al., 1998; Raina et al., 2017; Curson et al., 2018). The figure 1-12 considers all the previous statements regarding the cell's response to have a general overview of the antioxidant response.

This antioxidant system theory is further supported by the increase in DMS:Chl-*a* ratios due to the oxidative stress induced by solar radiation (Sunda et al., 2002). This idea is in line with the CLAW hypothesis : DMS released by the activation of the DMS(P,O) antioxidant system would act as a negative feedback mechanism on high light and UV oxidative stress by enhancing cloud albedo and thereby decreasing incoming solar radiation (Fig. 1-2a) (Sunda et al., 2002). This hypothesis is also supported by correlations between (seasonal) variations in DMS concentrations and local solar irradiance, UV radiation or the average radiation in the surface mixed layer, which is the solar radiation dose (SRD) that phytoplankton experience (Toole and Siegel, 2004; Vallina and Simó, 2007; Miles et al., 2009; Galí et al., 2011; 2013; Lizotte et al., 2012; Lana et al., 2012). Lana et al. (2012) showed that the climatological calculation used for SRD, the use of data grouping and binning as well as the use of different DMS climatologies will impact the proportionality between DMS and SRD. Nevertheless, DMS and light were significantly correlated even using exclusively in situ data of irradiance and light attenuation to calculate SRD ($R^2 > 0.80$, Vallina and Simó, 2007; Miles et al., 2009). In addition, Levine et al. (2012) found that the potential DMS production through the algal fraction (> 1.2 µm) was associated to radiation dose at 340 nm in the upper mixed layer. Galí et al. (2011; 2013) also confirmed that sunlight modulates DMS concentration since they observed an increase in gross DMS production with exposure to solar radiation, UV included.

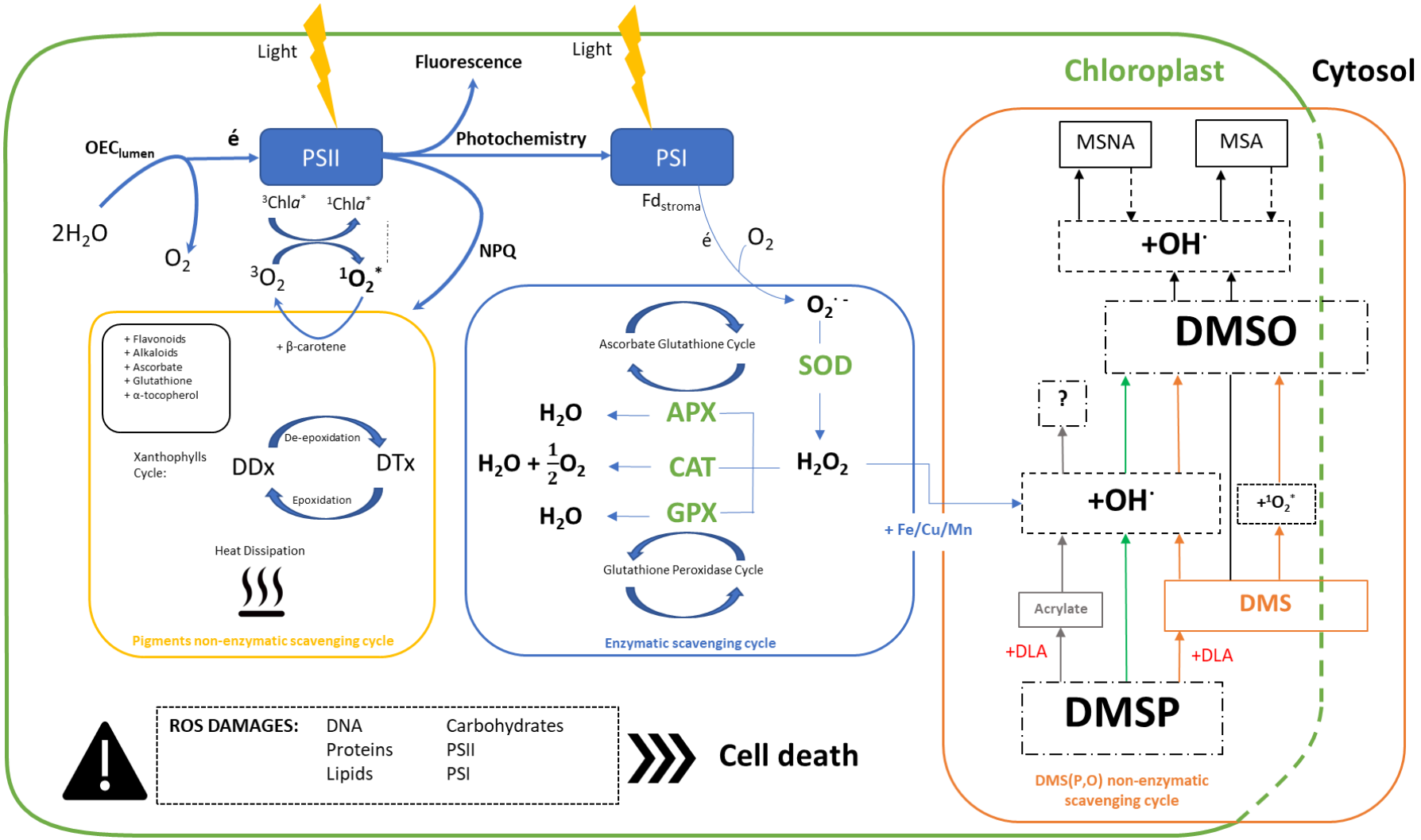

Figure 1-12: Schematic representation of the cellular site of the oxygen production (via the OEC: Oxygen-Evolving Complex) and of the reactive oxygen species (ROS) production at the photosystem I (PSI) and photosystem II (PSII) with the three possibilities of photochemistry, fluorescence or non-photochemical quenching (NPQ); in blue: the enzymatic scavenging cycle (SOD: Superoxide Dismutase; APX: Ascorbate Peroxidase; CAT: Catalase; GPX: Glutathione Peroxidase); in orange the DMS(P,O) non-enzymatic system including the dimethylsulfoniopropionate (DMSP)-dimethylsulfoxide (DMSO)-dimethylsulfide (DMS)-Acrylate with the presence of the DMSP-lyase (DL) activity and the oxidation products Methane Sulfinic Acid (MSNA) and methane sulfonate (MSA); in yellow the pigments non-enzymatic cycle representing the β-carotene and the Xanthophylls cycle (DDx: Diadinoxanthin; DTx: Diatoxanthin) to scavenge the excess of energy as heat dissipation; and the ROS production effect of the Menadone Bisulfite (MSB), DCMU and High Light (HL) added for the oxidative stress experiments; as well as the possible damages to DNA, Proteins and Lipids in case of this ROS production exceeds the ability of the organism to scavenge it.

Nevertheless, it has been suggested that the solar radiation enhancement of DMS may be also related to the inhibition of bacterial activity (~48% of suppression in bacterial growth was due to UV-B radiation and ~40% caused by PAR+UV-A; Herndl et al., 1993). In addition, Deschaseaux et al. (2014) observed a correlation between DMS(P,O) concentrations and direct sunlight. The DL activity has been shown to correlate with radiative stress conditions (Bell et al., 2007; Harada et al., 2004) while it might also decrease under high PAR and UV (Darroch et al., 2015). For any given exposure to irradiance, each phytoplankton population will contribute to the DMS production through the overflow, antioxidant, or damage mechanisms, depending on their sunlight sensitivity, their photoprotection strategies and their DMSP-cleaving capacity (Galí et al., 2013). In addition, DMS(P,O) and DL activity are often significantly correlated with algal photoprotective pigments in seawater (Belviso et al., 2001; Steinke et al., 2002; Harada et al, 2004; Riseman and DiTullio, 2004; Bell et al., 2010). Without excluding the potential reaction between DMSP and ROS, Archer et al. (2018) indicate that DMSP production on a diel timescale is not linked to photooxidative stress in natural communities. The DMSP production was generally inhibited in PAR+UV treatment compared to the photoprotective xanthophylls that were enhanced by 60-200%. The debate is still open since the physiological reactions between DMS(P,O) and the ROS production differ depending on the methodology used, the studied microorganisms, or the natural community observed.

The "DMS summer paradox", so called after high DMS concentration in summer coupled with low Chl-*a* in some part of the globe (Simó and Pedrós-Alió, 1999), could also be explained thanks to the understanding of the microbial food web and the antioxidant function. During the summer, the increase in solar inputs due to longer days and higher solar intensity, coupled with the thermal stratification of the seawater, will simultaneously lead to increased nutrient limitation with lower supply coming from deeper waters, and solar exposure (Sunda et al., 2007). Five mechanisms could explain the higher DMS concentration encountered (Fig. 1-13): (1) The photoinhibitory effect of UV on bacterial activity leads to the decrease (>90%) in the biological DMS(P) consumption (Slezak et al., 2001; Toole et al., 2006; Slezak et al., 2007) and simultaneously, (2) since the demand for bacterial sulfur is reduced, more consumed $DMSP_d$ is diverted to the bacterial cleavage pathway leading to DMS production (Slezak et al., 2007); (3) the high light and UV damage on phytoplankton cells could increase the cell lysis increasing the potential DL activity (Simó et al., 2018) while the zooplankton grazing rate is lower during summer and is then not responsible for the elevated rates of biological DMS release (Toole and Siegel, 2004); (4) nutrient limitation can lead to an oxidative stress

promoting DMS(P) production (Bucciarelli and Sunda, 2003; Harada et al., 2004; Sunda et al., 2007); (5) phytoplankton DMS(P) production is enhanced due to greater exposure to irradiance (Sunda et al., 2002) and have to be higher than the DMS photolysis that is promoted under UV radiation (Toole et al., 2006). However, the photooxidation of DMS depends upon the presence of chromophoric dissolved organic matter (CDOM) which is at the lowest concentrations at the summer (Siegel and Michaels, 1996). All this previous argument are apparently sufficient to overcome the negative effect of lower algal biomass during the summer, which would otherwise restrict DMS production (Sunda et al., 2007).

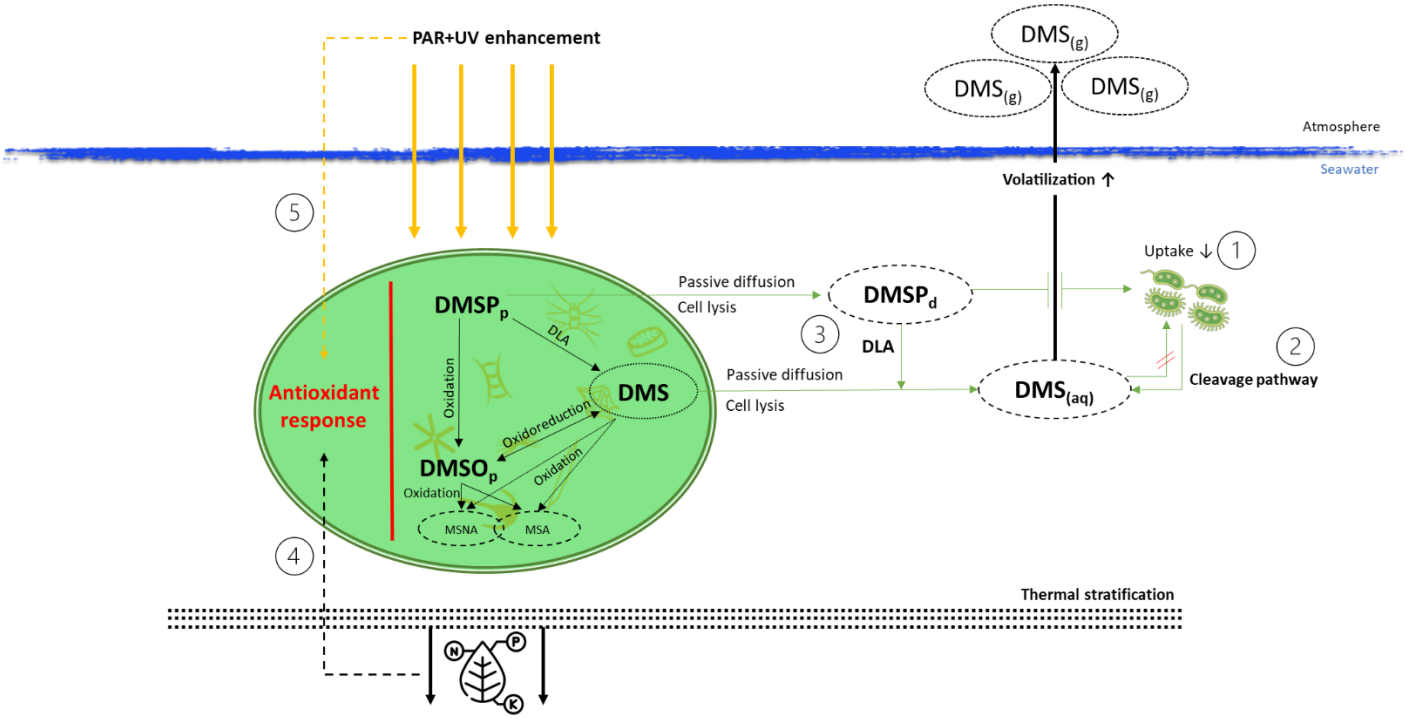

Figure 1-13: Schematic representation of the "DMS summer paradox" explained by (1) the photoinhibitory effect on the bacterial $DMSP_d$ uptake while (2) the cleavage pathway are promoted; (3) the PAR+UV enhancement promotes the cell lysis and the mixing of the DMSP lyases with its substrate during the physical degradation; (4) the nutrient limitation and (5) the higher PAR+UV due to the thermal stratification promote an oxidative stress within the phytoplankton cell, increasing the DMS(P) production.

5.4 Physiological impact of ROS formation

Under severe stress such as high light, when ROS concentration exceeds the cell's capability to scavenge them, PSII proteins and lipids might be oxidised and damaged by ROS (Aro et al., 1993). Nevertheless, at low level, ROS could serve as signalling molecules leading to an acclimation response or cell death (Apel and Hirt, 2004). Due to high light doses or high temperature, ROS might be transmitting a signal from the chloroplast to the nucleus through products of protein oxidation or lipid peroxidation (Fischer et al., 2012 and citations therein). ROS might also change gene expression by targeting and modifying the activity of transcription

factors (Apel and Hirt, 2004). The production of ROS might also be genetically programmed, inducing complex downstream effects on both primary and secondary metabolism (Foyer and Noctor, 2005). Erickson et al. (2015) already demonstrated the role of $^1O_2$ to signal the nucleus to turn on defence mechanisms to minimize its deleterious effects. Thanks to its relative stability and its diffusion over large distances within the cell, H_2O_2 also might be a signal molecule (Sharma et al., 2012). It regulates expression of genes by the activation of proteins signalling pathways associated as well to the acclimation or program cell death (Pospíšil, 2016 and citations therein). More recently, it has been demonstrated that the H_2O_2 formed in the thylakoid membrane leads to the regulation of the PSII antennae size during the acclimation responses (Borisova-Mubarakshina et al., 2015).

Lipid peroxidation (LPO) is one of the cellular damages that might produce ROS. It is initiated by $^1O_2$ and OH· and produces lipid hydroperoxides (LOOH) which decompose to secondary lipid peroxidation products, lipid hydroxides (LOH). Lipid hydroperoxide is stable but might be oxidised or reduced to lipid peroxyl radical (LOO·) or alkoxyl radical (LO·) that could lead to high energy intermediates, which is highly unstable and might transfer, via its decomposition to triplet excited carbonyls ($^3L^*$), its energy to O_2 to form $^1O_2$. Yadav and Pospíšil (2012) already have shown evidence that $^1O_2$ is produced through lipid peroxidation under light stress. Nevertheless, the amount of $^1O_2$ produced is considerably lower than from triplet chlorophyll (Pospíšil, 2016), but could aggravate the oxidative stress with new damage to proteins or DNA (Sharma et al., 2012).

6 Study cases for batch monoculture

6.1 Diatoms - *Skeletonema costatum*

Diatoms are a major component of the phytoplankton community (Sarthou et al., 2005). The diatoms are unicellular but can sometimes form colonial forms. They are classified as centric if their symmetry is radial, or pennate if it is bilateral. They are present in a wide distribution in all kinds of habitats in fresh or marine waters (Fritsch, 1971), even in the brine channels of sea ice (Trevena et al., 2000). They are responsible of 40% of the global oceanic primary production and therefore play an important roles in natural cycles (Sarthou et al., 2005 and citations therein). Diatoms can also rapidly sink from the upper ocean to deep waters, dominating the export production of carbon and silica (Sarthou et al., 2005). The micro-architectural complexity of their silicified cell-walls make diatoms remarkable and fascinating. This wall (or frustule) is composed of two, usually equal halves, the older (epitheca) fitting closely over the

younger (hypotheca). This thick siliceous envelope shuts off the cell from the environment but admits gaseous diffusion and osmotic exchange in thin areas, or even by direct apertures (i.e. pores) communicating with the exterior (Fritsch, 1971). Characterized by a low surface:volume ratio, the diatoms generally grow in natural high-nutrient concentrations and dominate the phytoplankton efflorescence in spring till silicate becomes limited (Sarthou et al. 2005). The diatom life cycle is presented and described at the figure 1-14. This life cycle is unique because of the presence of the rigid silicate cell wall and the size reduction at each vegetative step.

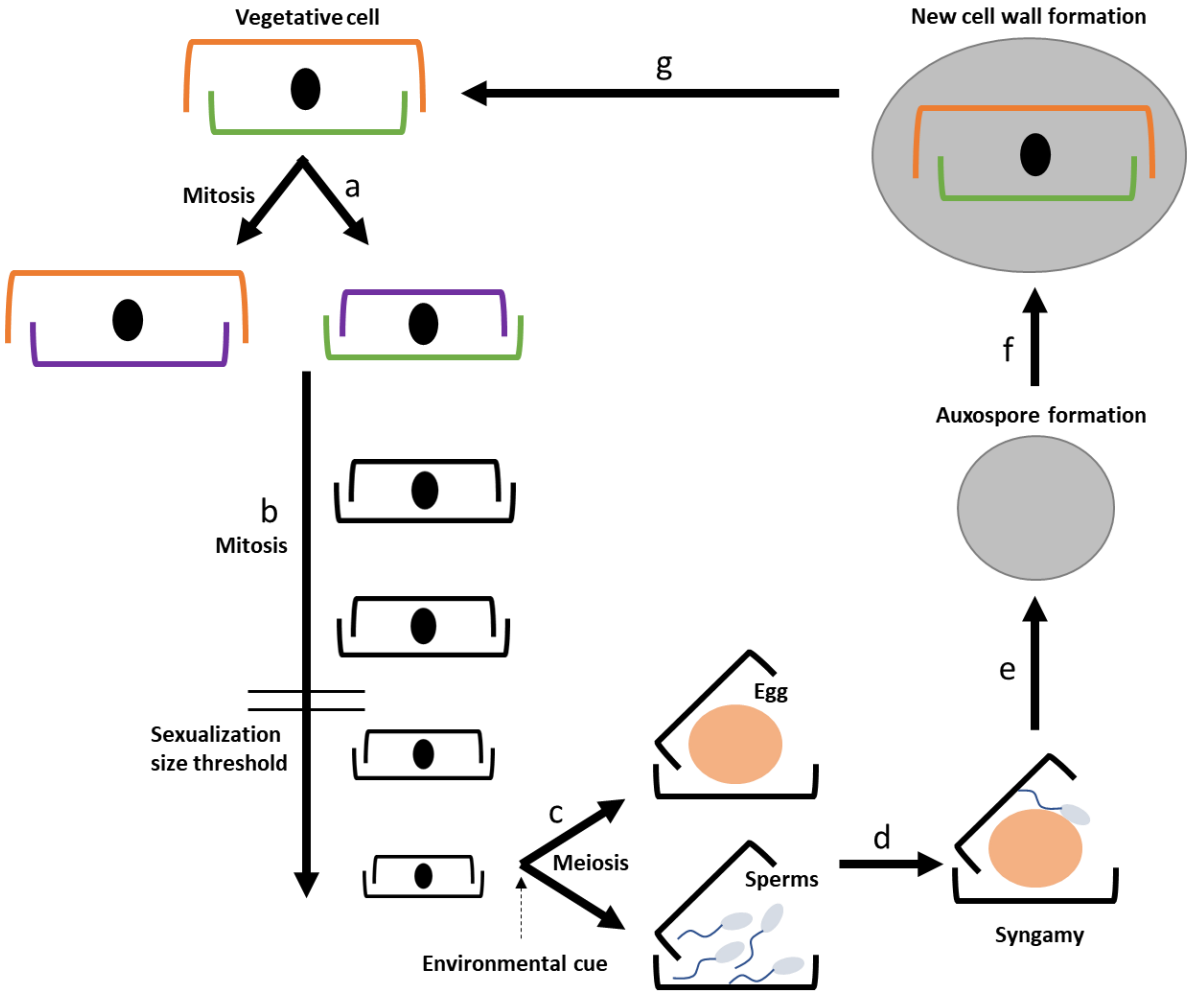

Figure 1-14: Schematic representation of the life cycle of a centric diatom: (a) the vegetative cell divides mitotically and produces two cells that inherit one of the two halves (thecae) of the rigid cell wall (orange and green line) and build a new smaller one (purple line). (b) This vegetative cell reproduction leads to a progressive reduction of the cell size of the cell population. Above a species-specific sexualisation size threshold, the cells are incapable of sexual reproduction. Below this threshold and if a proper trigger is present (i.e. salinity shock), meiosis is induced and produces egg and sperms. (d) The gametes conjugation (syngamy) leads to the formation of a zygote that (e) becomes an auxospore, a soft stage which can expand. (f) The new cell walls are built inside the auxospore, which (g) eventually becomes the initial vegetative cell. Representation based on Kaczmarska et al. (2013) and Ferrante et al. (2019).

Skeletonema costatum is a centric diatom characterized by cylindrical cells with a diameter between 2 to 21 µm. The colonial form is made up of individuals joined by the poles thanks to several silicified processes in long, straight, or slightly undulate chains. This species is present

in coastal waters and might bloom seasonally in spring and fall (Hoppenrath et al., 2009). Regarding DMS(P,O) production, the diatoms are considered as low-DMSP producers since they are characterized by a $DMSP_p$:Chl-*a* ratio of 4 ± 6 mmolS:g Chl*a* (Stefels et al., 2007). Nevertheless, $DMSP_p$:Chl-*a* ratio of the diatom *S. costatum* is higher and can be very different from 8.3 to 35.3 mmolS:g Chl-*a* (Table 1-1) (Speeckaert et al., 2018; McParland and Levine, 2019). We only found one published data to recalculate the $DMSO_p$:Chl-*a* ratio of *S. costatum* that was very low with 0.03 mmolS:g Chl-*a* (Table 1-1)

Table 1-1: Resume of the $DMSP_p$:Chl-*a* and $DMSO_p$:Chl-*a* ratio found from the published data available for the species *S. costatum*, *P. globosa* and *H. triquetra*.

Class	Class	Genus	Species	$DMSP_p$:Chla (mmol:g)	$DMSO_p$:Chl-*a* (mmol:g)	Data from
Diatom	Diatom	*Skeletonema*	*S. costatum*	**35.3**		1
Diatom	Diatom	*Skeletonema*	*S. costatum*	**8.3**		2
Diatom	Diatom	*Skeletonema*	*S. costatum*		**0.03**	3
Dinophyceae	Dinophyceae	*Heterocapsa*	*H. triquetra*	**98.8**		4
Dinophyceae	Dinophyceae	*Heterocapsa*	*H. triquetra*	**153.7**	**8.6**	5
Prymnesiophyceae	Prymnesiophyceae	*Phaeocystis*	*P. globosa*	**78.4**		2
Prymnesiophyceae	Prymnesiophyceae	*Phaeocystis*	*P. globosa*	**95.2**		1
Prymnesiophyceae	Prymnesiophyceae	*Phaeocystis*	*P. globosa*		**1.2**	6
Prymnesiophyceae	Prymnesiophyceae	*Phaeocystis*	*P. globosa*	**73.3**	**1.3**	5
Prymnesiophyceae	Prymnesiophyceae	*Phaeocystis*	*P. globosa*		**0.5**	3

1. Speeckaert et al. (2018); 2. McParland and Levine (2019); 3. Hatton and Wilson (2007); 4. Niki et al. (2000); 5. Speeckaert et al. (2019); 6. Simó et al. (1998)

6.2 Prymnesiophyceae - *Phaeocystis globosa*

The phytoplankton group Prymnesiophyceae (or Haptophyte) concerns *only* 300 different known species. They are important to primary production, the structure of the food chain and also for sedimentary rock formation. Their most important accessory pigment is fucoxanthin (Hoppenrath et al., 2009). This class is also known to produce DMSP with the two representatives *E. huxleyi* and *Phaeocystis* sp. that we already cited previously. They are also studied due to their capacity to form monospecific and large-scale blooms in the North Atlantic, Arctic, and Antarctic ocean (Caruana and Malin, 2014). This phytoplankton group includes Harmful Algal Bloom (HAB - rapid proliferation and/or high biomass accumulation of toxic or otherwise noxious microalgae; Anderson et al., 2012) species, either ichthyotoxic such as *Chrysochromulina* sp., *Prymnesium* sp. or high biomass forming species such as *Phaeocystis* sp. The latter can form colonies with mucilaginous matrix in the Barents Sea, Norwegian fjords, the Southern Ocean, and coastal waters of the North Sea (Lancelot et al., 1998). The harmful effect of the bloom is related to the deposition of thick layers of odorous foam on the beaches, thus affecting tourism and recreational activities, but are also responsible of clogging fishing

nets, repulsing fish, and probably having negative impacts on benthic life (Rousseau et al., 2000). In the Belgian Coastal Zone discussed in the next section, *Phaeocystis globosa* occurs as a single spring event lasting between 4 – 13 weeks and representing some 70% of the spring net primary production (Rousseau et al., 2000; Breton et al., 2006). This high biomass is related to its ability to form gelatinous colonies containing thousands of cells and making them unpalatable to the mesozooplankton. If turbulent conditions co-occur with the bloom, the colony matrix (polysaccharides) is whipped into a soapy foam that regularly accumulates on beaches along the coast (Rousseau et al., 2000).

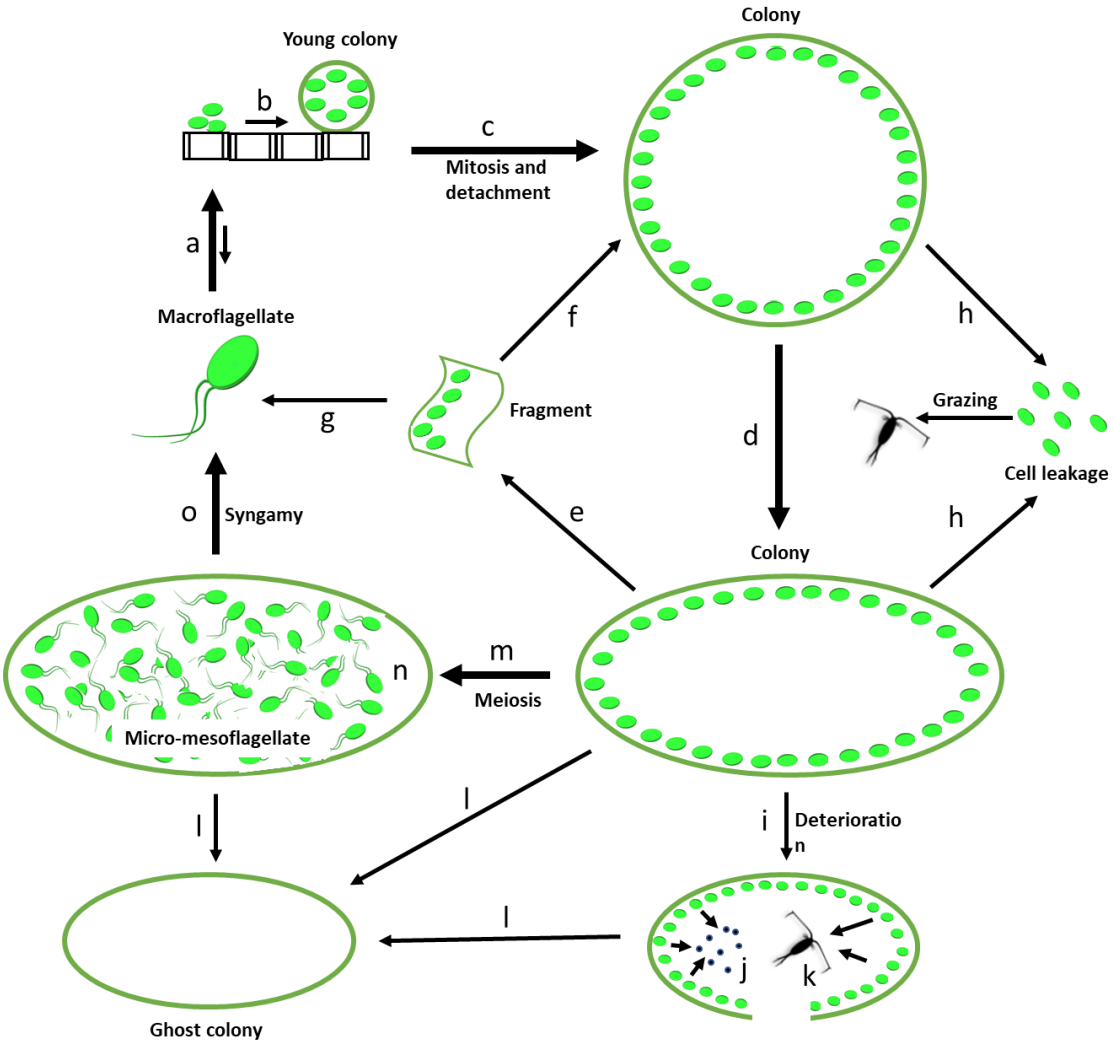

Figure 1-15: *P. globosa* haploid-diploid life cycle. The syngamy of two haploid micro or mesoflagellates cells produces the diploid macroflagellate that (a) can aggregate on a substrate (i.e. diatoms) and (b) grow to form a young colony. Under high turbulence, the young colony can return to single cells. (c) The colony size increases to finally detach from the substrate. (d) The spherical colony can change to a prolate spheroid. Under high turbulence, the colony can be split and (e) form fragments which will produce (f) a new colony or (g) furnish the pool of macroflagellates. Cells from the colony can leak from the colony and (h) are grazed by the microzooplankton. (i) At the end of the bloom, when the daily irradiance increase and the nutrient are depleted, the colony begins to deteriorate with (j) the cell lysis inside the colony and (k) cells are grazed by intruding microzooplankton. (m) At low irradiance and during sedimentation, the colony performs meiosis to form (n) new meso- or microflagellates. (o) The haploid cells might escape and perform the syngamy to produce the diploid macroflagellate. Representation based on Rousseau et al. (2007) and Peperzak and Gäbler-Schwarz (2012).

It has a complex life cycle consisting of three different flagellates and one non-motile cell stage embedded in carbohydrate matrix-forming colonies of different size and forms (Fig. 1-15). Briefly, the cycle can begin with (a) a diploid macroflagellate attaches to a solid substrate and from there (b) into a colony with diploid nonflagellate cells - The transition between the young colony and the macroflagellate is reversible under high turbulence; (c) The colony detaches of the substrate and grows (mitosis), with (d) eventually changes from a spherical to a prolate spheroid - Environmental factors influence the colony development (i.e. daily irradiance, nutrient such as vitamin B1, or zooplankton exudates); (e) With high turbulence, the colony fragments and (f) forms new colonies or (g) the colony cells transform intro macroflagellates; (h) Cells leaking from the colony are grazed by microzooplankton; (i) When the daily irradiance is high and the nutrients low, the colony begin to deteriorate with (j) cell lysis inside the colony, and (k) cells are grazed by intruding microzooplankton (l) until a "ghost" colony remains. When both the irradiance and nutrients are low, due to (m) sedimentation to the seafloor, (n) haploid micro- and mesoflagellates are formed (meiosis), (o) might escape the colony, and perform syngamy producing the diploid macroflagellate (Rousseau et al., 2007; Peperzak and Gäbler-Schwarz, 2012).

Stefels et al. (2007) calculated for the Prymnesiophyceae a $DMSP_p$:Chl-*a* ratio of 52 ± 37 mmolS:g Chl-*a*. *P. globosa* is characterized by a $DMSP_p$:Ch-*a* ratio varying from 73.3 to 95.2 (82.3 ± 11.5) mmolS:g Chl-*a* (Table 1-1). The $DMSO_p$:Chl-*a* ratio was lower with an average of 1.0 ± 0.4 mmolS:g Chl-*a* (Table 1-1).

6.3 Dinoflagellates - *Heterocapsa triquetra*

The dinoflagellates comprise more than 2000 species and are found in the most aquatic environments worldwide, including both photosynthetic, heterotrophic and mixotrophic species (Caruana, 2010). They play an important role as plankton organisms both in sea and fresh waters (Fritsch, 1971). They are mostly unicellular but rare species are filamentous or able to form chains (i.e. *Alexandrium*) (Caruana, 2010). Cellular sizes vary between 20 to 200 µm with minima and extrema of 3 µm and 2 mm. The best-known species might be the genus *Symbodinium* that lives in symbiosis with scleractinian corals (Goodson et al., 2001). They are characterized by "naked" or "armoured" form, where the first is more oceanic while the second concerns neritic plankton (Fritsch, 1971). The armoured form involves a thecae composed of a cellulose plate beneath the cellular membrane, providing a rigid structure and the diversity of this class (Fritsch, 1971; Caruana, 2010). The dinoflagellates include motile unicells but also a

sedentary phase and has a complex life cycle (Fig. 1-16). Motile individuals feature two flagella arising close together but different in structure and orientation (Fritsch, 1971; Caruana, 2010). This mobility confers the advantage to perform diel vertical migration in calm waters: migrating to the surface during the day to capture light and to deeper waters where nutrients may be more available during the night (Raven and Richardson, 1984).

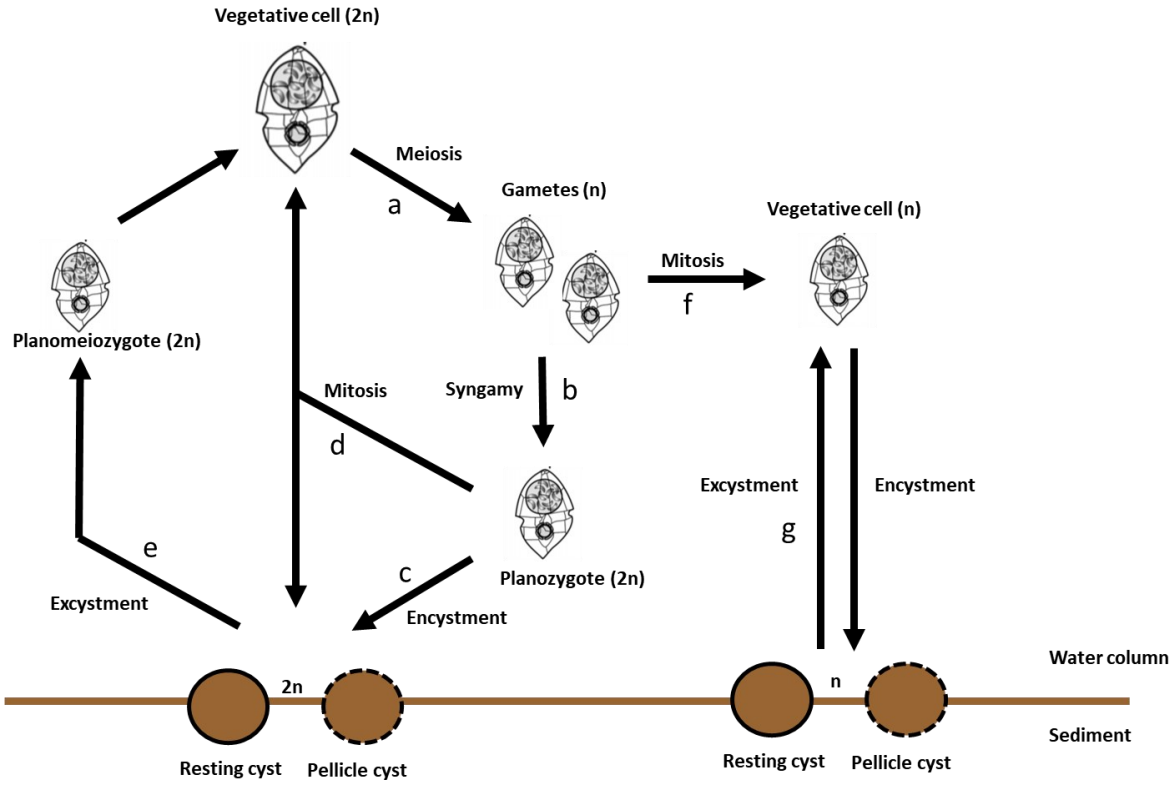

Figure 1-16: Schematic diagram of a dinoflagellate life cycle including the cyst formation. More than 10% of the 2000 known species produce cysts as part of their life cycle. The cyst remains in the sediment during unfavourable conditions for vegetative growth. The vegetative diploid cell triggers (a) the meiosis to produce haploid gametes. (b) The fusion of two haploid gametes forms the diploid planozygote that (c) eventually form cysts, also called hypnozygote. The excystment is subject to endogenous (maturation minimum period or dormancy) and exogenous (favourable environmental parameters) controls. The pellicle cyst is characterized by thin-wall and has no dormancy. (d) The mitosis of the planozygote produces diploid vegetative cells. (e) The excystment of the diploid cyst produce the planomeiozygote leading to the vegetative cell. (f) The haploid gametes can also have a vegetative life cycle and (g) endures the en- and excystment. Representation based on Iwataki et al. (2008) and Bravo and Figueroa (2014).

Dinoflagellates were highlighted in the earliest research on DMS(P) as high-DMS(P) producers. They were used as a model class to various studies including the DL activity or the biosynthesis pathway of DMSP production (Caruana and Malin, 2014 and citations therein). It is assumed that dinoflagellates are one of the most significant groups in term of DMSP production (Keller et al., 1989; Stefels et al., 2007; McParland and Levine, 2019). Nevertheless, this idea hides the high variability within this phytoplankton group where some dinoflagellates have very high intracellular DMSP whereas little to none DMSP was detected in others (Keller et al., 1989; Stefels et al., 2007; Caruana and Malin, 2014; McParland and Levine, 2019). The reasons for this high variability are still unknown (Caruana and Malin, 2014). In addition, high intraspecific

variability (14 – 220%) is observed between different strains or between multiple analyses in the same strain. This variability might come from the different genotypes or phenotypes when the strains are different or might also result from different environmental conditions at the time of sampling (Caruana and Malin, 2014). Their DL activity is covering 2 order of magnitude from 0.15 to 13.26 mmol L^{-1}_{cell} h^{-1} regarding the inter- and intra-specific variability. Nevertheless, only few dinoflagellates were investigated for DL activity (n = 12) (Caruana and Malin, 2014).

Table 1-2: Resume of the $DMSP_p$:Chl-*a* and $DMSO_p$:Chl-*a* ratio found from the published data available for the phytoplankton group of dinoflagellates for species characterizing the North Sea.

Class	Genus	Species	DMSPp:Chla (mmol:g)	DMSOp:Chl-*a* (mmol:g)	Data from
Dinoflagellate	*Gymnodinium*	*G. simplex*	**195.1**	**0.1**	1, 2
Dinoflagellate	*Gyrodinium*	*G. aureolum*	**0.4**		1
Dinoflagellate	*Heterocapsa*	*H. rotundata*	**18.8**		3
Dinoflagellate	*Heterocapsa*	*H. rotundata*	**17.7**		4
Dinoflagellate	*Heterocapsa*	*H. rotundata*	**19.5**		4
Dinoflagellate	*Heterocapsa*	*H. triquetra*	**98.8**		5
Dinoflagellate	*Heterocapsa*	*Heterocapsa sp.*	**116.2**		1
Dinoflagellate	*Heterocapsa*	*H. triquetra*	**153.7**	**8.6**	6
Dinoflagellate	*Karenia*	*K. mikimotoi*	**0.1**		7
Dinoflagellate	*Karlodinium*	*K. veneficum*	**3.9**		8
Dinoflagellate	*Katodinium*	*Katodinium sp.*	**41.2**		9
Dinoflagellate	*Tripos*	*T. fusus*	**0.1**		10

1. McParland and Levine (2019); 2. Hatton and Wilson (2007); 3. Cooney et al. (2019); 4. Cooney (2016); 5. Niki et al. (2000); 6. Speeckaert et al. (2019); 7. Archer et al. (2009); 8. Lee et al.

The mean $DMSP_p$:Chl-*a* ratio calculated in Stefels et al. (2007) is 111 ± 168 mmolS:g Chl-*a*. In this ratio, it is including for instance genera from *Heterocapsa, Gymnodinium* or *Tripos* that are characterized by $DMSP_p$:Chl-*a* significantly different (Table 1-2). The $DMSO_p$ concentration is less studied since we only found two studies allowing us to obtain the $DMSO_p$:Chl-*a* ratio of 4.4 ± 6.0 mmolS:g Chl-*a* (Hatton and Wilson, 2007; Speeckaert et al., 2019).

Heterocapsa triquetra is considered from the armoured dinoflagellates of the order of Peridiniales, characterized by a series of unequal polygonal cellulose plate. Its size is comprised between 16 – 30 µm with a width of 9 – 18 µm. *H. triquetra* is distributed throughout a neritic or estuarine habitat generally during summer when extensive bloom can occur in low salinity in temperate coastal waters. It is a mixotroph with both sexual and asexual reproduction.

7 Study cases for field sampling

7.1 The North Sea

We realised during this thesis two field samplings including one year of sampling in 2018 in the Belgian Coastal Zone (BCZ) in the Southern North Sea, and one month of sampling in August 2018 in the Northern North Sea (NNS). The North Sea is then described as a whole, englobing the NNS, while the BCZ characteristics are explained further.

The North Sea is a semi-enclosed marginal sea of the North Atlantic Ocean and is situated on the European continental shelf. It is connected to the Atlantic Ocean in the South through the English Channel and in the North with the Norwegian Sea. There is also a connection with the Baltic Sea in the East (Quante et al., 2016). The average bathymetry is about 90 meters even if the water depths can exceed 700 meters in the Norwegian trench. The current circulation will depend on the major inflow coming from the Northwest and a minor warm and more saline input from the English Channel (Paramor et al., 2009; Quante et al., 2016). This leads to an anti-clockwise rotation along the edges (Fig. 1-17). Nutrient inputs come principally from the inflow of the North Atlantic, while the highest concentrations come from the riverine inputs and atmospheric depositions of nitrogen (Druon et al., 2004; Paramor et al., 2009, Quante et al., 2016). The major rivers discharging freshwater are the Forth, Humber, Thames, Seine, Meuse, Scheldt, Rhine, Ems, Weser, Elbe, and Glomma. The melt water from Norway and Sweden contribute about a third of the annual input of freshwater (Quante et al., 2016). The North Sea is one of the most productive and biologically rich regions of the world (Emeis et al., 2015). The North Sea's ecosystem variability will depend on human and natural causes of change. For instance, the nutrient loads from terrestrial and anthropogenic sources are one of the major contributors of high levels of primary production in coastal waters (Quante et al., 2016).

As a temperate sea, the North Sea is characterized by a clear seasonal production cycle with: (1) in winter, the primary production is limited by light availability; (2) in spring and due to higher light levels and rising temperatures, distinct phytoplankton bloom occurs at the sea surface. In summer and/or autumn, dinoflagellates blooms might also occur (Cushing, 1959 in Quante et al., 2016), as well as diatoms to a lesser extent (Reid, 1978 in Quante et al., 2016). The spring phytoplankton bloom is initiated in the Southern North Sea (SNS) in late winter/early spring while it develops later in the northern part (Colebrook, 1979). Primary productivity in the SNS relies on terrestrial nutrient inputs to a far greater degree than in the

NNS, and nutrients can be a limiting factor during the productive period of spring. The nutrient cycle can be seen as follows (Quante et al., 2016 and citations therein): (1) nutrients accumulate in autumn and winter due to intense mineralisation with the peak generally occurring in late winter; (2) silicate and phosphate become the first nutrients to be depleted in coastal waters in spring, slowing the growth of diatoms; (3) excess nitrate will be taken by flagellates; (4) nutrients become depleted in most of the North Sea due to the summer stratification; (5) surface nutrient concentrations increase in autumn after mineralisation has occurred in deeper water layers and are brought to the euphotic zone by stormy autumn weather. Nitrogen is considered to be the limiting nutrient in the Central North Sea while in the Coastal Zones it is generally phosphate.

Figure 1-17: Map of the North Sea including the circulation system according to OSPAR (2000) in Quante et al. (2016).

7.2 The particular case of the Belgian Coastal Zone

The South Bight of the North Sea that includes the BCZ is surrounding by industrialized countries (Belgium, France, England, and Holland) (Fig. 1-18). The seawater in this area is well-mixed and under the influence of riverine inputs from the Rhine, the Meuse, the Seine, the Scheldt, and the Thames. As in the case of many other marine coastal areas, the BCZ is largely eutrophied due to riverine, atmospheric, and transboundary inputs of land-based nutrients

(Rousseau et al., 2002). Indeed, the North Sea is subjected to anthropogenic loads of nitrogen and phosphorus that lead to important biomass in most coastal zone between March and October (Desmit et al., 2019 and citations therein). This eutrophication results in excessive development of undesirable phytoplankton species, affecting the structure of the food web as well as the services and goods provided by the coastal environment (Rousseau et al., 2002). The nutrient contributions have led to an excess of nitrate compared to phosphate and silica, resulting in the proliferation of non-siliceous phytoplankton such as *Phaeocystis globosa*. As it was mentioned previously, this species can be at the origin of high biomass in spring when the silica becomes the limiting nutrient for diatoms (Lancelot et al., 2005). The coastal zones in the area are also under the threat of increased Sea Surface Temperature (SST) since the 80's. The consequences of these external drivers are the changes in the physiology, abundance, and phenology of marine phytoplankton (Desmit et al., 2019).

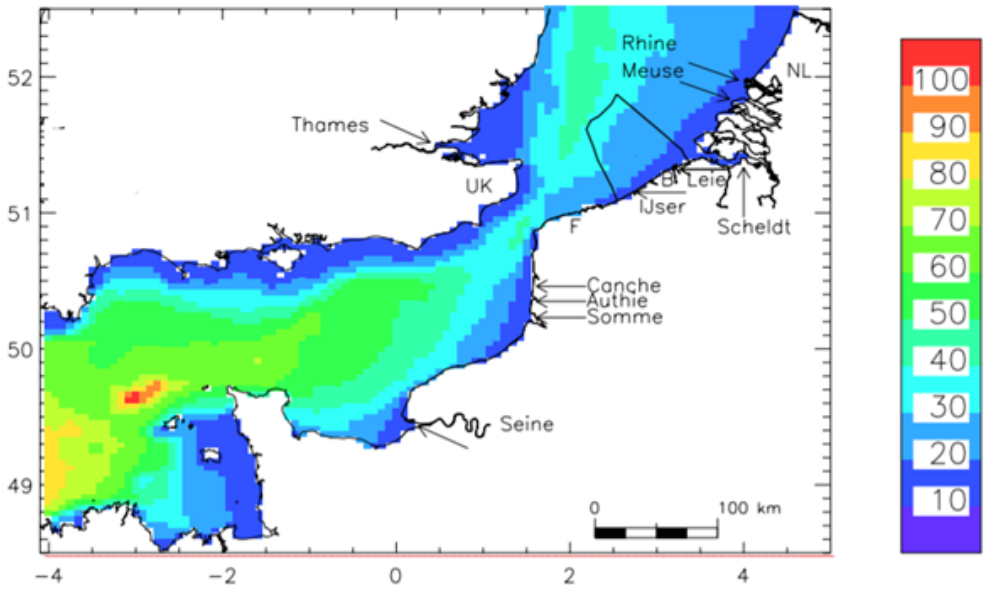

Figure 1-18: Maps of the Southern Bight of the North Sea with the Belgian Coastal Zone (in dark lines), the water depth (in meters) and the main rivers discharges (arrows) (Ruddick and Lacroix, 2006).

The BCZ is characterized by a very high phytoplankton biomass and phytoplankton succession as following: (1) the first bloom occurs in late February - March with diatoms, (2) directly followed by a huge biomass peak of *Phaeocystis globosa* in April-May, and (3) another diatom bloom at the end of summer-beginning of autumn (Rousseau et al., 2002). The first bloom is mainly dominated by colonial diatoms such as *Asterionellopsis* sp., *Thalassiosira* sp., *Thalassionema* sp., or *Skeletonema* sp. but they are rapidly limited by silica inputs. The species *Chaetoceros* sp. will also be present and will coexist temporally with the *Phaeocystis globosa* efflorescence. Finally, the last bloom of summer-autumn are characterized by the same colonial diatoms that were present in early spring. Each of these blooms occur because of changes in

SST, light intensity, and nutrient availability. The light intensity is, for example, one of the most important factors in the onset of the early diatom spring bloom. The *Phaeocystis* efflorescence will depend on the remaining nitrate concentrations after the diatom bloom (Rousseau et al., 2002). More details will be provided in Chapter III with the analysis of the phytoplankton succession during the year 2016 and 2018.

Since the DMS emissions result from bacterioplankton processes and the production of their two precursors (DMS(P,O)), their concentration throughout the year will depend on a succession of low- and high-DMSP producers. It was mentioned previously that the diatoms are considered to be low-DMSP producers while the Prymnesiophyceae, *Phaeocystis globosa*, produce high amounts of DMSP. These prerequisites lead to important DMS(P) concentrations during the *Phaeocystis* bloom in April – May, as consequence that the South Bight of the North Sea is considered as high-DMS producing regions at global scale (Lana et al., 2011). The seasonal DMS(P) variations were studied by field measurements and modelization in the two last decades (Turner et al., 1988; Kwint and Kramer, 1996; van den Berg et al., 1996; van Duyl et al., 1998; Archer et al., 2002; Gypens et al., 2014, Speeckaert et al., 2018). The seasonal and spatial variations of DMS(P,O) will be discussed in Chapter III and V.

8 Research objectives

As it was mentioned previously, DMS(P,O) play several hypothetical roles within phytoplankton cells. These roles depend on environmental drivers such as salinity, temperature, nutrient concentration, or light intensity. In addition, phytoplankton will produce DMS(P,O) in several orders of magnitude depending on the phytoplankton species.

Thus, the main idea driving this thesis is to study the influence of **phytoplankton diversity** or **taxonomy** as well as **external drivers** that promote DMS(P,O) production inside the cell. Indeed, after many years of research, the understanding of biological DMS(P,O) production within the main phytoplankton classes and regarding adverse environmental conditions is still in some parts unknown. This thesis is then built around experiments in laboratory and measurements on field samples.

In this context, the laboratory experiments involve three phytoplankton species present in the SNS and including a low-DMSP producer – the diatom *S. costatum* – and two high-DMSP producers – the Prymnesiophyceae *P. globosa*, and the dinoflagellate *H. triquetra*. They cover three phytoplankton groups with different initial $DMS(P,O)_p$ concentrations (Keller et al., 1989; McParland and Levine, 2019). They were grown in monoculture with controlled temperature and salinity conditions to study the influence of increasing light intensity and pro-oxidant molecules on the $DMS(P,O)_p$ production. The following assumptions arise from the antioxidant cascade reactions suggested by Sunda et al. (2002) and are discussed in Chapter III:

- **Hypothesis n°1**

  The oxidative stress produced by increasing light intensity or pro-oxidant molecules induces variations in $DMS(P,O)_p$ content.

- **Hypothesis n°2**

  These $DMS(P,O)_p$ variations are different between the three phytoplankton species because of their initial $DMS(P,O)_p$ concentration.

In the second part of this thesis, the field sampling covers the BCZ during the year 2018 (Chapter IV) that will be compared to the year 2016 (Speeckaert et al., 2018) to analyse the interannual variation. A second field sampling was also performed in the NNS in August 2018 (Chapter V). The field measurements force us to consider all the abiotic conditions – salinity, temperature, nutrient concentrations, and incident light – to explain the variations in

phytoplankton biomass and diversity to understand and explain the resulting $DMS(P,O)_p$ concentrations.

- **Hypothesis n°3**

  The seasonal or spatial variation of abiotic parameters affects the biomass and composition of marine phytoplankton (Chapter IV and V).

- **Hypothesis n°4**

  These changes in phytoplankton biomass do not necessarily have an impact on the DMS(P,O) concentrations which depend on the relative abundance of low- or high-DMSP producers (Chapter IV).

- **Hypothesis n°5**

  Considering the antioxidant function, the $DMS(P,O)_p$ concentrations are linked to the incident light as well as ancillary parameters such as the photoprotective pigments (Chapter V).

- **Hypothesis n°6**

  The $DMS(P,O)_p$ evolution during the year (Chapter IV) or along the latitude (Chapter V) can be estimated based on the taxonomic composition.

Since DMS(P,O) play a central role in the global sulfur cycle, addressing the previous hypothesis is critical to better constrain DMS(P,O) concentrations in the water column, but also understanding their physiological roles, especially with respect to their potential function as antioxidant. Furthermore, adding cellular DMS(P,O) concentrations and regulation of their production in three main phytoplankton groups will lead ultimately to better constrain and improve the modelization of the ocean-atmosphere DMS flux and its climate impact.

Chapter II – Material and methods: Overview

"The best way to show that a stick is crooked is not to argue about it or to spend time denouncing it, but to lay a straight stick alongside it".

- D.L. Moody

1 Phytoplankton culture

1.1 Culture equipment

This thesis was based on a cell approach and three phytoplankton species were chosen within three phytoplankton groups. The species were a diatom (1) *Skeletonema costatum* isolated from the Southern North Sea; the Prymnesiophyceae *Phaeocystis globosa* RCC1719 originating from Roscoff Culture Collection (English Channel, France), known for its bloom in the North Sea; and the dinoflagellate *Heterocapsa triquetra* RCC4800 originating from Roscoff Culture Collection (English Channel, France). The Prymnesiophyceae and dinoflagellates exhibit DL activity (Stefels and Dijkhuizen, 1996; Caruana and Malin, 2014). The species were maintained axenically in exponential growth at salinity of 34 (S34) and a temperature of 15°C with a 12:12h light: dark cycle under an irradiance of 100 µmol quanta $m^{-2}s^{-1}$. The seawater used for the culture was collected in the BCZ at 3 meters depth, kept in the dark for several months, filtered and autoclaved to avoid bacterial contamination. The seawater was enriched with nutrients according to f/2 culture medium from Guillard and Ryther (1962). Silica (Na_2SiO_3; final concentration 107 µmol L^{-1}) was added in the culture medium for *S. costatum*.

1.1 Experimental setup

Oxidative stress and its effects on DMS(P,O) production were analysed by three different methods using (Fig. 2-1):

1) High light (HL) intensities (600 and 1200 µmol quanta $m^{-2}s^{-1}$) to produce a natural oxidative stress. The irradiance of 100 µmol quanta $m^{-2}s^{-1}$ will be referred as the control light or I0 while 600 and 1200 µmol quanta $m^{-2}s^{-1}$ as I1 and I2, respectively. We performed long- (8-12 days) and short-term (6h) treatments to create this high light oxidative stress.
2) *Menadione Sodium Bisulfite* (MSB) was used to chemically produce $O_2^{\cdot -}$ inside the cell. It is widely used in the study of oxidant stress in plants (Sun et al., 1999). The treatment was inflicted during 6h.
3) *3-(3,4-dichlorophenyl)-1,1-dimethylurea* (DCMU) was used to inhibit the photosystem II and promote the ROS production. DCMU is generally used as an herbicide to block the electron flux in the PSII from the electron acceptor quinone Q_A to the secondary quinone acceptor Q_B (Haynes et al., 2000; Baker, 2008). This results in a rapid reduction of Q_A and an increase in fluorescence as photochemical quenching is prevented (Baker, 2008). DCMU maintains all the reaction centres closed under incident irradiance (Huot

and Babin, 2010). The phytoplankton cultures was exposed to DCMU under I2 during 6h.

1.2 Sampling

For the long-term HL treatment, phytoplankton cultures were sampled at mid-exponential growth stage to determine the cell density, the Chl-*a*, and the DMS(P,O) concentrations.

For the 6h treatment of MSB, DCMU and HL, cultures were sampled at t0h and t6h to analyse the Chl-*a* concentration, the ROS production, the LPO, the PSII activity, and the DMS(P,O) concentrations.

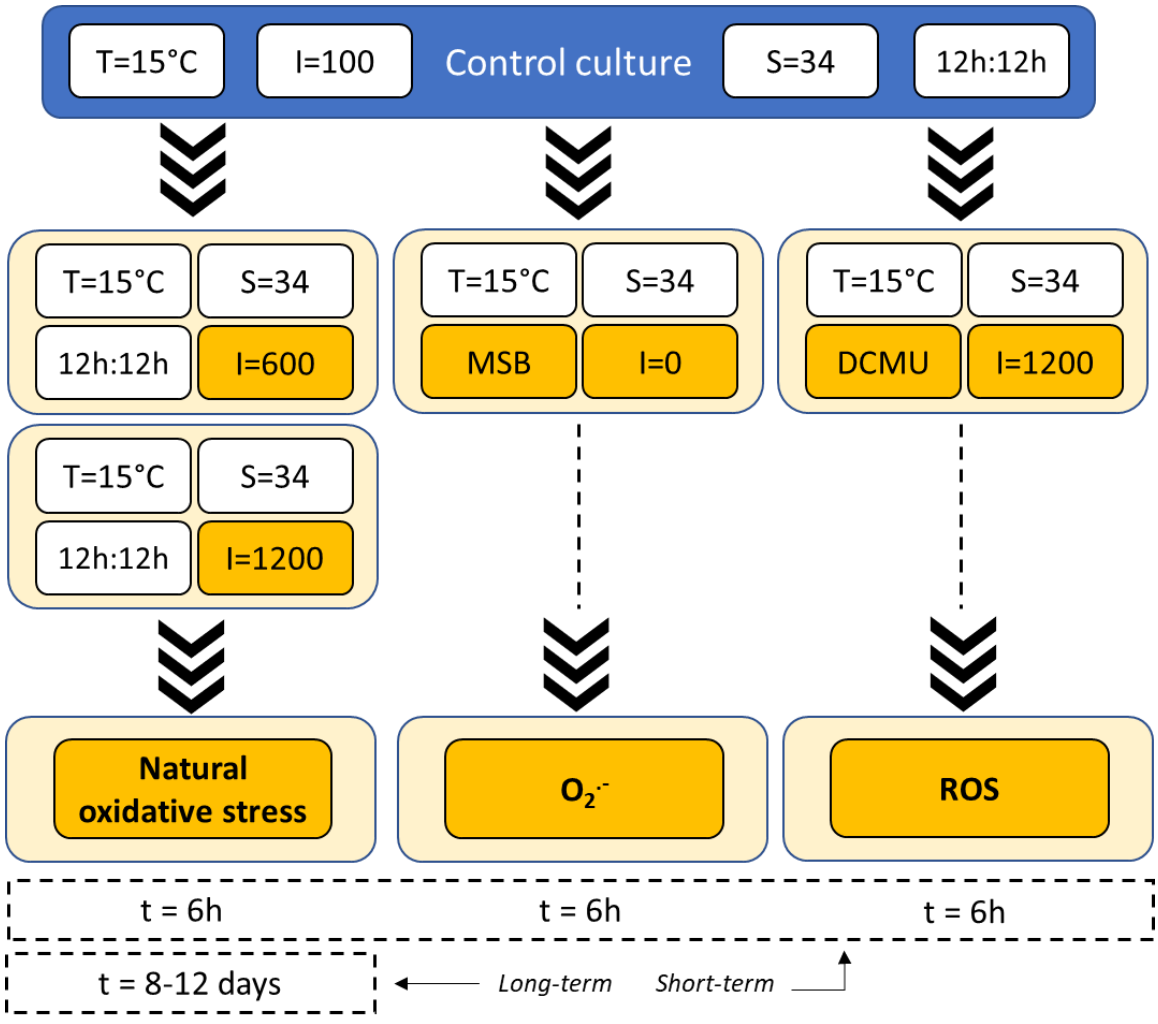

Figure 2-1: Experimental setup for the oxidative stress experiments with T = temperature (°C); I = light intensity (µmol quanta $m^{-2}s^{-1}$; S = salinity and t = time (h or days).

1.3 Analyses

1.3.1 Cell density

The cellular density for the long-term HL treatment was performed at different growth stages by microscopy according to Utermöhl method (Hasle, 1978); or by using a Z2 Coulter Particle Count and Size Analyser for the DCMU short-term oxidative stress experiments. The cellular biovolume was calculated by measuring the dimensions of cells according to Hillebrand et al. (1999) and converted in carbon biomass with the equations proposed by Menden-Deuer et Lessard (2000).

1.3.2 Chlorophyll-*a*

The Chl-*a* concentration was analyzed by filtration of a known volume of phytoplankton culture and its further extraction with acetone 90% and its measure by fluorimetry (Strickland and Parsons, 1972). For the short-term oxidative stress experiments, MeOH was used for the extraction and the measurement was obtained by spectrophotometry (Ritchie, 2006).

1.3.3 DMS(P,O)

DMS(P,O) analyses were performed using a gas chromatography after the conversion of DMSP in DMS by sodium hydroxide (Dacey and Blough, 1987; Stefels, 2009), and the conversion of DMSO in DMS by $TiCl_3$ (Kiene and Gerard, 1994; Deschaseaux et al, 2014) in the same sample (Champenois and Borges, 2019). Samples were collected for total and dissolved DMS(P,O), allowing by their subtraction to obtain the intracellular DMS(P,O). The gas chromatography was associated with a purge and trap system to preconcentrate the DMS from the previous conversion before its injection in the GC. More details are provided for the sulfur analysis in the Chapter III.

1.3.4 Chlorophyll fluorescence

For the three oxidative stress applied, fluorescence *in vivo* was measured using a SpeedZen JBeamBio camera allowing us to analyse the efficiency of PSII (Φ_{PSII}). Dummermuth et al. (2003) have shown that the measurement of the *in vivo* fluorescence of Φ_{PSII} is a suitable tool to determine the effect of oxidative stress in algae and it is widespread in physiological and ecophysiological studies (Baker, 2008). As described previously, three competing pathways are dominant when light energy arrives to the photosystem: (1) photochemistry, (2) heat dissipation and (3) fluorescence. The sum of the quantum yields of each process is unity and then, changes in fluorescence yield reflect changes in the complementary pathways as well (Cosgrove and

Borowitzka, 2010). The measurement of this fluorescence provides a rapid method to characterize the PSII operating efficiency under different light conditions or other stress (Baker, 2008). The method used was the saturation pulse method (Fig. 2-2) to estimate the photochemical quantum yield. Minimum fluorescence yield (F_0) occurs after dark adaptation when all the reaction centres (RCs, Q_A) of the PSII are open (or oxidised). It means if energy reaches the RCs, it has the maximal chance of being utilised photochemically and negligible chance of being dissipated as heat or fluorescence (Baker, 2008; Cosgrove and Borowitzka, 2010). We then applied a pulse of high light intensity saturating all the RCs of the PSII (closure or reduction of the RCs, Q_A), the photochemistry is reduced to zero and the maximal fluorescence level is observed (F_m). The non-photochemical quenching is negligible since the samples were dark adapted. After this point and with actinic light, the sample is no longer adapted to the dark, and the non-photochemical quenching will act to quench the fluorescence yield. The achieved maximum fluorescence yield is now lower and noted $F_{m'}$. The difference between F_m and $F_{m'}$ can be used as a measure of the non-photochemical quenching (Baker, 2008; Cosgrove and Borowitzka, 2010).

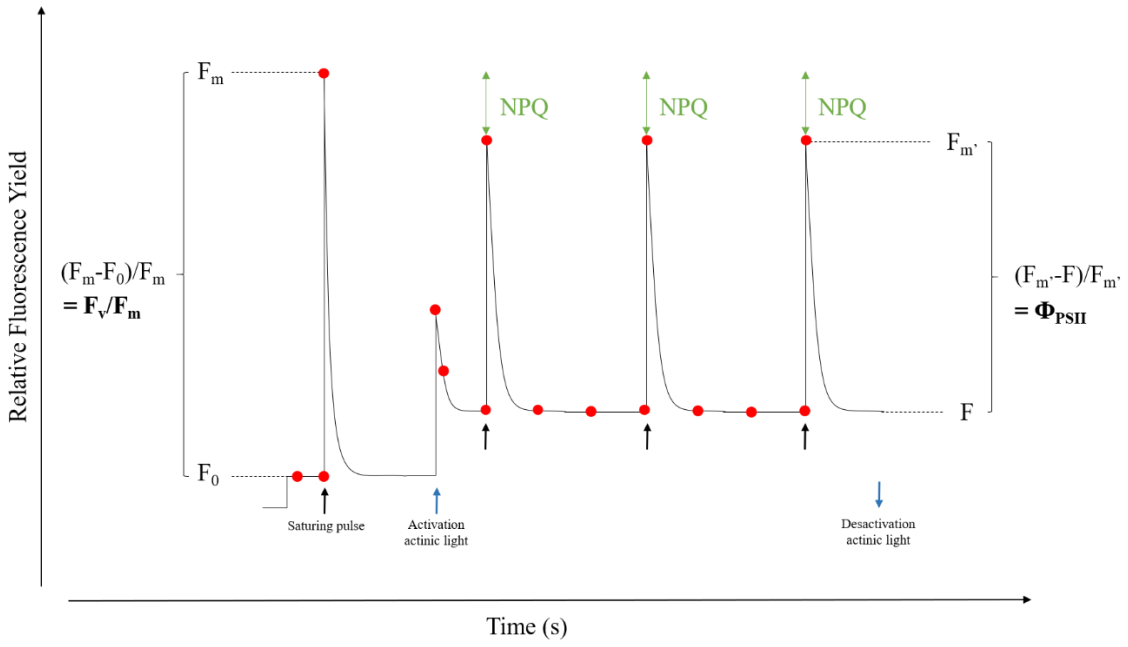

Figure 2-2: Schematic representation of the saturating pulse method use for the oxidative stress experiment.

In the oxidative stress experiments, this saturation pulse method can be used to estimate the efficiency of the PSII photochemistry (Φ_{PSII}) (Genty et al., 1989). Environmental factors such as the light intensity, nutrient concentrations, and temperature (Wozniak et al., 2002), that will impact the Φ_{PSII}, will directly or indirectly also impact the maximum theoretical yield of PSII (F_v/F_m) (Greene et al., 1992). These F_v/F_m values generally decrease when oxidative stress is

applied (Baker, 2008). The down-regulation of the PSII photochemistry may act as photoprotective mechanisms to reduce the formation of the triplet state Chlorophyll ($^3Chl^*$) in the PSII and the formation of ROS, as well as high levels of de-epoxidised xanthophyll cycle pigments (Krause and Jahns, 2004).

1.3.5 Reactive Oxygen Species concentration

The intracellular ROS concentration is visualized by spectrophotometry using the 5-(and-6)-carboxy-2',7'-dichlorodihydrofluorescein diacetate (carboxy-H_2DCFDA; Molecular Probes, Invitrogen) for the MSB treatments. For HL and DCMU stresses, a colourless probe Amplex Red (10-acetyl-3,7-dihydroxyphenoxazine; Invitrogen A12222) was used to determine the extracellular H_2O_2 concentration by spectrophotometry. More details are provided in Chapter III.

1.3.6 Lipid Peroxidation

Assessment of oxidative damage in phytoplankton cells exposed to each oxidative stress (HL, MSB, and DCMU) was achieved by the *Peroxidetect Kit* (Sigma Aldrich) and measured by spectrophotometry. The level of lipid peroxidation in parallel of ROS production has been widely used as an indicator of ROS mediated damage to cell membranes under stressful conditions (Sharma et al., 2012). More details are provided in Chapter III.

2 Field sampling

2.1 Belgian Coastal Zone

2.1.1 Sampling

Sampling was carried out on the *RV Simon Stevin* in 2016 and 2018 at 5 fixed stations chosen to cover both near-offshore gradient and a longitudinal gradient. The data from 2016 were published in Speeckaert et al. (2018). The samples were collected each month through the year and bimonthly between March and May during the spring phytoplanktonic bloom. Seawater samples were collected at 3 meters depth for further analysis of Chl-*a*, DMS(P,O) concentrations and DNA extraction. These analyses were performed using the same protocols as explained previously.

The abiotic measurements of sea-surface temperature (SST), sea-surface salinity (SSS), suspended particulate matter (SPM), nutrients concentrations were carried out by the Vlaams Instituut voor de Zee (VLIZ) (http://rshiny.lifewatch.be/Station%20data/) (Flanders Marine Institute, 2019) with the methodology found in Mortelmans et al. (2019). The daily global solar

radiation data was collected at the Oostende station of the Royal Meteorological Institute of Belgium.

2.1.2 DNA sequencing

DNA was sampled by filtering seawater on 0.2 µm filters (Tynes, 2013). The DNA was extracted using *DNeasy Plant Qiagen* following manufacturer's protocol. Sequencing was performed using Illumina MiSeq sequencer, analysed using R software package phyloseq (McMurdie and Holmes, 2013) and the taxonomic annotation database used was *Silva 1.32*. Several assumptions were decided for the analysis and more details can be found in the Chapter IV.

2.2 Northern North Sea

2.2.1 Sampling

Sampling of the physical, chemical, and biological parameters was carried out on the *RV Heincke* during the expedition HE517 that started the 19 August and ended the 04 September 2018. Three transects were chosen to be analysed to cover (1) the area from Bremerhaven (Germany) to the top of Scotland; (2) the continental rift between Scotland, the Shetlands Islands, and the Faeroe Islands; and (3) the Norway Coastal Zone. Seawater samples were collected at different depths to cover the vertical profile. All the samples were kept for further analysis of Chl-*a*, nutrients and DMS(P,O) concentrations. The abiotic measurements of temperature and salinity were carried out by Röttgers and Wizotzki (2018). The DNA sequencing protocol applied for the NNS was the same as the one explained previously for the BCZ.

2.2.2 Nutrients

The filtered seawater was analysed by colorimetry and the nutrients were measured for silicates, phosphates, and ammonium according to Koroleff (1983a, b, c) and according to Grasshoff (1983) for nitrates. More details are provided on Chapter V.

Chapter III – Response of DMSP and DMSO cell quotas to oxidative stress in three phytoplankton species

"Mostly I sit at home in the evenings watching the box and hoping that one day I'll evolve into plankton."

- Tom Holt.

Response of dimethylsulfoniopropionate (DMSP) and dimethylsulfoxide (DMSO) cell quotas to oxidative stress in three phytoplankton species

C. Royer[1,2*], N. Gypens[1], P. Cardol[3], A.V. Borges[2], & S. Roberty[4]

[1] Laboratoire d'Ecologie des Systèmes Aquatiques, Université Libre de Bruxelles, CP221, Boulevard du Triomphe, Brussels 1050, Belgium ;

[2] Unité d'Océanographie Chimique, FOCUS Research Unit, Institut de Physique (B5A), Université de Liège, Liège 4000, Belgium

[3] Laboratoire de génétique et physiologie des microalgues, InBioS Research Unit, Institut de Botanique, Université de Liège, Liège 4000, Belgium

[4] Lab of Animal Physiology and Ecophysiology, InBioS Research Unit, Institut de Botanique, Université de Liège, Liège 4000, Belgium

*corresponding author : croyer@ulb.ac.be

Keywords: Antioxidant; Reactive Oxygen Species; Light stress; Menadione; DCMU; *Skeletonema*; *Phaeocystis*; *Heterocapsa*

Status: Submitted and in review in **Journal of Plankton Research (18/01/2021).**

1 Abstract

A wide variety of phytoplankton species produce the metabolites dimethylsulfoniopropionate (DMSP) and dimethylsulfoxide (DMSO). These compounds are involved in the cycling of the climate active gas dimethylsulfide (DMS), but their intracellular roles need to be better understood. Sunda et al. (2002) have hypothesized an antioxidant cascade reaction from DMSP along with its oxidation products, DMS and DMSO. This DMSP antioxidant pathway would be partly regulated by the activity of DMSP-lyase (DL) and the cleavage products, DMS and acrylate, are even more efficient in Reactive Oxygen Species (ROS) scavenging. In order to improve the understanding of the DMSP antioxidant function, we exposed three phytoplankton species (the diatom *Skeletonema costatum*, the Prymnesiophyceae *Phaeocystis globosa* and the dinoflagellate *Heterocapsa triquetra*) to different experimental treatments known to cause oxidative stress (high light intensities (HL); HL in combination to 3-(3,4-dichlorophenyl)-1,1-dimethylurea (DCMU); menadione sodium bisulfite (MSB)). DMS(P,O) concentrations were found to decrease significantly after 6h in all treatments which indicates that these molecules reacted with ROS, whose production was increased during treatments. DMSP-to-cell ratios in control conditions were found to be lower in *S. costatum* and *P. globosa* than *H. triquetra*, with the later species being more sensitive and unable to grow under HL. During long-term treatment (10 days), DMS(P,O) concentrations were not increased in high-light grown cells of *P. globosa* and *S. costatum*. Overall these results indicate that (1) these molecules have the ability to lower cellular ROS concentration during an oxidative stress, and (2) the cellular DMS(P,O) concentration is not indicative of the capability of the cell/species to tolerate an oxidative stress.

2 Introduction

Light, temperature, and nutrient availability can be highly dynamic in aquatic ecosystems, varying at short (from seconds to hours; e.g. light) and long timescales (from day to season; e.g. temperature, nutrients, or light) (Litchman and Klausmeier, 2001; Müller et al., 2001; Jahns and Holzwarth, 2012; Erickson et al., 2015). Hence in phytoplanktonic cells light harvesting capacity has to be continuously adjusted to meet the cellular energetic demands, which in turn depend on the nutritional status of the cell (Goss and Jacob, 2010). With the evolution of processes such as photosynthesis or respiration, it has been established that all oxygen-metabolizing organisms produce reactive oxygen species (ROS) (Apel and Hirt, 2004; Lesser, 2006; Diaz and Plummer, 2018). ROS are a group of free radicals, reactive molecules, and ions derived from molecular dioxygen (O_2; Sharma et al., 2012). In phototrophic organisms, ROS are mainly produced within the chloroplasts by: (1) energy transfer from excited chlorophyll (Chl) to O_2, leading to the formation of singlet oxygen ($^1O_2$) at the photosystem II (PSII) (Jahns and Holzwarth, 2012; Ruban et al., 2012; Pospíšil, 2016); and (2) direct reduction of oxygen at the acceptor side of photosystem I (PSI) (Mehler reaction), leading to the formation of superoxide radicals ($O_2^{\cdot-}$). This latter can be subsequently dismutated to hydrogen peroxide (H_2O_2) and further hydroxyl radical ($OH\cdot$) in presence of transition metal via the Haber-Weiss/Fenton reaction (Mallick and Mohn, 2000; Apel and Kirt, 2004; Jahns and Holzwarth, 2012; Pospíšil, 2016). These ROS are scavenged by enzymatic antioxidants, such as dismutases, catalases and peroxidases (Apel and Hirt, 2004; Asada, 2006), and non-enzymatic antioxidant compounds comprising ascorbate, glutathione, α-tocopherol, flavonoids, alkaloids, and carotenoids (Dummermuth et al., 2003; Lesser, 2006). However, under adverse environmental conditions (i.e. high light intensity), the tight equilibrium between ROS production and the antioxidant network can be destabilized, and ROS in excess cause damages to proteins, lipids, carbohydrates, deoxyribonucleic acid (DNA), and ultimately trigger cell death (Apel and Kirt, 2004; Lesser, 2006; Van Alstyne, 2008; Gardner et al. 2016).

The dimethylsulfoniopropionate (DMSP), dimethylsulfoxide (DMSO) (here after DMS(P,O)) are biogenic sulphur molecules that play a key role in the cycling of dimethylsulfide (DMS), a climate active gas (Liss et al., 1997; Stefels et al., 2007). DMS(P,O) are ubiquitous in seawater and produced by a large variety of micro- and macroalgae as well as some angiosperms and corals (Keller et al., 1989; Stefels, 2000; Simó and Vila-Costa, 2006; Hatton and Wilson, 2007; Raina et al., 2013; Borges and Champenois, 2017; McParland and Levine, 2019). DMS(P,O) may act as cryoprotectants, osmolytes (Kirst et al., 1996; Bucciarelli and Sunda, 2003),

zooplankton deterrents (Wolfe et al., 1997; Strom et al., 2003) or as signalling compounds (Stefels, 2000; Seymour et al., 2010). In addition, both DMS and its precursors DMS(P,O) are suspected to act as antioxidant molecules because: (1) the potential for DMSP accumulation in chloroplasts is in line with the ROS production in this cellular compartment (Trossat et al., 1998; Raina et al., 2017; Curson et al., 2018); (2) they have been associated with oxidative stress caused by high light intensity, UV-radiation, nutrient limitation, or hyposalinity (Karsten et al., 1992; Stefels and van Leeuwe, 1998; Sunda et al., 2002; Bucciarelli and Sunda, 2003; Husband et al., 2012; Deschaseaux et al., 2014; Gardner et al., 2016); (3) the exogenous addition of DMSP and acrylate on plant leaves have been shown to reduce oxidative damages (Husband et al., 2012); and (4) they can readily scavenge ROS, in particular OH· (Scaduto, 1995; Lee and De Mora, 1999; Sunda et al., 2002). The antioxidant capacity of the DMSP pathway would be partly regulated by the activity of DMSP-lyase (DL) as the enzyme cleavage products, DMS and acrylate, are ~60 and ~20 times more efficient in OH· scavenging than DMSP (Sunda et al., 2002). In addition, DMS could also react with $^1O_2$ (Wilkinson et al., 1995). Finally, DMS released by the activation of the DMS(P,O) pathway would act as a negative feedback mechanism on daily dose of solar and UV radiation by enhancing cloud albedo and thereby decreasing the incoming solar radiation, supporting a potential climate-cooling feedback loop (CLAW hypothesis, Charlson et al., 1987; Sunda et al., 2002). Within marine phytoplankton, the Prymnesiophyceae and the dinoflagellates are considered as high-DMSP producers while the diatoms are low-DMSP producers even if a high variability within each group is observed (Keller et al., 1989; Stefels et al., 2007; McParland and Levine, 2019). Also, the DL activity has been found only in some Prymnesiophyceae and dinoflagellates (Stefels et al., 2007; Mohapatra et al., 2014; Caruana and Malin, 2014; Alcolombri et al., 2015). Overall, this suggests that the contribution of DMS(P,O) to the antioxidant network might differ among phytoplankton species.

Studies aiming at improving the knowledge on DMS(P,O) cell quotas and their regulation according to abiotic parameters are necessary to better estimate the DMS(P,O) concentrations based on Chl-*a* and the phytoplankton composition. The clarification of the biological role of DMS(P,O) within the phytoplankton cell can also improve our understanding of how any climate feedback loop might operate (Ayers and Cainey, 2007) and ultimately, will help to better assess the DMS fluxes in ocean-atmosphere modelling systems. In order to improve our understanding of the antioxidant role played by DMS(P,O) in marine phytoplankton, we investigated the impact of oxidative stress on DMS(P,O) cellular concentrations in three

phytoplankton species, characterized by different DMS(P,O):Chl-*a* contents. To this end, monospecific cultures of *Skeletonema costatum* (diatom), *Phaeocystis globosa* (Prymnesiophyceae) and *Heterocapsa triquetra* (dinoflagellate) were exposed to three different experimental treatments known to cause oxidative stress and consisting in: (1) a light stress; (2) an exposition to menadione sodium bisulfite (MSB), a prooxidant molecule; and (3) a light stress in presence of DCMU, a chemical agent blocking the photosynthetic electron transport.

3 Material and Methods

3.1 Algal species and culture conditions

The phytoplankton species studied were the diatom *Skeletonema costatum* isolated from the Southern North Sea; the Prymnesiophyceae *Phaeocystis globosa* RCC1719 originating from the Roscoff Culture Collection (English Channel, France); and the dinoflagellate *Heterocapsa triquetra* RCC4800 originating from the Roscoff Culture Collection (English Channel, France). Prymnesiophyceae and dinoflagellates exhibit a DL activity (Stefels and Dijkhuizen, 1996; Caruana and Malin, 2014). For all experiments, cells were cultured axenically in F/2 medium (Guillard and Ryther, 1962) made with 0.2 µm filtered and autoclaved natural seawater (collected at the Belgian Coastal Zone). Silica (Na_2SiO_3; final concentration 107 µmol L^{-1}) was added in the culture medium for *S. costatum*. Batch cultures of all the species were grown to the exponential growth phase in 2 L Nalgene bottles containing 1 L of F/2 medium. Cultures were maintained at 15°C under cool white fluorescent bulbs providing a total light intensity of 100 µmol photons m^{-2} s^{-1} (12h:12h light:dark cycle) in an Aralab Fitoclima S600 incubator. Light intensities were determined between 400 and 700 nm using a LI-250 light meter (Li-Cor, USA) with a US-SQS/A light sensor (Walz, Germany).

3.2 Experimental treatments

Three experimental treatments were designed to assess the impact of ROS production on DMS(P,O) cellular concentrations in the phytoplankton species investigated: (1) a high light (HL) stress; (2) a chemical stress with MSB; and (3) a stress combining the use of DCMU and high light intensity. For each treatment, the temperature was kept at 15°C.

During the long-term HL stress, cells cultured at 100 µmol photons m^{-2} s^{-1} (control; I0) were exposed to light intensities of 600 (I1) and 1200 (I2) µmol photons m^{-2} s^{-1} (12h:12h light:dark cycle) for up to 15 days. Cellular density, Chl-*a* and DMS(P,O) contents were analysed at mid-exponential growth stage (days 8-10) of this long-term stress.

A short-term HL treatment of 6h at 1200 µmol photons m^{-2} s^{-1} was applied to cells cultured at 100 µmol photons m^{-2} s^{-1} to determine the chlorophyll concentrations and fluorescence, ROS production and lipid peroxidation (see 3.3 Analyses).

During the second experimental treatment, cells were exposed in the dark and for 6h to 25 µmol L^{-1} of MSB diluted in F/2 medium. This water-soluble compound is commonly used as a chemical agent causing oxidative stress in plants and microalgae (e.g. Sun et al., 1999; Borges et al. 2009; Roberty et al. 2016). Once incorporated in the cell, MSB reacts with a variety of reductive enzymes and in presence of O_2, the unstable semiquinones formed enter into a redox cycle, causing the reformation of quinones with the concomitant generation of $O_2^{\bullet-}$ and H_2O_2 (Hassan and Fridovich, 1979). The MSB concentration applied was determined experimentally on the basis of photosynthetic activity measurements (ΦPSII) in dark adapted samples (see 3.3.3 Chlorophyll fluorescence measurements). A treatment of 6h at 25 µmol L^{-1} was chosen because it moderately impacted the photophysiology of the species investigated (i.e. by 25-50%).

And finally, for the third experimental treatment, cells were exposed for 6h to 1200 µmol photon m^{-2} s^{-1} in presence of 10 nmol L^{-1} DCMU. This inhibitor competes for the binding site of plastoquinone Q_B and blocks the electron flux from PSII, promoting the formation of ROS within the chloroplasts (Haynes et al., 2000; Baker et al., 2008). Based on the photosynthetic activity measurement (ΦPSII) after 30 min in dark adapted samples (see 3.3.3 Chlorophyll fluorescence measurements), the concentration chosen in this study inhibited PSII activity by 60, 70 and 40% in *S. costatum, P. globosa* and *H. triquetra*, respectively.

3.3 Analyses

The assessment of the oxidative stress applied was studied by the analyses of the cellular Chl-*a* quota, the Chl-*a* fluorescence, the ROS production, and the cellular damages with the LPO. Those observations were conducted in parallel with the DMS(P,O) cellular quota.

3.3.1 Carbon concentration

The cellular concentration (cell L^{-1}) for the long-term HL treatment was determined at mid-exponential growth stage with an inverted microscope (Leitz fluovert) by using the Utermöhl sedimentation procedure on samples fixed with lugol-gluteraldehyde (10 µL mL^{-1}) (Hasle, 1978). A minimum of 400 cells around the slide were counted to have a 10% maximum error within a confidence interval of 95% (Lund et al., 1958).

For the short-term DCMU treatment, the cellular density was obtained using a Z2 Coulter Particle Count and Size Analyser Version 1.01 with known volume of culture mixed with 10 mL of isoton. The isoton is composed of filtrated solution of demineralized water with 9 g L^{-1} of NaCl and 0.5% v:v of formaldehyde.

The cellular biovolume (μm^3) was calculated by measuring the dimensions of cells according to Hillebrand et al. (1999) and converted into biomass per cell (pgC $cell^{-1}$) with the equations proposed by Menden-Deuer and Lessard (2000).

3.3.2 Chlorophyll concentrations

For the long-term HL treatment, a determined volume of the phytoplankton cultures was filtered on Whatman glass microfiber filters GF/F 25 mm and immediately frozen and stored at -20°C until analysis (within 1 month after sampling). Chl-*a* was then extracted at 4°C in acetone 90% (v:v) and measured fluorometrically using a Kontron Instruments SFM 25 (Strickland and Parsons, 1972). Chl-*a* concentrations (µg mL^{-1}) were determined using a Chl-*a* standard solution (1000 µg L^{-1}; Chl-*a* analytical standard, Merck).

For the MSB and DCMU short-term treatments, Chl-*tot* (Chl-*a* + Chl-c_2) from concentrated aliquots of cultures (3 600 x g for 3 min) were extracted in ice-cold 100% MeOH in presence of 0.5 mL of glass beads (710-1180 µm; Sigma-Aldrich, USA). Samples were then vortexed during 5 min at 30 Hz and at 4°C using a Tissue Lyser II (Qiagen, Germany). After debris removal (centrifugation 10 000 x g 10 min with a MicroStar 17 (VWR, Belgium)), Chl-*tot* (µg mL^{-1}) were determined by using a SP2000 spectrophotometer (Safas, Monaco) and the equations of Ritchie (2006). The Chl-*tot* concentrations were determined at the beginning and the end of the treatment.

3.3.3 Chlorophyll fluorescence measurements

In vivo Chl-*a* fluorescence measurements were performed at room temperature using a fluorescence imaging system (SpeedZen, BeamBio, France) described in Vega de Luna et al. (2019). Briefly, aliquots of the cultures were harvested and concentrated by gentle centrifugation to reach 10 µg Chl-*tot* mL^{-1} in fresh F/2 medium. The maximum quantum yield of PSII was calculated as F_V/F_M, where $F_V = F_M - F_0$, F_0 is the initial fluorescence level in dark-adapted sample (~10 min) and F_M is the maximum fluorescence level after a saturating pulse of light (150 ms at 4000 µmol photons m^{-2} s^{-1}). The effective photochemical quantum yield (ΦPSII) was calculated as $(F_{M'}-F)/F_{M'}$, where F is the fluorescence signal and $F_{M'}$ is the

maximum fluorescence level obtained with a saturating pulse under the light (after 3 min at 230 µmol photons m^{-2} s^{-1}) (Genty et al., 1989). The Chl-*a* fluorescence measurements were performed at 0 and 6h.

3.3.4 ROS production

ROS production was monitored by using carboxy-H_2DCFDA (Molecular Probes, Life technologies) during the MSB treatment and the Amplex Red reagent (Molecular probes, Life technologies, USA) during the short-term HL and DCMU treatments. For both measurements, aliquots of cultures were harvested and concentrated by gentle centrifugation to contain 10 µg Chl-*tot* mL^{-1} in fresh F/2 medium. ROS production was normalized with initial Chl-*tot* concentration at t0h. For the AmplexRed treatment, 150 µmol L^{-1} of DTPA was added to the culture medium at least 24h prior to the analysis to form complexes with trace metals in order to prevent their reaction with $O_2^{\bullet-}$ (Saragosti et al., 2010).

Carboxy-H_2DCFDA is a general oxidative stress indicator. When this non-polar compound enters the cells, it is deacetylated by esterases to DCFH and converted by various reactive species into carboxy-DCF, a fluorescent compound. Conditions of this assay were similar to those described in Roberty et al. (2016). Briefly, 1 mL of each culture was incubated with 25 µmol L^{-1} carboxy-H2DCFDA for 30 min in the dark. Cells were then washed and resuspended into 1 mL of fresh F/2 medium and placed in a Binder KB115 incubator (Binder, Germany) set to the treatment conditions. The fluorescence of the samples was then measured in black 96-well microplates (Greiner Bio-One) at 528 nm with a 485 nm excitation wavelength provided by a Synergy Mx spectrofluorometer (Biotek, USA). The measurement was performed at 0 and 6h.

The relative production of ROS during the short-term HL and DCMU treatments was evaluated by using the Amplex Red reagent (Molecular probes, Life technologies, USA). This colourless probe reacts with H_2O_2 in the presence of peroxidase and forms a fluorescent compound, resorufin. As described in Roberty et al. (2015), aliquots of cultures were combined with Amplex Red (100 µmol L^{-1}) and horseradish peroxidase (0.2 U mL^{-1}), and placed in a Binder KB115 incubator (Binder, Germany) set to the treatment conditions. Then, samples were centrifuged, and the fluorescence emitted by the supernatant in black 96-well microplates was measured at 590 nm with a 540 nm excitation wavelength provided by a Synergy Mx spectrofluorometer (Biotek, USA). Concentrations of H_2O_2 were calculated by comparing fluorescence emitted by the samples to a H_2O_2 standard curve (0 – 10 µmol L^{-1}). As the Amplex

Red (AR) reagent is sensitive to photo-oxidation, a Rose Pink filter (Lee Filters, Andover, UK) was used during experimental treatments to exclude wavelengths of light strongly absorbed by the reagent, and the experimental treatment was also limited to 3h. Various controls were performed: without AR, and with AR (and DCMU) in the dark to evaluate basal cellular ROS production.

3.3.5 Lipid peroxidation assay

The level of lipid peroxidation (LPO; mmol t-BuOOH:g Chl-*tot*) was assessed in phytoplankton cells exposed to experimental treatments by using the PeroxiDetect Kit (Sigma Aldrich, USA). Aliquots of the cultures were harvested and concentrated to obtain a final Chl-*tot* concentration of 20 µg mL^{-1} in fresh F/2 medium. LPO was normalized with initial Chl-*tot* concentration at t0h. LPO was measured using a methanolic reagent containing xylenol orange and butylated hydroxytoluene (BHT). The determination of LPO was performed following manufacturer's instructions at the beginning and the end of the short-term treatments. Then, the absorbance of the samples was measured at 560 nm using a SP2000 spectrophotometer (Safas, Monaco).

3.3.6 DMS(P,O) analysis

The DMS(P,O) analyses were performed at mid-exponential growth stage for the long-term HL acclimation, and at the beginning and the end of the MSB and DCMU treatments. Three biological replicates of particulate DMS(P,O) ($DMS(P,O)_p$) were obtained by the difference between 10 mL of unfiltered seawater samples (total DMS(P,O) - $DMS(P,O)_t$) and dissolved DMS(P,O) ($DMS(P,O)_d$). $DMS(P,O)_d$ was obtained by gentle filtration of 15 mL and only the first 10 mL of filtrate were collected to avoid cell destruction at the end of the filtration that could release DMSP (Kiene and Slezak, 2006). Samples were then microwaved individually till boiling to inhibit the DL activity that converts DMSP into DMS (Kinsey and Kieber, 2016) and acidified with 5 µL mL^{-1} of 50 % H_2SO_4 (del Valle et al. 2011), to arrest any biological activity (Curran et al, 1998). Samples were crimped after cooling with gas tight PFTE coated silicone septa and kept 24h at room temperature in the dark to allow the DMS to degas or oxidise (Kiene and Slezak, 2006). Then, samples were stored at 4°C until GC analysis. The DMS(P,O) concentrations were determined using an Agilent 7890B purge and trap gas chromatography (GC) (Agilent column 30 m long, 0.32 mm internal diameter, 0.25 µm film thickness) equipped with sulfur selective Flame Photometric Detector (FPD) and the carrier gas was He (2 ml min^{-1}). 5 mL of 12 M NaOH were added to the 10 mL samples to obtain a pH > 12 and quantitatively cleave DMSP into DMS for 24h (Dacey and Blough, 1987; Stefels, 2009). For the DMSO

analysis, 5 mL HCl 37% (HCl 37% Normapur, VWR) and 1 mL $TiCl_3$ (30%, Merck) (Kiene and Gerard, 1994; Deschaseaux et al, 2014) were added into the precedent vial yet analyzed (Champenois and Borges, 2019). After 48h at room temperature, 3 mL of 12 M NaOH were added to avoid injecting acid fumes into the GC (Kiene and Gerard, 1994). The same procedure was applied for the calibration. The DMSP used was obtained from Research Plus and the DMSO from 99,9% pure stock solution (Merck). Working solutions were prepared with the successive dilution in MilliQ water but DMSP and DMSO were diluted in the same vial. Calibration curves were made weekly to ensure the GC stability for the detector by fitting a quadratic curve for the FPD. The average precision was 5 and 8% for DMSP and DMSO calibration, respectively. Any leaks during the analysis were detected by using a Thermo Scientific GLD Pro Gas Leak Detector every day.

3.4 Statistics

To investigate the correlation between the variables, the Pearson's *r* coefficient and its *p* value was used. In case of deviation of normality by the Shapiro-Wilk test ($p < 0.05$), the non-parametric Spearman's ρ coefficient was applied. The parametric paired-samples Student t-test was used to compare two related groups (i.e. at t0h and t(x)h) on the same continuous and dependent variable. The assumption of normality was checked using the Shapiro-Wilk test. In case of deviation of the normality ($p < 0.05$), the Wilcoxon t-test was applied. These statistics analyses were performed using JASP software (JASP Team (2019), Version 0.11.1) and the assumptions were based on Goss-Sampson (2018). Principal component analysis (PCA) was performed on $DMS(P,O)_p$ contents (nmol L^{-1}), Chl-*tot* (µg L^{-1}), F_V/F_M, ΦPSII, ROS production (mole:g Chl-*tot*; fluorescence:µg Chl-*tot*) and LPO (mmol:g Chl-*tot*), using JMP Pro 14.

4 Results

4.1 High light stress

The exposure of low light acclimated cells (i.e. 100 µmol photons m^{-2} s^{-1}) to 1200 µmol photons m^{-2} s^{-1} for 6h strongly impacted the photosynthetic activities of the three species investigated. The maximal photochemical quantum yield (F_V/F_M) was inhibited by 81, 46, and 66%, and the ΦPSII values were decreased by 45%, 48%, and 65% for *S. costatum*, *P. globosa*, and *H. triquetra*, respectively ($p < 0.01$; Fig. 3-1A, B). The extracellular ROS production increased significantly by 3.0 for *S. costatum*, 2.2 for *P. globosa*, and 2.7 for *H. triquetra* ($p < 0.05$; Fig. 3-1C), but the pool of peroxidised lipids remained unchanged at the end of the experimental

treatment (Fig. 3-1D). The short-term light stress did not have any significant impact on the chlorophyll content of the species investigated neither (data not shown).

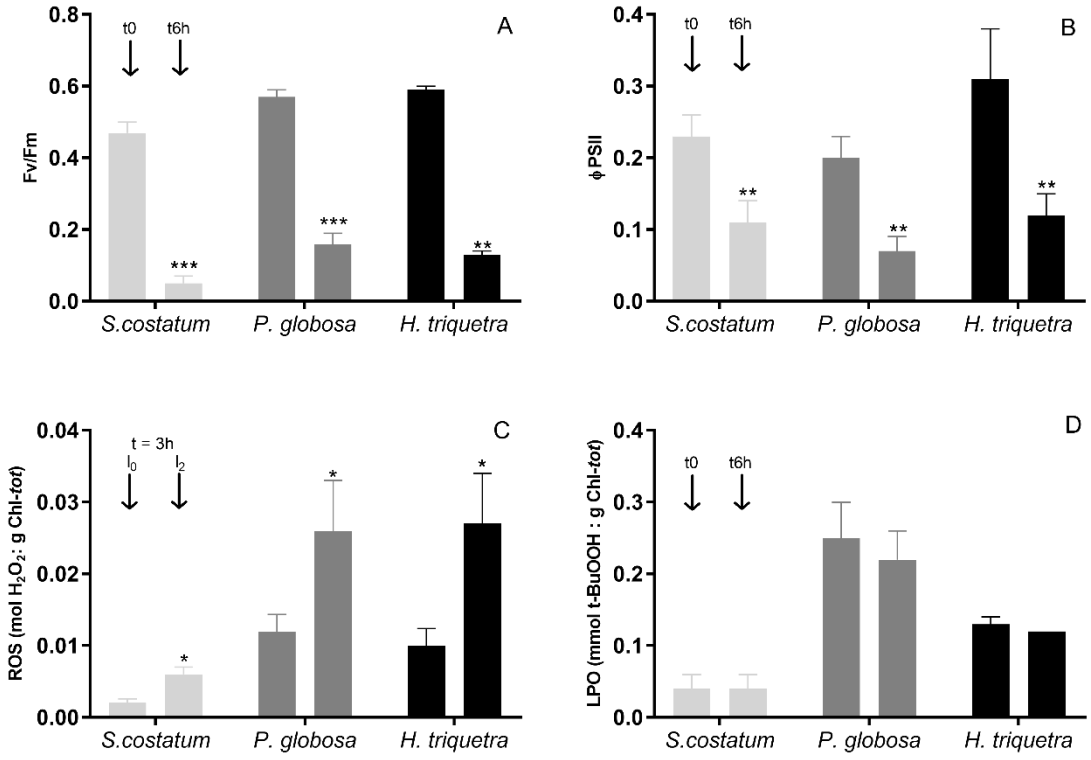

Figure 3-1: Evolution of (A) Maximum quantum yield of PSII (Fv/Fm), (B) Effective photochemical quantum yield of PSII (ΦPSII), (C) Reactive oxygen species (ROS) (mol H_2O_2:g Chl-*tot*) at the beginning and after 3h, (D) Lipid peroxidation (LPO) (mmol t-BuOOH:g Chl-*tot*) with increasing light intensity from 100 to 1200 µmol photon $m^{-2}s^{-1}$ during 6h for the three species *S. costatum*, *P. globosa* and *H. triquetra*. Error bars represent SD calculated from triplicates biological samples. Asterisks denote significant differences between the time point 0 and 6h (* $p < 0.05$; ** $p < 0.01$; *** $p < 0.001$).

In the long term, HL treatments (I1 and I2) did not impact the cell density observed of *S. costatum* and *P. globosa*, on the contrary to *H. triquetra* that was unable to grow at 1200 µmol photons m^{-2} s^{-1} (Fig. 3-2A). In contrast, the cellular Chl-*a* concentrations (Chl-a:C [g:g]) decreased significantly with increasing light intensities ($p < 0.05$; Fig. 3-2B). As a consequence, the $DMS(P,O)_p$ concentrations relative to Chl-*a* or cellular quota showed opposite trends with high variability between the species investigated. The $DMSP_p$:Cell (fmolS:cell) were similar between the treatments for *S. costatum*, while ratios were significantly lower at I1 for *P. globosa* (but not at I2) and *H. triquetra* compared to I0 ($p < 0.05$; Fig. 3-2C). The $DMSO_p$:Cell (fmolS:cell) did not change with light intensity whatever the species (Fig. 3-2D). When reported by chlorophyll amount, $DMSP_p$ ($DMSP_p$:Chl-*a*) contents were positively correlated with light intensities ($R^2 = 0.74$ and $p < 0.01$ for *S. costatum*; $R^2 = 0.55$ and $p < 0.05$ for *P. globosa*; and $R^2 = 0.90$ and $p < 0.01$ for *H. triquetra*). The $DMSP_p$:Chl-*a* ratio doubled from I1 for *P. globosa* and *H. triquetra* but at I2 for *S. costatum* ($p < 0.05$; Fig. 3-2E). The $DMSO_p$:Chl-*a* ratio of *S.*

costatum was significantly impacted by the light treatments and a 3- and a 4-fold increase of ratio was observed at I1 and I2, respectively ($p < 0.01$; Fig. 3-2F). A similar but not significant trend was observed in *P. globosa* and *H. triquetra*, respectively (Fig. 3-2F).

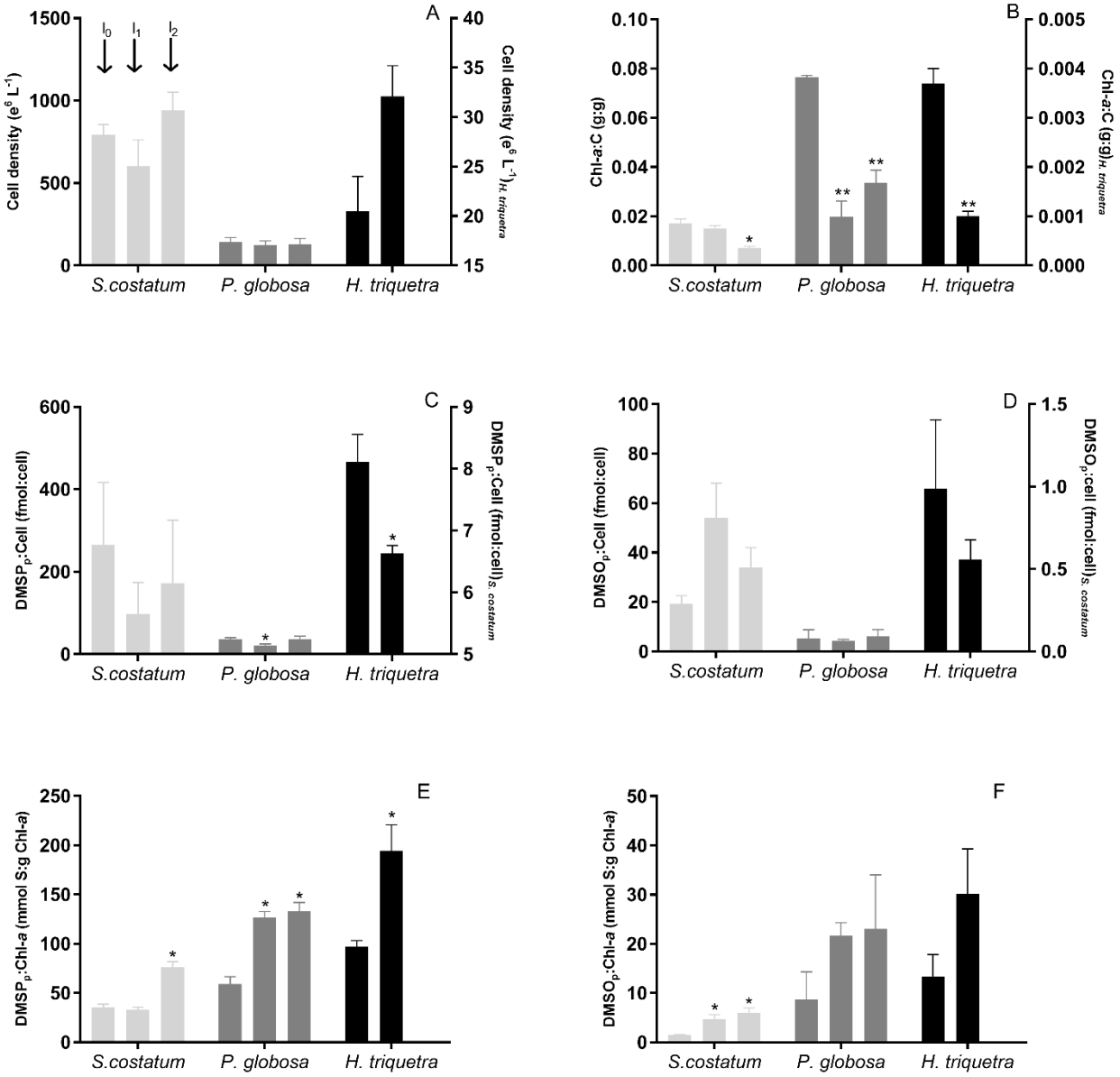

Figure 3-2: Evolution of (A) Cellular density (e^6 cells L^{-1}); (B) Cellular Chlorophyll-*a* content (Chl-*a*:C) (g:g), (C) the $DMSP_p$:Cell ratio (fmolS:cell); (D) the $DMSO_p$:Cell ratio (fmolS:cell); (E) the $DMSP_p$:Chl-*a* ratio (mmolS:g Chl-*a*), (F) the $DMSO_p$:Chl *a* ratio (mmolS:g Chl-*a*) at three light intensities of 100 (left column), 600 (centre column) and 1200 (right column) µmol photon $m^{-2}s^{-1}$ during the long-term HL treatment for the three species *S. costatum*, *P. globosa* and *H. triquetra*. Error bars represent SD calculated from triplicates biological samples. Asterisks denote significant differences between the control and the high light intensity considered (* $p < 0.05$; ** $p < 0.01$; *** $p < 0.001$).

4.2 DCMU treatment

Cultures of the three phytoplankton species were exposed to a PPFD of 1200 µmol photons m^{-2} s^{-1} (I2) in presence of 10 nmol L^{-1} of DCMU. As expected, the treatment strongly impacted the photosynthetic efficiency in the three species investigated. After 6h, F_V/F_M values decreased on average by 81, 93 and 77% in *S. costatum*, *P. globosa* and *H. triquetra* ($p < 0.001$; Fig. 3-3B) and the ΦPSII was totally inhibited (100%) in *P. globosa*, and at about 75% in the two remaining species ($p < 0.001$; Fig. 3-3D). The contributions of the HL treatment alone (controls without DCMU but exposed to I2) to the decrease of the later parameter accounted for 65, 44 and 75% in *S. costatum*, *P. globosa* and *H. triquetra* (data not shown). The treatment with DCMU also resulted in a significantly higher production of H_2O_2 comparatively to the HL treatment alone (33, 51 and 48% for *S. costatum, P. globosa* and *H. triquetra*, respectively; Fig. 3-3A). However, it is important to note that the cellular production of H_2O_2 in the dark in presence of DCMU was already high (Fig. Supp. 3-1A), thus indicating that a non-specific effect of DCMU stimulated the extracellular H_2O_2 production.

The peroxidised lipids content remained constant during the treatment, for the three species investigated (Fig. 3-3C). On the contrary, Chl-*tot* concentrations decrease significantly by 32, 97, and 85% in *S. costatum, P. globosa* and *H. triquetra*, respectively ($p < 0.05$; Fig. 3-3F). The $DMS(P,O)_p$:Chl-*tot* ratios were not significantly impacted by the treatment (Fig. Supp. 3-1B, C). The cell fractions collected at the start and the end of the experimental treatment came from the same cultures and cell concentrations did not vary significantly between the two time-points or between dark and treated samples for *S. costatum* and *P. globosa* (Table Supp. 3-1). Significant variation was found for *H. triquetra* between t0h and t6h but not between dark and treated samples (Table Supp. 3-1). We thus directly compared raw $DMS(P,O)_p$ data (i.e. non-normalized to Chl-*tot*) that revealed that the $DMSP_p$ content decreased by 37, 91 and 81% in *S. costatum, P. globosa* and *H. triquetra*, respectively (Fig. 3-3E) and the $DMSO_p$ content declined by 75 and 48% in *S. costatum* and *P. globosa* but not in *H. triquetra* (Fig. 3-3G). These observations indicate that the cellular content in $DMS(P,O)_p$ was impacted by ROS generated during the experimental treatment.

4.3 MSB treatment

The exposure of phytoplankton cell cultures to 25 µmol L^{-1} MSB for 6h resulted in the increase of the intracellular ROS concentration by 3.2, 2.5 and 3.0 compared to control concentrations

(i.e. without MSB), in *S. costatum*, *P. globosa*, and *H. triquetra,* respectively (Fig. 3-4A). The increased ROS concentration very likely impacted the photosynthetic apparatus in two of the three species. F_V/F_M was inhibited by more than 50% in *S. costatum* and *P. globosa* ($p < 0.05$; Fig. 3-4B) and ΦPSII decreased by 77 and 100% in *S. costatum* and *P. globosa*, respectively ($p < 0.05$; Fig. 3-4D). The photosynthetic activity of *H. triquetra* was unaffected by the treatment. The pool of peroxidised lipids remained stable for the diatom and the Prymnesiophyceae while a slight decrease of 28% was observed for the dinoflagellate ($p < 0.01$; Fig. 3-4C). The treatment with MSB did not significantly affect the Chl-*tot* content, except in *H. triquetra* where it decreased significantly ($p < 0.01$; Fig. 3-4F). The $DMSP_p$:Chl-*tot* ratio varied significantly in *H. triquetra* only ($p < 0.05$; Fig. Supp. 3-2A) and the $DMSO_p$:Chl-*tot* ratio remained stable in the three species investigated (Fig. Supp. 3-2B). Since the DCMU treatment did not impact the cellular density, we can conclude the same hypothesis for the MSB treatment and analyse raw $DMS(P,O)_p$ data. The $DMSP_p$ concentration decreased by 65, 88 and 28% in *S. costatum, P. globosa* and *H. triquetra*, respectively (Fig. 3-4E) and the $DMSO_p$ content decreased by 79 and 40% in *S. costatum* and *P. globosa* but increased by 33% in *H. triquetra* (Fig. 3-4G).

4.4 PCA

We further explored the similarities between all the variables combining the three experimental treatments applied. For HL treatment, the parameters correspond to the short-term treatment at t0h and t6h while the Chl and DMS(P,O) concentrations were from the long-term treatment at I0 (LL) and I2 (HL) to ensure a correct comparison. The figure 3-5 shows the distribution of the data within an orthogonal 2D-space along the first two PCs explaining 59.1% of the variance. The first PC has a large positive association with three variables ($DMSP_p$, Chl, and ΦPSII). This first component primarily measures strain's photosynthetic phenotype. The second PC has a positive association with ROS, $DMSO_p$, LPO and Fv/Fm (although Fv/Fm and LPO have also positive and negative association with PC1, respectively), reflecting the phenotype in terms of oxidative stress. This analysis further shows that some variables are uncorrelated to each other (i.e. Chl and Fv/Fm; ROS and $DMSP_p$; LPO and $DMSO_p$; LPO and Fv/Fm; LPO and ΦPSII) while Chl and LPO are anti-correlated.

This analysis also showed different visual separation in the distribution of the data related to each species regarding the controls and each treatment. When considering the control samples of each treatment (i.e. LL, MSB and DCMU 0 h), the data related to *H. triquetra* and *P. globosa* are closer to each other than *S. costatum,* characterized with more scattered data points for MSB

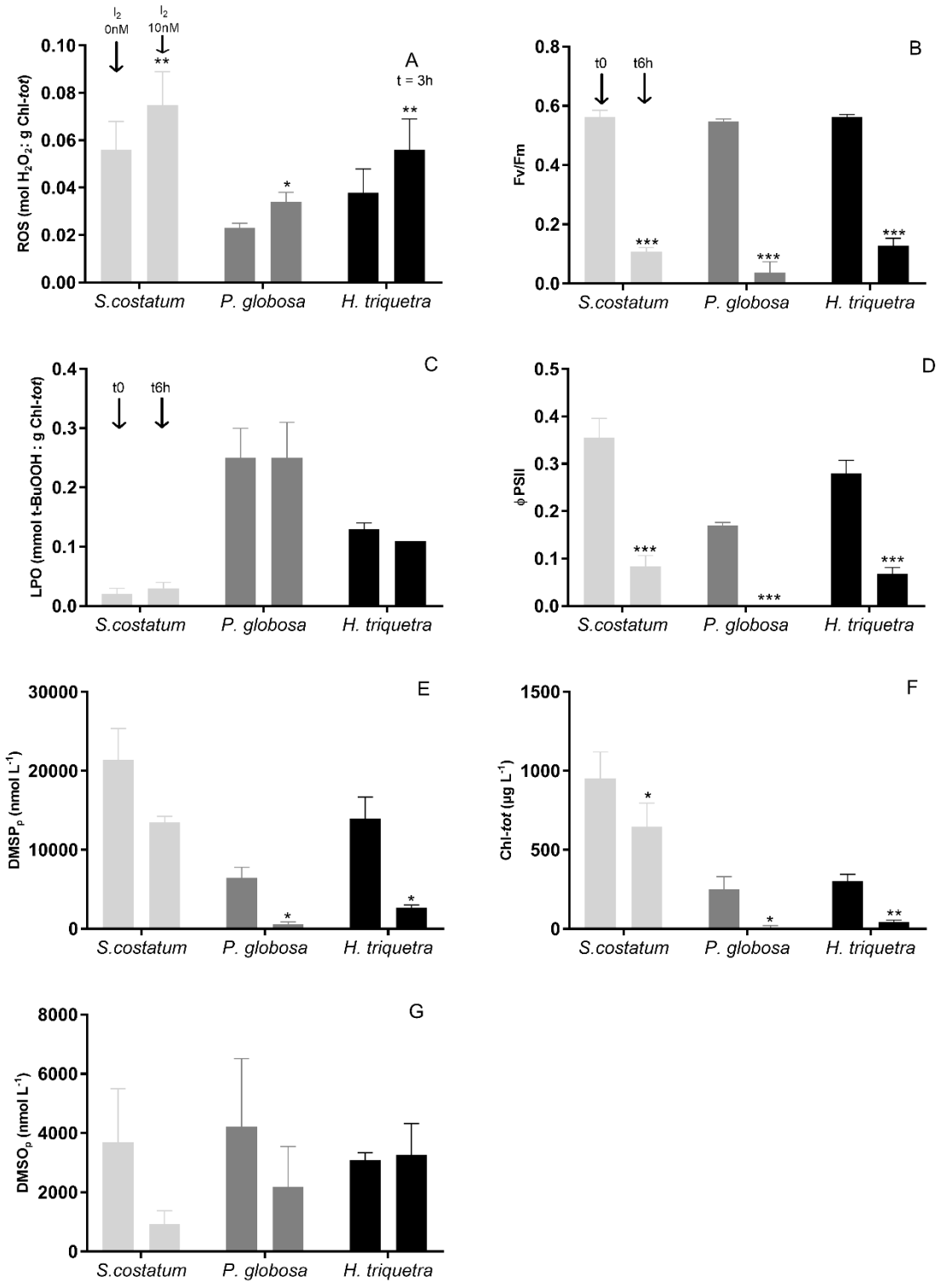

Figure 3-3: Evolution of (A) Reactive oxygen species (ROS) production (DCF-fluorescence:µg Chl-*tot*, (B) Maximum quantum yield of PSII (Fv/Fm), (C) Lipid Peroxidation (LPO) (mmol t-BuOOH:g Chl-*tot*), (D) Effective photochemical quantum yield of PSII (ΦPSII), (E) the $DMSP_p$:Chl-*tot* ratio (mmolS:g Chl-*tot*), (F) Chlorophyll-*tot* (Chl-*tot*) concentration (µg L^{-1}), and (G) the $DMSO_p$:Chl-*tot* ratio (mmolS:g Chl-*tot*) with 10 nmol L^{-1} DCMU + HL (1200 µmol photon $m^{-2}s^{-1}$) or in dark during 6h for the three species *S. costatum*, *P. globosa* and *H. triquetra*. Error bars represent SD calculated from triplicates biological samples. Asterisks denote significant differences between the two time-point (* $p < 0.05$; ** $p < 0.01$; *** $p < 0.001$).

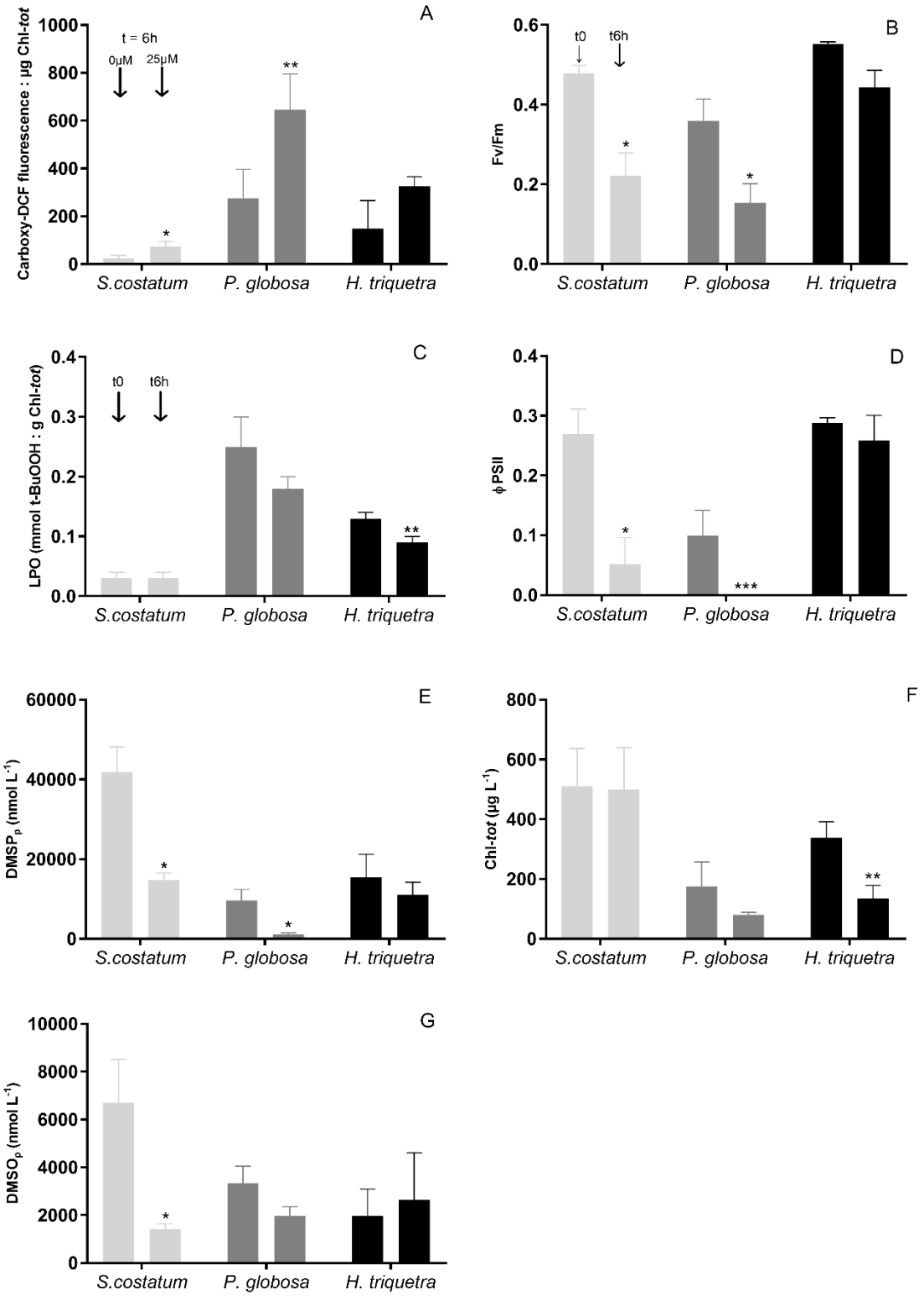

Figure 3-4: Evolution of (A) Reactive oxygen species (ROS) production (DCF-fluorescence:µg Chl-*tot*), (B) Maximum quantum yield of PSII (Fv/Fm), (C) Lipid Peroxidation (LPO) (mmol t-BuOOH:g Chl-*tot*), (D) Effective photochemical quantum yield of PSII (ΦPSII), (E) the $DMSP_p$:Chl-*tot* ratio (mmolS:g Chl-*tot*), (F) Chlorophyll-*tot* (Chl-*tot*) concentration (µg L^{-1}) and (G) the $DMSO_p$:Chl-*tot* ratio (mmolS:g Chl-*tot*) with 25 µmol L^{-1} MSB during 6h for the three species *S. costatum*, *P. globosa* and *H. triquetra*.. Error bars represent SD calculated from triplicates biological samples. Asterisks denote significant differences between the two time-point (* $p < 0.05$; ** $p < 0.01$; *** $p < 0.001$).

and DCMU controls (Fig. 3-5). Data related to the HL treatment (6h) were relatively well clustered, indicating that the cellular response to the treatment was similar between species. The same conclusion can be drawn for *H. triquetra* and *P. globosa* at the end of the treatment with DCMU, while *S. costatum* showed a more distinct response. And finally, the distribution of the data related to the MSB treatment was more scattered, indicating more species-specific responses to this treatment.

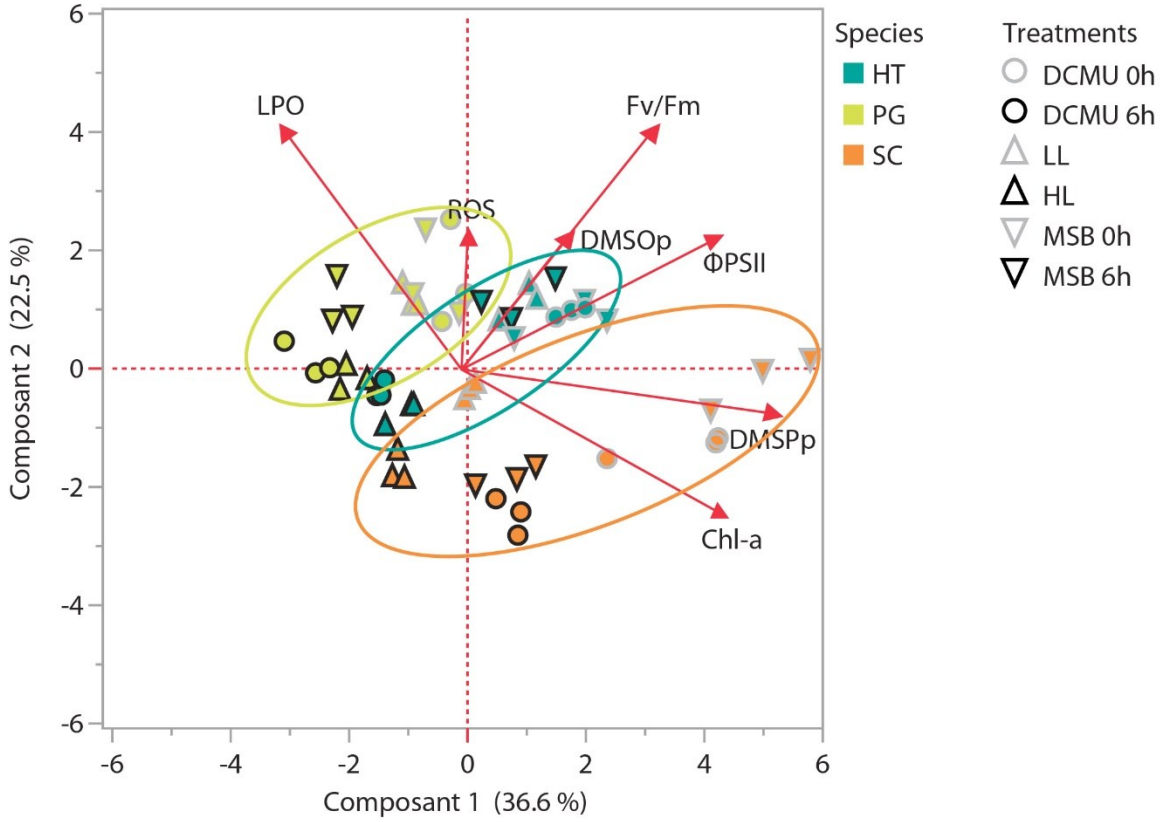

Figure 3-5: Principal component analysis (PCA) combining the three treatments at t0h and t6h for the short-term treatments and at I0 (LL) and I2 (HL) for the long-term HL treatment for the three species *S. costatum* (SC), *P. globosa* (PG) and *H. triquetra* (HT). The variables used are $DMSP_p$ and $DMSO_p$ concentrations, Reactive oxygen species concentration (ROS), Lipid peroxidation (LPO), Chlorophyll concentration (Chl), the maximum quantum yield of photosystem II (Fv/Fm) and the effective photochemical quantum yield of the photosystem II (ΦPSII).

5 Discussion

This study evaluated the impact of oxidative stress on $DMS(P,O)_p$ content in three phytoplankton species. ROS relative production is discussed further with no distinction between the methodologies used. Although all the experimental treatments did not impact $DMS(P,O)_p$ content in a similar way, short-terms oxidative stress (treatments with DCMU and MSB) were found to decrease DMSP, suggesting that this sulfur compound interacts with ROS.

5.1 $DMS(P,O)_p$ contents vary among phytoplankton species investigated.

As previously reported in the literature (i.e. Keller et al., 1989), $DMSP_p$:Chl-*a* ratios measured in control conditions (i.e. I0; 100 µmol photons m^{-2} s^{-1} and 15°C) were found to differ between species investigated, with the diatom possessing much less DMSP:Chl-*a* than the dinoflagellate and the Prymnesiophyceae. DMSP:Chl-*a* ratios measured in our cultures also agreed with previous studies conducted on *H. triquetra* (122.7 ± 27.7 mmolS:g Chl-*a* in average) and *P. globosa* (82.3 ± 11.5 mmolS:g Chl-*a*), maintained in similar environmental conditions (Keller et al., 1989; Niki et al., 2000; Speeckaert et al., 2018; 2019; Stefels et al. 2007). For *S. costatum*, values were similar to those of Speeckaert et al. (2018), who applied the same methodology on the same strain, but differed from other studies reporting lower DMSP:Chl-*a* ratio (4.5 to 11.8 mmolS:g Chl-*a,* in average; Sunda et al., 2007; Stefels et al., 2007; Spielmeyer et al., 2011; Speeckaert et al., 2019). The $DMSO_p$-to-chlorophyll-*a* ($DMSO_p$:Chl-*a*) ratios measured in this study were a bit higher than values reported in the literature, with 0.2 ± 0.2 for the diatoms, 1.5 ± 0.4 for the Prymnesiophyceae and 3.9 ± 4.3 mmolS:g Chl-*a* for the dinoflagellates (Simó et al., 1998; Hatton and Wilson, 2007; Bucciarelli et al., 2013; Speeckaert et al., 2019).

Reporting $DMS(P,O)_p$-to-Chlorophyll-*a* ratio is not convenient for oxidative stress experiments since the physiological conditions of the algal cells (i.e. growth stage) and the environmental constraints (i.e. salinity, temperature, nutrient limitation, and light intensity) were found to affect DMSP (Stefels, 2000; Sunda et al., 2002; Bucciarelli and Sunda, 2003) and chlorophyll cellular contents (Brunet et al., 2011). Since lugol-gluteraldehyde fixation caused significant changes in biomass predictions (Menden-Deuer et al., 2001), it is also preferable to report DMSP-to-cell ratio for studies focusing on the physiological roles of DMS(P,O).

Similar to $DMSP_p$:Chl-*a*, we observed much less $DMSP_p$:Cell for the diatom than for the Prymnesiophyceae or the dinoflagellate. Values of these ratios are in the same order of magnitude than those found in the literature, with an average ratio of 3.6 ± 0.1, 17.0 ± 1.0 and 605.6 ± 244.7 fmolS:cell for *S. costatum, P. globosa* and *H. triquetra*, respectively (Keller et al., 1989; Niki et al., 2000; Speeckaert et al., 2018; 2019). As the $DMSO_p$ comes from the oxidation of $DMSP_p$, it is not surprising that the trends observed between species for $DMSP_p$:Cell are similar for $DMSO_p$:Cell. Values obtained in this study was higher than data reported previously (i.e. 0.02 ± 0.01, 0.2 ± 0.1 and 23.9 ± 33.6 fmolS:cell for diatoms, Prymnesiophyceae and dinoflagellates; Simó et al., 1998; Hatton and Wilson, 2007; Bucciarelli et al., 2013; Speeckaert et al., 2019).

5.2 DMS(P,O) act as antioxidant compounds.

The experimental treatments involving changes in light intensity showed contrasting results. Three to six hours after the beginning of the HL treatment, cells from all species investigated displayed a sharp decrease of the photosynthetic efficiency (i.e. F_V/F_M and ΦPSII; Fig. 3-1A, B) indicating a photoinhibition phenomenon very likely caused by photodamages to PSII reactions centres (Murata et al., 2007). This physiological state is conducive to an increased production of ROS (Fig. 3-1C) potentially causing oxidative stress and important cellular damages. In this context, we would have expected increased levels of lipid peroxidation during the treatments, but those remained stable (Fig. 3-1D). Since the peroxidation of polyunsaturated fatty acids is mainly caused by $^1O_2$ and $OH^\bullet$ (Farmer and Mueller, 2013), we cannot rule out the possibility that $O_2^{\bullet-}$ and H_2O_2 were the main ROS produced during the treatment. It would have been interesting to also monitor other biomarkers of oxidative stress such as protein carbonylation or ubiquitination (Sharma et al., 2012; Roberty et al. 2016).

In contrast to the previous observation, the results of the DCMU+HL treatment indicate that cells suffered from oxidative stress. Indeed, ROS production was enhanced for the three species due to the strong inhibition of photosynthesis (Fig. 3-3A, B, D), and Chl-*tot* concentrations were drastically reduced (Fig. 3-3F). The concomitant decrease of $DMSP_p$ concentrations (Fig. 3-3E) suggests that these molecules are interacting with ROS and are part of the antioxidant network. In support of this assumption is the location of the DMSP production site within the chloroplasts (Raina et al., 2017; Curson et al., 2018) which is also the main cellular site impacted during the HL short-term treatments. The antioxidant properties of DMS(P,O) were also supported by the results obtained during the experimental treatment involving MSB. This molecule promotes the production of $O_2^{\bullet-}$ that will spontaneously or enzymatically be converted into H_2O_2 (Hassan and Fridovich, 1979), and $OH^\bullet$ in presence of transition metals (Apel and Kirt, 2004). The production of ROS by MSB occurs mainly in the cytosol but H_2O_2 can easily diffuse to the chloroplasts and cause damages to the photosynthetic apparatus. Indeed, as this experimental treatment was conducted in the dark, ROS produced by MSB were very likely the cause of the decline of the photosynthetic efficiency (i.e. F_V/F_M and ΦPSII in *S. costatum* and *P. globosa*; Fig. 3-4B, D). Although the Chl-*tot* content remained stable for the two species, $DMSP_p$ concentrations decreased significantly, further supporting the antioxidant role of these molecules. At the opposite, *H. triquetra* seemed not to suffer from MSB at this concentration. The reason of this result is very likely related to the cellulose thecae characterizing the armoured

H. triquetra (Caruana, 2010) that may act as a physical barrier decreasing the passive diffusion of the molecule within the cell, which is consistent with the higher concentration used on another dinoflagellate species by Roberty et al. (2016).

ROS produced in the cells can also act as signalling molecules. Thus, thanks to its relative stability and its half-life (1 ms; Møller et al., 2007), H_2O_2 can diffuse over a "large" distance within the cell and regulate gene expression by the activation of proteins signalling pathways associated with acclimation processes or programmed cell death (Sharma et al., 2012; Pospíšil, 2016). For instance, H_2O_2 formed in the thylakoid membranes can lead to the regulation of the PSII antennae size during the acclimation response (Borisova-Mubarakshina et al., 2015). ROS can also indirectly transmit a signal from the chloroplasts to the nucleus through products of protein oxidation or lipid peroxidation (Fischer et al., 2012). Data obtained during the long-term exposure to highest light intensity indicate that ROS produced early (see short-term HL treatment) led to photoacclimation in *S. costatum* and *P. globosa*, but to cell death in *H. triquetra*. Indeed, while *H. triquetra* was unable to grow at the highest light intensity, the two other species showed similar cellular density to the controls but a lower cellular Chl-*a* concentration (Fig. 3-2A, B). This last is part of a well-known strategy allowing photosynthetic cells to decrease the excitation pressure over the light harvesting complexes and photosystems (Brunet et al., 2011). It can also involve the adjustment of the relative amount of accessory pigments (Chl-*c* and fucoxanthin) or modifies the size and the number of photosynthetic units, thus changing photosynthetic capacity of the cell (Nymark et al., 2009).

The $DMSP_p$:Cell ratios of *S. costatum* were similar among the different light levels while it decreased at I1 (but not at I2) for *P. globosa*, demonstrating that cells of these two species have reached a new redox equilibrium thanks to the adjustment of the photosynthetic apparatus. Furthermore, while *H. triquetra* was characterized by a much higher $DMSP_p$:Cell ratio than the two other species, the dinoflagellate was not able to grow at I2 indicating that the cellular DMSP concentration do not provide any information about the antioxidant capacity of the cell to a subsequent oxidative stress (also suggested by the PCA, Fig. 3-5).

Further studies addressing the antioxidant role of DMSP should include other components of the antioxidant network (i.e. enzymatic antioxidants, carotenoids, and cellular buffers), the DMS(P,O) by-products (i.e. acrylate, methane sulfonate (MSA), methane sulfinic acid (MSNA), and DMS) and the DL activity to better understand their interactions (Stefels et al., 2007). For instance, recent findings demonstrated diatoms' ability to produce flavonoids which

display relevant antioxidant capacity and act as signalling compounds able to up-regulate cellular defences under high light intensity (i.e. at 600 µmol photons $m^{-2}s^{-1}$ during 6h) (Pietta, 2000; Goiris et al., 2015; Smerilli et al., 2019). The DL activity has also been correlated with photoprotective pigments (Steinke et al., 2002; Harada et al., 2004), higher light intensities encountered in the upper sea layer (Harada et al., 2004; Bell et al., 2007), and oxidative stress caused by a nitrogen limitation (Sunda et al., 2007). A better understanding of the mechanisms and the conditions controlling the activation of DL in phytoplankton should also be addressed to provide better insights on the involvement of this enzyme and DMSP in the regulation of the antioxidant network (Stefels et al., 2007).

The common technique for DMS(P,O) determination we applied in this study does not measure the fluxes between DMSP and its by-products (i.e. DMSO, DMS, acrylate, MSA and MSNA) (Stefels et al., 2007). Recent studies are now working with incorporation of stable isotope (D_2O or $NaH^{13}CO_3$) into DMSP to measure *de novo* DMSP synthesis rates (Stefels et al., 2009; Archer et al., 2018). Using this approach within natural communities, Archer et al. (2018) reported that DMSP production on a diel timescale was coupled to carbon fixation rather than being stimulated at high light intensity. This does not exclude the chemical reaction between DMSP and ROS but indicates that regulation of DMSP production is not linked to photooxidative stress (Archer et al., 2018).

5.3 Species ecological characteristics explain the experimental results.

In the concept of C-S-R model (Reynolds, 2006; revised by Glibert, 2016), which builds on Margalef's mandala model (Margalef, 1978), the phytoplankton succession is linked to the nutrient accessibility and light availability. The species investigated here stand out by their succession in temperate seas (Johns and Reid, 2001), in adequation with the previous ecological model. In the Southern North Sea, the diatom *S. costatum* (R-strategy; light stress tolerant) occurs in spring and autumn (Rousseau et al., 2002; Speeckaert et al., 2018); the Prymnesiophyceae *P. globosa* (C-strategy; fast growing when nutrients and light are highly available) blooms in late spring after the diatom efflorescence (Rousseau et al., 2002); and the dinoflagellate *H. triquetra* (S-strategy; nutrient stress tolerant) becomes abundant in coastal waters during summer (Smayda and Reynolds, 2001). The analysis of phytoplankton abundance time-series in the North Atlantic also showed that diatoms were most likely found in colder waters, rich in nutrients and at lower light intensities than the dinoflagellates (Irwin et al., 2012).

The photophysiological responses of our species are not fully in line with the supposed ecological traits. These observations can come from the high light treatment applied (i.e. 1200 µmol photons m^{-2} s^{-1}) that was not ecologically realistic, but species investigated were exposed to the same treatment and *S. costatum* and *P. globosa* were able to grow at the highest light treatment while *H. triquetra* was not. In support of this observation, Cooney et al. (2019) recently reported that *Heterocapsa rotundata* cells lysed during short-term experiments involving similar light levels. This may seem counterintuitive since the first two species occur mainly in spring, when the coastal waters are turbulent and the light intensity rarely exceeds 400 µmol photons m^{-2} s^{-1} (Flanders Marine Institute, 2019; Royer et al., 2021), and *H. triquetra* blooms in summer, when the light could be higher than 750 µmol photons m^{-2} s^{-1} at sub-surface (Anderson and Stolzenbach, 1985). Therefore, the occurrence of this species in summer could be related to various strategies, as the capacity to (1) perform diel vertical migration (Anderson and Stolzenbach 1985; Olli and Seppälä, 2001; Jephson et al., 2011) allowing to avoid excessive light intensity during the day; (2) synthesise mycosporine-like amino acids (MAAs) (Korbee et al., 2010), acting as UV filters (Neale et al., 1998) or antioxidants (Shick and Dunlap, 2002).

Consequently, for *P. globosa*, which is a colonist taxa (C-strategy) that grows fast in areas where nutrients and light are richly available (Reynolds, 2006), its absence during summer months is not related to its capacity to tolerate high light intensity but results from the low nutrient concentration during this period (Lancelot et al., 1998).

Finally, *S. costatum* managed to survive and grow during each treatment, displaying the greatest physiological plasticity from the three species investigated. This plasticity might be interpreted as a functional trait that contributes to its ecological success (Dimier et al., 2007) in the turbulent and well-mixed area of the Southern Bight of the North Sea (Rousseau et al., 2002). Considered as a R-strategist and able to efficiently harvest light, this species might also quickly adjust its photosynthetic apparatus to support sudden light intensity changes. The physiological plasticity observed for *S. costatum* is determining and may explain the ecological success of this group (Dimier et al., 2007; Smerilli et al., 2019), that are present in a wide range of habitats, from fresh to marine waters (Fritsch, 1971), or even in the brine channels of sea ice (Trevena et al., 2000).

6 Conclusions

This study highlights that cellular $DMS(P,O)_p$ contents decrease when cells of key phytoplankton species are subjected to ROS-generating high-light and chemically-induced stresses; thus supporting the antioxidant function of these molecules. However, the initial $DMS(P,O)_p$ concentrations were found to vary between species investigated and were not indicative of the capability of the cell/species to tolerate a subsequent oxidative stress. Furthermore, DMS(P,O) cellular content were not increased in HL grown cells (i.e. long-term treatment). Overall these results suggest that these molecules have the ability to lower cellular ROS concentration during an oxidative stress. Further studies monitoring more constituents of the antioxidant network (i.e. enzymes, carotenoids, redox buffer) along with the metabolic pathway of DMSP (DMS(P,O) by-products and DL activity) are however needed to better grasp the cellular functions of DMSP.

7 Acknowledgments

This project has received funding from the European Union's Horizon 2020 research and innovation programme under the Marie Skłodowska-Curie grant agreement No 766327, the European Research Council (ERC; H2020-EU BEAL project No 682580) and the Belgian Fonds National de la Recherche Scientifique (FNRS; 2.4.637.10; CDR J.0014.18). NG and CR received financial support from the Fonds David et Alice Van Buuren. CR is FRIA grantee while PC and AVB are senior research associate and research director at the FNRS, respectively.

8 Appendix

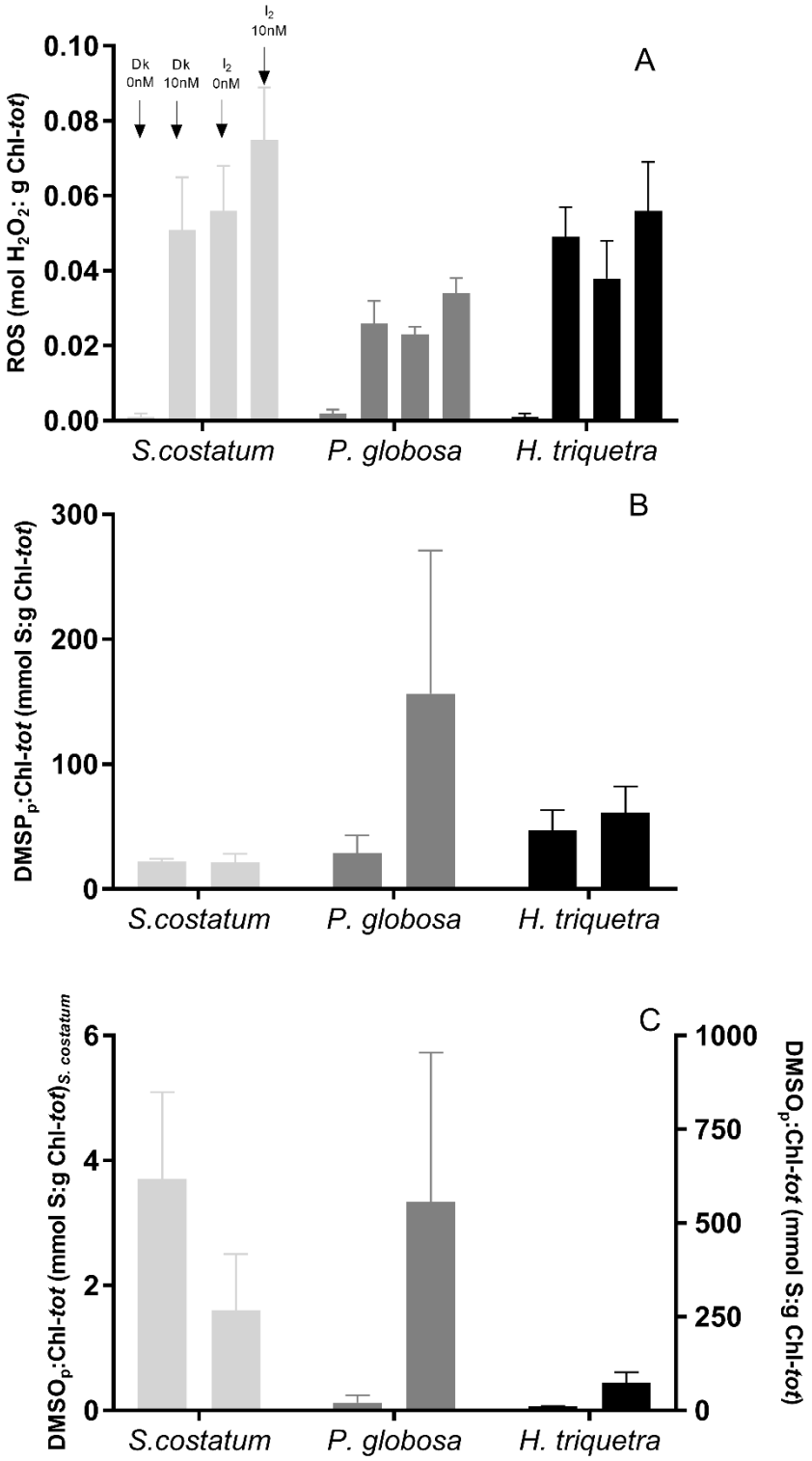

Figure Supp. 3-1: Evolution of (A) Reactive oxygen species (ROS) production (DCF-fluorescence:µg Chl-tot, (B) $DMSP_p$ (nmol L^{-1}), (C) $DMSO_p$ concentrations (nmol L^{-1}) with 10 nmol L^{-1} DCMU + HL (1200 µmol photon $m^{-2}s^{-1}$) or in dark during 6h for the three species *S. costatum, P. globosa* and *H. triquetra*. Error bars represent SD calculated from triplicates biological samples. Asterisks denote significant differences between the two time-point (* $p < 0.05$; ** $p < 0.01$; *** $p < 0.001$).

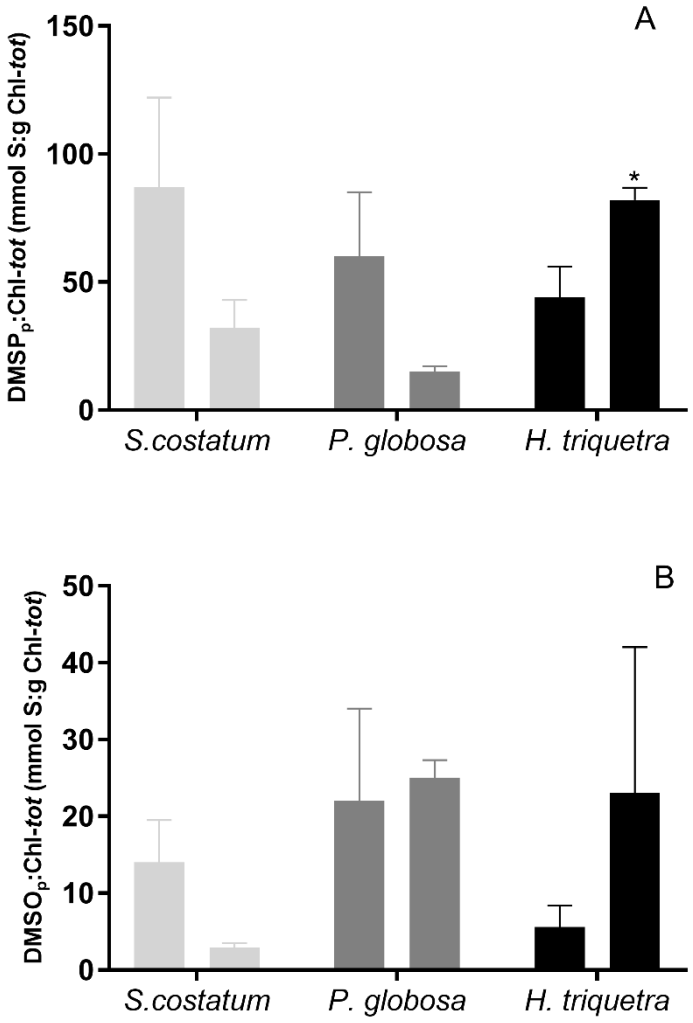

Figure Supp. 3-2: Evolution of (A) $DMSP_p$ (nmol L^{-1}) and (B) $DMSO_p$ concentrations (nmol L^{-1}) for the *S. costatum, P. globosa* and *H. triquetra* with 25 µmol L^{-1} MSB during 6h. Error bars represent SD calculated from triplicates biological samples. Asterisks denote significant differences between the two time-point (* $p < 0.05$; ** $p < 0.01$; *** $p < 0.001$).

Table Supp. 3-1: Averaged cellular density for the three species during the DCMU treatment. Data are expressed in 10^6 cells mL^{-1}. SD into brackets calculated from triplicates biological samples (Dk : Dark; HL: high light). Paired samples student t-test associated with comparison between t0h and t6h or between controls samples (Dk at t6h) and the treatments at t6h. Asterisks denote significant differences between the two time-point (* $p < 0.05$; ** $p < 0.01$; *** $p < 0.001$).

	T0	**T6h (Dk)**	**T6h (HL)**	**T6h (DCMU+HL)**
S. costatum	17.35 (1.45)	20.90 (1.00)	20.90 (1.00)	23.64 (4.87)
P. globosa	7.06 (0.48)	6.56 (2.07)	6.88 (0.88)	7.73 (0.51)
H. triquetra	6.66 (1.70)	11.29 (1.85)	9.33 (2.98)	11.09 (2.22)

Paired samples Student t-test		**T6h**	**P value**
S. costatum	T0h	Dk	0.061
		HL	0.061
		DCMU+HL	0.090
	Dk	HL	
		DCMU+HL	0.393
P. globosa	T0h	Dk	0.735
		HL	0.784
		DCMU+HL	0.054
	Dk	HL	0.871
		DCMU+HL	0.496
H. triquetra	T0h	Dk	0.039*
		HL	0.070
		DCMU+HL	0.006***
	Dk	HL	0.319
		DCMU+HL	0.856

Chapter IV – Drivers of the variability of DMSP and DMSO in the Southern North Sea

« Avec la mer du Nord pour dernier terrain vague
Et des vagues de dunes pour arrêter les vagues
Et de vagues rochers que les marées dépassent
Et qui ont à jamais le cœur à marée basse […] »

- Jacques Brel (1962).

Drivers of the variability of dimethylsulfoniopropionate (DMSP) and dimethylsulfoxide (DMSO) in the Southern North Sea

C. Royer[1,2*], A.V. Borges[2], J. Lapeyra Martin[1], & N. Gypens[1]

[1]Laboratoire d'Ecologie des Systèmes Aquatiques, Université Libre de Bruxelles, CP221, Boulevard du Triomphe, Brussels 1050, Belgium

[2]Unité d'Océanographie Chimique, Institut de Physique (B5A), Université de Liège, Liège 4000, Belgium

*corresponding author : croyer@ulb.ac.be

Keywords: Dimethylsulfoniopropionate – Dimethylsulfoxide – Phytoplankton diversity – Southern North Sea

Status: Published in **Continental Shelf Research (CSR)** : https://doi.org/10.1016/j.csr.2021.104360

1 Abstract

The influence of abiotic and biotic factors on the concentration of dimethylsulfoniopropionate (DMSP) and dimethylsulfoxide (DMSO) was investigated and compared during two annual cycles in 2016 and 2018 in the Belgian coastal zone (BCZ) in the southern North Sea at five fixed stations. These stations covered a near-offshore gradient from stations close to the mouth of the Scheldt estuary to most offshore stations. Significant differences of Chlorophyll-*a* (Chl-*a*) concentrations were observed between the two years with higher values in early spring 2018 (due to better light and nutrient conditions coupled to colder temperatures) and in summer 2018 (due to warmer conditions) compared to 2016. Nevertheless, the seasonal and spatial DMSP and DMSO (DMS(P,O)) patterns, as well as the yearly average were nearly identical in 2016 and 2018. This can be explained by the fact that the phytoplankton groups responsible for the large differences in Chl-*a* in 2018 and 2016 were low DMSP-producers characterized by several diatom and dinoflagellate species, occurring in early spring and summer. Further, the Prymnesiophyceae *Phaeocystis globosa*, occurring in late spring and responsible of most of DMS(P,O) measured in the area, reached similar biomass both years. The DMSP:Chl-*a* ratio obtained from the field measurements were similar to those previously published for the main observed phytoplankton groups, but more differences were observed for the DMSO:Chl-*a* ratio. DMS(P,O) estimations based on Chl-*a* linear regressions for the whole dataset need to account on two relationships discriminating the low and high-DMSP producing species.

2 Introduction

Dimethylsulfoniopropionate (DMSP; $(CH_3)_2S^+CH_2CH_2COO^-$) and dimethylsulfoxide (DMSO; $(CH_3)_2SO$) are organic sulfur compounds produced by numerous species of marine micro-algae. DMSP is the main precursor of the climate active gas dimethylsulfide (DMS) that once in the atmosphere might affect the Earth's radiative budget (Charlson et al., 1987; Quinn and Bates, 2011). Prymnesiophyceae and dinoflagellates are high-DMSP producers, and the low-DMSP producers include some members of Chrysophyceae and diatoms (Keller et al. 1989; McParland and Levine, 2019). The intracellular physiological functions of DMS(P,O) are still poorly understood. DMSP might play roles such as antioxidant (Sunda et al., 2002), cryoprotector, osmolyte (Kirst et al. 1991; Bucciarelli and Sunda, 2003), methyl donor (Kirst, 1996), zooplankton deterrent (Wolfe et al., 1997; Strom et al., 2003), or signaling compound (Stefels, 2000; Seymour et al., 2010). DMSO could be involved in a complex cascade reaction in the antioxidant system alongside with DMS and acrylate (Sunda et al., 2002). The DMS(P,O) production by marine micro-algae varies considerably depending on the growth stage, salinity, temperature, nutrient availability, and light intensity. Seawater phytoplankton diversity is the factor that affects the most DMSP production (Townsend and Keller, 1996; Stefels et al., 2007). Phytoplankton composition and its seasonal succession might depend on the seasonal change in day length (Litchman and Klausmeier, 2001), although water temperature has been found to be the most significant factor affecting the phytoplankton community structure in some parts of the globe (Suikkanen et al., 2007). Changes in temperature will affect the growth-irradiance relationship (Edwards et al., 2016) and the competitive dominance of algal communities (Striebel et al., 2016) which is a key factor for the species' composition (Schabhüttl et al., 2013). In deeper pelagic systems, the influence of increasing temperature on thermal stratification induces an increase in light availability that is usually the phytoplankton bloom trigger (Wiltshire et al., 2008; Sommer et al., 2012). In well-mixed coastal waters, stratification rarely plays a role, and the amount of light will be the limiting factor rather than the nutrients concentration (Wiltshire et al., 2008). The spring phytoplankton seasonal succession will also depend on the Sea Surface Temperature (SST) during winter influencing the overwintering zooplankton and its grazing pressure (Sommer and Lewandowska, 2011).

SST has increased in the North Sea since the 1980s affecting the physiology, abundance, and phenology of marine phytoplankton (Richardson and Schoeman, 2004; Hunter-Cevera et al., 2016; Barton et al., 2018). In addition, high anthropogenic loads of inorganic nutrients (nitrogen

and phosphorus) led to important phytoplankton blooms and biomass in most coastal zones between March and October (Desmit et al., 2019). In the Southern North Sea, the Belgian Coastal Zone (BCZ) is a eutrophic and well-mixed area under the influence of the Scheldt and the Rhine rivers. It is characterized by a very high phytoplankton biomass and three phytoplankton blooms: (1) the first occurs in late February-March with diatoms, (2) directly followed by a huge biomass peak of *Phaeocystis globosa* in April-May, and (3) another diatom bloom at the end of summer-beginning of autumn (Rousseau et al., 2002). This phytoplankton taxonomic succession was very constant from 1988 to 2000 despite the variability in salinity, temperature, and light (Rousseau et al. 2002). The onset of the diatom spring bloom in the BCZ is dependent on a specific light threshold. Furthermore, the adaptation to low irradiance and temperature prevailing in late winter-early spring coupled with high nutrient concentrations explains the first diatom bloom, followed by *Phaeocystis globosa* when the ambient dissolved silicate is depleted (Rousseau et al., 2002). *Phaeocystis globosa* blooms are responsible for 95% of the phytoplankton late spring community biomass (Rousseau et al., 1990, 2000). Yet, since 1990, de-eutrophication measures have led to the decrease of nutrient concentrations in coastal waters of the Southern North Sea (van Beusekom et al., 2009; Prins et al., 2012). Both the warming and the de-eutrophication trends may have an impact on the long-term annual mean of Chl-*a* (Desmit et al., 2019) and the phytoplankton community (Nohe et al. 2020). This should also affect the DMS(P,O) concentrations, since they strongly depend on phytoplankton composition and biomass, as shown by a modelling study in the area (Gypens et al. 2014). A better understanding of the intracellular DMS(P,O) concentration in response to external drivers or phytoplankton diversity could improve their prediction, and ultimately the related DMS emissions with its potential climate effect (Charlson et al., 1987).

This study presents an interannual comparison of DMS(P,O) concentrations measured in the BCZ in 2016 and 2018 on a regular grid of 5 fixed stations. The year-to-year variation was analyzed in light of nutrient concentrations, SST, and light availability; the key factors influencing the phytoplankton production and community structure in general and in the study area (Nohe et al., 2020). The phytoplankton composition was studied for both years to investigate the possible variations on species dominance and biomass, and corresponding impact on the DMS(P,O) content.

3 Material and Methods

3.1 Field sampling

Sampling was carried out on the *RV Simon Stevin* in 2016 and 2018 at 5 fixed stations chosen to cover a near-offshore gradient from station 700 (close to the Scheldt estuary) to the most marine station (ZG02) covering a major part of the BCZ (Fig. 4-1). The data from 2016 were published in Speeckaert et al. (2018). The samples were collected each month through the year and twice a month between March and May during the spring phytoplanktonic bloom. Seawater samples were collected at 3 meters depth using 4L Niskin bottles on a rosette sampler attached to a Conductivity-Temperature-Depth (CTD) probe (Seabird SBE25), for further analysis of Chl-*a*, DMS(P,O) concentrations and DNA extraction. The abiotic measurements at 3 meters depth of SST, sea-surface salinity (SSS), suspended particulate matter (SPM), photosynthetic active radiation (PAR) and nutrients concentrations were carried out by the Vlaams Instituut voor de Zee (VLIZ) in the frame of the LifeWatch sampling campaigns (http://rshiny.lifewatch.be/Station%20data/) (Flanders Marine Institute, 2019) with the methodology found in Mortelmans et al. (2019). The daily global solar radiation data was collected at the Oostende station of the Royal Meteorological Institute of Belgium and allowed us to calculate the surface incident PAR.

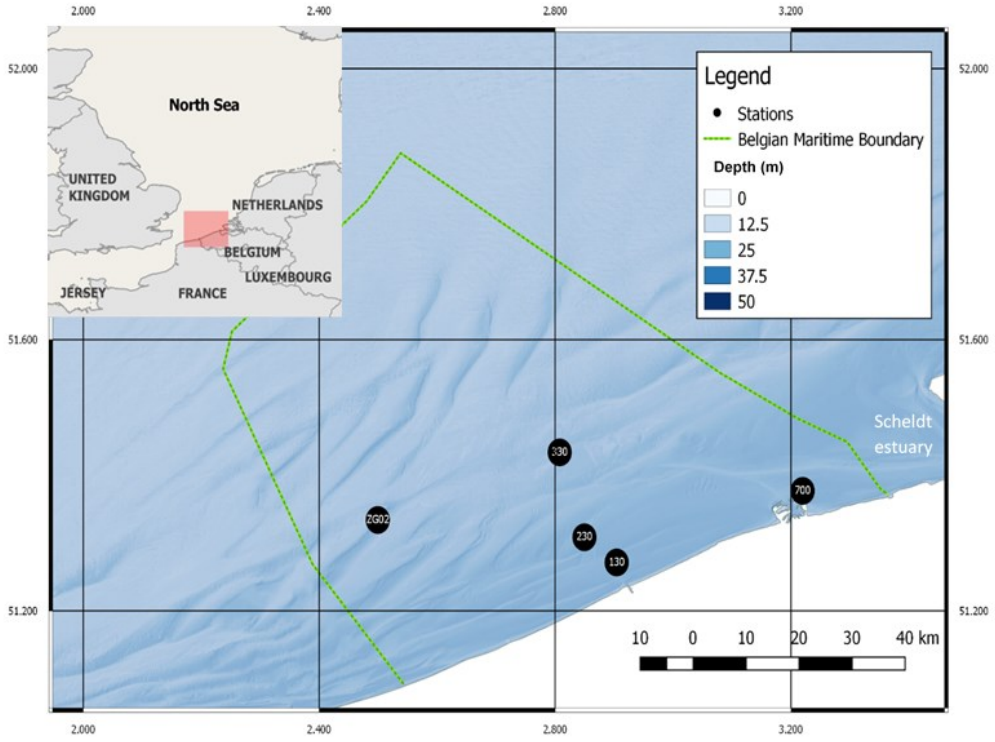

Figure 4-1: Map of the sampling area with the five key stations (black circle) and the bathymetry (m) in the Belgian Coastal Zone (BCZ, North Sea).

3.2 Chlorophyll-*a*

A determined volume of the seawater collected was filtered on Whatman glass microfiber filters GF/F 25 mm. The filters were immediately frozen and stored at -20°C until analysis (within 1 month after sampling). Chl-*a* (µg L^{-1}) was then extracted at 4°C in 90% acetone (v:v) and measured fluorometrically using a Kontron Instruments SFM 25 (Strickland and Parsons, 1972).

3.3 Phytoplankton diversity

In 2016 and 2018, samples from station 330 were fixed with lugol-gluteraldehyde (1% v:v) and stored at 4°C for species identification and cell density measurements by using inverted microscope. The station 330 is representative of the area (Rousseau et al., 2002). In 2018, DNA was sampled from March to December for the five stations. The DNA was collected by filtering seawater on 0.2 µm 47 mm polycarbonate Durapore filters (Tynes, 2013). The filter was preserved at -80°C. DNA was extracted using *DNeasy Plant Qiagen* following manufacturer's protocol and libraries were prepared. 18S rDNA amplicon sequencing was performed using Illumina MiSeq sequencer which produced 2x300 bp paired-end sequences. Decomplexed sequences were analyzed using R software package *phyloseq* (McMurdie and Holmes, 2013) and the taxonomic annotation database used was *Silva 1.32*. The phytoplankton diversity was investigated based on several assumptions: (1) non-autotrophic kingdoms were removed; (2) as well as the unclassified genera by *Silva*; (3) Operational Taxonomic Units (OTUs) with same taxonomic annotations were merged; (4) singletons and genera not seen more than 3 times in at least 10% of the samples were eliminated; (5) the 50 most abundant genera were chosen to analyze the phytoplankton diversity over time.

The DMS(P,O):Chl-*a* ratio were recalculated from published data (Table 1, 2; Keller et al., 1989b; Townsend and Keller, 1996; Simó et al., 1998; Hatton and Wilson, 2007; Bucciarelli et al., 2013; Cooney, 2016; Cooney et al., 2019; Speeckaert et al., 2018; 2019; McParland and Levine, 2019; Royer et al. *in review*). The carbon per cell was calculated from cell volumes found in the literature or with the median cell volumes from Olenina et al. (2006), and according to the formula given by Menden-Deuer and Lessard (2000). The biomass was converted to Chl-*a* per cell assuming the C:Chl-*a* ratio of 60 g g^{-1} (Geider, 1987).

3.4 DMS(P, O) analysis

The 60 mL borosilicate glass vials were acid-washed (HCl 10%) and rinsed with high purity water obtained from a milli-Q system. The vials were covered with aluminum foil and baked at

350°C for at least 1h in a muffle furnace before the sampling (Kiene and Gerard, 1994). The 25 mm Whatman glass microfiber filters GF/F were baked at 450°C for 4h (Kiene and Slezak, 2006). Intracellular DMS(P,O) ($DMS(P,O)_p$) were obtained by the difference between 10 mL of unfiltered seawater samples (total DMS(P,O) ($DMS(P,O)_t$)) and dissolved DMS(P,O) ($DMS(P,O)_d$). $DMS(P,O)_d$ was obtained by gentle filtration of 15 mL and only the first 10 mL filtrate was collected to avoid cell destruction at the end of the filtration that could release DMSP (Kiene and Slezak, 2006). All the samples were microwaved individually at 900 W till boiling (~15sec) (Kinsey and Kieber, 2016) and then acidified with 5 µL mL^{-1} of 50% H_2SO_4 (del Valle et al. 2011). The acid stopped the biological activity and preserved the DMSP (Curran et al, 1998). The acidification may produce rapid conversion of DMSP to DMS and presumably acrylate, inducing substantial losses of DMSP (del Valle et al. 2011). But Kinsey and Kieber (2016) have recently observed that microwaving samples to boiling point are an alternative method for sample preservation prior to the addition of acid. The samples were crimped after cooling with gas-tight PFTE coated silicone septa and stored 24h at dark before the refrigerator to allow the DMS to degas or oxidize (Kiene and Slezak, 2006).

The samples were sparged to remove the potential DMS left for 20 min. 5 mL of 12 M NaOH were added to the 10 mL samples to obtain a pH > 12 and quantitatively cleave DMSP into DMS for 24h (Dacey and Blough, 1987; Stefels, 2009). An Agilent 7890B gas chromatography with a purge and cryogenic trap system (Agilent column 30 m long, 0.32 mm internal diameter, 0.25 µm film thickness) was applied to analyze the DMS released. The GC was equipped with sulfur selective Flame Photometric Detector (FPD) and the carrier gas was He (2 ml min^{-1}). The FPD was kept at 350°C with a H_2 flow of 72 ml min^{-1}, a synthetic air flow of 72 ml min^{-1} and a makeup (N_2) flow of 20 ml min^{-1}. The capillary column was kept at 60°C. DMS was quantitatively purged from the vial by the He flow carried through a long stainless-steel needle inserted through the septum into the liquid phase and during 20 min. The DMS flew through two Dewar maintained cold around -30°C with liquid nitrogen to trap residual water vapor (Andreae and Barnard, 1984). The DMS is then trapped in a PFTE loop immersed in liquid nitrogen (-196°C). At the end of the purge, the loop was transferred in boiling water and the DMS is injected in the GC.

For the DMSO analysis, 5 mL HCl 37% (HCl 37% Normapur, VWR) and 1 mL $TiCl_3$ (30%, Merck) (Kiene and Gerard, 1994; Deschaseaux et al, 2014) were added into the precedent vial yet analyzed. Even if we consider the reaction efficiency < 100%, it will not interfere with the

analysis since the system is calibrated against DMSO standards, assuming the same reduction efficiency for both standards and samples (Champenois and Borges, 2019). After 48h at room temperature, 3 mL of 12 M NaOH were added to avoid injecting acid fumes into the GC (Kiene and Gerard, 1994). The DMS produced from the reduction of DMSO was analyzed as described previously. The DMS(P,O) quantified in arrow in the same sample was validated by Champenois and Borges (2019). The same procedure was applied for the calibration. The DMSP used was obtained from Research Plus and the DMSO from 99.9% pure stock solution (Merck). Working solutions were prepared with the successive dilution in MilliQ water but DMSP and DMSO were diluted in the same vial. Calibration curves were made weekly to ensure the GC stability for the detector by fitting a quadratic curve for the FPD. The average precision was 5 and 8% for DMSP and DMSO calibration, respectively. Any leaks during the analysis were detected by using a Thermo Scientific GLD Pro Gas Leak Detector every day.

3.5 Statistical analysis

The statistical comparison of the variables between the two years was performed using the parametric paired-samples Student t-test. The assumption of normality was checked using the Shapiro-Wilk test and the Q-Q plot. In case of deviation of the normality ($p < 0.05$), the Wilcoxon t-test was applied. To investigate the correlation between the variables, the Pearson's *r* coefficient and its *p* value was used. In case of deviation of normality by the Shapiro-Wilk test ($p < 0.05$) and the Q-Q plot, the non-parametric Spearman's ρ coefficient was applied.

The Kaiser-Meyer-Olkin index (> 0.50) and Bartlett sphericity test ($p < 0.05$) were used to ensure the application of Principal Component Analysis (PCA) for which we assumed the application of an Oblimin rotation. The principal components (PCs) have to explain at least 50% of the total percentage of variance between all the variables. The loading component (LC) explaining the correlation between the PC and the variable was considered significant when $\geq \pm 0.60$. These statistics were realized using the IBM SPSS Statistics software (version 23.0.0.0) and the assumptions were based on Goss-Sampson (2018).

4 Results and discussion

The years 2016 and 2018 were characterized by the typical phytoplankton succession for the area (Rousseau et al., 2002) with an early spring diatom bloom followed by a huge *Phaeocystis globosa* (here after *Phaeocystis*) bloom. Yet, in early spring, Chl-*a* concentrations for the coastal stations were higher in 2018 than 2016. A summer diatom bloom was also observed during both years, with higher Chl-*a* concentrations in 2018 compared to 2016.

4.1 Spring phytoplankton bloom

As previously described in the BCZ (Rousseau et al., 2002), the *Phaeocystis* bloom occurred at the end of April both in 2016 and 2018. The values were not significantly different between the two years with an average Chl-*a* concentration of 13.6 ± 6.0 µg L^{-1} and 15.7 ± 7.8 µg L^{-1} in 2016 and 2018 respectively ($p = 0.653$) (Fig. 4-2).

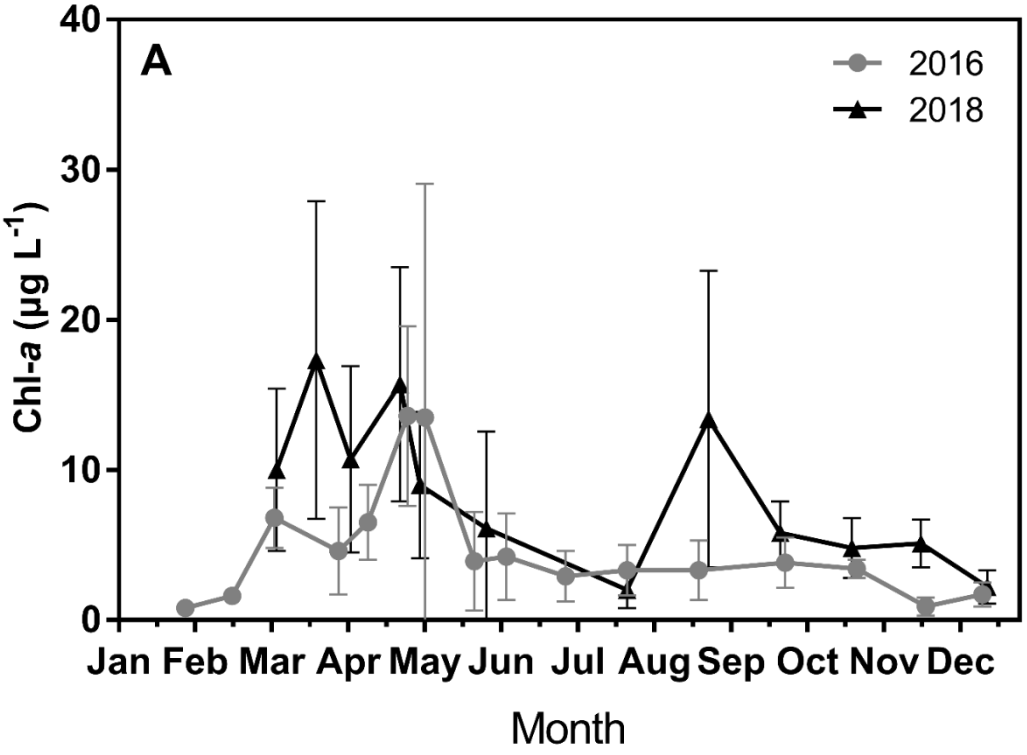

Figure 4-2: Seasonal evolution of average (± standard deviation) Chlorophyll-*a* (Chl-*a*) concentration (µg L^{-1}) for the five stations sampled in the Belgian coastal zone in 2016 and 2018. Location of the sampling stations are shown in Figure 4-1.

However, both years differed significantly with respect to the early spring bloom of diatoms occurring during the month of March in 2016, and from the first days of March until early April in 2018 (5.6 ± 2.6 and 12.8 ± 8.0 µg L^{-1} respectively; $p < 0.05$) (Fig. 4-2). The higher Chl-*a* values were due to the Chl-*a* concentrations from the coastal stations (700, 130, and 230) (Fig. 4-3a, b) with an average Chl-*a* at these three stations and for the diatom bloom period of 6.9 ± 1.9 and 16.7 ± 7.5 µg L^{-1} for 2016 and 2018 respectively ($p = 0.073$).

We tested if differences in light intensity, SST and nutrient concentrations might be responsible of the earlier and higher diatom spring bloom in 2018 compared to 2016. The light availability

is the primary control on spring phytoplankton onset in the North Sea (Wiltshire et al., 2008) and depends on the combination of incoming solar radiation and the SPM content that attenuates light penetration. During the early diatom bloom, SPM for the coastal stations was significantly higher in 2018 (173.3 ± 32.1 mg L^{-1}) than 2016 (48.7 ± 53.2 mg L^{-1}) ($p < 0.01$) (Fig. 4-3i, j). However, the incident light was more favorable in 2018 and allowed an earlier onset of the diatom bloom (Rousseau, 2000) (Pearson's correlation between Chl-*a* and incident light, $p < 0.05$). The incoming PAR was indeed 1.5 times higher in February 2018 than 2016 (204.2 ± 85.9 and 137.6 ± 81.6 µE $m^{-2}s^{-1}$ respectively; $p < 0.001$) (Fig. 4-3o).

SST for the coastal stations was less favorable for the diatom growth (Montagnes et al., 2001) in February 2018 (5.3 ± 0.5°C) than in 2016 (6.5 ± 0.2°C) ($p < 0.05$) and during the bloom in 2018 (4.2 ± 2.2°C) than 2016 (7.6 ± 1.0°C) ($p = 0.063$) (Fig. 4-3m, n). The SST in winter 2018 was the lowest during the last 13 years (Borges et al., 2019). Nevertheless, lower temperature during winter-spring bloom period might induce higher phytoplankton biomass resulting from a lower grazing rate of the zooplankton (Sommer and Lewandowska, 2011).

In addition, we observed a higher nutrient supply coming from the Scheldt estuary during the early blooming period with SSS lower in 2018 than in 2016 (30.9 ± 1.3 and 32.9 ± 1.8 respectively; $p = 0.086$) (Fig. 4-3c, d). The DIN concentration was higher in 2018 than in 2016 with respectively 45.8 ± 9.6 and 19.6 ± 17.9 µmol L^{-1} ($p = 0.084$) (Fig. 4-3k, l) and PO_4 concentration was significantly differentiated with 0.6 ± 0.2 and 0.2 ± 0.2 µmol L^{-1} ($p < 0.05$) (Fig. 4-3g, h). The DSi concentration was not significantly different even if we also observed higher values with 16.3 ± 4.7 in 2018 and 4.3 ± 5.1 µmol L^{-1} in 2016 ($p = 0.250$) (Fig. 4-3e, f).

In conclusion, the timing of the early spring diatom bloom in 2018 compared to 2016 seems to be the result of better light conditions in late winter. Furthermore, the higher biomass observed during the blooming period might be the consequence of higher nutrient concentrations and possibly lower zooplankton grazing resulting from lower SST.

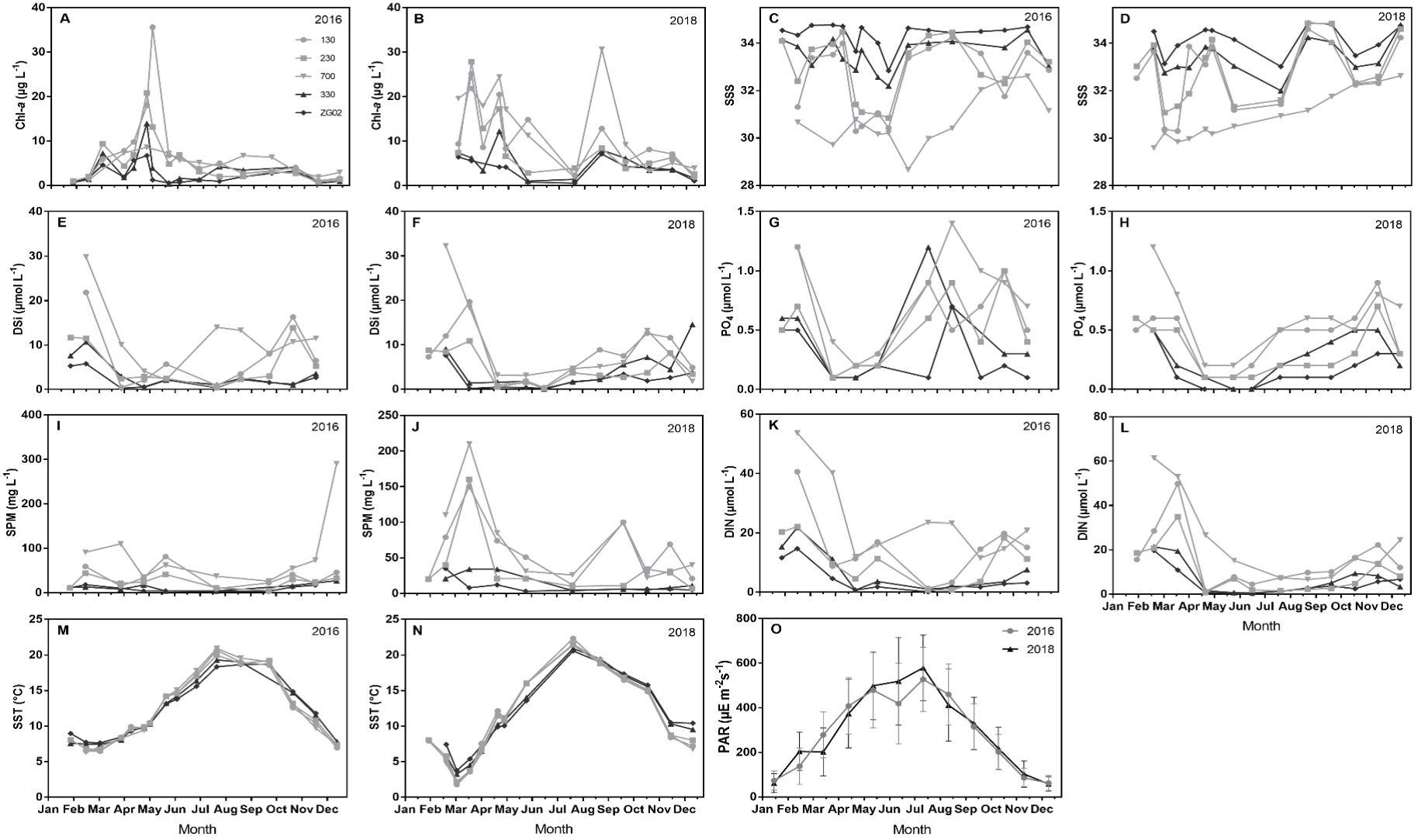

Figure 4-3: Seasonal and spatial evolution of (a) Chlorophyll-*a* (Chl-*a*) concentration (µg L^{-1}) in 2016, (b) in 2018; (c) Sea Surface Salinity (SSS) in 2016, (d) in 2018; (e) Dissolved Silica (DSi) concentration (µmol L^{-1}) in 2016, (f) in 2018; (g) phosphate (PO_4) concentrations (µmol L^{-1}) in 2016, (h) in 2018; (i) Suspended Particulate Matter (SPM) (mg L^{-1}) in 2016, (j) in 2018; (k) Dissolved Inorganic Nitrogen (DIN) concentration (µmol L^{-1}) in 2016, (l) in 2018; (m) Sea Surface Temperature (SST) (°C) in 2016, (n) in 2018; and (o) seasonal evolution of daily averaged Photosynthetic Active Radiation (PAR) (µE $m^{-2}s^{-1}$) for the five stations sampled in the Belgian coastal zone in 2016 and 2018 (Fig. 4-1).

The relative cellular density (%) was analyzed in 2016 and 2018 for the station 330, representative for the BCZ area (Rousseau et al., 2002). For March 2016, diatoms represented ~40% and *P. globosa* ~60% (Fig. 4-4). In April 2016, the relative abundance of the Prymnesiophyceae increased up to 96% while the diatoms decreased to 4% (Fig. 4-4). At the beginning of May 2016, *P. globosa* still represented 99% while only 1% of diatoms characterized the phytoplankton community (Fig. 4-4). In May 2018, the phytoplankton community was represented by 94% of *P. globosa* and 3% of diatoms (Fig. 4-4). The dinoflagellates were for both years almost absent for this period (< 0.2%). With genomic data, we can additionally explore the phytoplankton composition during the early spring bloom for the station 330. The diatom community was mainly composed by the genus *Thalassiosira,* including *T. rotula, T. tenera* and *T. lundiana*, as well as *Guinardia delicatula, Rhizosolenia shubsholei* and *Minutocellus polymorphus.* Some diatom genera from 2016 were not observed in 2018 such as *Asterionella, Coscinodiscus, Thalassionema, Biddulphia* and *Nitzschia*. The dinoflagellates observed were the species *Heterocapsa rotundata* and *Karlodinium veneficum*. Other species such as *Gyrodinium aureolum, G. spirale, Sinophysis sp., Tripos fusus, Katodinium glaucum*, or *Warnowia* sp. among others were also detected.

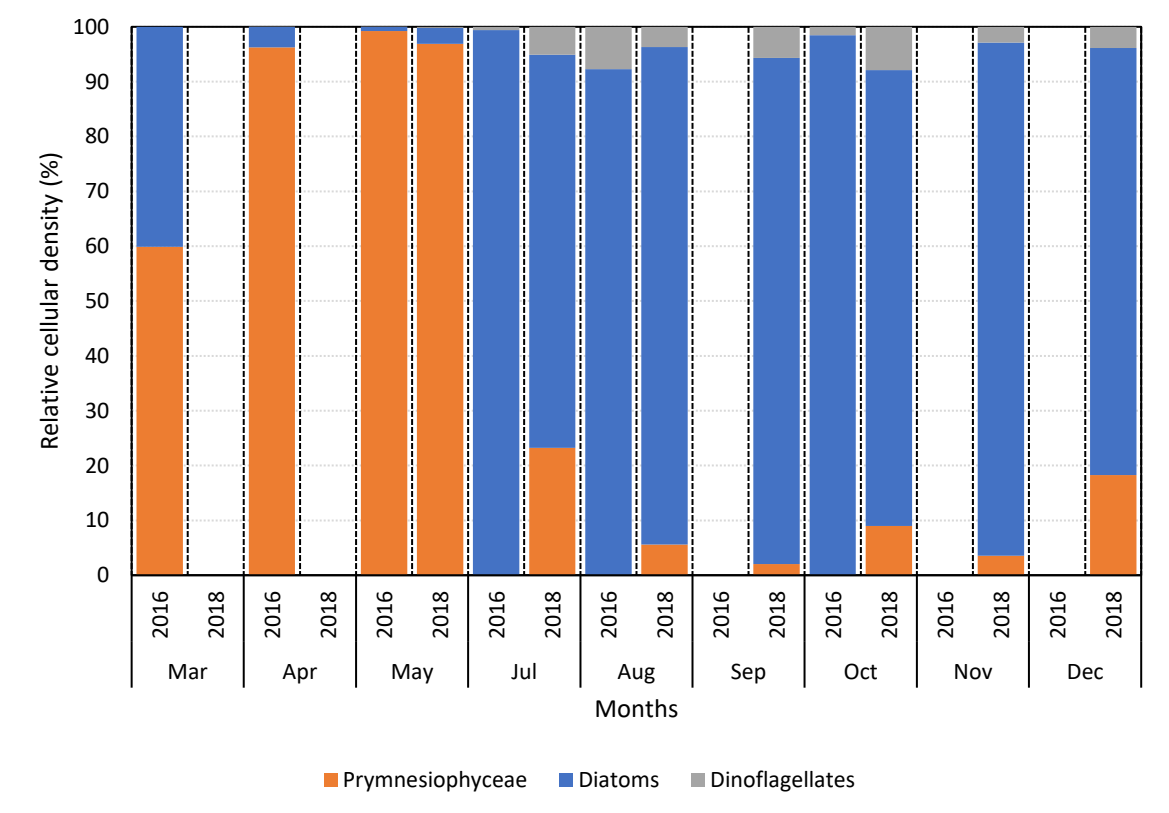

Figure 4-4: Seasonal evolution of the relative cellular density (%) for the station 330 in the Belgian coastal zone (Fig. 4-1) analysed for the phytoplankton diversity from March to October in 2016 and from March to December in 2018 with distinction between the Prymnesiophyceae, diatoms and dinoflagellates.

4.2 Summer phytoplankton bloom

The Chl-*a* concentrations in August (Fig. 4-2) were also different between 2016 and 2018 ($p = 0.090$). The concentration was 4.1 times higher in 2018 (13.4 ± 9.9 µg L^{-1}) than in 2016 (3.4 ± 2.0 µg L^{-1}). The PAR was 1.2 times higher in June 2018 than in 2016 ($p < 0.05$) (Fig. 4-3o). This explains the significant higher average SST for all the stations observed in July 2018 compared to 2016 (21.3 ± 0.7 °C and 19.8 ± 1.0 °C respectively; $p < 0.01$), in response to a large-scale heatwave in Europe (Magnusson et al., 2018; Borges et al., 2019). As a matter of fact, the temperature was significantly higher at the coastal stations in 2018 than in 2016 from late April to July ($p < 0.05$) (Fig. 4-3m, n). Temperature is one of the most important drivers of the phytoplankton community composition (Schabhüttl et al., 2013; Striebel et al., 2016; Hunter-Cevera et al., 2016), and the higher biomass results from higher cell division rates in warmer conditions (Richardson and Schoeman 2004; Hunter-Cevera et al., 2016).

In July 2016, the community was dominated by diatoms (99%) with a small increase of dinoflagellates (1%) (Fig. 4-4). In 2018, the diatoms represented 72% with 23% of Prymnesiophyceae and 5% of dinoflagellates (Fig. 4-4). During August 2016, diatoms still dominated the community (92%) with a slight increase of dinoflagellate (8%) (Fig. 4-4). Diatoms represented up to 91% in August 2018 while Prymnesiophyceae and dinoflagellates were represented by 6 and 4%, respectively (Fig. 4-4). October was the last month sampled in 2016 for the phytoplankton diversity characterized with 98% and 2% of diatoms and dinoflagellates, respectively (Fig. 4-4). From September to December 2018, the community was composed by 87 ± 8, 8 ± 7 and 5 ± 2% of diatoms, Prymnesiophyceae and dinoflagellates, respectively. Diatom community in August 2018 was mainly composed by *Thalassiosira sp.* (*T. rotula, T. tenera* and *T. lundiana*), *M. polymorphus*, *G. delicatula* and *Chaetoceros socialis*. The dinoflagellate community was still characterized by *H. rotundata* while some unclassified *Syndiniales*, *Gyrodinium sp., G. aureolum*, *G. spirale, T. fusus, Lepidodinium sp., Warnowia sp.*, *K. glaucum* and *Sinophysis sp* were observed. From September to December 2018, *Thalassiosira sp., M. polymorphus, G. delicatula* still represented the diatom community while the presence of the dinoflagellates *H. rotundata, K. veneficum, Gyrodinium sp* or *Syndiniales* sp. was detected.

4.3 Spatial and seasonal variations of DMS(P,O) concentrations

While the annual average Chl-*a* was significatively higher in 2018 (8.5 ± 7.2 µg L^{-1}) than in 2016 (5.1 ± 5.5 µg L^{-1}) ($p < 0.001$), the annual average $DMSP_p$ concentration between the two years was similar (162 ± 246 nmol L^{-1} in 2018 and 207 ± 374 nmol L^{-1} in 2016; $p = 0.438$). Even if there was slight difference in $DMSP_p$ in early may (448 ± 183 in 2018 and 1142 ± 487 nmol L^{-1} in 2016), no significant difference was observed ($p = 0.086$) (Fig. 4-5a) and the Chl-*a* concentration was similar ($p = 0.752$) (Fig. 4-2). Despite a higher biomass in August 2018 than 2016, there was no difference in $DMSP_p$ concentrations during both years, with a low value of 49 ± 20 and 54 ± 14 nmol L^{-1} in 2016 and 2018, respectively ($p = 0.732$). Even if the Chl-*a* concentrations were different between the two years during both the early spring and summer blooms, the similarities in $DMSP_p$ concentrations could be explained by the phytoplankton composition. The early spring bloom was mainly characterized by low-DMSP producers such as the diatom *Thalassiosira sp.* and the dinoflagellates *H. rotundata* and *K. veneficum* (Table 4-1). The same conclusion was observed during summer with the diatoms *Thalassiosira sp.* and *M. polymorphus*, or the dinoflagellates *H. rotundata, Gyrodinium sp.* and *Syndiniales sp.* (Table 4-1).

The seasonal pattern of $DMSO_t$ concentration was similar between both years (Fig. 4-5b) but the yearly mean was significantly different (88 ± 107 and 48 ± 68 nmol L^{-1} in 2016 and 2018 respectively; $p < 0.01$). The average value of $DMSO_t$ during the *Phaeocystis* bloom was 246 ± 205 and 163 ± 193 nmol L^{-1} for 2016 and 2018, respectively ($p = 0.597$) (Fig. 4-5b). Significant difference was only observed at the beginning of May, as it was for the $DMSP_p$, with concentration 1.9 times higher in 2016 than in 2018 ($p < 0.05$). In 2018, $DMSO_p$ represents 66% of the $DMSO_t$ pool and showed a similar seasonal evolution (Fig. 4-6a). $DMSO_d$ was generally lower than $DMSO_p$ and presented a different seasonal pattern since the peak of $DMSO_d$ occurred just before the $DMSO_p$ peak in late April (Fig. 4-6a, b).

The spatial variations (coastal-offshore) observed for Chl-*a* (Fig. 4-3a) also occurred for $DMSP_p$ in 2016 but the $DMSO_t$ concentrations did not clearly differ among the stations, except for station 700 (Fig. 4-5c, d). The high concentration observed at station 700 was related to the high SPM concentration and linked to the resuspension of sediment (Speeckaert et al., 2018). In 2018, the $DMSP_p$ concentration was associated with the *Phaeocystis* bloom with a nearshore-offshore gradient and concentrations from 536 to 1353 nmol L^{-1} (Fig. 4-5e). This gradient did not occur in late May nor during the summer. $DMSO_t$ and $DMSO_p$ in 2018 showed a seasonal

pattern with the same gradient during the *Phaeocystis* bloom with values varying from 62 to 500 nmol L^{-1} (Fig. 4-5f) and from 33 to 498 nmol L^{-1} (Fig. 4-6c), respectively. The distinction between coastal and offshore stations for the $DMSO_d$ variations was no longer clearly identified (Fig. 4-6d). Following the Chl-*a* peak during August 2018 for station 700 (Fig. 4-3b), the $DMSO_t$ and the $DMSO_p$ concentration reached a value of 69 and 59 nmol L^{-1} respectively, which were the highest concentrations observed for this period (Fig. 4-5f, 4-6c).

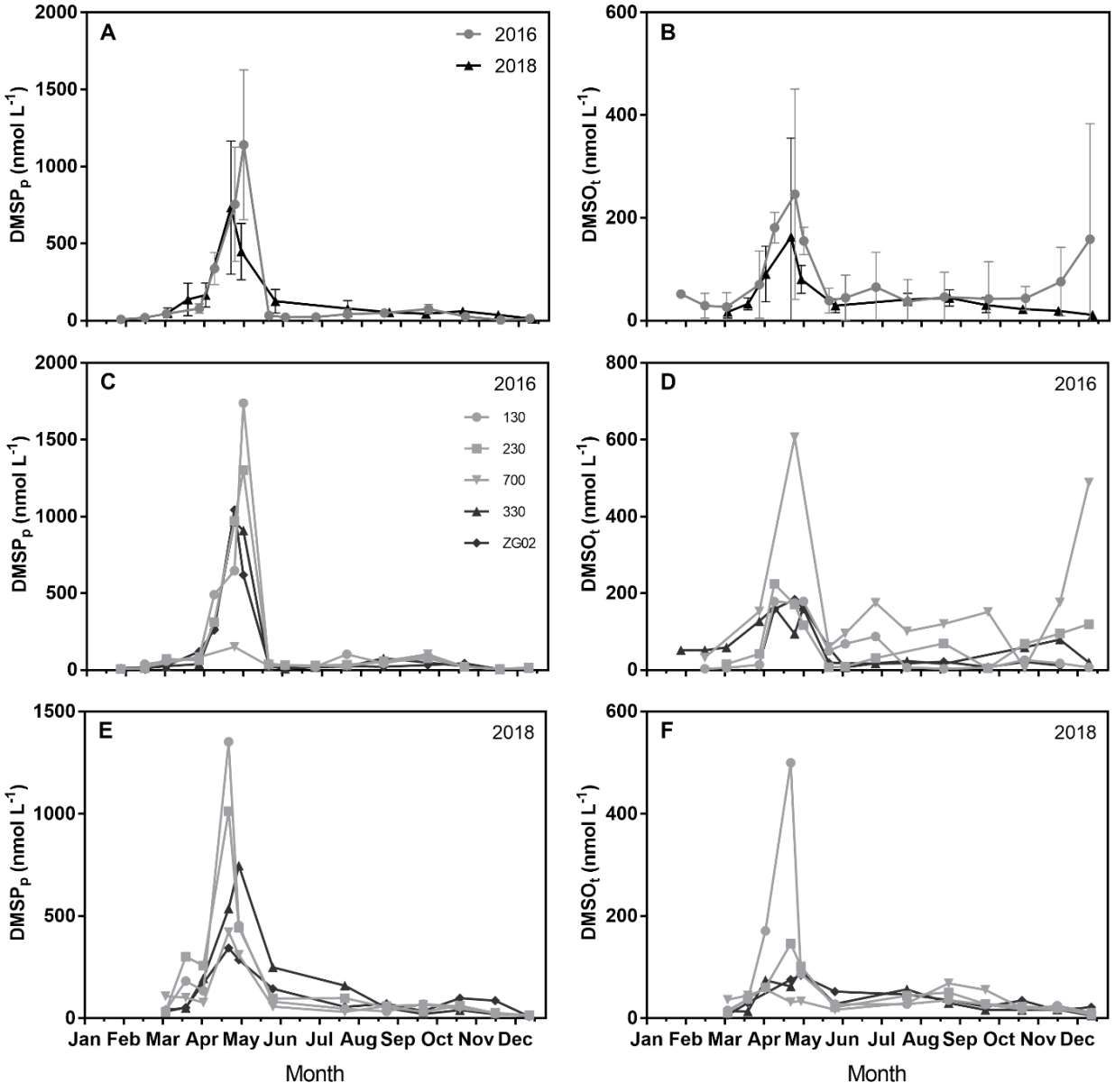

Figure 4-5: Seasonal evolution in 2016 and 2018 of average (± standard deviation) (a) particulate dimethylsulfoniopropionate ($DMSP_p$) (nmol L^{-1}); (b) total dimethylsulfoxide ($DMSO_t$) (nmol L^{-1}); and seasonal and spatial evolution of (c) $DMSP_p$ (nmol L^{-1}) and (d) $DMSO_t$ (nmol L^{-1}) in 2016; (e) $DMSP_p$ (nmol L^{-1}) and (f) $DMSO_t$ (nmol L^{-1}) in 2018 for the five stations sampled in the Belgian coastal zone (Fig. 4-1).

Tableau 4-1: Ratio of particulate dimethylsulfoniopropionate ($DMSP_p$) to Chlorophyll-*a* (Chl-*a*) concentration ($DMSP_p$:Chl-*a*) (mmol:g), cell biovolume (µm³), cell carbon (C) content (pgC cell^{-1}) compiled from published literature for species found in the Belgian coastal zone (Fig. 4-1).

Class	Genus	Species	Biovolume (µm³)	C (pgC cell^{-1})	Chl-*a* (pgChl-*a* cell^{-1})	$DMSP_p$ (fmol cell^{-1})	$DMSP_p$:Chl-*a* (mmol:g)	Data from
Diatom	*Rhizosolenia*	*R. setigra*	69080.0	7561.5	126.0	112.5	**0.9**	1
Diatom	*Guinardia*	*G. delicatula*	58139.0	2105.6	35.1		**1.9**	2
Diatom	*Thalassiosira*	*T. rotula*	15072.0	704.5	11.7	1.9	**5.4 ± 7.3**	1, 2
Diatom	*Thalassiosira*	*Thalassiosira sp.*	13713.0	652.5	10.9	40.8	**3.2 ± 0.8**	1, 2
Diatom	*Thalassiosira*	*T. pseudonana*	80.1	10.1			**4.8**	3
Diatom	*Rhizosolenia*	*Rhizosolenia sp.*	69080.0	2421.6	40.4	112.5	**2.8**	1
Diatom	*Pseudo-Nitzschia*	*Pseudo-Nitzschia sp.*	120.0	14.0	0.2	0.2	**0.9**	1
						Average ± s.d. :	**3.2 ± 3.1**	
Dinoflagellates	*Heterocapsa*	*H. rotundata*	234.0	66.3	1.1	20.8	**18.7 ± 0.9**	4, 5
Dinoflagellates	*Gyrodinium*	*G. aureolum*	5007.6	814.3	13.6	5.3	**0.4**	1
Dinoflagellates	*Katodinium*	*Katodinium sp.*	1439.0	293.3	4.9	201.2	**41.2**	6
Dinoflagellates	*Karlodinium*	*K. veneficum*	739.0	106.7	1.8	7.0	**3.9**	1
Dinoflagellates	*Gymnodinium*	*G. simplex*	265.0	73.4	1.2	238.5	**195.1**	1
Dinoflagellates	*Tripos*	*T. fusus*	19500.0	2479.4	41.3	2.8	**0.1**	7
						Average ± s.d. :	**37.1 ± 65.3**	
Prymnesiophyceae	*Phaeocystis*	*P. globosa*	75.0	12.4	0.2	16.3	**82.3 ± 11.5**	3, 2 ,8
Prymnesiophyceae	*Phaeocystis*	*Phaeocystis sp.*	46.6	8.0			**59.0**	1
						Average ± s.d. :	**76.5 ± 15.0**	

1. McParland and Levine (2019); 2. Speeckaert et al. (2018); 3. Royer et al. (in review); 4. Cooney et al. (2019); 5. Cooney (2016); 6. Townsend and Keller (1996); 7. Keller et al. (1989)b; 8. Speeckaert et al. (2019)

Tableau 4-2: Ratio of particulate dimethylsulfoxide ($DMSO_p$) to Chlorophyll-*a* (Chl-*a*) concentration ($DMSO_p$:Chl-*a*) (mmol:g), cell biovolume (µm³), cell carbon (C) content (pgC $cell^{-1}$) compiled from published literature for species found in the Belgian coastal zone (Fig. 4-1).

Class	Genus	Species	Biovolume (µm³)	C (pgC $cell^{-1}$)	Chl-*a* (pgChl-*a* $cell^{-1}$)	$DMSO_p$ (fmol $cell^{-1}$)	$DMSO_p$:Chl-*a* (mmol:g)	Data from
Diatom	*Thalassiosira*	*T. oceanica*					**0.4**	1
Diatom	*Thalassiosira*	*T. pseudonana*	119.5	13.9	0.2	0.02	**1.0 ± 1.4**	2, 3
Diatom	*Skeletonema*	*S. costatum*	264	26.5	0.4	0.01	**0.8 ± 1.0**	2, 3
						Average ± s.d. :	**0.8 ± 0.9**	
Dinoflagellates	*Heterocapsa*	*H. triquetra*					**11.0 ± 3.4**	2, 4
Dinoflagellates	*North Sea dominated by dinoflagellates*						**2.9**	5
Dinoflagellates	*Gymnodinium*	*G. simplex*	265.0	73.4	1.2	0.1	**0.1**	3
						Average ± s.d. :	**6.3 ± 5.9**	
Prymnesiophyceae	*Phaeocystis*	*P. globosa*					**5.0 ± 5.2**	2, 4
Prymnesiophyceae	*North Sea dominated by P. globosa*						**1.2**	5
Prymnesiophyceae	*Emiliania*	*E. huxleyi*	39.5	6.8	0.1	0.2	**2.0**	3
						Average ± s.d. :	**3.3 ± 3.6**	3

1. Bucciarelli et al. (2013); 2. Royer et al. (in review); 3. Hatton and Wilson (2007); 4. Speeckaert et al. (2019); 5. Simó et al. (1998)

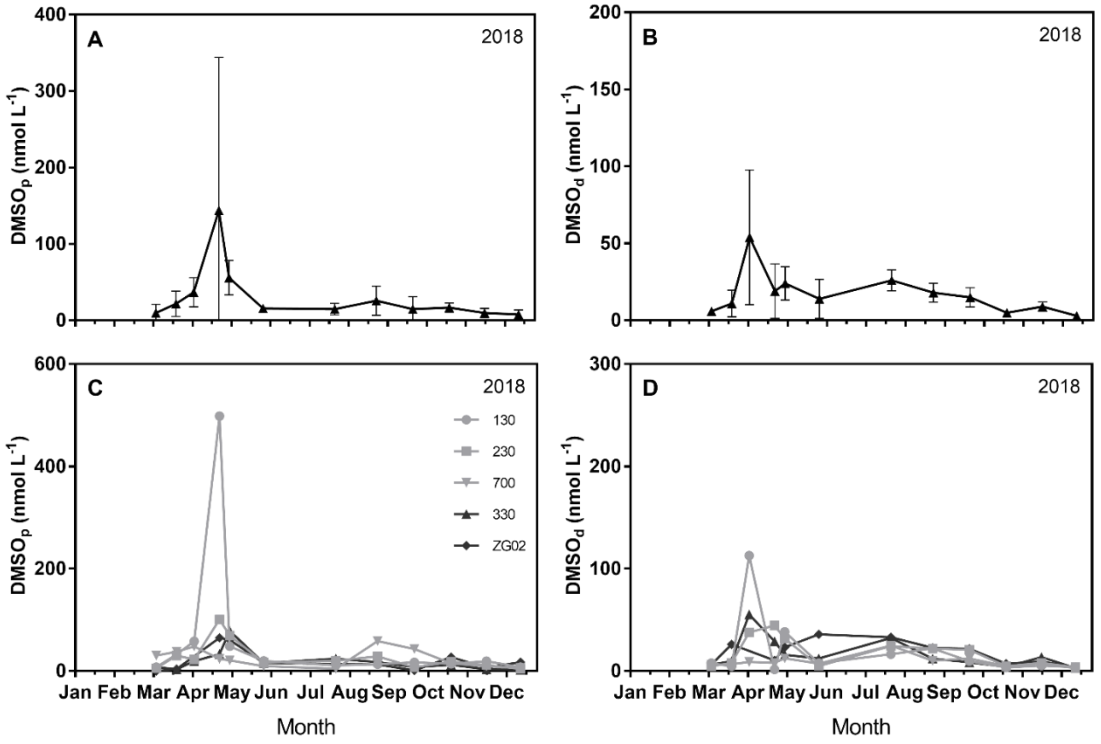

Figure 4-6: Seasonal evolution of average (± standard deviation) (a) particulate dimethylsulfoxide ($DMSO_p$) (nmol L^{-1}), (b) dissolved dimethylsulfoxide ($DMSO_d$) (nmol L^{-1}); and seasonal and spatial evolution of (c) $DMSO_p$ (nmol L^{-1}), (d) $DMSO_d$ (nmol L^{-1}) in 2018 for the five stations sampled in the Belgian coastal zone (Fig. 4-1).

4.4 DMS(P,O) relations and $DMSO_p$: $DMSP_p$ ratio

We further explored the similarities between all the variables in 2016 and 2018 by PCA. The figure 4-7a shows the grouping of variables within an orthogonal 2D-space along the two most relevant PCs explaining 57.8% of the total variance (n = 86). $DMSP_p$, $DMSO_t$ and Chl-*a* explained more than 69.2% of variation along the PC2. With only the 2016 data (Fig. 4-7b; n = 41), two PCs characterized 61.7% of the variance where the variables were clustering together as previously (>67.3%). With only the 2018 data (Fig. 4-7c; n = 45), 61.6% of the variance were explained by two PCs where $DMSP_p$ and $DMSO_p$ correlated (>84.7%). The combining 2016-2018 PC analysis brings statistical support for the link between the Chl-*a* and the DMS(P,O) that are varying together. The previous observation was not noticed for the data in 2018 since the $DMS(P,O)_p$ were not clustered with Chl-*a*. The Spearman correlation analysis followed the same information with significant non-parametric correlation between $DMSP_p$ and Chl-*a* ($\rho = 0.62$; $p < 0.01$) with data from 2016 and 2018. More precisely, $DMSP_p$ and Chl-*a* were highly correlated in 2016 ($\rho = 0.71$; $p < 0.001$) but to a lesser extent in 2018 ($\rho = 0.42$; $p < 0.001$) that was reflected in the PCA.

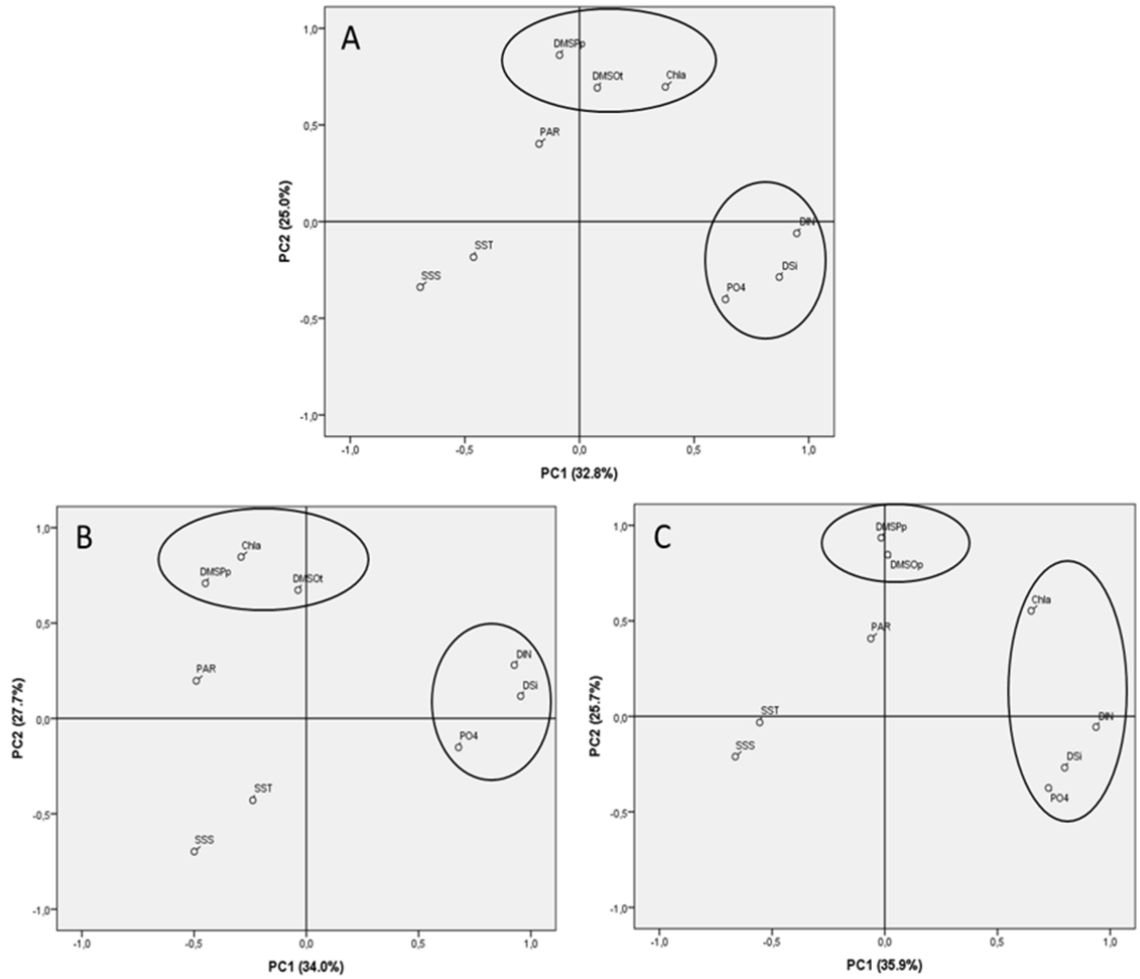

Figure 4-7: Principal Component Analysis (PCA) with all the variables after Oblimin rotation for (a) the data from 2016 and 2018, (b) with data from 2016 and (c) with data from 2018 including Chlorophyll-*a* (Chl-*a*), total dimethylsulfoxide ($DMSO_t$), particulate dimethylsulfoxide ($DMSO_p$), particulate dimethylsulfoniopropionate ($DMSP_p$), Sea Surface Salinity (SSS), Sea Surface Temperature (SST), Photosynthetic Active Radiation (PAR), Dissolved Inorganic Nitrogen (DIN), Dissolved Silica (DSi), phosphate (PO_4) in the Belgian coastal zone (Fig. 4-1).

The figure 4-8a represents the linear regression between $DMSP_p$ and Chl-*a* for the two years. The slope of the regression of $DMSP_p$ and Chl-*a* was higher in 2016 than that in 2018 (Fig. 4-8a). This is due to the fact that in 2018 many data points for high Chl-*a* values corresponded to low DMSP-producing diatoms and dinoflagellates (Table 4-1), while in 2016 the data points for low DMSP-producing species usually exhibited low Chl-*a*. This led to the steeper regression of $DMSP_p$ and Chl-*a* in 2016 compared to 2018, as well as lower correlation coefficient in 2018 ($R^2 = 0.38$) due to more scatter in data points. Yet, when comparing the $DMSP_p$ and Chl-*a* correlations separating the *Phaeocystis* bloom dominated data point from the rest of the year (Fig. 4-8b), the slopes of the regressions are similar during both years: 42.0 and 53.9 for *Phaeocystis* in 2018 and 2016, respectively, and 6.8 and 9.1 for the rest of the year in 2018 and 2016, respectively. The first values were in the same range as the $DMSP_p$:Chl-*a* ratio given by

Stefels et al. (2007) (52 ± 37 mmol:g) or recalculated from published literature with 76.5 ± 15.0 mmol:g for the Prymnesiophyceae *P. globosa* (Table 4-1). The ratio obtained for the rest of the year corresponds to the ratio given by Stefels et al. (2007) (4 ± 6 mmol:g) or recalculated in Table 4-1 (3.2 ± 3.1 mmol:g) for the diatoms. The presence of dinoflagellates was not reflected in the slope of the linear regressions since they were mainly composed by *H. rotundata* characterized by a low $DMSP_p$:Chl-*a* ratio of 18.7 ± 0.9 mmol:g (Table 4-1).

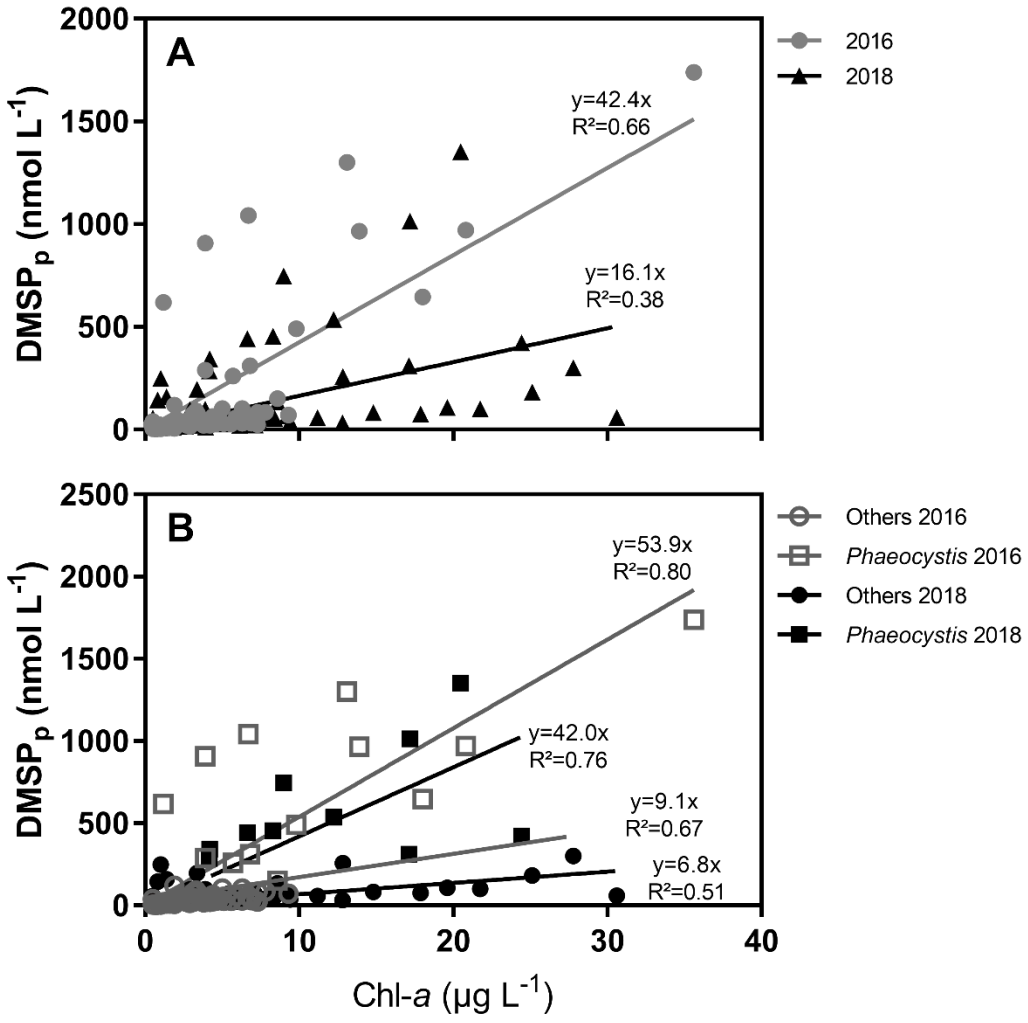

Figure 4-8: (a) Particulate dimethylsulfoniopropionate ($DMSP_p$) (nmol L^{-1}) versus Chlorophyll-*a* (Chl-*a*) concentration (µg L^{-1}) in 2016 and 2018 and (b) $DMSP_p$ (nmol L^{-1}) versus Chl-*a* concentration (µg L^{-1}) with discrimination between *Phaeocystis* and others with data for 2016 and 2018 in the Belgian coastal zone (Fig. 4-1).

The $DMSO_p$ concentration was significantly correlated with $DMSP_p$ concentration ($\rho = 0.79$; $p < 0.001$), as also observed in a global dataset by Simó and Vila-Costa (2006). The slope of the regression of $DMSO_p$ and $DMSP_p$ (Fig. 4-9a) ($R^2 = 0.74$) was lower in the BCZ (0.1) than in the global dataset reported by Simó and Vila-Costa (2006) (0.2). This difference cannot be

analyzed because Simó and Vila-Costa (2006) did not report the phytoplankton composition. The $DMSO_p$:$DMSP_p$ ratio in the BCZ driven by the data points related to *Phaeocystis* bloom (0.16 ± 0.13) was very close to the value of 0.15 ± 0.09 reported in the literature for pure *Phaeocystis* cultures (Hatton and Wilson, 2007; Royer et al., in progress). $DMSO_p$ was also highly correlated to Chl-*a* ($\rho = 0.79$; $p < 0.001$) and the slope of the regression was higher for *Phaeocystis* (3.3 mmol:g) ($R^2 = 0.51$) than for the rest of the year (1.8 mmol:g) ($R^2 = 0.71$) (Fig. 4-9b). The first value was in the same range than those reported in literature for the $DMSO_p$:Chl-*a* ratio with 3.3 ± 3.6 mmol:g for the Prymnesiophyceae (Table 4-2). The second value was higher than the ratio found for the diatoms (0.8 ± 0.9 mmol:g; Table 4-2). The higher value could be explained by the presence of dinoflagellates for which we found $DMSO_p$:Chl-*a* ratio of 6.3 ± 5.9 mmol:g (Table 4-2).

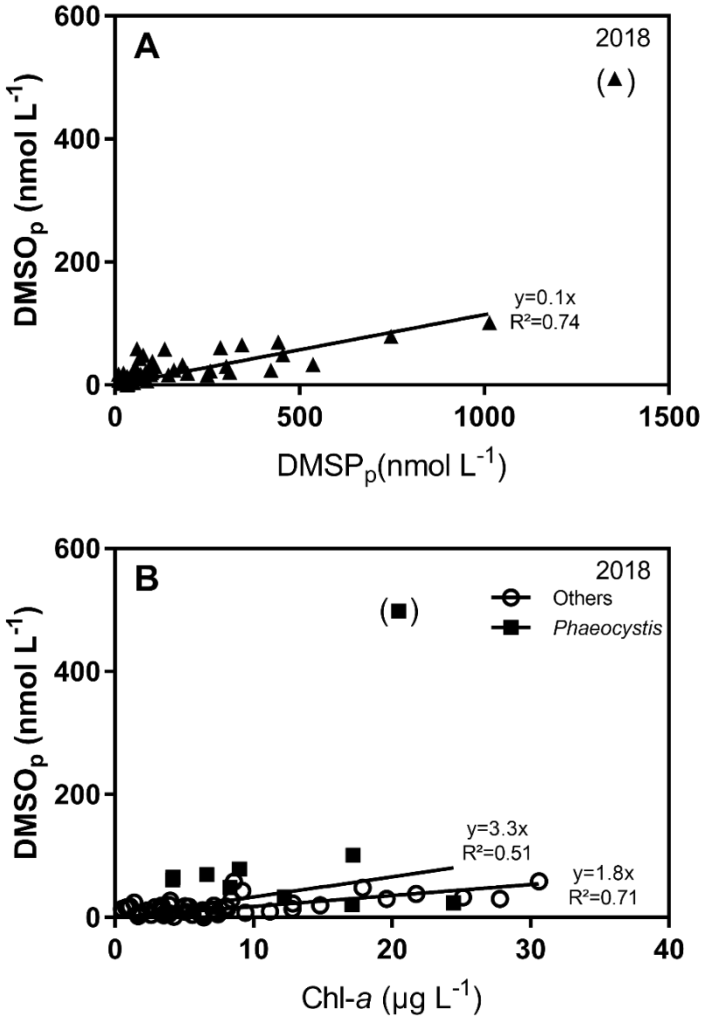

Figure 4-9: (a) Particulate dimethylsulfoxide ($DMSO_p$) (nmol L^{-1}) versus particulate dimethylsulfoniopropionate ($DMSP_p$) concentration (nmol L^{-1}) in 2018 and (b) $DMSO_p$ (nmol L^{-1}) versus Chlorophyll-*a* (Chl-*a*) concentration (µg L^{-1}) with discrimination between *Phaeocystis* and others with data from 2018 in the Belgian coastal zone (Fig. 4-1). The linear regressions exclude the outlier data points in brackets.

4.5 Phytoplankton diversity and DMS(P,O) estimation

$DMSP_p$ was estimated from the linear regression with Chl-*a* ($DMSP_p$ (nmol L^{-1}) = 23.1 * Chl-*a* (µg L^{-1}), R^2 = 0.46) computed for the whole dataset (2016 and 2018) and compared with the measured $DMSP_p$. For both years, the magnitude of the calculated *Phaeocystis* $DMSP_p$ peak was underestimated compared to measurements (Fig. 4-10a, b). Calculated $DMSP_p$ was also higher than spring and summer observed concentrations in particular in 2018 due to higher Chl-*a* values (Fig. 4-10b). As shown by Speeckaert et al. (2018), using a unique DMSP:Chl-*a* ratio is inappropriate to estimate DMSP concentration associated to either high- or low-DMSP producers. We thus used two different $DMSP_p$ *versus* Chl-*a* relationships to discriminate the two main blooming phytoplankton groups: for *Phaeocystis* ($DMSP_p$ (nmol L^{-1}) = 48.0 * Chl-*a* (µg L^{-1})) and for diatoms ($DMSP_p$ (nmol L^{-1}) = 8.0 * Chl-*a* (µg L^{-1})). The use of these specific $DMSP_p$:Chl-*a* relationships led to a better fit of modelled $DMSP_p$ compared to field measurements for both years (Fig. 4-10a, b).

The same procedure was applied for the $DMSO_p$ estimation. We compared $DMSO_p$ computed for the whole dataset in 2018 from the linear regression with Chl-*a* ($DMSO_p$ (nmol L^{-1}) = 2.1 * Chl-*a* (µg L^{-1}), R^2 = 0.54). The regression model tends to fit with the observed $DMSO_p$ except during the *Phaeocystis* blooming period where it was underestimated but still within the standard deviation (Fig. 4-10c). When using the relationships deduced from the figure 4-9b, with one corresponding for the *Phaeocystis* ($DMSO_p$ (nmol L^{-1}) = 3.3 * Chl-*a* (µg L^{-1})) and one for the diatoms ($DMSO_p$ (nmol L^{-1}) = 1.8 * Chl-*a* (µg L^{-1})), we mainly observed the same evolution (Fig. 4-10c).

In conclusion, simple relationships between $DMS(P,O)_p$ and Chl-*a* are not sufficiently robust to describe the seasonal variability of $DMS(P,O)_p$. We thus recommend considering two separate DMS(P,O)-Chl-*a* relationships for low and high-DMSP producing groups to estimate $DMS(P,O)_p$ based on Chl-*a* in global models.

5 Conclusions

Phytoplankton biomass in the BCZ was higher during the diatom blooming period in spring 2018 than 2016, and to a lesser extent, in August 2018 than 2016. The difference among years in spring was explained by lower SST during winter, higher nutrients supply coming from the Scheldt estuary and better light conditions in 2018 compared to 2016.

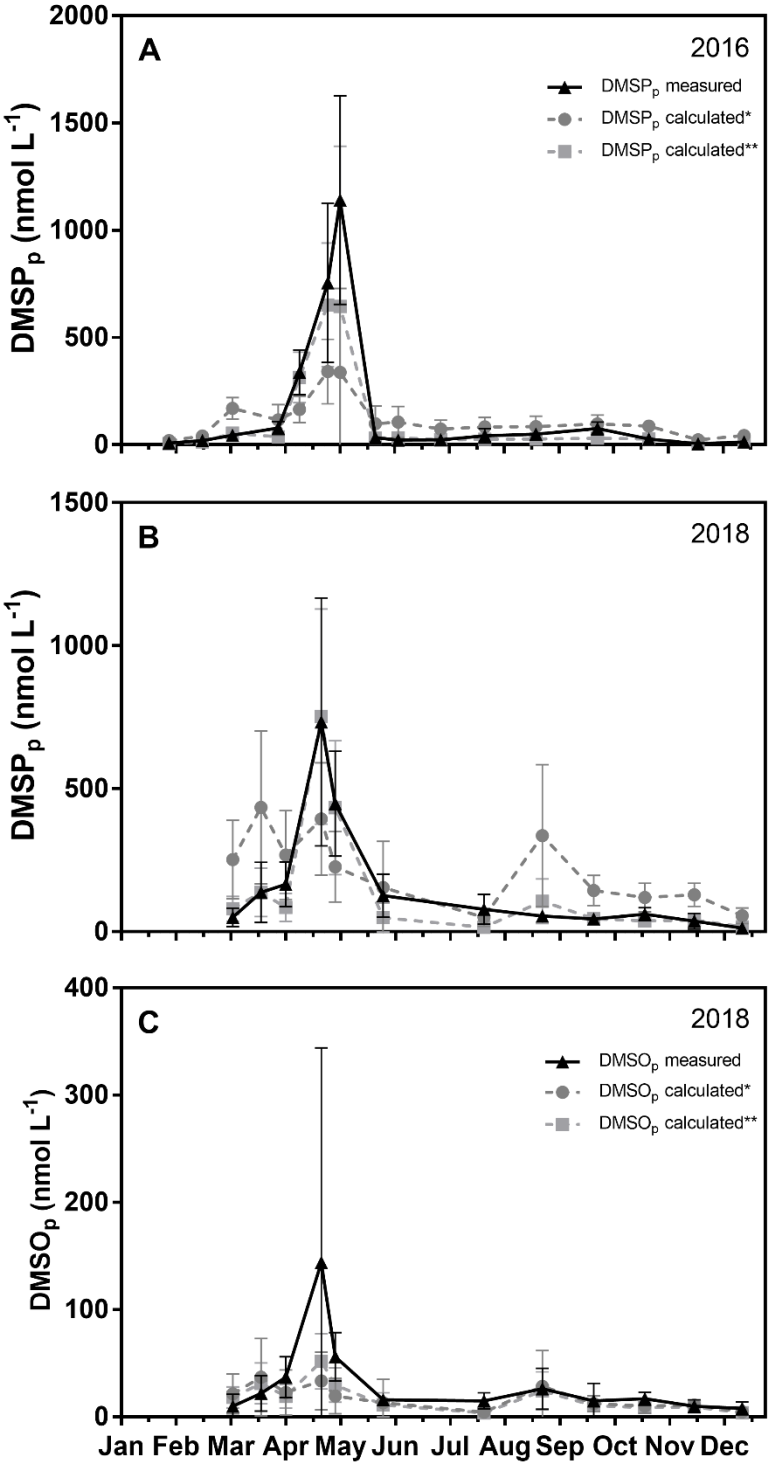

Figure 4-10: Seasonal evolution in the Belgian coastal zone of average (± standard deviation) particulate dimethylsulfoniopropionate ($DMSP_p$) measured (nmol L^{-1}) (in black) and $DMSP_p$ calculated* based on Chlorophyll-*a* (Chl-*a*) concentration using a relationship for all phytoplankton species [$DMSP_p$ (nmol L^{-1}) = 25.1 * Chl-*a* (µg L^{-1})] or $DMSP_p$ calculated** using a relationship for the diatoms [$DMSP_p$ (nmol L^{-1}) = 8.0 * Chl-*a* (µg L^{-1})] and another one for Phaeocystis globosa [$DMSP_p$ (nmol L^{-1}) = 48.0 * Chl-*a* (µg L^{-1})] for (a) 2016 and (b) 2018. (c) Seasonal evolution of particulate dimethylsulfoxide ($DMSO_p$) measured (nmol L^{-1}) (in black) and $DMSO_p$ calculated* based on Chl-*a* using a relationship for all phytoplankton species [$DMSO_p$ (nmol L^{-1}) = 2.1 * Chl-*a* (µg L^{-1})] or $DMSO_p$ calculated** using a relationship for the diatoms [$DMSO_p$ (nmol L^{-1}) = 1.8 * Chl-*a* (µg L^{-1})] and another one for Phaeocystis globosa [$DMSO_p$ (nmol L^{-1}) = 3.3 * Chl-*a* (µg L^{-1})] for 2018.

The difference among years in August seemed related to higher SST in 2018 compared to 2016. Despite these major differences in phytoplankton biomass, the seasonal and spatial $DMS(P,O)_p$ patterns were similar in 2016 and 2018. This was explained by the peak of biomass occurring both years in spring due to *Phaeocystis. Phaeocystis* is a high-DMS(P,O) producer and dominates the annual $DMSP_p$ production in the BCZ. On the contrary, low-DMSP producing diatom and dinoflagellate species dominated the spring and summer bloom for which we observed strong differences in Chl-*a* between both years. This illustrates why Chl-*a* concentration alone could not be used to describe the $DMS(P,O)_p$ variations. The phytoplankton diversity had to be taken into consideration to analyze and better predict the $DMS(P,O)_p$ variations. The impact of current or future phytoplankton biomass changes on $DMS(P,O)_p$ marine concentrations will thus mainly depend on the species composition rather than the total phytoplankton biomass.

Coastal marine areas are expected to show changes in phytoplankton biomass in response to several human pressures such as nutrient inputs and changes in temperature that can also affect $DMS(P,O)_p$ concentration (and possibly DMS emissions). We pointed out the significance of considering two separate $DMS(P,O)_p$-Chl-*a* relationships for low and high-DMSP producing species to properly estimate the $DMS(P,O)_p$ concentrations. Better constrain the $DMS(P,O)_p$ in the water column linked to the phytoplankton diversity and abiotic parameters will ultimately lead to improvements in the modelling of the ocean-atmosphere DMS flux and its potential climate impact.

6 Acknowledgements

We are grateful to the crew of the *RV Simon Stevin* for assistance during the cruises, to André Cattrijsse and Jonas Mortelmans (VLIZ) for organizing the schedule of cruises. Nutrient data were acquired as part of the VLIZ contribution to the LifeWatch ESFRI. This project has received funding from the European Union's Horizon 2020 research and innovation program under the Marie Skłodowska-Curie grant agreement No 766327. The GC was acquired with funds from the Fonds National de la Recherche Scientifique (FNRS) (2.4.637.10). NG and CR received financial support from the Fonds David et Alice Van Buuren. CR has a PhD grant from the FRIA (Fund for Research Training in Industry and Agriculture, FNRS). AVB is a research director at the FNRS.

Chapter V – DMSP and DMSO variability along latitudinal transects and depths in the North Sea.

"Der little lea anunder a lang-backit sea"

The rolling ocean provides no shelter in a storm.

- Shetlands Proverbs and Sayings

1 Introduction

As suggested in the general introduction, scientific understanding of the processes playing key roles in the DMS cycle and its interaction between the upper ocean and the atmosphere has improved, and with this, an appreciation of its complexity (Quinn and Bates, 2011). In particular, the central role of DMSP, the dominant biological precursor of DMS, is now well established. In addition, the biological production of DMSO resulting of DMS(P) oxidation add another step into this cycle (Stefels et al., 2007).

A wide variety of marine microalgae produces DMS(P,O) (McParland and Levine, 2019). The usual classification between high-DMSP producers (dinoflagellates and Prymnesiophyceae) and low-DMSP producers (diatoms) (Keller et al., 1989; McParland and Levine, 2019) leads to good correlations between Chlorophyll-*a* (Chl-*a*) and DMSP for restricted areas where DMSP-producing phytoplankton dominate. For studies crossing a wide range of geographical zones, accessory pigments could provide additional details on phytoplankton community composition (Bell et al., 2010). With this approach, significant relationships were found between the Prymnesiophyceae characterized by the accessory pigments Hex+But (19'-Hexanoyloxyfucoxanthin plus 19'-Butanoyloxyfucoxanthin) and DMSP (Belviso et al., 2001). Correlations were also observed between peridinin, the dinoflagellates and the intracellular DMSP (Sunda et al., 2005). In the Norwest Atlantic, significant correlation has been found between the abundance of dinoflagellates and Prymnesiophyceae and the concentrations of DMSP (Scarratt et al., 2002). The same correlation has been established in the Southern North Sea (SNS) and the Wadden Sea between abundance of the Prymnesiophyceae *Phaeocystis globosa* and DMS(P,O) concentration (van Duyl et al., 1998; Speeckaert et al., 2018; *cf.* Chapter IV). Seawater phytoplankton diversity is thus the factor affecting the community-DMSP production the most (McParland et al., 2019), rather than the overall phytoplankton biomass (Townsend and Keller, 1996; *cf.* Chapter IV).

As explained in the Chapter III, DMS(P,O) and its breakdown products have been suggested to play as antioxidants within the phytoplankton cells (Sunda et al., 2002). This function was observed on field measurements with positive correlations between DMS(P,O) and photoprotective pigments DDx+DTx (Bell et al., 2010) or β-carotene (Riseman and DiTullio, 2004). Similar trends with the xanthophylls pigments or UV sunscreen compounds and $DMSP_t$ provide indirect support to the photoprotective role of DMSP (Archer et al., 2009). Significant relationship was found between DMSP-Lyase (DL) activity (partially regulating the antioxidant

response) and DDx and DTx (Steinke et al., 2002; Harada et al., 2004). Recent modelling studies have shown that DMS concentrations in surface waters can be linked to UV radiation (Toole and Siegel, 2004), full-spectrum of sunlight (Galí et al., 2011; 2013), Photosynthetic Active Radiation (PAR) (Lizotte et al., 2012), or the Solar Radiation Dose (SRD) (Vallina and Simó, 2007; Belviso and Caniaux, 2009; Miles et al., 2009; Lana et al., 2012).

As a temperate sea, the North Sea is mainly characterized by a diatom bloom in spring followed by other groups such as flagellates and later (i.e. during summer) by dinoflagellates (Reid et al., 1990; Johns and Reid, 2001). In the Northern North Sea (NNS), the most abundant phytoplankton genus are the dinoflagellate *Ceratium* and the diatom *Thalassiosira.* In the SNS, the dominant species included *Ceratium* and the diatom *Chaetoceros* (Johns and Reid, 2001). The dinoflagellate *Protoperidinium* is also present in the two areas (Johns and Reid, 2001). There has been a gradual decrease in the abundance of the majority of diatoms' species (Reid et al., 1990), excepted for the genus *Thalassiosira* (Johns and Reid, 2001). Reid et al. (1990) affirmed that in the Central and NNS, the armoured dinoflagellates are the most abundant and are governed by the hydrographic conditions of the summer months.

With respect to DMS(P,O), the North Sea area are under-sampled, and measurements already reported include only data from the 90's and most of all for coastal regions. An increase number of field measurements should have to be carried on to better understand the phytoplankton evolution regarding DMS(P,O) concentrations. For instance, Malin et al. (1993) observed in June-July 1987 in the northeast Atlantic (between England and Iceland) $DMSP_p$ concentrations from 10.8 to 280.0 nmol L^{-1}. Simó et al. (1998) reported $DMSP_p$ and $DMSO_p$ values from 5.2 to 340.0 and from 2.7 to 16.0 nmol L^{-1} respectively, with Chl-*a* concentration of 1.3 and 13.3 µg L^{-1} for the month of June, July, and August 1996 near the coast of England (Great Yarmouth). Simó and Villa-Costa (2006) observed $DMSP_p$ concentration from 28.2 to 173.4 nmol L^{-1} for Chl-*a* concentration from 0.7 to 1.9 µg L^{-1} in the northeast Atlantic (South of Iceland) in June 1998. In June 1999, $DMSP_p$ concentrations from 54.0 to 121.0 nmol L^{-1} were analysed in the NNS for Chl-*a* concentrations between 0.4 and 1.0 µg L^{-1}. High $DMSP_p$ concentrations in June-July 1996 were also reported in waters off the western coast of Ireland, up to 50 – 635 nmol L^{-1} (Locarnini et al., 1998). To our knowledge, DMS(P,O) concentrations along the transect from the coast of Germany till Scotland, neither along the continental rift between Scotland, the Shetlands Islands, and the Faeroe Islands, or along the Norwegian coast (Fig. 5-1) were reported.

Thus, this chapter aims at providing new field data measurements for DMS(P,O) concentrations and phytoplankton diversity in the North Sea along the depth and three different transects for the month of August 2018. Statistical links between DMS(P,O) and ancillary data characterizing the phytoplankton community physiology, taxonomic composition, and its ability to cope with light were explored. The DMS(P,O) estimations realized in the Chapter IV were also tested to ensure its application within another environment. Since DMS(P,O) are playing a central role in the global sulfur cycle, better understanding the link between abiotic parameters, phytoplankton diversity and DMS(P,O) concentrations will lead to a better appreciation of their variation in the water column, and ultimately a better estimation of the resulting DMS flux.

2 Material and Methods

2.1 Field sampling and abiotic parameters

The monitoring of physical, chemical, and biological parameters was carried out on the *RV Heincke* during the expedition HE517 that started the 19 August and ended the 04 September 2018. Different stations (Fig. 5-1) were analysed and covered: (1) the transect from Bremerhaven (Germany) to the top of Scotland, referred to the transect *BS* and the stations (St.) 1 to 10; (2) the transect along the continental rift between Scotland, the Shetlands Islands, and the Faeroe Islands, referred to the transect *SSF* and the St.11 to 16; and (3) the transect along the Norwegian Coastal Zone, referred to the transect *NCZ* and the St.17 to 23.

Seawater samples were generally collected at different depth to cover the vertical profile, typically between 0 - 20m, 20 - 40m and 40 - 100m. Only the surface water was sampled when the vertical profile was not covered (St.2, 3, 6, 7 and 10). The sampling was realized using Niskin bottles on a rosette sampler attached to a Conductivity-Temperature-Depth (CTD) probe (SEA-BIRD SBE 911plus, SN 1015). All the samples were kept for further analysis of Chl-*a*, nutrients and DMS(P,O) concentrations. The abiotic measurements of seawater temperature and salinity were carried out by Röttgers and Wizotzki (2018).

The nutrients were measured by filtering the sample by a Whatman polycarbonate filter 0.6 µm 47 mm and stored separately for each nutrient: for nitrogen and phosphate, frozen at -20°C; for silicate, acidified with 2 µL mL^{-1} of fuming HCl and stored at 4°C. The nutrients were measured by colorimetry using a Perkin Elmer Lambda 650S UV/Vis spectrophotometer according to

Koroleff (1983a, b, c) and Grasshoff (1983). The reagents and chemical reactions were realized with UltraPure water (Merck).

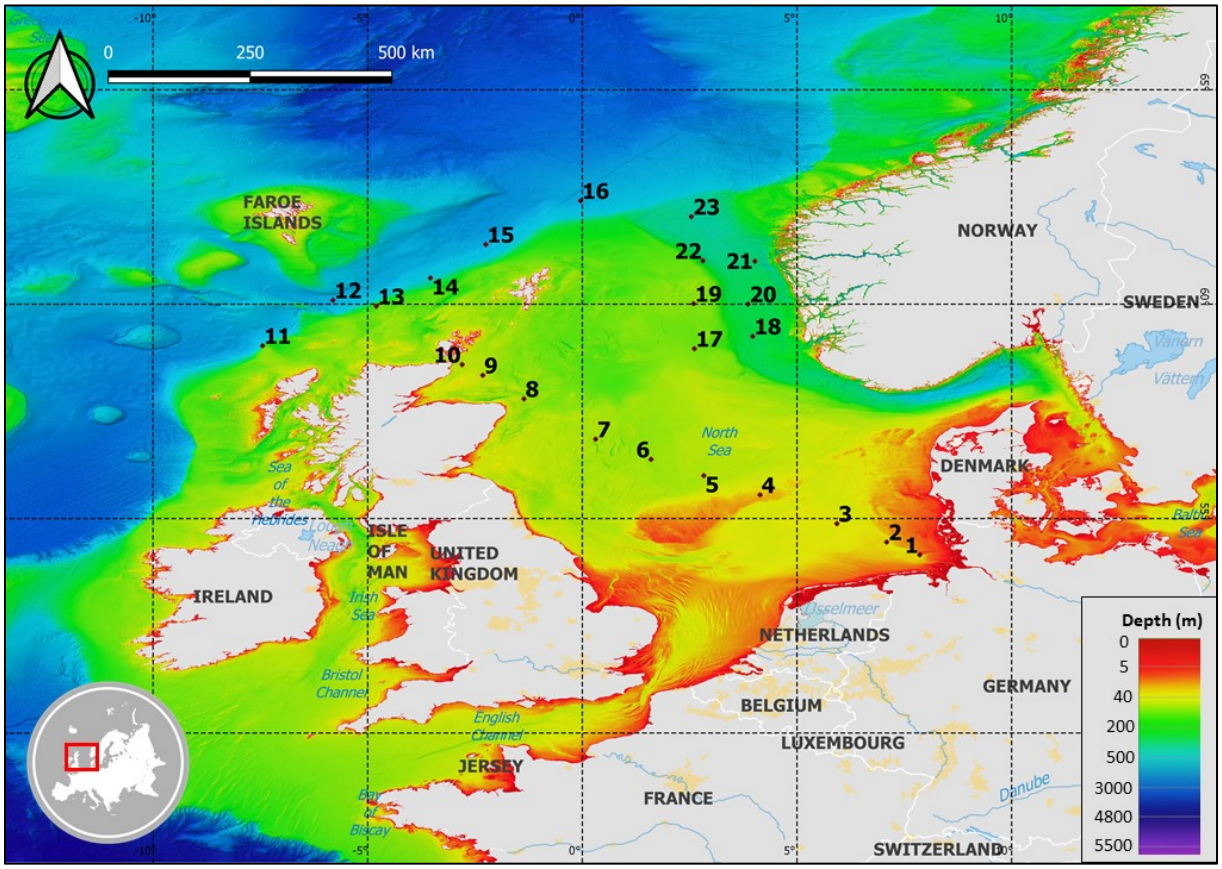

Figure 5-1: Map of the sampling area with the main countries around, the stations numerated from station 1 to station 23, and the bathymetry (m) in the North Sea.

Averaged all sky insolation incident on a horizontal surface (MJ m^{-2} d^{-1}) for a specific date and single site was downloaded from POWER Data Access Viewer v1.1.1, converted in W m^{-2} and multiplied by 2.02 to obtain the Photosynthetic Active Radiation (PAR) (µmol m^{-2} s^{-1}) (Thimijan and Heins, 1983; Mavi and Tupper, 2004; Reis and Ribeiro, 2020).

2.2 Biotic parameters analysis

Chl-*a* was sampled and analyzed fluorometrically as it was for the Chapter III and IV. The photosynthetic and photoprotective pigments – diadinoxanthin (DDx), Diatoxanthin (DTx), Neoxanthin (Neox), Alloxanthin (Allox), Zeaxanthin (Zeax), α-carotene (α-car), β-carotene (β-car), 19'-Butanoyloxyfucoxanthin (But), Fucoxanthin (Fucox), Peridinin (Perid), Lutein (Lut), 19'-Hexanoyloxyfucoxanthin (Hex), 19-hex 4 Keto-Fucoxanthin (4-k-Hex), Antheraxanthin (Anthera), Prasinoxanthin (Prasi), Chlorophyllide-*a* (Chlid-*a*), Chlid-*b*, Chl-c_3, Chl-c_2, Chl-*a*, Chl-*c2* MGDGxanthin (Chl-*c2* MGDG), Pheophorbide-*a* (Phb-*a*) and Pheophytin-*a* (Pheo-*a*) –

were analysed by High Performance Liquid Chromatography (HPLC) LC-2030C Plus 3D RoHS Prominence (Shimadzu and LabSolutions Software) (Zapata et al., 2000). The pigment analysis was only performed for the first depth and for St.4, 5, 8, 9, 11 – 23 (17 stations on 23). The estimate relative abundance of algal types was realized using the CHEMTAX methodology. The matrix inversion method CHEMTAX (Mackey et al., 1996) assumes that pigments ratio are known for each phytoplankton group and that linear relationships exist among phytoplankton pigment ratios for a given dataset. The relative abundance is then based on the contribution of each group to total Chl-*a* based on pigment ratios (Wright and Jeffrey, 2006; Kramer and Siegel, 2019).

DNA extraction and analysis, as well as the DMS(P,O) measurements were realized with the same methodology found in the Chapter IV. The student t-test, the non-parametric Spearman correlation, or the Principal Component Analysis (PCA) were performed as it was described in the Chapter IV.

3 Results and discussion

The data was plotted for the first depth for the three transects (Fig. 5-2) to analyse its evolution along the latitude. The data was then sorted into fixed depth bins based upon the depths typically sampled during the campaign: 0-20m, 20-40m and 40-100m. For these three depths, the median, inter-quartile range (delimited by the 25th and 75th percentile), data range and outliers (defined as values less than the 25th percentile or greater than the 75th percentile by 150% of the inter-quartile range) were calculated (Fig. 5-3 and 5-4).

3.1 The abiotic parameters and the Chl-*a* concentrations.

Despite covering different latitude, only few data points for Chl-*a* were considered as outliers. These latter pointed out the difference between coastal or open sea regions. The spatial Chl-*a* evolution followed a profile nearshore-offshore with higher values near the coast of Germany (St.1: 5.01 µg L^{-1}) and Scotland (St.9: 2.41 µg L^{-1}), decreasing rapidly to reach 0.13 µg L^{-1} at St.7 in open sea (Fig. 5-2f). Little variations were observed for the SSF (0.86 ± 0.40) and NCZ transects (0.71 ± 0.17 µg L^{-1}) with only a small peak at St.15 with 1.65 µg L^{-1} (Fig. 5-2f). Considering the Chl-*a* evolution with depth (Fig. 5-4a, b), we observed that the maximum median concentration was more likely at 29.5m of depth with 1.01 ± 0.50 µg L^{-1} with no significant difference with the surface (0.75 ± 0.51 µg L^{-1}). This concentration dropped to 0.10 ± 0.32 µg L^{-1} at 80m of depth (Fig. 5-4a, b).

Higher Chl-*a* concentrations near the coast of Germany or Scotland could be explained by higher concentrations of PO_4, DSi and DIN than in open sea (Fig. 5-2c, d, e). The St.1 was closed to the Elbe riverine input while the St.8, 9 and 10 were at the mouth of Moray Fifth (i.e. Cromarty, Dornoch or Inverness firth) and close to the firth of Tay or Forth (Lyons et al., 1993; Webster et al., 2004). Along the SSF or NCZ, the parallel between nutrients variations and Chl-*a* concentrations are sparser since the peak of PO_4 and DSi at St.14 (Fig. 5-2c, d) did not follow the peak Chl-*a* at St.15 (Fig. 5-2f).

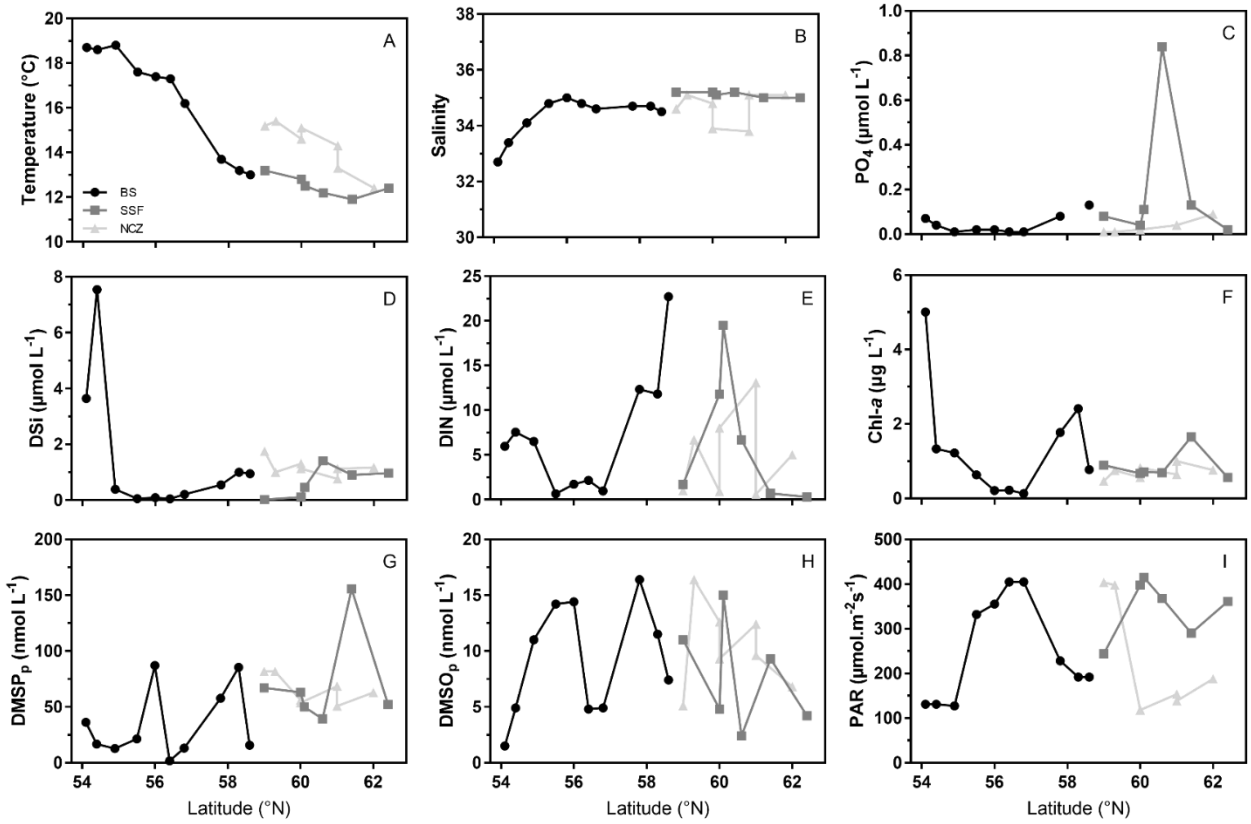

Figure 5-2: Latitudinal profiles along the BS, SSF and NCZ transects for (a) temperature (°C), (b) salinity, (c) phosphates (PO_4), (d) Dissolved Silicate (DSi), (e) Dissolved Inorganic Nitrogen (DIN) concentrations (µmol L^{-1}), (f) Chlorophyll-a (Chl-a) concentrations (µg L^{-1}), (g) particulate dimethylsulfoniopropionate ($DMSP_p$), (h) particulate dimethylsulfoxide ($DMSO_p$) concentrations (nmol L^{-1}) and (i) Photosynthetic Active Radiation (µmol $m^{-2}s^{-1}$).The $DMS(P,O)_p$ profiles followed the Chl-*a* concentrations.

PAR was ranging from 118 to 415 µmol $m^{-2}s^{-1}$ with an increase from St.1 to St.7, to slowly decrease near the coast of Scotland (Fig. 5-2i). The average incident PAR was higher during the SSF (346 ± 66) and lower during the NCZ transects (217 ± 128) than it was during the BS transect (250 ± 114 µmol $m^{-2}s^{-1}$).

The salinity followed the coastal-oceanic variations as it was for the nutrients and remained stable along the SSF or the NCZ (Fig. 5-2b). A steady increase of the salinity with depth was

analysed with 34.8 ± 0.6, 35.0 ± 0.3 and 35.2 ± 0.2 (Fig. 5-3c, d) while the median temperature followed a steady decrease of ~2°C (14.3 ± 3.9, 12.3 ± 0.9 and 9.9 ± 1.2°C respectively for each depth; Fig. 5-3a, b). The temperature was influenced by the warm water coming from the English Channel (Paramor et al., 2009) and the large-scale heatwave that occurred in Europe (Magnusson et al., 2018), with higher temperature (~18°C) at the beginning of summer and near the coast of Germany (Fig. 5-2a). We observed lower temperatures (~13°C) along the SSF or the NCZ, influenced by the nearby Atlantic Ocean and the North Sea currents (Paramor et al., 2009). As a matter of fact, the summer months are characterized by a permanent thermocline (Richardson et al., 1998) that induces a sink of the colder and nutrient-rich waters away from the photic zone (Johns and Reid, 2001; Kraberg et al., 2012), explaining the nutrient evolution with depth observed for DIN, PO_4 and DSi concentrations (Fig. 5-3e, f, g, h, i, j).

3.2 The $DMS(P,O)_p$ profiles followed the Chl-*a* concentrations.

Chl-*a* and $DMS(P,O)_{p,d}$ profiles along the latitude for the three transects and along the depth are presented at the figure 5-3 and 5-4.

$DMSP_p$ along the BS transect followed the coastal-offshore gradient as it was for the Chl-*a* concentrations, except for St.5 characterized with 87.0 nmol L^{-1} (Fig. 5-2g). The $DMSP_p$ concentration was higher along the SSF transect with an average of 71.2 ± 42.5 nmol L^{-1} with the highest concentration encountered at St.15 with 155.6 nmol L^{-1} (Fig. 5-2g), where the Chl-*a* was at the highest. The NCZ was more consistent with an average $DMSP_p$ of 65.1 ± 12.9 nmol L^{-1} with no significant variations among the stations (Fig. 5-2g). The $DMSO_p$ concentrations followed the $DMSP_p$ peaks (St.5, 9 and 15). The lowest concentration was analysed for the St.1 with an increase towards the open sea (Fig. 5-2h) and an average for the BS transect of 9.1 ± 5.1 nmol L^{-1}. An average $DMSO_p$ concentrations of 7.8 ± 4.8 and 10.3 ± 3.8 nmol L^{-1} were observed for the SSF and NCZ transects with higher values at St.11, 13, 15 and 18 (Fig. 5-2h).

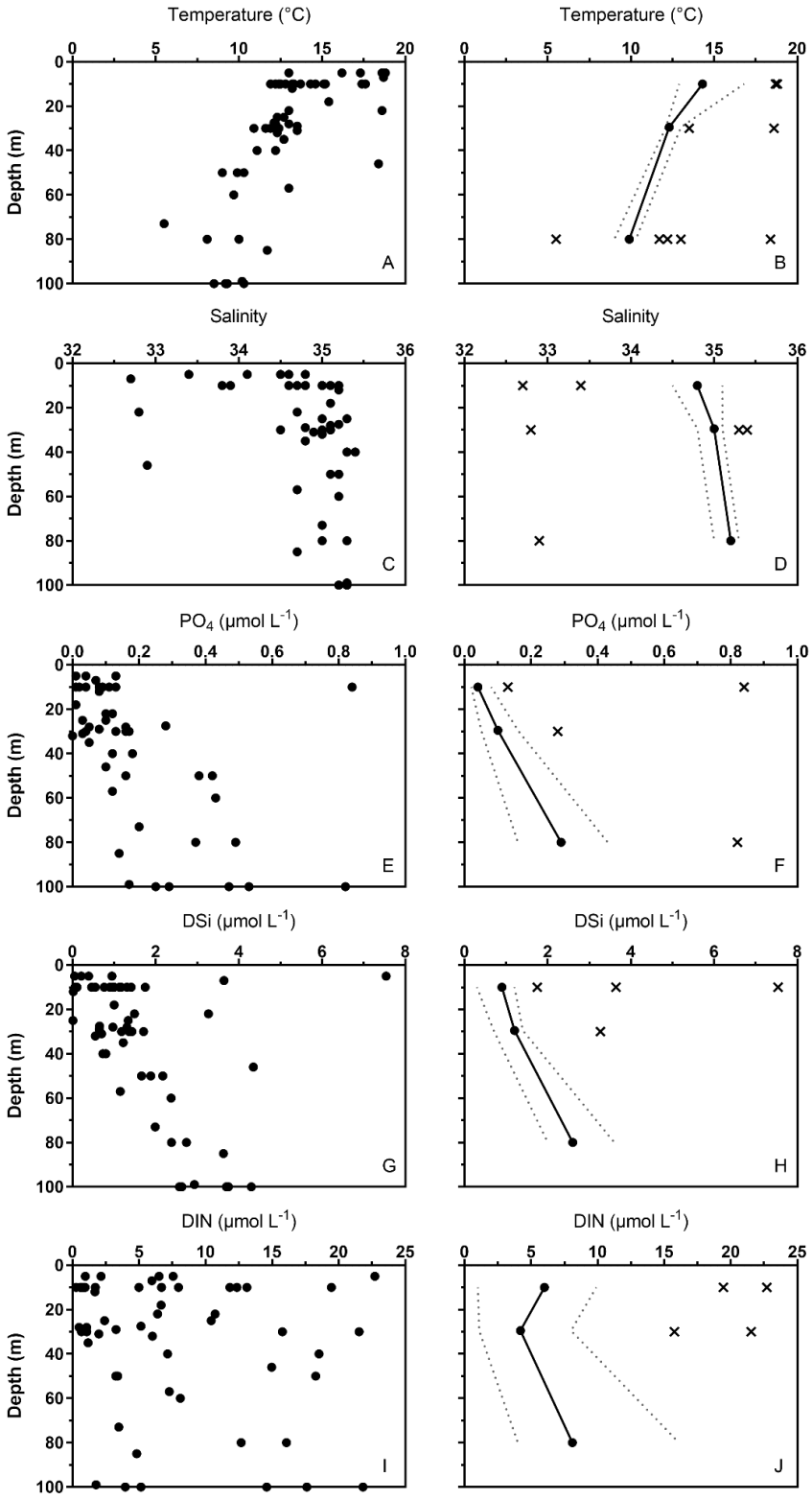

Figure 5-3: Depth profiles for temperature (°C) (a - b), salinity (c – d), phosphates (PO_4) (e – f), Dissolved Silicates (DSi) (g – h) and Dissolved Inorganic Nitrogen (DIN) (i – j) concentrations (µmol L^{-1}) for the three transects. On the left: the individual profiles; and the right: depth-binned data represented by median values (black line with circles), range excluding outliers and delimited by 25th and 75th percentiles (dotted lines) and outliers (stars) for each depth.

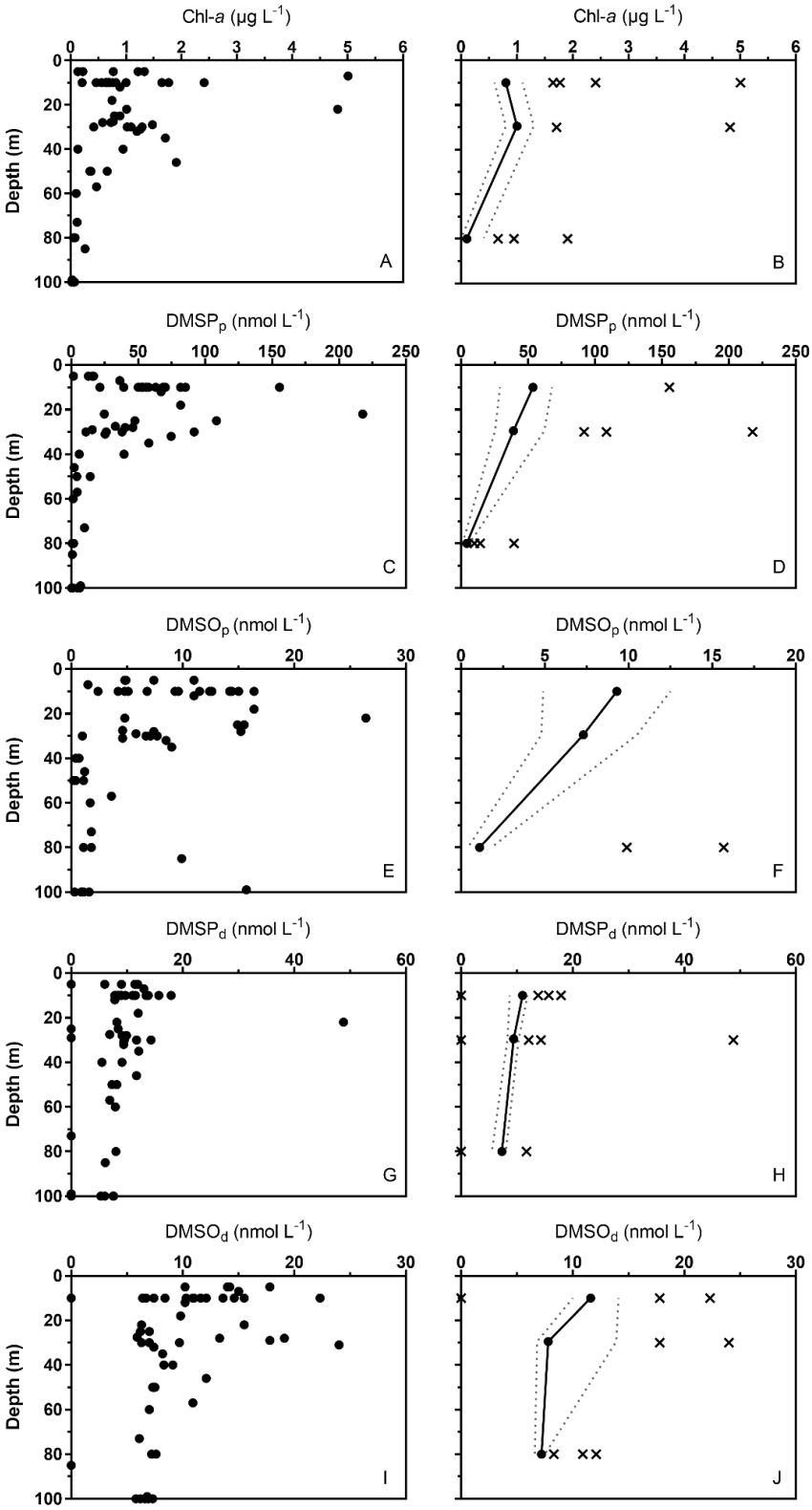

Figure 5-4: Depth profiles for Chlorophyll-*a* (Chl-*a*) (µg L^{-1}) (a - b), particulate dimethylsulfoniopropionate ($DMSP_p$) (c – d), particulate dimethylsulfoxide ($DMSO_p$) (e – f), dissolved dimethylsulfoniopropionate ($DMSP_d$) (g – h) and dissolved dimethylsulfoxide ($DMSO_d$) (i – j) concentrations (nmol L^{-1}) for the three transects. On the left: the individual profiles; and the right: depth-binned data represented by median values (black line with circles), range excluding outliers and delimited by 25th and 75th percentiles (dotted lines) and outliers (stars) for each depth.

Regarding their profiles along the depth, $DMSP_p$ trends to decrease with median value of 53.7 ± 39.0, 39.1 ± 36.9 and 4.3 ± 5.3 nmol L^{-1} respectively for each depth (Fig. 5-4c, d). The same observation could be noted for $DMSO_p$ with 9.3 ± 7.6, 7.3 ± 5.7 and 1.1 ± 1.3 nmol L^{-1} (Fig. 5-4e, f). While the $DMSP_p$ were ranging from 0.4 to 217.7 nmol L^{-1} (Fig. 5-4c), the $DMSP_d$ concentrations observed were between the detection limit and 48.8 nmol L^{-1} (Fig. 5-4g), with no significant variations along the transects and following the $DMSP_p$ peaks (data not shown). On the contrary, the $DMSO_p$ concentrations were lower from 0.2 to 26.4 nmol L^{-1} (Fig. 5-4e) while the dissolved part was ranging between the detection limit and 24.0 nmol L^{-1} (Fig. 5-4i). The median value for $DMSO_d$ was higher at each depth than the $DMSO_p$ (Fig. 5-4j). DMSO levels in seawater can actually exceed those of both DMS and $DMSP_d$ (Hatton et al., 1998). Nevertheless, this affirmation was not observed in our field measurements as it was for the SNS in 2018 (*cf.* Chapter IV).

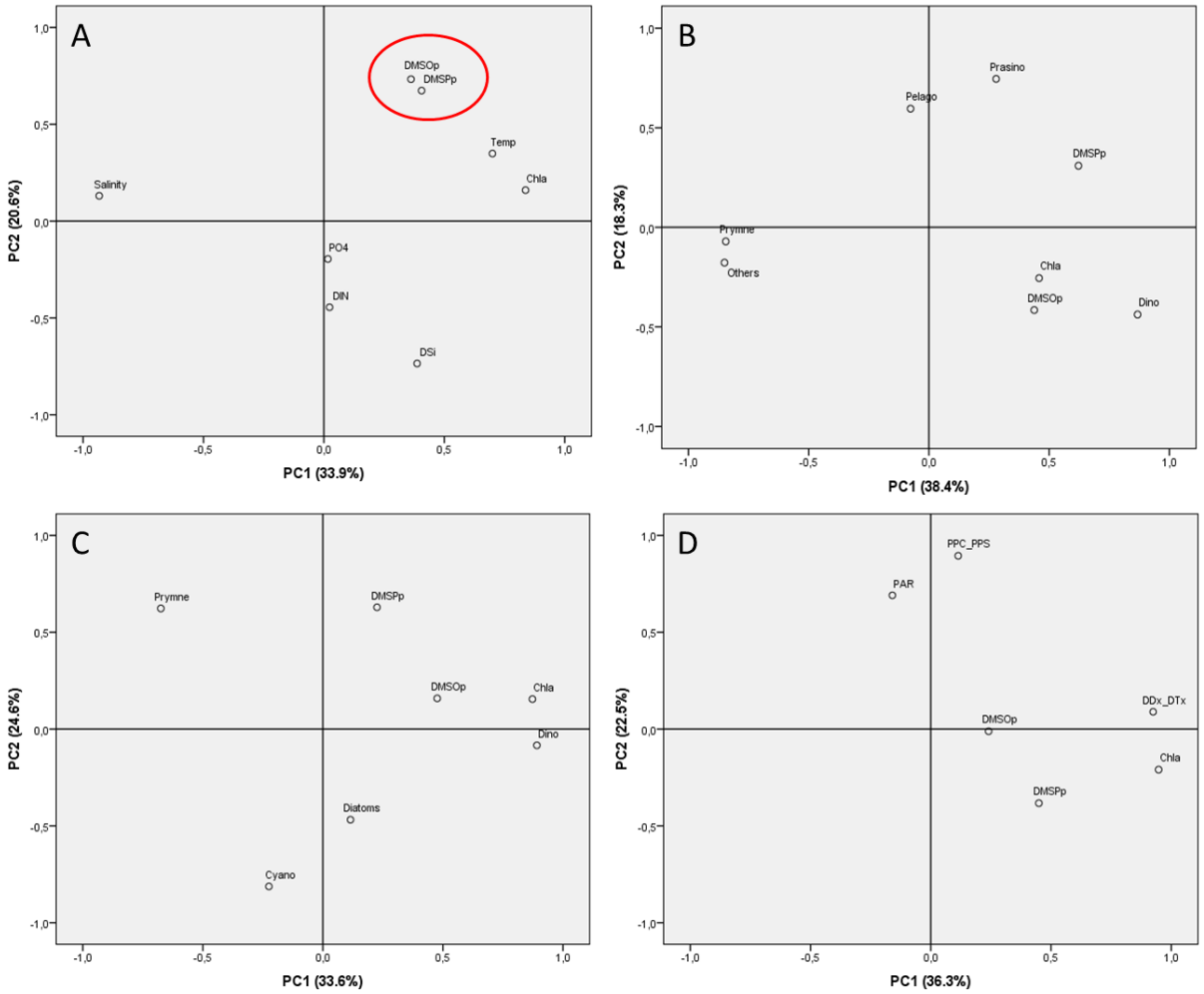

Figure 5-5: Principal Component Analysis with (a) the three depths combined, (b) the first depth including the genomic diversity, (c) the first depth including the pigment biomarkers analysed by CHEMTAX methodology, and (d) the first depth including the photoprotective pigments and the incident Photosynthetic Active Radiation (PAR). The variables included are the Chlorophyll-*a* (Chl-*a*), particulate dimethylsulfoniopropionate ($DMSP_p$), particulate dimethylsulfoxide ($DMSO_p$), temperature (Temp), salinity, phosphates (PO_4), Dissolved Silicates (DSi) and Dissolved Inorganic Nitrogen (DIN).

We then explored the similarities between all the variables to understand their links with the sulfur compounds. Combining the three depths, the figure 5-5a shows the grouping of variables within an orthogonal 2D-space along the two most relevant PCs explaining 54.5% of the variability among the samples.

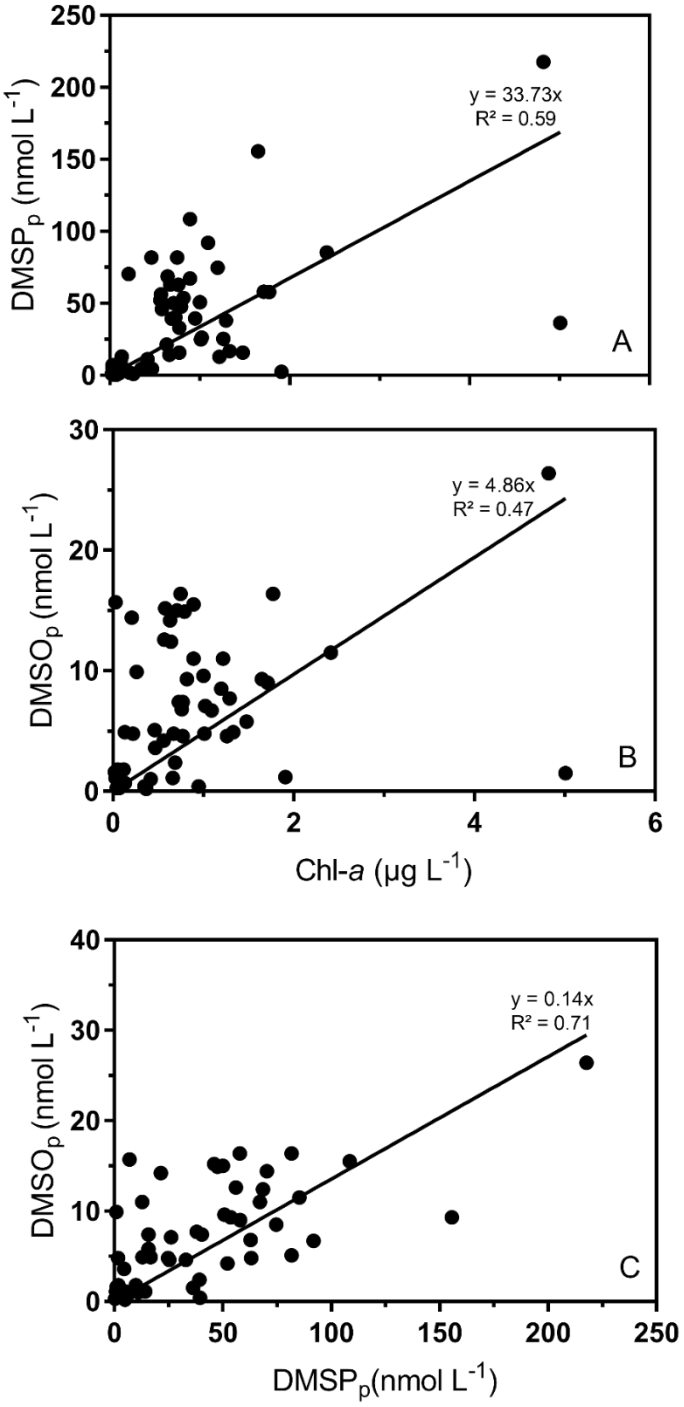

Figure 5-6: (a) Particulate dimethylsulfoniopropionate ($DMSP_p$) and (b) particulate dimethylsulfoxide ($DMSO_p$) concentrations (nmol L^{-1}) versus Chlorophyll-*a* concentrations (Chl-*a*) (µg L^{-1}); and (c) $DMSO_p$ (nmol L^{-1}) versus $DMSP_p$ concentrations (nmol L^{-1}) for the three transects including the three depths. Linear regression was applied for each relationship.

The $DMS(P,O)_p$ were clustering together and with Chl-*a* while the salinity was at the opposite (Fig. 5-5a). The nutrients were varying in the same way as expected. We observed indeed a strong correlation between $DMSP_p$ and Chl-*a* ($\rho = 0.595$, $p < 0.001$, $n = 56$; $R^2 = 0.59$; Fig. 5-6a) as it was for $DMSO_p$ ($\rho = 0.403$, $p < 0.01$, $n = 56$; $R^2 = 0.47$; Fig. 5-6b). Actually, the $DMSP_p$ was positively correlated with Chl-*a* concentrations during the transect SSF ($\rho = 0.849$, $p < 0.001$, $n = 17$) as it was also for $DMSP_p$ ($\rho = 0.524$, $p < 0.05$, $n = 21$) and $DMSO_p$ ($\rho = 0.498$, $p < 0.05$, $n = 21$) for the NCZ transect. As suggested with the PCA (Fig. 5-5a), the two sulfur compounds were positively correlated ($\rho = 0.661$, $p < 0.001$, $n = 56$; Fig. 5-6c), as it was observed recently in the SNS (*cf.* Chapter IV), or in a global data set (Simó and Vila-Costa, 2006). The $DMSP_p$ and $DMSO_p$ were correlated for the three transects BS ($\rho = 0.629$, $p < 0.01$, $n = 18$), SSF ($\rho = 0.698$, $p < 0.01$, $n = 17$), and NCZ ($\rho = 0.749$, $p < 0.001$, $n = 21$). This strong correlation was only pointed out for the second depth for all the data ($\rho = 0.845$, $p < 0.001$, $n = 16$) where the maximum of Chl-*a* was observed. Since it is largely assumed than the phytoplankton is the main DMSP producer, it was not surprising that the vertical distribution patterns of DMSP followed those of phytoplankton (Zhang et al., 2019).

Considering night and day sampling, the dynamics between DMSP concentration and other cellular processes entrained by circadian rhythms might influence its concentration (Berdalet et al., 2011). Nevertheless, we did not observe significant differences between the morning (5 – 13h), the afternoon (13 – 21h) or the night (21 – 5h) sampling for the three transects (data not shown). Variations of DMSP content was observed between dark and light periods with higher concentrations observed during the light for diatoms (Spielmeyer and Pohnert, 2012), *E. huxleyi* (Bucciarelli et al., 2007), or natural communities (Sunda et al., 2005), but with no variations for corals during 24h of sampling (Tapiolas et al., 2013). The spatial heterogeneity of our sampling might influence the results observed regarding the DMSP evolution along a diel timescale.

3.3 Antioxidant function for $DMS(P,O)_p$

The antioxidant function described previously (*cf.* Chapter III) and suggested by Sunda et al. (2002) provide motivation for investigating *in situ* $DMS(P,O)_p$ concentrations in terms of ancillary data that might indicate shift in the physiological status of the phytoplankton cells (Bell et al., 2010). The phytoplankton community was classified using the photoprotective carotenoids (PPC: DDx, Allox, Zeax and β-car) in the context of the photosynthetic carotenoids (PPS: But, Hex, Fucox, Perid and Prasi) (Gibb et al., 2000; Bell et al., 2007; Bell et al., 2010). The percentage of PPC (%PPC) is defined as follows (Gibb et al., 2000; Bell et al., 2010):

%PPC = (PPC/(PPC+PPS))*100.

Correlations between $DMS(P,O)_p$ or $DMS(P,O)_p$:Chl-*a* ratio and %PPC were very weak (Fig. 5-7a, b) even if the %PPC signal along the campaign tends to be dominated by Hex, a major pigment in the Prymnesiophyceae (Bell et al., 2010), known to be high-DMSP producing group (Keller et al., 1989).

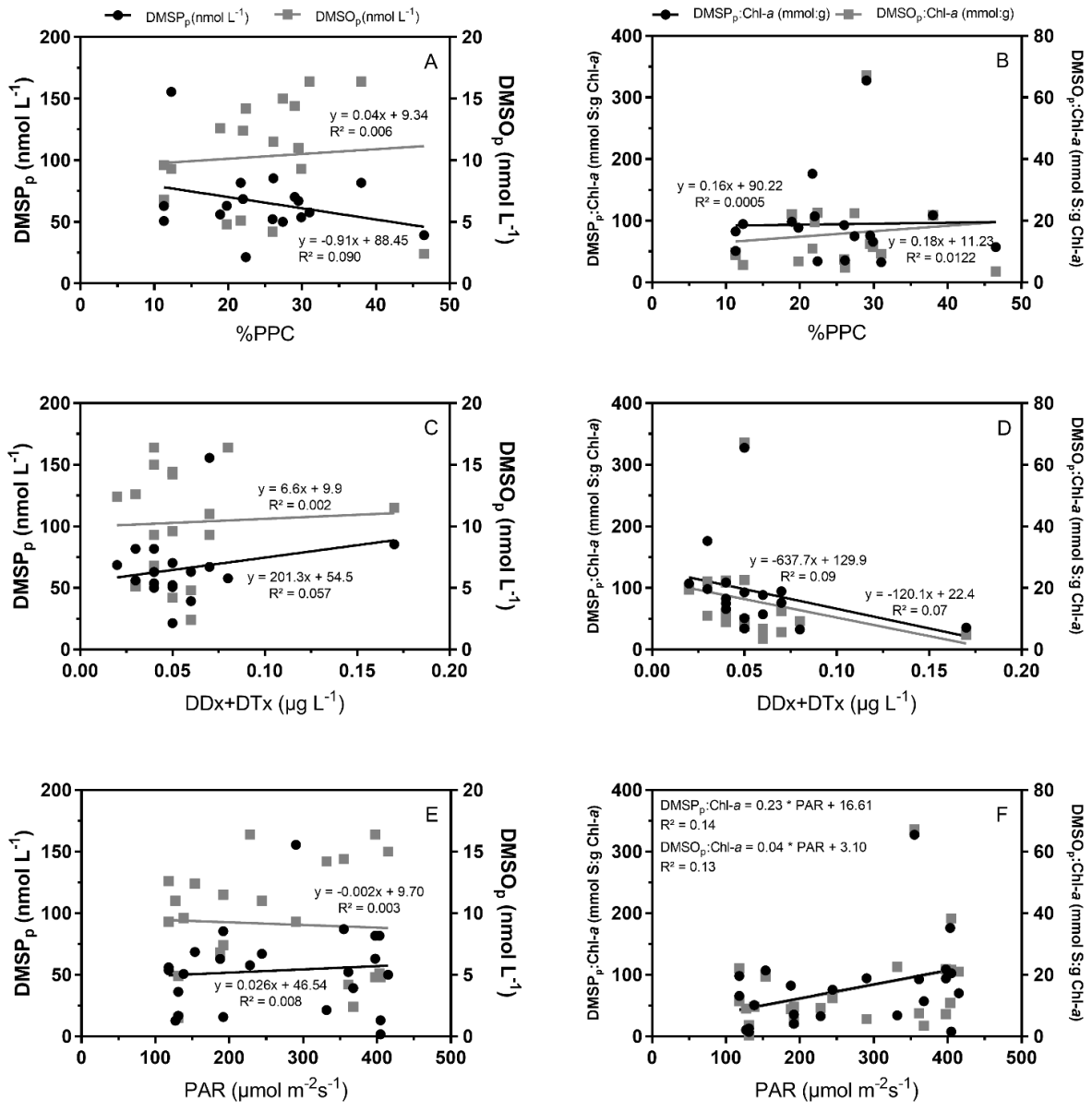

Figure 5-7: *On the left:* Particulate dimethylsulfoniopropionate ($DMSP_p$) and particulate dimethylsulfoxide ($DMSO_p$) concentrations (nmol L^{-1}) and *on the right:* $DMSP_p$:Chl-*a* and $DMSO_p$:Chl-*a* in function of (a-b) %PPC; (c-d) DDx+DTx concentration (µg L^{-1}) and (e-f) Photosynthetic Active Radiation (PAR) (µmol $m^{-2}s^{-1}$) for the three transects including the first depth. Linear regression was applied for each relationship.

Since DDx and DTx are part of the same photoprotective xanthophyll cycle, the total concentration of both could be also used as indicator of the prominence of this cycle within the

cell metabolism (Bell et al., 2010). No correlation was found in our field measurements (Fig. 5-7c, d) as it was during the Atlantic Meridional Transect (Bell et al., 2007) but at the opposite of the strong association found between DMS and $DMSP_t$ with DDx+DTx in the sub-tropical Atlantic (Bell et al., 2010). Furthermore, we tested if the $DMS(P,O)_p$ concentrations or ratio could be linked to PAR as it was for DMS in previous studies. As a matter of fact, no significant correlations were found (Fig. 5-7d, e). No clustering between $DMS(P,O)_p$ with PAR was indeed denoted with the PCA in the figure 5-5d.

The difficulty to determine whether the variation in correlations strength with the pigments or PAR are driven by the sampling, the spatial heterogeneity or difference in phytoplankton community (Bell et al., 2010). However, studies reporting significant correlations were mainly from the subtropical region between DMSP and photoprotective pigments (Riseman and DiTullio, 2004; Bell et al., 2010) or between DMS and seasonal variation of light intensity. Daily PAR variation from our field measurement (from 118 to 415 µmol $m^{-2}s^{-1}$ (Fig. 5-2i)) was in the same range than the following studies. PAR was varying between 158 and 653 µmol $m^{-2}s^{-1}$ in the oligotrophic gyres of the Atlantic Ocean from April to June 2003-2004 and September-October 2003 (Miles et al., 2009). Under light intensity from 95 to 455 µmol $m^{-2}s^{-1}$, Galí et al. (2011) observed correlations with gross DMS production from deck incubations with seawater from the Northwest Mediterranean Sea (throughout the seasonal cycle), the Southern Indian Ocean, and the Tasman sea (during the austral summer). Including the incident light and the mixed layer depth, the Solar Radiation Dose (SRD) from Vallina and Simó (2007) was varying from 20 to 606 µmol $m^{-2}s^{-1}$ in the Norwest Mediterranean Sea during the year 2003, and in the Sargasso Sea from January 1992 to November 1994. Lizotte et al. (2012) also found correlation between DMS and PAR, from 26 to 282 µmol $m^{-2}s^{-1}$, for a dataset extending from the subtropical gyre to the Greenland current and from spring to fall 2003.

DMS(P,O) antioxidant function thus do not seem to be dominant in temperate regions for small temporal sampling characterized by small $DMS(P,O)_p$ concentrations due to lower biomass, and daily PAR variation. The correlations were significant for long period of sampling and mainly with the DMSP oxidation products, DMS, resulting from the antioxidant response (Sunda et al., 2002) (*cf.* Chapter I – 5. Antioxidant function). Additional measurement such as DL activity or the efficiency of the photosystem II would lead to a better appreciation of the physiological status of the phytoplankton community within the water column. The physiological status would provide useful information regarding the oxidative stress that might occur during these periods of sampling.

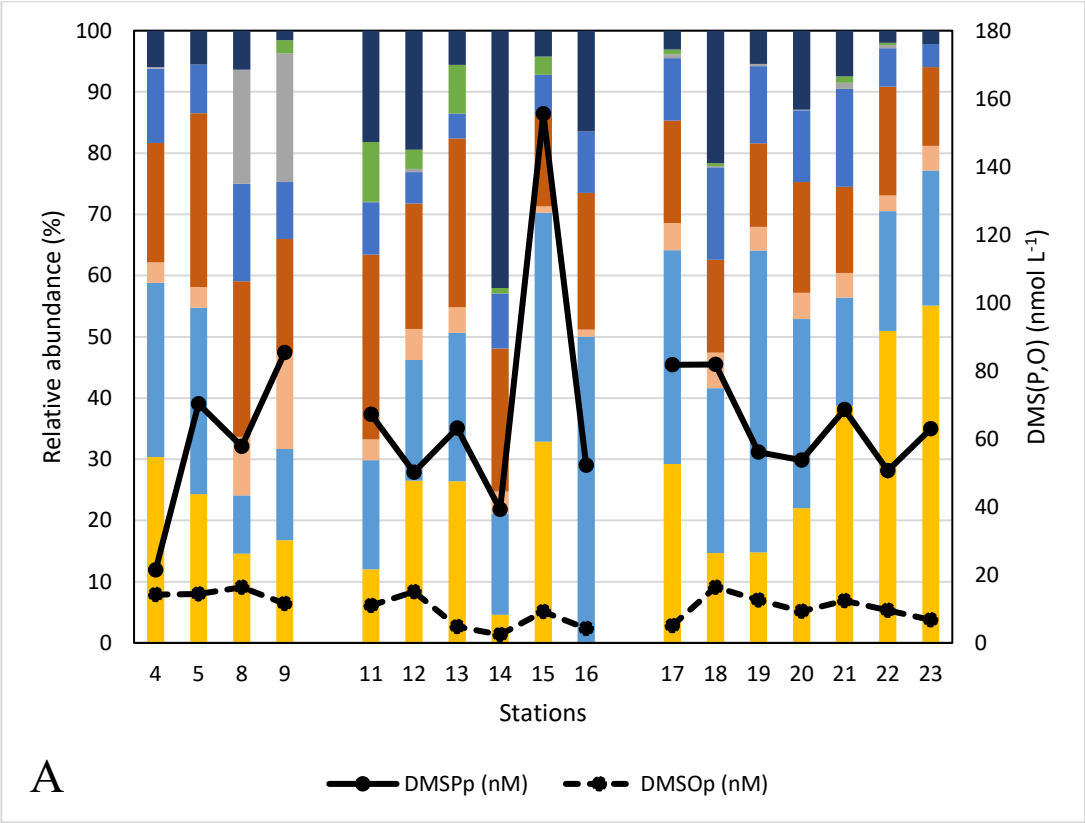

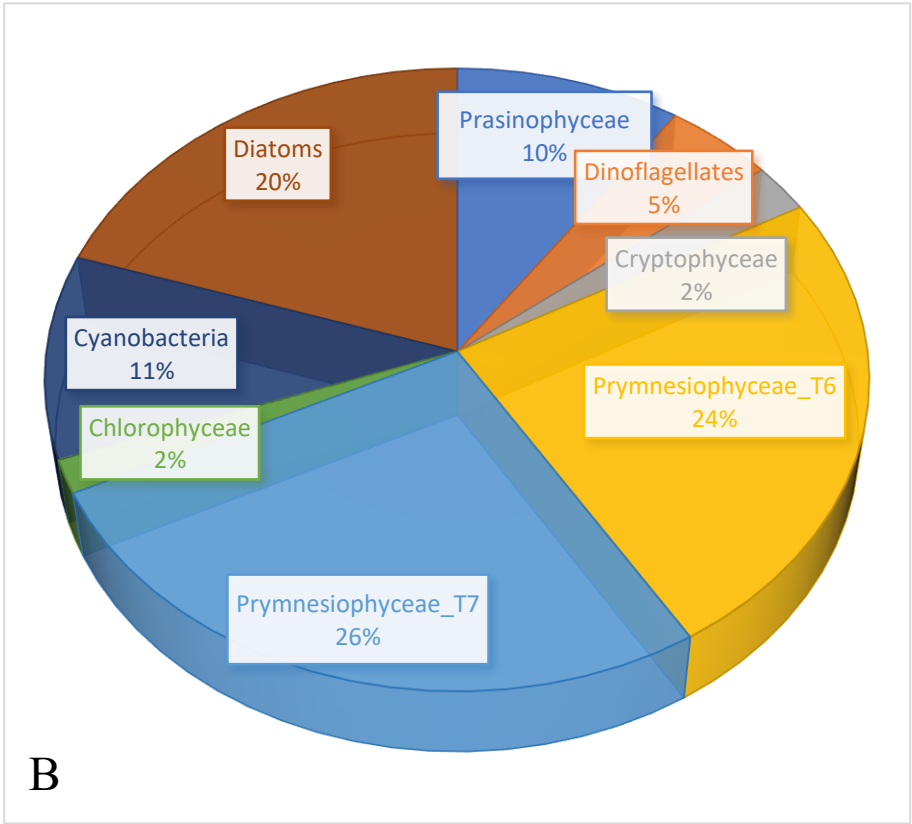

Figure 5-8: Biomarkers analysed by CHEMTAX methodology for (a) each stations and the main phytoplankton groups encountered with the particulate dimethylsulfoniopropionate ($DMSP_p$) and particulate dimethylsulfoxide ($DMSO_p$) concentrations (nmol L^{-1}) variation, and (b) with the averaged biomarkers for all the stations for the three transects including the first depth.

3.4 DMS(P,O) production resulted from a mixed phytoplankton community.

We further use two methodologies to explore the phytoplankton diversity based on specific pigments or DNA extraction. Each method presents an incomplete picture of phytoplankton community and often complement each other (Kramer et al., 2020). HPLC pigments (Chl and carotenoids) provide an opportunity to characterize the community at low taxonomic resolution (i.e. group level) since they occur in all algal taxa with variable degrees of specificity (Table Supp. 5-1) (Jeffrey et al., 2011; Kramer et al., 2020). We thus decided to estimate the relative abundance of algal types using the CHEMTAX methodology (Mackey et al., 1996) and described the phytoplankton groups with the genomic data.

The Prymnesiophyceae were the most abundant for the three transects with an average of 51 ± 17% (Fig. 5-8b). We distinguished the Prymnesiophyceae_T6 (Type 6; 24 ± 15%) and the Prymnesiophyceae_T7 (Type 7; 26 ± 11%) based on Jeffrey and Wright (2005). Both were present with similar proportions during the campaign (Fig. 5-8b). With the genomic analysis, the Prymnesiophyceae was represented mainly by *Phaeocystis sp, Prymnesium sp.* and *Chrysochromulina strobilus.* The Cryptophytes and dinoflagellates were present at St.8 and 9 while the Chlorophytes were at St.11 and 13 (Fig. 5-8a). The Cryptophytes detected were mostly *Teleaulax amphioxeia* while the dinoflagellates regrouped species such as *Heterocapsa rotundata, Karlodinium veneficum, Tripos sp., Gyrodinium sp., Karenia mikimotoi, Katodinium sp*., *Pelagodinium beii*, and *Gymnodinium sp.* (data not shown).

The relative abundance of diatoms were constant during the three transects with 20 ± 5% (Fig. 5-8b). The Prasinophyte were mainly present during the NCZ transect (Fig. 5-8a) and with an average relative abundance for the three transects of 10 ± 4% (Fig. 5-8b). Some Mamiellyophyceae (*Micromonas pusilla* and *Bathycoccus prasinos*) and Pelagophyceae (*Aureococcus anophagefferens*) were also observed with the genomic analysis. The Cyanobacteria were important during the SSF transect with a relative abundance of 42% at St.14 (Fig. 5-8a) but an average of 11 ± 10% (Fig. 5-8b).

However, no distinct patterns were observed between the relative abundance of biomarker algal types and the $DMS(P,O)_p$ concentrations (Fig. 5-8a). In addition, any strong $DMS(P,O)_p$ correlations or linear regressions with any pigment biomarkers, pigments alone, or algal groups based on genomic data were identified ($p > 0.05$; data not shown). The PCA brought the same ascertainment since no cluster was identified with the CHEMTAX or genomic analysis (Fig. 5-5b, c). Our results are in contradiction with Belviso et al. (2001) that identified strong

correlation between $DMSP_p$ and Hex+But within more than 200 surface-water samples collected over contrasting ocean regions and time sampling. Same observation was also encountered between $DMSP_p$, Hex and *Phaeocystis* sp. in the Ross Sea, Antarctica during February 1992 (DiTullio and Smith, 1995) or through the Drake Passage during October to December 1992 (Turner et al., 1995). In the Belize coastal lagoon and adjacent barrier reef systems, Sunda et al. (2005) observed relations between $DMSP_p$ and peridinin ($R^2 = 0.92$), indicator pigments for dinoflagellates. The absence of significant and positive correlations in our field measurements demonstrated that $DMS(P,O)_p$ production cannot be easily related to algal group based on biomarker, as it was in the oligotrophic subtropical and tropical regions analysed by Bell et al. (2010).

The use of biomarkers or genomic analysis for mixed phytoplankton community could also affect the view of the community structure. First of all, most pigments are not perfect indicators of taxonomy and many pigments are shared between taxonomic groups (Higgins et al., 2011; Jeffrey et al., 2011). For instance, the dinoflagellates harbour different plastid types including peridinin, prymnesiophyte-like, diatom-like, cryptomonad-like, prasinophyte-like plastids. We observed indeed the presence of *K. veneficum, K. mikimotoi, Gyrodinium sp.,* and *Gymnodinium sp.* that are characterized by prymnesiophyte-like plastid (Tengs et al., 2000; Caruana and Malin, 2014). The pigment analysis thus did not detect these species since they lack peridinin (Coupel et al, 2015). In addition, the heterotrophic and mixotrophic dinoflagellates can lead to misinterpretation since CHEMTAX potentially considers other pigments present in algae ingested by dinoflagellates (Coupel et al., 2015). CHEMTAX methodology also assumes that individual or combinations of pigments correspond to unique phytoplankton groups, and the contribution of individual phytoplankton pigments to each taxonomic class are known (Kramer and Siegel, 2019). On global or even on local scales, direct comparisons between CHEMTAX and other methods of phytoplankton identification are often inconsistent (Kramer and Siegel, 2019 and citations therein).

3.5 DMS(P,O) estimations

Since $DMSP_p$ was significantly correlated with Chl-*a* concentrations, we compared $DMSP_p$ computed for the three surface transects from the linear regression with Chl-*a* ($DMSP_p$ (nmol L^{-1}) = 52.0 * Chl-*a* (µg L^{-1}), $R^2 = 0.67$; excluding the first station; data not shown) with the measured $DMSP_p$ data as it was realized in Chapter IV.

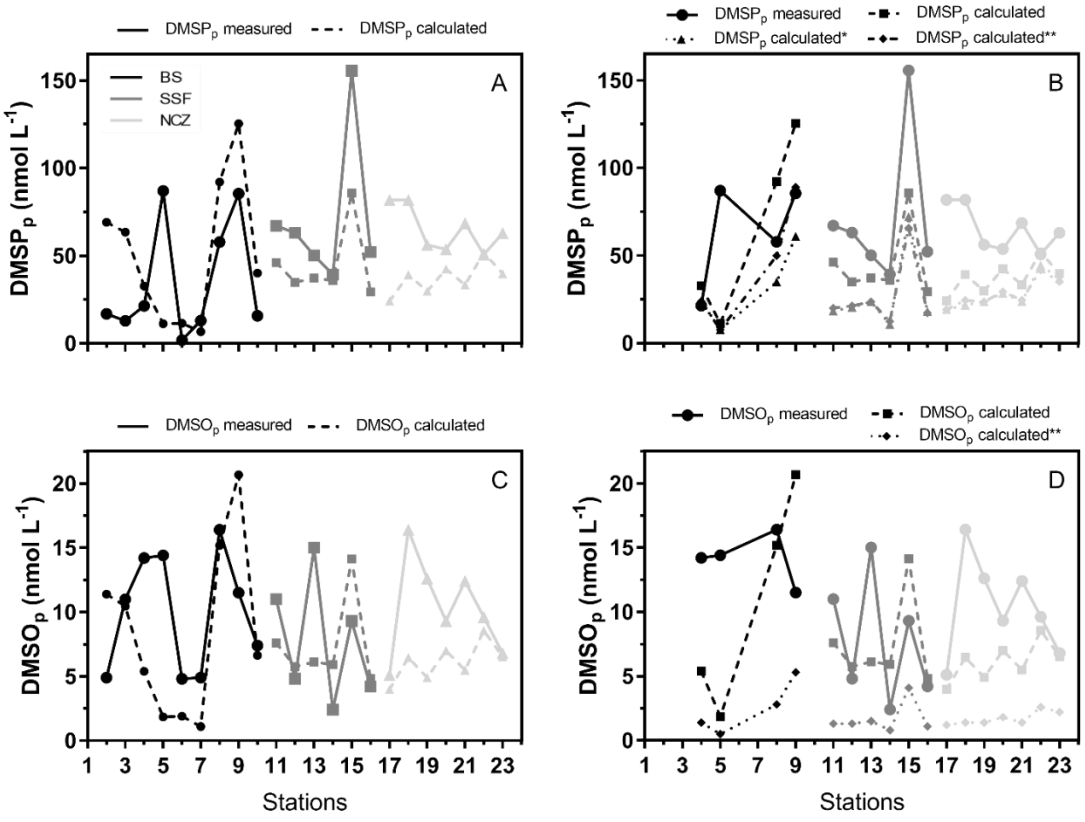

Figure 5-9: Seasonal evolution for the three surface transects of (a) particulate dimethylsulfoniopropionate ($DMSP_p$) measured (nmol L^{-1}) and $DMSP_p$ calculated (in dotted lines) based on Chlorophyll-*a* (Chl-*a*) using one relationship for all phytoplankton species [$DMSP_p$ (nmol L^{-1}) = 52.0 * Chl-*a* (µg L^{-1})] for all the stations; of (b) $DMSP_p$ measured compared to $DMSP_p$ calculated based on the Chl-*a* linear regression ($DMSP_p$ calculated), based on the pigment relative abundance and specific $DMSP_p$:Chl-*a* ratio (Table Supp. 5-1) ($DMSP_p$ calculated*) or $DMSP_p$:Chl-*a* ratio from Stefels et al. (2007) ($DMSP_p$ calculated**); (c) particulate dimethylsulfoxide ($DMSO_p$) measured (nmol L^{-1}) and $DMSO_p$ calculated (in dotted lines) based on Chlorophyll-*a* (Chl-*a*) using one relationship for all phytoplankton species [$DMSO_p$ (nmol L^{-1}) = 8.6 * Chl-*a* (µg L^{-1})] for all the stations; of $DMSO_p$ measured compared to $DMSO_p$ calculated based on the Chl-*a* linear regression ($DMSO_p$ calculated), based on the pigment relative abundance and $DMSO_p$:Chl-*a* ratio for the main phytoplankton groups (Table. Supp. 5-2) ($DMSP_p$ calculated**).

First of all, the $DMSP_p$:Chl-*a* ratio from the linear regressions was in the same range than the value from Stefels et al. (2007) (52 ± 37 mmol:g) or recalculated from published literature (Table Supp. 5-2: 60.4 ± 25.5 mmol:g) for the Prymnesiophyceae, possibly confirming the dominance of this group in the area. However, while the spatial variation was well represented for some stations (St.6 – 10; St.14 – 16), others were at the opposite of what we observed (St.2 – 5) (Fig. 5-9a). We also noticed an underestimation for the transect NCZ with a spatial evolution that was not similar (Fig. 5-9a). Same procedure was applied for the $DMSO_p$ estimation from the linear regressions with Chl-*a* ($DMSO_p$ (nmol L^{-1}) = 8.6 * Chl-*a* (µg L^{-1}), $R^2 = 0.69$; excluding the first station; data not shown). The same observations could mainly be drawn for the DMSO estimation with a more chaotic evolution of the $DMSO_p$ measured that was not reflected in the $DMSO_p$ calculated (Fig. 5-9c).

We then used the relative abundance deduced from the pigment biomarkers (Fig. 5-8a) to estimate the $DMS(P,O)_p$ using $DMS(P,O)_p$:Chl-*a* ratio specific to each phytoplankton group. The relative abundance of each phytoplankton group was multiplied by the Chl-*a* concentration at each station (Fig. 5-2f) as well as the average $DMS(P,O)_p$:Chl-*a* ratio from Table Supp. 5-2 or 5-3 for each group ($DMS(P,O)_p$ calculated*), or from Stefels et al. (2007) ($DMS(P,O)_p$ calculated**). Using the three methodologies (Chl-*a* linear regressions based on field measurements, specific and group $DMS(P,O)_p$:Chl-*a* ratio from published literature) brought an underestimation of the $DMSP_p$ calculated (Fig. 5-9b). The spatial evolution of the $DMSP_p$ estimated was similar than the $DMSP_p$ measured for most of the stations since $DMSP_p$ followed the Chl-*a* concentrations (*c.f. 4.2*). The $DMSP_p$ calculated from the Chl-*a* linear regression was the less underestimated since the $DMSP_p$:Chl-*a* ratio used was deduced from the field measurements (Fig. 5-9b). With the same methodology, the following ascertainment could be drawn for the $DMSO_p$ estimation: underestimation when using $DMSO_p$:Chl-*a* ratio ($DMSO_p$ calculated**) while the $DMSO_p$ calculated from the Chl-*a* linear regression from field measurements was mainly within the same range than the $DMSO_p$ measured, without the spatial evolution. However, the difference in the average $DMSO_p$ estimation was not significant with 10.3 ± 4.4 and 7.7 ± 4.7 nmol L^{-1} for $DMSO_p$ measured and calculated, respectively.

In conclusion, the $DMS(P,O)_p$ variation along the three transects was explained by the phytoplankton diversity but no distinct patterns could be extrapolated to understand and predict the observed $DMS(P,O)_p$. In the previous Chapter IV, the calculated $DMS(P,O)_p$ fitted with the $DMS(P,O)_p$ observed thanks to relationships discriminating the diatoms and *Phaeocystis* community. The mixed phytoplankton community during this campaign did not provide an easy way to characterize and estimate the $DMS(P,O)_p$. The $DMSO_p$ estimation, even in the range of the calculated $DMSO_p$, did not follow its spatial evolution. Its passive diffusion and physiological reactions within the cells (i.e. antioxidant response) might explain its unpredictable variation along this short period of time. $DMS(P,O)_p$ can be thus mainly estimated when the phytoplankton community is dominated by low and high-DMSP producing species as it was in the SNS. The correlation with biomarkers have also been suggested for small spatial and temporal scales such as blooms (DiTullio and Smith, 1995; Turner et al., 1995; Sunda et al., 2005). In addition, the high inter- and intraspecific variability regarding the $DMS(P,O)_p$:Chl-*a* production within each phytoplankton group (Table Supp. 2, 3) (Stefels et al., 2007) could also lead to unpredictable DMS(P,O) variations in our field analysis characterized by mixed phytoplankton communities.

4 Conclusions

The study of twenty days of sampling in the North Sea in August 2018 demonstrated coastal-oceanic variations in terms of Chl-*a* concentrations that were mainly explained by the nutrients' gradient. We tried to understand and explain the $DMS(P,O)_p$ evolution regarding ancillary measurements such as photoprotective pigments, incident light or phytoplankton diversity. We did not observe the antioxidant function within our field samples. As a result of DMSP cascade reaction due to oxidative stress, DMS measurements would probably lead to a better appreciation of this hypothesis. This function was mainly observed with DMS measurements from long-term sampling period and for subtropical area, contrasting with our short-term sampling in a temperate sea.

Furthermore, the phytoplankton diversity based on pigment biomarkers or genomic analysis did not provide in our study an easy way to observe distinct $DMS(P,O)_p$ patterns. This resulted from the mixed phytoplankton community without the dominance of low or high-DMSP producing species. The wide range of DMSP production resulting from this mixed phytoplankton community leads to unpredictable DMSP variations. Previous correlations were mainly observed between the sulfur compounds, pigments, and phytoplankton diversity during phytoplankton efflorescence, at the opposite of our mixed phytoplankton community.

In order to understand the antioxidant function within field samples, further work would have to conduct DMS analysis in parallel of ancillary parameters to englobe the physiological status of the community. A better understanding of the DMS(P,O) function within the cell and between the phytoplankton groups would lead to a better appreciation of their production and evolution along diverse abiotic profiles.

5 Acknowledgements

We are grateful to the crew of the *RV Heincke* for assistance during the cruises, to Rüdiger Röttgers (HZG) for organizing the schedule of the cruise and the on-board organization, to Rüdiger Röttgers (HZG) and Kerstin Heymann (HZG) for the HPLC pigments' analysis. The GC was acquired with funds from the Fonds National de la Recherche Scientifique (FNRS) (2.4.637.10). NG and CR received financial support from the Fonds David et Alice Van Buuren. CR have a PhD grant from the FRIA (Fund for Research Training in Industry and Agriculture, FNRS). AVB is a senior research director at the FNRS.

6 Appendix

Table Supp. 5-1: Summary of the 18 pigments used for the CHEMTAX analysis and the distribution of these pigments across the taxonomic groups (based on Kramer and Siegel, 2019).

	Diatoms	Dinoflagellates	Prymnesiophyceae T6	Prymnesiophyceae T7	Cryptophyceae	Prasinophyceae	Chlorophyceae	Cyanobacteria
But								
Hex								
Allo								
DTx								
DDx								
Perid								
Fuco								
Zea								
MVChl-*a*								
DV-Chl-*a*								
MV-Chl-*b*								
DV-Chl-*b*								
Chl-*c1+c2*								
Chl-*c2*-MGDG								
Chl-*c3*								
MV-Chl-*c3*								
Neo								
Viola								
Lut								
Pras								

	Unique		Rarely present
	Always often		Not present
	Often present		

Table Supp. 5-2: Ratio of particulate dimethylsulfoniopropionate ($DMSP_p$) to Chlorophyll-*a* (Chl-*a*) concentration ($DMSP_p$:Chl-*a*) (mmol:g), cell biovolume (µm³), cell carbon (C) content (pgC $cell^{-1}$) compiled from published literature for species found during the campaign.

Class	Genus	Species	Biovolume (µm³)	C (pgC $cell^{-1}$)	Chl-*a* (pgChl-*a* $cell^{-1}$)	$DMSP_p$ (fmol $cell^{-1}$)	$DMSP_p$:Chl-*a* (mmol:g)	Data from
Cryptophyceae	*Teleaulax*	*T. amphioxeia*	90.7	14.9	0.2	0.2	**0.9**	1
Diatom	*Rhizosolenia*	*R. setigra*	69080.0	7561.5	126.0	112.5	**0.9**	2
Diatom	*Guinardia*	*G. delicatula*	58139.0	2105.6	35.1		**1.9**	3
Diatom	*Thalassiosira*	*T. rotula*	15072.0	704.5	11.7	1.9	**0.2**	2
Diatom	*Thalassiosira*	*T. rotula*					**10.5**	3
Diatom	*Thalassiosira*	*Thalassiosira sp.*	13713.0	652.5	10.9	40.8	**3.8**	2
Diatom	*Thalassiosira*	*Thalassiosira sp.*					**2.6**	3
Diatom	*Thalassiosira*	*T. pseudonana*	80.1	10.1			**4.8**	4
Diatom	*Rhizosolenia*	*Rhizosolenia sp.*	69080.0	2421.6	40.4	112.5	**2.8**	2
Diatom	*Pseudo-Nitzschia*	*Pseudo-Nitzschia sp.*	120.0	14.0	0.2	0.2	**0.9**	2
						Average ± s.d. :	**3.2 ± 3.1**	
Dinoflagellates	*Heterocapsa*	*H. rotundata*	234.0	66.3	1.1	20.8	**18.8**	5
Dinoflagellates	*Heterocapsa*	*H. rotundata*	173.3	51.8	1.2	21.4	**17.7**	6
Dinoflagellates	*Heterocapsa*	*H. rotundata*	181.2	53.7	1.4	27.3	**19.5**	6
Dinoflagellates	*Gyrodinium*	*G. aureolum*	5007.6	814.3	13.6	5.3	**0.4**	2
Dinoflagellates	*Gyrodinium*	*G. aureolum*	5007.6	814.4	13.6	0.0	**0.0**	7
Dinoflagellates	*Pelagodinium*	*P. beii*	29187.0	3449.9	57.5	900	**15.7**	2
Dinoflagellates	*Karenia*	*K. mikimotoi*	80178.9	7892.9	131.5	7.5	**0.1**	8
Dinoflagellates	*Katodinium*	*Katodinium sp.*	1439.0	293.3	4.9	201.2	**41.2**	9
Dinoflagellates	*Karlodinium*	*K. veneficum*	739.0	106.7	1.8	7.0	**3.9**	1
Dinoflagellates	*Gymnodinium*	*G. simplex*	265.0	73.4	1.2	238.5	**195.1**	2
Dinoflagellates	*Tripos*	*T. fusus*	19500.0	2479.4	41.3	2.8	**0.1**	7
						Average ± s.d. :	**28.4 ± 56.7**	
Mamiellyophyceae	*Micromonas*	*M. pusilla*	4.2	0.8	0.0	0.2	**10.9**	2

Mamiellyophyceae	*Bathycoccus*	*B. prasinos*	1.8	0.4	0.0	0.0	**5.5**	2
						Average ± s.d. :	**8.2 ± 3.8**	
Pelagophyceae	*Aureococcus*	*A. anophagefferens*	33.51	5.84	0.1	1.0	**10.0**	7
Prasinophyceae	*Pycnococcus*	*P. provasolii*	8.0	1.5	0.0	0.2	**9.5**	2
Prymnesiophyceae	*Phaeocystis*	*P. globosa*	75.0	12.4	0.2	16.3	**78.4**	4
Prymnesiophyceae	*Phaeocystis*	*P. sp.*	46.6	8.0			**59.0**	2
Prymnesiophyceae	*Phaeocystis*	*P. globosa*					**95.3**	3
Prymnesiophyceae	*Phaeocystis*	*P. globosa*					**73.3**	10
Prymnesiophyceae	*Prymnesium*	*Prymnesium sp.*	368.0	55.4	0.9	14.4	**15.7**	2
Prymnesiophyceae	*Chrysochromulina*	*Chrysochromulina sp.*	156.5	24.8	0.4	21.7	**52.4**	2
Prymnesiophyceae	*Emiliania*	*E. huxleyi*	39.5	6.8	0.1	5.5	**48.4**	2
						Average ± s.d. :	**60.4 ± 25.5**	

1. Lee et al. (2012); 2. McParland and Levine (2019); 3. Speeckaert et al. (2018); 4. Royer et al. (in review); 5. Cooney et al. (2019); 6. Cooney (2016); 7. Keller et al. (1989)b; 8. Archer et al. (2009); 9. Townsend and Keller (1996); 10. Speeckaert et al. (2019)

Table Supp. 5-3: Ratio of particulate dimethylsulfoxide ($DMSO_p$) to Chlorophyll-*a* (Chl-*a*) concentration ($DMSO_p$:Chl-a) (mmol:g), cell biovolume (µm³), cell carbon (C) content (pgC cell^{-1}) compiled from published literature for species found during the campaign.

Class	Genus	Species	Biovolume (µm³)	Carbon (pgC cell^{-1})	Chl-*a* (pgChl-*a* cell^{-1})	$DMSO_p$ (fmol cell^{-1})	$DMSO_p$:Chl-*a* (mmol:g)	Data from
Diatom	*Thalassiosira*	*T. oceanica*					**0.4**	1
Diatom	*Thalassiosira*	*T. pseudonana*					**2.0**	2
Diatom	*Thalassiosira*	*T. pseudonana*	119.5	13.9	0.23	0.01937	**0.1**	3
Diatom	*Skeletonema*	*S. costatum*					**1.5**	2
Diatom	*Skeletonema*	*S. costatum*	264	26.5	0.44	0.01192	**0.03**	3
						Average ± s.d.:	**0.8 ± 0.9**	
Dinoflagellates	*Heterocapsa*	*H. triquetra*					**8.6**	4
Dinoflagellates	*Heterocapsa*	*North Sea dominated by Dinoflagellates*					**2.9**	5
Dinoflagellates	*Heterocapsa*	*H. triquetra*					**13.4**	2
Dinoflagellates	*Gymnodinium*	*G. simplex*	265.0	73.36	1.22	0.1	**0.1**	3
						Average ± s.d.:	**6.3 ± 5.9**	
Prymnesiophyceae	*Phaeocystis*	*P. globosa*					**1.3**	4
Prymnesiophyceae	*Phaeocystis*	*North Sea dominated by P. globosa*					**1.2**	5
Prymnesiophyceae	*Phaeocystis*	*P. globosa*					**8.7**	2
Prymnesiophyceae	*Emiliania*	*E. huxleyi*	39.5	6.8	0.11	0.22355	**2.0**	3
						Average ± s.d. :	**3.3 ± 3.6**	3

1. Bucciarelli et al. (2013); 2. Royer et al. (in review)); 3. Hatton and Wilson (2007); 4. Speeckaert et al. (2019); 5. Simó et al. (1998)

Chapter VI – Discussion and perspectives

"Discussion is impossible with someone who claims not to seek the truth, but already to possess it."

- Romain Rolland (Above the battle, 1917).

1 Discussion and perspectives

The main objective of this thesis was to study DMS(P,O) production under oxidative stress (Chapter III) while we brought additional support information between phytoplankton diversity, environmental parameters, and field DMS(P,O) measurements (Chapter IV and V). We tried to explain the spatial and temporal variability of the DMS(P,O) regarding ancillary data measurements such as phytoplankton pigments, community composition, and how the species cope with light stress. The main issues investigated throughout this thesis will be described in this section. The results are summarized and discussed in relation with the progress achieved and from the perspective of future research that could be developed.

1.1 Antioxidant function

The phytoplankton community has to endure various adverse environmental conditions during the day or throughout the seasonal changes. The nutrient availability, the temperature as well as the light intensity influence and impact the cell's adjustments to stabilise the physiological status of the cell. Depending on how the cell reacts according to these environmental variations, the latter can be responsible of the production of Reactive Oxygen Species (ROS) that might be harmful for the cell. This ROS production can lead to cell's damages that will be reflected in the efficiency of the photosystem II (PSII), the increase of the Chlorophyll-*a* (Chl-*a*) fluorescence, the lipid peroxidation, or the decrease in Chl-*a* concentrations (photoacclimation), among others.

To analyse the antioxidant response, we designed an experimental setup to study the impact of light increase and chemical oxidative treatments on three emblematic phytoplankton producing DMS(P,O) groups: the diatom *S. costatum,* the Prymnesiophyceae *P. globosa*, and the dinoflagellate *H. triquetra*. The first is normally considered as low-DMSP producer while the two others are high-DMSP producers (Stefels et al., 2007). This experimental setup allowed us to study the impact of **oxidative stress** while also considering the **taxonomy** as potential drivers of DMS(P,O) production.

The actual consideration in the literature is to cleave the phytoplankton groups between low or high DMSP-producing species such as said previously. This cleavage might be useful to quickly understand the DMSP dynamics within an ecosystem but might hide some potential useful information. For instance, the accepted $DMSP_p$:Chl-*a* ratio are the one gave by Stefels et al. (2007), that already reflected the high variability within each group. We did find significant differences between the diatom, the Prymnesiophyceae and the dinoflagellate as expected

(Chapter III). However, the diatom *S. costatum* already had an elevated $DMSP_p$:Chl-*a* (~35 mmolS:g Chl-*a*), much higher than normally considered (4 ± 6 mmolS:g Chl-*a*) (Stefels et al., 2007). Recently, the homologous gene DSYB, coding for the methyltransferase needed for the DMSP synthesis (Curson et al., 2018) was found within all the Prymnesiophyceae and dinoflagellates tested but only within 20% of diatoms. This low gene presence might explain the variability within the diatoms and within our diatom's species.

Furthermore, reporting the $DMS(P,O)_p$:Chl-*a* ratio is convenient for global models based on satellite-derived Chl-*a* data as proxy for $DMS(P,O)_p$ (Bopp et al., 2003). However, the DMS(P,O) production is taxon-specific, and a wide diversity of microalgae do not produce these sulfur compounds (Keller et al., 1989). In addition, the experimental design (i.e. light, temperature or salinity variation) might influence the Chl-*a* cellular content (Brunet et al., 2011) in addition to affect DMSP (Stefels et al., 2007). We thus suggest reporting $DMS(P,O)_p$-to-cells ratio for further research focusing on the physiological roles of DMS(P,O).

Furthermore, we did not measure the DL activity that would provide useful information regarding the physiological reactions. Caruana and Malin (2014) showed that the DL activity varied considerably between species or even between strains of the same species within the dinoflagellates. The next question arises then: why have some species conserved the capability to produce DMSP and to convert it into DMS thanks to DL, while some others not, or not in the same proportion? The answer to this question might reside in the successive or ancestral endosymbiosis or horizontal gene transfers characterizing the phytoplankton (Keeling, 2010; Fan et al., 2020).

Laboratory experiments mentioned in Chapter III confirmed the DMS(P,O) antioxidant function and this research brought observational support to this hypothesis. The three oxidative treatments did not impact in the same way the $DMS(P,O)_p$ content. We observed a decrease in the $DMSP_p$ during the short-term DCMU and MSB treatments that suggested an interaction between the sulfur compound and ROS produced. Since we did not observe an increase of the lipid peroxidation, this might join the antioxidant definition provided by Halliwell (1995) since $DMSP_p$ delays or prevents the oxidation of oxidizable substrate such as lipids. However, the initial $DMS(P,O)_p$ concentrations did not provide information about how the species will endure a further oxidative stress and the DMS(P,O) cellular contents were not upregulated during long-term high-light treatments. The previous results joined the observations realized by Archer et

al. (2018): the regulation of DMSP is not linked to photooxidative stress without excluding a chemical reaction between ROS and the sulfur compound.

In addition, there are still uncertainties regarding the importance of this function in natural environment. We tried during our field measurements to find any relevant correlation between DMS(P,O) concentrations and photoprotective pigments (Chapter V). These ancillary data did not provide us novel insights for answering our scientific hypothesis, but future research might focus on developing easy-field measurements to understand the DMS(P,O) dynamics. For instance, additional measurements such as the efficiency of the PSII or F_v/F_m would lead to a better appreciation of the physiological status of the cells within the water column, as well as the potential identification of the phytoplankton taxonomy (Maxwell and Johnson, 2000; Suggett et al., 2009). Nevertheless, proper *in situ* measurements of variable fluorescence require careful attention to a number of operational, instrumental, and environmental factors that are not encountered in the laboratory: *in situ* light influence, methodology and instruments used, assumptions made for considering a large number of cells of different phytoplankton population, presence of optically active constituents such as the coloured dissolved organic matter, among others (Laney, 2010).

To support the antioxidant function, we also tested if significant relationships can be found between the sulfur compounds and the incident light. Thanks to the BCZ and NNS campaigns (Chapter IV and V), we can combine the whole dataset to explore the correlations with the incident Photosynthetic Active Radiation (PAR). We found significant correlations between $DMSP_p$ ($\rho = 0.423$, $p < 0.001$), $DMSO_t$ ($\rho = 0.235$, $p < 0.01$) and the incident PAR combining the data from the BCZ (2016 and 2018; Chapter IV) and the first depth of the NNS campaign (Chapter V). These results are driven by the BCZ campaigns for which we found relevant correlation between incident PAR and the sulfur compounds: $DMS(P,O)_{p,t}$ were correlated positively with the incident PAR mainly from January to May ($DMSP_p$: $\rho = 0.642$, $p < 0.001$; $DMSO_t$: $\rho = 0.388$, $p < 0.01$). From July to December, the correlation was less significant for the $DMSP_p$ ($p < 0.05$) and absent for the $DMSO_t$ ($p = 0.380$). As the $DMSP_p$ increased in parallel of the incident PAR during the spring period, it is not surprising to observe significant correlation for this area. However, the NNS campaign, occurring only in August, did not provide any correlation (Chapter V).

We thus suggested that the antioxidant function is difficult to study for a short-term period of sampling in a temperate sea as it was for the NNS campaign. As explained in the Chapter V,

significant correlations between DMSP and photoprotective pigments were mainly observed in the subtropical oligotrophic gyres in the Atlantic Ocean or along the Peruvian coast (Riseman and DiTullio, 2004; Bell et al., 2010). In addition, the correlations generally found concern the resulting DMSP oxidation product which is DMS. It might be interesting to analyse DMS concentrations to increase the opportunity to observe and understand the antioxidant function. Indeed, significant relationships with UV solar radiation or the Solar Radiation Dose (SRD; calculated with the incident PAR and the Mixed Layer Depth (MLD)) were mainly detected with DMS in the subtropical part of: the Atlantic Ocean (i.e. Sargasso Sea and with UVR (Toole and Siegel, 2004); the oligotrophic gyres of the Atlantic Ocean and with SRD (Miles et al., 2009); the coastal northwest Mediterranean Sea (i.e. Blanes Bay (Vallina and Simó, 2007); with the gross DMS production and exposure to full spectrum sunlight (Galí et al., 2011); the Southern Indian Ocean and the Tasman Sea (Galí et al., 2011). In the Northeast Atlantic, no strong relationship was found between DMS and SRD, accounting only for 19 – 24% of the variance and depending mainly on the k_d used (Belviso and Caniaux, 2009). Only Lizotte et al. (2012) found correlation between DMS and SRD for a dataset extending from the subtropical gyre to the Greenland current. Only the DL activity was actually correlated with irradiance or photoprotective pigments for temperate latitude (Steinke et al., 2002; Harada et al., 2004; Bell et al., 2007). Nonetheless, when considering the extended model developed by Lana et al. (2012), they did find positive DMS response to SRD, irrespective of latitude and covering a large variability of temperature and trophic status. Nevertheless, Derevianko et al. (2009) found that SRD only accounted for 14% of total DMS variance using minimum aggregation methods (i.e. averaging the data across small spatial regions (2.5° x 2.5°)). This correlation was reduced further when controlling the confounding effect that SRD and DMS decrease when MLD increases.

In conclusion, to expand the opportunity to observe the antioxidant function in the natural environment, we suggest analysing DMS coupled with DMS(P,O) measurements and photoprotective pigments. In addition of the daily averaged incident light, it could be interesting to have the PAR evolution along each day with several measurements of the three sulfur compounds (DMS, DMSP and DMSO) and photoprotective pigments along this evolution. It could lead to a better appreciation of the diel antioxidant responses. If there is the possibility to include the analyse of DMS(P,O) by-products (acrylate, methane sulfonate and methane sulfinic acid), the DL activity, and the physiological status of the community, it would lead to a better completion of the antioxidant response. The previous measurements could lead to the

same conclusion than we observed in Chapter III: an antioxidant function for DMS(P,O) without being part of the antioxidant response.

The main question resides finally in the following sentence: which factor, if it is not the solar radiation, plays a leading role in determining the global DMS emissions? And, subsequently, which factor determines the DMS(P,O) production the most ? Both factors, if they are not the same, are determinant to better understand the climate cooling feedback loop.

1.2 $DMS(P,O)_p$ estimations

In the Chapter IV, we estimated the $DMS(P,O)_p$ concentrations based on the Chl-*a* linear regressions from the field measurements. In the Chapter V, same methodology was applied in addition of $DMS(P,O)_p$ estimations based on relative pigment abundance and specific $DMS(P,O)_p$:Chl-*a* ratio. We have the opportunity to combine the two datasets from the two chapters to extrapolate a common linear regression that might be used for temperate seas as the North Sea, including coastal and open sea regions. The Chl-*a* linear regressions obtained with the whole dataset ($DMSP_p$ (nmol L^{-1}) = 25.6 * Chl-*a* (µg L^{-1}), R^2 = 0.47; $DMSO_p$ (nmol L^{-1}) = 3.4 * Chl-*a* (µg L^{-1}), R^2 = 0.28) are driven by the BCZ results and would unfortunately lead to the same conclusion for the BCZ results: we would overestimate the $DMSP_p$ during the main part of the year and underestimate it during the *Phaeocystis* bloom. When applying this regression for the NNS results, normally characterized by a $DMSP_p$:Chl-*a* ratio of 52.0 mmol:g (Chapter V), it would lead to an underestimation for all the stations. The $DMSO_p$ estimation would fit with the $DMSO_p$ measured for the BCZ while it would be underestimated for the NNS campaign.

As we suggested to use preferentially the $DMS(P,O)_p$:Cell ratio for experimental treatments, we denote here the easy way to use the $DMS(P,O)_p$:Chl-*a* ratio. Even if a wide variety of microalgae do not produce DMS(P,O) and account on the Chl-*a* concentrations, the time-consuming measurement of cell density and biomass by inverted microscope do not lead to cost and time effective way to estimate the resulting DMS(P,O).

In Chapter IV and V, the use of the genomic diversity helped the understanding of which species were present in our field measurements and we recalculated $DMS(P,O)_p$:Chl-*a* ratio for the species for which we found DMS(P,O) concentrations in the published literature. These ratio were then used to estimate the DMS(P,O) concentrations in the Chapter V. However, from the 50 most abundant species in the samples, we only recalculated the DMSP ratio for ~25 species

and only ~7 for the DMSO ratio. We thus do not have a complete overview of the DMS(P,O) production within our samples. Increasing the knowledge about the DMSP, and above all the DMSO production, within more species would help to better constrain and predict the DMS(P,O) concentrations.

The previous observations lead to the conclusion that it is difficult to extrapolate a common $DMS(P,O)_p$:Chl-*a* ratio that could be used to understand the DMS(P,O) evolution along different regions. The use of one single relationship to describe and estimate correctly the $DMSP_p$ concentration for distinct area, even closed and similar to each other, is not appropriate. We have already pointed out the necessity to use two distinct relationships for the BCZ area since it is characterized by a succession of low- and high-DMSP producing species (Chapter IV). However, for the NNS campaign, the application of different relationships was not helpful since the phytoplankton community was mixed (Chapter V). Regarding the $DMSO_p$ estimation, it mainly reproduces the range of values observed in the field but do not reproduce its evolution during the *Phaeocystis* bloom in the Chapter IV, and for most stations in the Chapter V. A better understanding of the processes behind its production would allow a better fit. The previous suggestions regarding the analysis of the physiological status of the community would help to apply a more appropriate $DMSO_p$:Chl-*a* ratio.

Finally, phytoplankton taxonomic composition of the ocean can be described based on colour satellite radiometry (Nair et al., 2008; Mouw et al., 2017). Taxonomic groups can be discriminated thanks to their pigment signatures, which, in turn, impact their absorption spectra, given that different pigments have different absorption windows in the visible (Zhang et al., 2018). Using the $DMS(P,O)_p$:Chl-*a* ratio from Stefels et al. (2007), Chl-*a* concentrations from remote sensing, we thus could use satellite-derived data to properly estimate the $DMSP_p$ concentrations and to a lesser extent the $DMSO_p$ concentrations, based on the discrimination of low- and high-DMSP producers (i.e. diatoms, dinoflagellates or Prymnesiophyceae). A direct comparison of the assumptions, strengths, limitations, required satellite input and output products between different approaches is provided in Mouw et al. (2017).

1.3 Limits and perspectives

In this thesis, we assumed that the taxonomy and light variations would partially drive the DMS(P,O) cell quotas. Some experimental aspects should be addressed in future work to better estimate and consider a potential oxidative stress.

1.3.1 Issues on the experimental design

1) Our experimental setup was designed considering a nutrient replete medium and variation only in light intensity. However, we did not control the pH, oxygen or CO_2 variations that could cause physiological stress in the photosynthetic apparatus (Apel and Hirt, 2004). The cultures were mixed gently to avoid any O_2 or CO_2 over- or subsaturation at the bottom of the culture flasks. However, we cannot assure that there was no limitation during all the culture growth or when we were using microplates during the different oxidative treatments. These potential other cellular stress could influence the photosynthesis response.

2) We did analyse the pigment profiles by High Performance Liquid Chromatography (HPLC) during our oxidative stress treatments for 6h. Nevertheless, the results brought contradictory conclusions compared to the spectrophotometric measurements and the results were withdraw. In addition, we did not observe any significant variations during the HL and MSB treatments that suggest that 6h of treatment was not long enough to see any physiological response (data not shown in the Chapter III). Improvement with the use of liquid nitrogen to preserve the pigments is needed to ensure that variations observed is due to the treatment and not due to experimental methodology. The analysis of pigment profiles would bring additional information on the antioxidant response.

1.3.2 Improvements of the experimental design

1) The use of light intensity of 600 and 1200 µmol quanta m^{-2} s^{-1} during a complete growth cycle (12h:12h for 8-12 days) was not realistic for natural understanding purpose. It would be interesting to design light diel variations for a particular season and analyse the corresponding $DMS(P,O)_p$ changes. Adding the proportional UV-A and UV-B radiations would improve the physiological understanding of the DMS(P,O) production response.

2) Singlet oxygen can also be artificially produced inside the phytoplankton cell thanks to Rose Benghal, Methylene Violet, Neutral Red, or Indigo Carmine (Kovács et al., 2014). This artificial production coupled with Chl fluorescence analysis and DMS measurements might be interesting to understand the role of DMS for scavenging $^1O_2$.

3) In addition, in order to have a better understanding of the cell's antioxidant response, we also recommend analysing the antioxidant capacity (AOC) as a whole with the aim to understand the role of DMS(P,O) play in a complex antioxidant system. This analysis can be realized using the oxygen radical absorbance capacity (ORAC) assay (Ou et al., 2001; Deschaseaux et al.,

2014). Specific and key antioxidants such as the Superoxide Dismutase (SOD) or Glutathione (GSH) could also be analyzed using manufacturer's assay kit (Gardner et al., 2016). This would provide insights in the first line of defence, or primary antioxidants, against ROS: SOD converts superoxide anions into hydrogen peroxide and oxygen close to the site of production (Lesser, 2006), whereas the glutathione system is tightly linked in the regeneration of ascorbate peroxidase, enzyme responsible for scavenging hydrogen peroxide (Foyer and Noctor, 2005).

4) As mentioned in Chapter III, our experimental methodology used to measure DMS(P,O) concentrations produced results as cellular stocks. Other approaches based on molecular studies or other analytical methods could improve our understanding of the DMS(P,O) fluxes in the cell (Stefels et al., 2009). For instance, Archer et al. (2018) coupled direct measurements of DMS on board with further $DMSP_t$ analyses by purge-and-trap gas chromatography, and incorporation of ^{13}C analysed by proton-transfer-reaction mass spectrometry as suggested by Stefels et al. (2009). The DMSP production was then calculated from the initial $DMSP_t$ concentration and the μDMSP measurement, resulting from the mass ratio progress method (Stefels et al., 2009). Nevertheless, even if these new methods can provide better insight within the cell's reaction, they have to be cost effective and logistically viable on the field.

1.4 Cellular location, isotopic measurements, and molecular toolbox

The antioxidant function is based on variation of DMSP cell quotas under various abiotic stresses. This role is supported by the fact that the DMSP production seems to be located in the chloroplast for the plant *Wollastonia biflora* (Trossat et al., 1998), for the dinoflagellate *Symbiodinium* sp. (Raina et al., 2017) and most likely for the Prymnesiophyceae *Prymnesium parvum* (Curson et al., 2018). Raina et al. (2017) also confirmed the DMSP production in the cytoplasm and vacuoles. The presence of DMSP in these locations supports its proposed role in protecting the cell from salinity variations and oxidative damages. However, a major issue that remains regarding the DMSP production is the confirmation of the DMSP pathway and its subcellular location in most marine microalgae (Caruana, 2010). Since the diatoms, the Prymnesiophyceae and the dinoflagellates have different DMSP concentrations, its role within each group might be different as it could be for its main place of production. This future research perspective can improve our result's interpretation considering better survival during the high light treatments than with the chemical treatments that produced ROS in the cytosol (Chapter III).

Following the measurements of isotopic signature of DMS(P) could provide new insights regarding the fractionation and potentially in the pathway of production of the sulfur compounds. Natural isotopes measurements is an effective approach to trace sources and potential transformation processes in biogeochemical cycle (Canfield, 2011). Using gas chromatography with multicollector inductively coupled plasma mass spectrometry (MC-ICPMS) (Said-Ahmad and Amrani, 2013) it has been shown that the isotopic variability could originate from distinct DMSP metabolism in microalgae (Carnat et al., 2018). Variation of light intensity or other drivers such as salinity potentially affect the DMSP pathway production and degradation, resulting in different fractionation as it has been observed for the cleavage of DMSP to DMS (Oduro et al., 2012; Amrani et al., 2013). Development of new protocols accounting for these changes in the isotopic signature would therefore increase our knowledge of the DMS(P) cycle within the cell.

In addition, the analysis of DMSOP found by Thume et al. (2018) might also help to understand the DMS(P,O) variations within the cell. Since the phytoplankton can directly produce this molecule but also might result from the oxidation of DMSP, our results interpretation in the Chapter III did not account of this DMSP lost pathway. Moreover, DMSOP measurement would add a better insight within the oxidation system, the DMSP by-products, and maybe the potential antioxidant role that might play this new intermediate as it is for DMS(O)?

The microalgae DMSP pathway is assumed to be similar to the one described for the green macroalgae *Enteromorpha intestinalis* (Gage et al., 1997) and some key genes were identified by Lyon et al. (2011) and Curson et al. (2018). These key genes have not been fully verified since similar studies have not detected them (Kettles et al., 2014; Kageyama et al., 2018). Furthermore, the DMSP lyase gene identification (*Alma1*) suggests an entire family of DL present in a wide variety of algae (Alcolombri et al., 2015). If these genes are conserved between phytoplankton species, such key genes could be used to rapidly screen a wide variety of phytoplankton species and strains.

The physiological roles and the benefits of DMSP production could be also analyzed by comparative eco-physiological experiments with the generation of mutant deficient, or gene silencing, in DMSP-production in comparison with control clones (Raina et al., 2017). Nowadays, it is possible to knock-down and overexpress genes of interest (De Riso et al., 2009) but also permanently modify the genome obtaining knock-out (loss of function) or knock-in (gain of function) mutants by means of clustered regularly interspaced short palindrome repeats

(CRISPRs) (Russo et al., 2018). This was already realized in the diatoms *Phaeodactylum tricornutum* (Nymark et al., 2016) and *Thalassiosira pseudonana* (Hopes et al., 2016) for which the whole genome was sequenced (Armbrust et al., 2004; Montsant et al., 2007; Bowler et al., 2008). Another solution would be to analyse the variation among the gene expression under diverse physiological stress (i.e. salinity, temperature, or light) thanks to Reverse Transcriptase quantitative PCR or proteomic studies (Siaut et al., 2007; Lyon et al., 2011). The previous molecular techniques would allow to withdraw the production/consumption issue encountered with the classical DMSP measurement. However, the possible gene diversity among the DMSP or DL synthesis within each taxa or strain might be important as it was suggested before (Lyon et al., 2011; Kettles et al., 2014). Recent works have shown that the bacterial genes involved in DL synthesis appear to be rather diverse (Johnston et al., 2008; Todd et al., 2009) as it is for the six different genes coding for the bacterial DMSP cleavage pathway (Curson et al., 2011; Bullock et al., 2017). If the same diversity exist within the phytoplankton, this will limit their application even if they would be of great interest.

2 Conclusions

As a conclusion, we would like to point the progress achieved and the complexity of the DMS(P,O) cycle within the cell coupled with the metabolism machinery. We brought observational support to the $DMS(P,O)_p$ antioxidant function, without excluding not being part of the antioxidant response. Regarding the field measurements, the knowledge of the phytoplankton taxonomy was emphasized to ensure a correct $DMS(P,O)_p$ estimation for community characterized by monospecific phytoplankton groups. However, we recommend improving the experimental setup to better understand the DMS(P,O) fluxes and the physiological reactions. Increasing field sampling and experiments (i.e. oxidative stress analysis) to ensure better insight in the physiological cell responses within the natural environment would improve our understanding of the DMS(P,O) cycle. We recommend four methodological pathways with (1) adding other physiological stress by testing other environmental drivers such as the salinity, temperature, pH, oxygen, or nutrient concentrations and by combining them to analyse the natural fluctuation experienced by the phytoplankton; (2) comparing the physiological response of a larger set of phytoplankton species coupled to non-DMSP producing species; (3) analysing the entire antioxidant system along with DMS(P,O) by-products and DL activity; (4) using molecular approaches combining molecular toolbox and isotopic measurements.

References

"Choice of sources can shield extreme bias behind a facade of objectivity."

- Noam Chomsky.

Albrecht, B. A. Aerosols, Cloud Microphysics, and Fractional Cloudiness. *Science* **245**, 1227–1230 (1989).

Alcolombri, U. *et al.* Identification of the algal dimethyl sulfide-releasing enzyme: A missing link in the marine sulfur cycle. *Science* **348**, 1466–1469 (2015).

Amiotte Suchet, P., Probst, A. & Probst, J.L. Influence of acid rain on CO_2 consumption by rock weathering: Local and Global scales. *Water, Air, and Soil Pollution* **85**: 1563 – 1568 (1995).

Amrani, A., Said-Ahmad, W., Shaked, Y. & Kiene, R. P. Sulfur isotope homogeneity of oceanic DMSP and DMS. *Proceedings of the National Academy of Sciences* **110**, 18413–18418 (2013).

Anderson, D. M. & Stolzenbach, K.D. Selective retention of two dinoflagellates in a well-mixed estuarine embayment: the importance of diel vertical migration and surface avoidance. *Marine Ecology Progress Series* **25**, 39 – 50 (1985)

Anderson, D. M., Cembella, A. D. & Hallegraeff, G. M. Progress in Understanding Harmful Algal Blooms: Paradigm Shifts and New Technologies for Research, Monitoring, and Management. *Annu. Rev. Mar. Sci.* **4**, 143–176 (2012).

Andreae, M. O. & Barnard, W. R. The marine chemistry of dimethylsulfide. *Marine Chemistry* **14**, 267–279 (1984).

Andreae, M. O., & Jaeschke, W. A. Exchange of sulphur between biosphere and atmosphere over temperate and tropical regions, in Sulphur cycling on the Continents: Wetlands, Terrestrial Ecosystems, and Associated Water Bodies. *SCOPE* **48**, edited by R. W. Howarth, J. W. B. Stewart, & M. V. Ivanov, pp. 27-61, Wiley, Chichester (1992).

Apel, K. & Hirt, H. Reactive oxygen species: Metabolism, Oxidative Stress, and Signal Transduction. *Annu. Rev. Plant Biol.* **55**, 373–399 (2004).

Archer, S. D. *et al.* Contrasting responses of DMS and DMSP to ocean acidification in Arctic waters. *Biogeosciences* **10**, 1893–1908 (2013).

Archer, S. D. *et al.* Limitation of dimethylsulfoniopropionate synthesis at high irradiance in natural phytoplankton communities of the Tropical Atlantic: DMSP synthesis in the tropical ocean. *Limnol. Oceanogr.* **63**, 227–242 (2018).

Archer, S. D. *et al.* Transformation of dimethylsulphoniopropionate to dimethyl sulphide during summer in the North Sea with an examination of key processes via a modelling approach. *Deep Sea Research Part II: Topical Studies in Oceanography* **49**, 3067–3101 (2002).

Archer, S. D., Gilbert, F.J., Allen, J.I., Blackford, J. & Nightingale, P.D. Modelling of the seasonal patterns of dimethylsulfide production and fate during 1989 at a site in the North Sea. *Canadian Journal of Fisheries and Aquatic Sciences* **61**, 765–787 (2004).

Archer, S. D., Safi, K., Hall, A., Cummings, D. G. & Harvey, M. Grazing suppression of dimethylsulphoniopropionate (DMSP) accumulation in iron-fertilised, sub-Antarctic waters. *Deep Sea Research Part II: Topical Studies in Oceanography* **58**, 839–850 (2011).

Archer, S., Cummings, D., Llewellyn, C. & Fishwick, J. Phytoplankton taxa, irradiance and nutrient availability determine the seasonal cycle of DMSP in temperate shelf seas. *Mar. Ecol. Prog. Ser.* **394**, 111–124 (2009).

Archer, S., Widdicombe, C., Tarran, G., Rees, A. & Burkill, P. Production and turnover of particulate dimethylsulphoniopropionate during a coccolithophore bloom in the northern North Sea. *Aquat. Microb. Ecol.* **24**, 225–241 (2001).

Armbrust, E. V. The Genome of the Diatom Thalassiosira Pseudonana: Ecology, Evolution, and Metabolism. *Science* **306**, 79–86 (2004).

Aro, E.-M., Virgin, I. & Andersson, B. Photoinhibition of Photosystem II. Inactivation, protein damage and turnover. *Biochimica et Biophysica Acta (BBA) - Bioenergetics* **1143**, 113–134 (1993).

Asada, K. Production and Scavenging of Reactive Oxygen Species in Chloroplasts and Their Functions. *Plant Physiology* **141,** 391–396 (2006).

Ayers, G. P. & Cainey, J. M. The CLAW hypothesis: a review of the major developments. *Environ. Chem.* **4**, 366 (2007).

Baker, N. R. Chlorophyll Fluorescence: A Probe of Photosynthesis In Vivo. *Annu. Rev. Plant Biol.* **59**, 89–113 (2008).

Barton, S. *et al. Universal metabolic constraints on the thermal tolerance of marine phytoplankton*. http://biorxiv.org/lookup/doi/10.1101/358002 (2018).

Behrenfeld, M. J. *et al.* Climate-driven trends in contemporary ocean productivity. *Nature* **444**, 752–755 (2006).

Bell, T. G., Malin, G., Kim, Y.-N. & Steinke, M. Spatial variability in DMSP-lyase activity along an Atlantic meridional transect. *Aquat. Sci.* **69**, 320–329 (2007).

Bell, T. G., Poulton, A. J. & Malin, G. Strong linkages between dimethylsulphoniopropionate (DMSP) and phytoplankton community physiology in a large subtropical and tropical Atlantic Ocean data set: DMS(P) and phytoplankton community links. *Global Biogeochem. Cycles* **24** (2010).

Belviso, S. & Caniaux, G. A new assessment in North Atlantic waters of the relationship between DMS concentration and the upper mixed layer solar radiation dose. *Global Biogeochem. Cycles* **23** (2009).

Belviso, S. *et al.* Production of dimethylsulfonium propionate (DMSP) and dimethylsulfide (DMS) by a microbial food web. *Limnol. Oceanogr.* **35**, 1810–1821 (1990).

Belviso, S., Claustre, H. & Marty, J.-C. Evaluation of the utility of chemotaxonomic pigments as a surrogate for particulate DMSP. *Limnol. Oceanogr.* **46**, 989–995 (2001).

Berdalet, E., Llaveria, G. & Simó, R. Modulation of dimethylsulfoniopropionate (DMSP) concentration in an Alexandrium minutum (Dinophyceae) culture by small-scale turbulence: A link to toxin production?. *Harmful Algae* **11** (2011).

Bidle, K. D. & Falkowski, P. G. Cell death in planktonic, photosynthetic microorganisms. *Nat Rev Microbiol* **2**, 643–655 (2004).

Bopp, L., Aumont, O., Belviso, S. & Monfray, P. Potential impact of climate change on marine dimethyl sulfide emissions. 12 (2003).

Borges, A. A. *et al.* Molecular analysis of menadione-induced resistance against biotic stress in Arabidopsis. *Plant Biotechnology Journal* **7**, 744–762 (2009).

Borges, A. V. & Champenois, W. Preservation protocol for dimethylsulfoniopropionate and dimethylsulfoxide analysis in plant material of the Mediterranean seagrass Posidonia oceanica, and re-evaluation of dimethylsulfoniopropionate leaf content. *Aquatic Botany* **143,** 8–10 (2017).

Borges, A. V., Royer, C., Lapeyra Martin, J. & Gypens, N. Response of marine methane dissolved concentrations and emissions in the Southern North Sea to the European 2018 heatwave. *Continental Shelf Research* **8** (2019).

Borges, A. V., Royer, C., Martin, J. L., Champenois, W. & Gypens, N. Response of marine methane dissolved concentrations and emissions in the Southern North Sea to the European 2018 heatwave. *Continental Shelf Research* **190**, 104004 (2019).

Borisova-Mubarakshina, M. M. *et al.* Long-term acclimatory response to excess excitation energy: evidence for a role of hydrogen peroxide in the regulation of photosystem II antenna size. *EXBOTJ* **66**, 7151–7164 (2015).

Borodina, E. *et al.* Enzymes of dimethylsulfone metabolism and the phylogenetic characterization of the facultative methylotrophs Arthrobacter sulfonivorans sp. nov., Arthrobacter methylotrophus sp. nov., and Hyphomicrobium sulfonivorans sp. nov. *Arch Microbiol* **177**, 173–183 (2002).

Bowler, C. *et al.* The Phaeodactylum genome reveals the evolutionary history of diatom genomes. *Nature* **456**, 239–244 (2008).

Boyd, C. M. & Gradmann, D. Impact of osmolytes on buoyancy of marine phytoplankton. *Marine Biology* **141**, 605–618 (2002).

Bravo, I. & Figueroa, R. Towards an Ecological Understanding of Dinoflagellate Cyst Functions. *Microorganisms* **2**, 11–32 (2014).

Breton, E., Rousseau, V., Parent, J.-Y., Ozer, J. & Lancelot, C. Hydroclimatic modulation of diatom/ *Phaeocystis* blooms in nutrient-enriched Belgian coastal waters (North Sea). *Limnology and Oceanography* **51**, 1401–1409 (2006).

Brimblecombe, P. The Global Sulfur Cycle. in *Treatise on Geochemistry* 559–591 (Elsevier, 2014).

Brimblecombe, P., & Shooter, D. Photo-Oxidation of Dimethylsulphide in Aqueous Solution. *Marine Chemistry* **19** (4): 343–53 (1986).

Brooks, S. D. & Thornton, D. C. O. Marine Aerosols and Clouds. *Annu. Rev. Mar. Sci.* **10**, 289–313 (2018).

Brun, P. *et al.* Ecological niches of open ocean phytoplankton taxa: Niches of open ocean phytoplankton. *Limnol. Oceanogr.* **60**, 1020–1038 (2015).

Brunet, C., Johnsen, G., Lavaud, J. & Roy, S. Pigments and photoacclimation processes. in *Phytoplankton Pigments* (eds. Roy, S., Llewellyn, C., Egeland, E. S. & Johnsen, G.) 445–471 (Cambridge University Press, 2011).

Bucciarelli, E. & Sunda, W. G. Influence of CO2, nitrate, phosphate, and silicate limitation on intracellular dimethylsulfoniopropionate in batch cultures of the coastal diatom Thalassiosira pseudonana. *Limnology and Oceanography* **48,** 2256–2265 (2003).

Bucciarelli, E. *et al.* Increased intracellular concentrations of DMSP and DMSO in iron-limited oceanic phytoplankton *Thalassiosira oceanica* and *Trichodesmium erythraeum*. *Limnology and Oceanography* **58**, 1667–1679 (2013).

Bucciarelli, E., Sunda, W., Belviso, S. & Sarthou, G. Effect of the diel cycle on production of dimethylsulfoniopropionate in batch cultures of Emiliania huxleyi. *Aquat. Microb. Ecol.* **48**, 73–81 (2007).

Bullock, H. A., Luo, H. & Whitman, W. B. Evolution of Dimethylsulfoniopropionate Metabolism in Marine Phytoplankton and Bacteria. *Front. Microbiol.* **8**, (2017).

Cainey, J. & Harvey, M. Dimethylsulfide, a limited contributor to new particle formation in the clean marine boundary layer. *Geophys. Res. Lett.* **29**, 1128 (2002).

Caldeira, K. Evolutionary pressures on planktonic production of atmospheric sulphur. *Nature* **337**, 732–734 (1989).

Canfield, D.E. Biogeochemistry of Sulfur Isotopes. Reviews in *Mineralogy and Geochemistry* **43** (1): 607–636. (2011).

Carnat, G. *et al.* Variability in sulfur isotope composition suggests unique dimethylsulfoniopropionate cycling and microalgae metabolism in Antarctic sea ice. *Commun Biol* **1**, 212 (2018).

Carslaw, K. S. *et al.* A review of natural aerosol interactions and feedbacks within the Earth system. *Atmos. Chem. Phys.* **10**, 1701–1737 (2010).

Carslaw, K. S. *et al.* Large contribution of natural aerosols to uncertainty in indirect forcing. *Nature* **503**, 67–71 (2013).

Caruana, A. M. N. & Malin, G. The variability in DMSP content and DMSP lyase activity in marine dinoflagellates. *Progress in Oceanography* **120**, 410–424 (2014).

Caruana, A. M. N. DMS and DMSP production by marine dinoflagellates. A thesis submitted to the School of Environmental Sciences, at the University of East Anglia. (2010).

Champenois, W. & Borges, A. V. Determination of dimethylsulfoniopropionate and dimethylsulfoxide in Posidonia oceanica leaf tissue. *MethodsX* **6**, 56–62 (2019).

Chang, R. Y.-W. *et al.* Relating atmospheric and oceanic DMS levels to particle nucleation events in the Canadian Arctic. *J. Geophys. Res.* **116**, D00S03 (2011).

Charlson, R. J. *et al.* Climate Forcing by Anthropogenic Aerosols. *Science* **255**, 423–430 (1992).

Charlson, R. J., Lovelock, J. E., Andreae, M. O. & Warren, S. G. Oceanic phytoplankton, atmospheric sulphur, cloud albedo and climate. *Nature* **326**, 655–661 (1987).

Chen, Y. & Schäfer, H. Towards a systematic understanding of structure–function relationship of dimethylsulfoniopropionate-catabolizing enzymes. *Mol Microbiol* **111**, 1399–1403 (2019).

Chin, M. & Jacob, D. J. Anthropogenic and natural contributions to tropospheric sulfate: A global model analysis. *J. Geophys. Res.* **101**, 18691–18699 (1996).

Cloern, J. Our evolving conceptual model of the coastal eutrophication problem. *Mar. Ecol. Prog. Ser.* **210**, 223–253 (2001).

Colebrook, J. M. Continuous Plankton Records: Seasonal cycles of phytoplankton and copepods in the North Atlantic Ocean and the North Sea. *Marine Biology* **51**, 23–32 (1979).

Cooney, E. C. The Effect of High-Intensity Visible Light on the Bloom Niches of the Phototrophic Dinoflagellates Alexandrium fundyense and Heterocapsa rotundata. *WWU Graduate School Collection* **529** (2016).

Cooney, E. C., Fredrickson, K. A., Bright, K. J. & Strom, S. L. Contrasting effects of high-intensity photosynthetically active radiation on two bloom-forming dinoflagellates. *J. Phycol.* **55**, 1082–1095 (2019).

Cosgrove, J. & Borowitzka, M. A. Chlorophyll Fluorescence Terminology: An Introduction. in *Chlorophyll a Fluorescence in Aquatic Sciences: Methods and Applications* (eds. Suggett, D. J., Prášil, O. & Borowitzka, M. A.) 1–17 (Springer Netherlands, 2010).

Coupel, P. *et al.* Pigment signatures of phytoplankton communities in the Beaufort Sea. *Biogeosciences* **12**, 991–1006 (2015).

Curran, M. A. J. & Jones, G. B. Spatial distribution of dimethylsulfide and dimethylsulfoniopropionate in the Australasian sector of the Southern Ocean. *Journal of Geophysical Research* **103,** 16 667-16 689 (1998).

Curson, A. R. J. *et al.* Dimethylsulfoniopropionate biosynthesis in marine bacteria and identification of the key gene in this process. *Nature microbiology* **2**, 17009 (2017).

Curson, A. R. J. *et al.* DSYB catalyses the key step of dimethylsulfoniopropionate biosynthesis in many phytoplankton. *Nat Microbiol* **3**, 430–439 (2018).

Curson, A. R. J., Todd, J. D., Sullivan, M. J. & Johnston, A. W. B. Catabolism of dimethylsulphoniopropionate: microorganisms, enzymes, and genes. *Nat Rev Microbiol* **9**, 849–859 (2011).

Dacey, J. W. H. & Blough N. V. Hydroxide decomposition of dimethylsulfoniopropionate to form dimethylsulfide. *Geophysical Research Letters* **14**:1246–1249 (1987).

Damm, E. *et al.* Methane production in aerobic oligotrophic surface water in the central Arctic Ocean. 10 (2010).

Damm, E. Methane excess production in oxygen-rich polar water and a model of cellular conditions for this paradox. *Polar Science* 8 (2015).

Dang, H. & Li, J. Climate tipping-point potential and paradoxical production of methane in a changing ocean. *Sci. China Earth Sci.* **61**, 1714–1727 (2018).

Darroch, L. *et al.* Effect of short-term light- and UV-stress on DMSP, DMS, and DMSP lyase activity in Emiliania huxleyi. *Aquat. Microb. Ecol.* **74**, 173–185 (2015).

De Bont, J. A. M., Van Dijken, J. P. and Harder. W. Dimethyl Sulphoxide and Dimethyl Sulphide as a Carbon, Sulphur and Energy Source for Growth of Hyphomicrobium S. *Microbiology*, **127** (2): 315–23 (1981).

De Riso, V. *et al.* Gene silencing in the marine diatom Phaeodactylum tricornutum. *Nucleic Acids Research* **37**, e96–e96 (2009).

del Valle, D. A. *et al.* Effect of acidification on preservation of DMSP in seawater and phytoplankton cultures: Evidence for rapid loss and cleavage of DMSP in samples containing Phaeocystis sp. *Mar. Chem.* **124,** 57–67 (2011).

del Valle, D. A., Kieber, D. J., Toole, D. A., Bisgrove, J. & Kiene, R. P. Dissolved DMSO production via biological and photochemical oxidation of dissolved DMS in the Ross Sea, Antarctica. *Deep Sea Research Part I: Oceanographic Research Papers* **56**, 166–177 (2009).

Derevianko, G. J., Deutsch, C. & Hall, A. On the relationship between ocean DMS and solar radiation. *Geophys. Res. Lett.* **36**, L17606 (2009).

Deschaseaux, E. S. M. *et al.* Dimethylsulphoxide (DMSO) in biological samples: A comparison of the $TiCl_3$ and $NaBH_4$ reduction methods using headspace analysis. *Marine Chemistry* **164,** 9–15 (2014).

Deschaseaux, E. S. M. *et al.* Effects of environmental factors on dimethylated sulfur compounds and their potential role in the antioxidant system of the coral holobiont. *Limnol. Oceanogr.* **59**, 758–768 (2014).

Desmit, X. *et al.* Changes in chlorophyll concentration and phenology in the North Sea in relation to de-eutrophication and sea surface warming. *Limnology and Oceanography* lno.11351 (2019).

Diaz, J. M. & Plummer, S. Production of extracellular reactive oxygen species by phytoplankton: past and future directions. *Journal of Plankton Research* (2018).

Dickson, D. M. J., and G. O. Kirst. The Role of β-Dimethylsulphoniopropionate, Glycine Betaine and Homarine in the Osmoacclimation of *Platymonas Subcordiformis*. *Planta* **167** (4): 536–43 (1986).

Dimier, C., Corato, F., Tramontano, F. & Brunet, C. Photoprotection and xanthophyll-cycle activity in three marine diatoms [1]. *Journal of Phycology* **43**, 937–947 (2007).

DiTullio, G. R. & Smith, W. O. Relationship between dimethylsulfide and phytoplankton pigment concentrations in the Ross Sea, Antarctica. *Deep Sea Research Part I: Oceanographic Research Papers* **42**, 873–892 (1995).

Druon, J., Schrimpf, W., Dobricic, S. & Stips, A. Comparative assessment of large-scale marine eutrophication: North Sea area and Adriatic Sea as case studies. *Mar. Ecol. Prog. Ser.* **272**, 1–23 (2004).

Dummermuth, A. L., Karsten, U., Fisch, K. M., König, G. M. & Wiencke, C. Responses of marine macroalgae to hydrogen-peroxide stress. *Journal of Experimental Marine Biology and Ecology* **289**, 103–121 (2003).

Durack, P. Ocean Salinity and the Global Water Cycle. *Oceanog* **28**, 20–31 (2015).

Edwards, K. F., Thomas, M. K., Klausmeier, C. A. & Litchman, E. Phytoplankton growth and the interaction of light and temperature: A synthesis at the species and community level: Light-Temperature Interactions. *Limnology and Oceanography* **61**, 1232–1244 (2016).

Edwards, M., Reid, P.C. and Planque, B. Long-term and regional variability of phytoplankton biomass in the Northeast Atlantic (1960-1995). *ICES Journal of Marine Science* **58**: 39-49 (2001).

Emeis, K.-C. *et al.* The North Sea — A shelf sea in the Anthropocene. *Journal of Marine Systems* **141**, 18–33 (2015).

Endoh, T. *et al.* Characterization and identification of genes essential for dimethyl sulfide utilization in Pseudomonas putida strain DS1. *Applied Microbiology and Biotechnology* **62**, 83–91 (2003).

Erickson, E., Wakao, S. & Niyogi, K. K. Light stress and photoprotection in *Chlamydomonas reinhardtii*. *Plant J* **82**, 449–465 (2015).

Evans, C. *et al.* The relative significance of viral lysis and microzooplankton grazing as pathways of dimethylsulfoniopropionate (DMSP) cleavage: An *Emiliania huxleyi* culture study. *Limnol. Oceanogr.* **52**, 1036–1045 (2007).

Falkowski, P.G. & Chen, YB. Photoacclimation of Light Harvesting Systems in Eukaryotic Algae. In: Green B.R., Parson W.W. (eds) Light-Harvesting Antennas in Photosynthesis. *Advances in Photosynthesis and Respiration*, **13**. Springer, Dordrecht (2003).

Falkowski, P.G., Barber, R.T. and Smetacek, V. Biogeochemical controls and feedbacks on ocean primary production. Science **281**, 200–206 (1998).

Fan, X. *et al.* Phytoplankton pangenome reveals extensive prokaryotic horizontal gene transfer of diverse functions. *Sci. Adv.* **6**, eaba0111 (2020).

Farmer, E. E. & Mueller, M. J. ROS-Mediated Lipid Peroxidation and RES-Activated Signaling. *Annu. Rev. Plant Biol.* **64**, 429–450 (2013).

Fernanda Pessoa, M. Harmful effects of UV radiation in Algae and aquatic macrophytes – A review. *EJFA* **24**, (2012).

Fernandes, M. The influence of Stress conditions on intracellular Dimethylsulfoniopropionate (DMSP) and Dimethylsulfide (DMS) release in *Emiliania huxleyi.* A thesis submitted to the School of Environmental Sciences, at the University of East Anglia, United Kingdom. (2012).

Ferrante *et al.* Exploring Molecular Signs of Sex in the Marine Diatom Skeletonema marinoi. *Genes* **10**, 494 (2019).

Figueroa, R. I. & Bravo, I. Sexual reproduction and two different encystment strategies of lingulodinium polyedrum (dinophyceae) in culture. *Journal of Phycology* **41**, 370–379 (2005).

Fischer, B. B. *et al.* Singlet oxygen resistant: links reactive electrophile signalling to singlet oxygen acclimation in *Chlamydomonas reinhardtii*. *Proceedings of the National Academy of Sciences* **109**, E1302–E1311 (2012).

Flanders Marine Institute (VLIZ), Belgium: LifeWatch observatory data: nutrient, pigment, suspended matter and secchi measurements in the Belgian Part of the North Sea (2019).

Foyer, C. H. & Noctor, G. Oxidant and antioxidant signalling in plants: a re-evaluation of the concept of oxidative stress in a physiological context. *Plant Cell Environ* **28**, 1056–1071 (2005).

Foyer, C. H., Lopez-Delgado, H., Dat, J. F. & Scott, I. M. Hydrogen peroxide- and glutathione-associated mechanisms of acclimatory stress tolerance and signalling. *Physiol Plant* **100**, 241–254 (1997).

Fredrickson, K. A. & Strom, S. L. The algal osmolyte DMSP as a microzooplankton grazing deterrent in laboratory and field studies. *Journal of Plankton Research* **31**, 135–152 (2008).

Fritsch, F. E. The structure and reproduction of the algae - Volume I – Class IV. Bacillariophyceae, 564–643; and Class VI. Dinophyceae, 664–715. Cambridge University Press (1971).

Fuse, H., Takimura, O., Murakami, K., Yamaoka, Y. & Omori, T. Utilization of Dimethyl Sulfide as a Sulfur Source with the Aid of Light by Marinobacterium sp. Strain DMS-S1. *Appl. Environ. Microbiol.* **66**, 5527–5532 (2000).

Gage, D. A. *et al.* A new route for synthesis of dimethylsulphoniopropionate in marine algae. *Nature* **387**, 891–894 (1997).

Galí, M. & Simó, R. A meta-analysis of oceanic DMS and DMSP cycling processes: Disentangling the summer paradox. *Global Biogeochem. Cycles* **29**, 496–515 (2015).

Galí, M. *et al.* Diel patterns of oceanic dimethylsulfide (DMS) cycling: Microbial and physical drivers: DIEL PATTERNS OF DMS CYCLING. *Global Biogeochem. Cycles* **27**, 620–636 (2013).

Galí, M. *et al.* Spectral irradiance dependence of sunlight effects on plankton dimethylsulfide production. *Limnol. Oceanogr.* **58**, 489–504 (2013).

Galí, M., Levasseur, M., Devred, E., Simó, R. & Babin, M. Sea-surface dimethylsulfide (DMS) concentration from satellite data at global and regional scales. *Biogeosciences* **15**, 3497–3519 (2018).

Galí, M., Saló, V., Almeda, R., Calbet, A. & Simó, R. Stimulation of gross dimethylsulfide (DMS) production by solar radiation. *Geophys. Res. Lett.* **38**, (2011).

Gao, C. *et al.* Single-cell bacterial transcription measurements reveal the importance of dimethylsulfoniopropionate (DMSP) hotspots in ocean sulfur cycling. *Nat Commun* **11**, 1942 (2020).

Gardner, S. G. *et al.* Dimethylsulfoniopropionate, superoxide dismutase and glutathione as stress response indicators in three corals under short-term hyposalinity stress. *Proc. R. Soc. London B Biol. Sci.* **283,** (2016).

Geider, R. J. Light and temperature dependence of the carbon to chlorophyll a ratio in microalgae and cyanobacteria: implications for physiology and growth of phytoplankton. *New Phytol* **106**, 1–34 (1987).

Genty, B., Briantais, J.-M. & Baker, N. R. The relationship between the quantum yield of photosynthetic electron transport and quenching of chlorophyll fluorescence. *Biochimica et Biophysica Acta (BBA) - General Subjects* **990**, 87–92 (1989).

Gibb, S. W. *et al.* Surface phytoplankton pigment distributions in the Atlantic Ocean: an assessment of basin scale variability between 50°N and 50°S. *Progress in Oceanography* **45**, 339–368 (2000).

Giordano, M., Norici, A. & Hell, R. Sulfur and phytoplankton: acquisition, metabolism, and impact on the environment. *New Phytologist* **166**, 371–382 (2005).

Glibert, P. M. Margalef revisited: A new phytoplankton mandala incorporating twelve dimensions, including nutritional physiology. *Harmful Algae* **55**, 25–30 (2016).

Goiris, K. *et al.* Impact of nutrient stress on antioxidant production in three species of microalgae. *Algal Research* **7**, 51–57 (2015).

Gondwe, M., Krol, M., Gieskes, W., Klaassen, W. & de Baar, H. The contribution of ocean-leaving DMS to the global atmospheric burdens of DMS, MSA, SO_2, and NSS $SO_4^=$: DMS, MSA, SO_2, NSS $SO_4^=$ BURDENS OF OCEANIC DMS ORIGIN. *Global Biogeochem. Cycles* **17**, n/a-n/a (2003).

Goodson, M.S., Whitehead, L.F. and Douglas, A.E. Symbiotic dinoflagellates in marine Cnidaria: diversity and function. Hydrobiologia **461**, 79-82 (2001).

Goss, R. & Jakob, T. Regulation and function of xanthophyll cycle-dependent photoprotection in algae. *Photosynth Res* **106**, 103–122 (2010).

Goss-Sampson, M. A. Statistical analysis in JAsP: A guide for students (2018).

Govindjee & Govindjee, R. The Absorption of Light in Photosynthesis. *Sci Am* **231**, 68–82 (1974).

Grasshoff, K. Determination of nitrate. In: Methods of seawater analysis. Grasshoff K., Ehrhardt M., and K. Kremling (eds). Verlag Chemie. Basel: 143-150 (1983)

Green, T. K. & Hatton, A. D. The Claw Hypothesis: A New Perspective on the Role of Biogenic Sulphur in the Regulation of Global Climate. in *Oceanography and Marine Biology* (eds. Hughes, R., Hughes, D. & Smith, I.) vol. 20141169 315–336 (CRC Press, 2014).

Greene, R. M., Geider, R. J., Kolber, Z. & Falkowski, P. G. Iron-Induced Changes in Light Harvesting and Photochemical Energy Conversion Processes in Eukaryotic Marine Algae. *Plant Physiol.* **100**, 565–575 (1992).

Gries, C., Nash, T. H. & Kesselmeier, J. Exchange of reduced sulfur gases between lichens and the atmosphere. *Biogeochemistry* **26**, 25–39 (1994).

Guillard, R.R.L. & Ryther, J.H. Studies of marine planktonic diatoms. I. *Cyclotella nana* Hustedt and *Detonula confervacea* Cleve. *Can. J. Microbiol.* **8:** 229-239 (1962).

Gunson, J. R., S. A. Spall, T. R. Anderson, A. Jones, I. J. Totterdell, and M. J. Woodage. Climate Sensitivity to Ocean Dimethylsulphide Emissions'. *Geophysical Research Letters* **33** (7) (2006)

Gypens, N. & Borges, A. V. Increase in dimethylsulfide (DMS) emissions due to eutrophication of coastal waters offsets their reduction due to ocean acidification. *Front. Mar. Sci.* **1**, (2014).

Gypens, N., Borges, A. V., Speeckaert, G. & Lancelot, C. The Dimethylsulfide Cycle in the Eutrophied Southern North Sea: A Model Study Integrating Phytoplankton and Bacterial Processes. *PLoS ONE* **9**, e85862 (2014).

Halliwell, B. Antioxidant characterization, methodology and mechanism. *Biochemical Pharmacology* **49**, 1341 – 1348 (1995).

Halmer, M. M., Schmincke, H.-U. & Graf, H.-F. The annual volcanic gas input into the atmosphere, in particular into the stratosphere: a global data set for the past 100 years. *Journal of Volcanology and Geothermal Research* **115**, 511–528 (2002).

Hamilton, W. D. & Lenton, T. M. Spora and Gaia: how microbes fly with their clouds. *Ethology Ecology & Evolution* **10**, 1–16 (1998).

Harada, H., Rouse, M.-A., Sunda, W. & Kiene, R. P. Latitudinal and vertical distributions of particle- associated dimethylsulfoniopropionate (DMSP) lyase activity in the western North Atlantic Ocean. **61**, 12 (2004).

Hasle, G.R. The Inverted Microscope Method. Phytoplankton Manual. UNESCO, Paris, pp. 8896 (1978).

Hassan, H. M. & Fridovich, I. Intracellular production of superoxide radical and of hydrogen peroxide by redox active compounds. *Archives of Biochemistry and Biophysics* **196**, 385–395 (1979).

Hatton, A. D. & Wilson, S. T. Particulate dimethylsulphoxide and dimethylsulphoniopropionate in phytoplankton cultures and Scottish coastal waters. *Aquatic Sciences* **69,** 330–340 (2007).

Hatton, A. D. Influence of Photochemistry on the Marine Biogeochemical Cycle of Dimethylsulphide in the Northern North Sea. *Deep Sea Research Part II: Topical Studies in Oceanography, Dimethyl Sulphide Biogeochemistry within a Coccolithophore Bloom: An Overview,* **49** (15): 3039–52 (2002).

Hatton, A. D., Turner, S. M., Malin, G. et Liss, P. S. Dimethylsulphoxide and other biogenic sulphur compounds in the Galapagos Plume. *Deep. Res. Part II Top. Stud. Oceanogr.* **45,** 1043–1053 (1998).

Havlin, J. L., S. L. Tisdale, W. L. Nelson, and J. D. Beaton. Soil Fertility and Fertilizers. 8 edition. Upper Saddle River, N.J: Pearson. (2013).

Haynes, D., Ralph, P., Prange, J. & Dennison, B. The Impact of the Herbicide Diuron on Photosynthesis in Three Species of Tropical Seagrass. *Marine Pollution Bulletin* **41**, 288–293 (2000).

Herndl, G. J. Major role of ultraviolet-8 in controlling bacterioplankton growth in the surface layer of the ocean. **361**, 3 (1993).

Higgins, HW, Wright, SW et Schluter, L. Quantitative interpretation of chemotaxonomic pigment data. In Phytoplankton Pigments: Characterization, Chemotaxonomy and Applications in Oceanography, Cambridge University Press, S Roy, C A. Llewellyn, ES Egeland and G Johnsen (ed), United Kingdom, pp. 257-313 (2011).

Hill, R., White, B., Cottrell, M. & Dacey, J. Virus-mediated total release of dimethylsulfoniopropionate from marine phytoplankton: a potential climate process. *Aquat. Microb. Ecol.* **14**, 1–6 (1998).

Hillebrand, H., Dürselen, C.-D., Kirschtel, D., Pollingher, U. & Zohary, T. Biovolume calculation for pelagic and benthic microalgae. *Journal of Phycology* **35**, 403–424 (1999).

Hoegh-Guldberg, O. & Bruno, J. F. The Impact of Climate Change on the World's Marine Ecosystems. *Science* **328**, 1523–1528 (2010).

Holmer, M. & Storkholm, P. Sulphate reduction and sulphur cycling in lake sediments: a review. *Freshwater Biol* **46**, 431–451 (2001).

Hopes, A., Nekrasov, V., Kamoun, S. & Mock, T. Editing of the urease gene by CRISPR-Cas in the diatom Thalassiosira pseudonana. *Plant Methods* **12**, 49 (2016).

Hoppenrath, M., Elbrächter, M. & Drebes, G. Marine Phytoplankton: selected microphytoplankton species from the North Sea around Helgoland and Sylt. *Kleine Senckenberg-Reihe* **49** (2009).

Huang, Q. B., X. Q. Qin, P. Y. Liu, L. K. Zhang, & C. T. Su. Influence of Sulfuric Acid to Karst Hydrochemical and δ13CDIC in the Upper and Middle Reaches of the Wujiang River. *Huan jing ke xue= Huanjing kexue* **36** (9): 3220–29 (2015).

Hunter-Cevera, K. R. *et al.* Physiological and ecological drivers of early spring blooms of a coastal phytoplankter. *Science* **354**, 326–329 (2016).

Huot, Y. & Babin, M. Overview of Fluorescence Protocols: Theory, Basic Concepts, and Practice. In *Chlorophyll a Fluorescence in Aquatic Sciences: Methods and Applications* (eds. Suggett, D. J., Prášil, O. & Borowitzka, M. A.) 31–74 (Springer Netherlands, 2010).

Husband, J. D., Kiene, R. P. & Sherman, T. D. Oxidation of dimethylsulfoniopropionate (DMSP) in response to oxidative stress in Spartina alterniflora and protection of a non-DMSP producing grass by exogenous DMSP+acrylate. *Environmental and Experimental Botany* **79**, 44–48 (2012).

Hussherr, R. *et al.* Impact of ocean acidification on Arctic phytoplankton blooms and dimethyl sulfide concentration under simulated ice-free and under-ice conditions. *Biogeosciences* **14**, 2407–2427 (2017).

Irwin, A. J., Nelles, A. M. & Finkel, Z. V. Phytoplankton niches estimated from field data. *Limnol. Oceanogr.* **57**, 787–797 (2012).

Iwataki, M. Taxonomy and identification of the armored dinoflagellate genus Heterocapsa (Peridiniales, Dinophyceae). *Plankton Benthos Res* **3**, 135–142 (2008).

Jacob, S. W. & Wood, D. C. Dimethyl Sulfoxide (DMSO) Toxicology, Pharmacology, and Clinical Experience. *The American Journal of Surgery, Symposium on Diseases of the Small Intestine*, **114** (3): 414–26 (1967).

Jahns, P. & Holzwarth, A. R. The role of the xanthophyll cycle and of lutein in photoprotection of photosystem II. *Biochimica et Biophysica Acta (BBA) - Bioenergetics* **1817**, 182–193 (2012).

Jeffrey, S.W. & Wright, S.W. Photosynthetic pigments in marine microalgae. In Algal cultures, Analogues of Blooms and Applications, Science Publishers, Subba Rao DV (ed), New Hampshire, USA (2005).

Jeffrey, SW, Wright, SW & Zapata, M, Microalgal classes and their signature pigments, Phytoplankton Pigments: Characterization, Chemotaxonomy and Applications. In Oceanography, Cambridge University Press, S Roy, C A. Llewellyn, ES Egeland and G Johnsen (ed), United Kingdom, pp. 3-77. ISBN 9780511732263 (2011).

Jephson, T., Fagerberg, T. & Carlsson, P. Dependency of dinoflagellate vertical migration on salinity stratification. *Aquat. Microb. Ecol.* **63**, 255–264 (2011).

Jian, S., Zhang, J., Zhang, H.-H. & Yang, G.-P. Effects of ocean acidification and short-term light/temperature stress on biogenic dimethylated sulfur compounds cycling in the Changjiang River Estuary. *Environ. Chem.* **16**, 197 (2019).

Johns, D. G. & Reid, P. C. An overview of plankton ecology in the North Sea. *Sir Alister Hardy Foundation for Ocean Science: Technical Report* **30** (2001).

Johnston, A. W. B. *et al.* Molecular diversity of bacterial production of the climate-changing gas, dimethyl sulphide, a molecule that impinges on local and global symbioses. *Journal of Experimental Botany* **59**, 1059–1067 (2008).

Kaczmarska, I. *et al.* Proposals for a terminology for diatom sexual reproduction, auxospores and resting stages. *Diatom Research* **28**, 263–294 (2013).

Kageyama, H., Tanaka, Y., Shibata, A., Waditee-Sirisattha, R. & Takabe, T. Dimethylsulfoniopropionate biosynthesis in a diatom Thalassiosira pseudonana : Identification of a gene encoding MTHB-methyltransferase. *Archives of Biochemistry and Biophysics* **645**, 100–106 (2018).

Karl, D. M. *et al.* Aerobic production of methane in the sea. *Nature Geosci* **1**, 473–478 (2008).

Karl, D. M. Microbial oceanography: paradigms, processes, and promise. *Nat Rev Microbiol* **5**, 759–769 (2007).

Karsten, U., K. Kück, C. Vogt, and G. O. Kirst. Dimethylsulfoniopropionate Production in Phototrophic Organisms and Its Physiological Functions as a Cryoprotectant. In *Biological and Environmental Chemistry of DMSP and Related Sulfonium Compounds*, edited by R. P. Kiene, P. T. Visscher, M. D. Keller, and G. O. Kirst, 143–53. Springer US (1996).

Karsten, U., Kirst, G. O. & Wiencke, C. Dimethylsulphoniopropionate (DMSP) accumulation in green macioalgae from polar to temperate regions: interactive effects of light versus salinity and light versus temperature. *Polar Biol* **12**, (1992).

Karsten, U., Wiencke, C. & Kirst, G. O. The effect of light intensity and daylength on the beta-dimethylsulphoniopropionate (DMSP) content of marine green macroalgae from Antarctica*. *Plant Cell Environ* **13**, 989–993 (1990).

Karuppanapandian, T., Moon, J.-C., Kim, C. & Manoharan, K. Reactive oxygen species in plants: their generation, signal transduction, and scavenging mechanisms. *Australian Journal of Crop Science* **5** (6): 709–725 (2011).

Keeling, P. J. The endosymbiotic origin, diversification and fate of plastids. *Phil. Trans. R. Soc. B* **365**, 729–748 (2010).

Keller, M. D., Bellows, W. K. & Guillard, R. R. L. Dimethylsulfide production and marine phytoplankton: an additional impact of unusual blooms. *Novel Phytoplankton Blooms* (1989)b.

Keller, M. D., Bellows, W.K., & Guillard, R.R.L. Dimethyl sulfide production in marine phytoplankton. In: Saltzman ES, Cooper WJ (eds) Biogenic sulfur in the environment. American Chemical Society, Washington DC, pp 167– 182 (1989).

Kettle, A. J. & Andreae, M. O. Flux of dimethylsulfide from the oceans: A comparison of updated data sets and flux models. *J. Geophys. Res.* **105**, 26793–26808 (2000).

Kettles, N. L., Kopriva, S. & Malin, G. Insights into the Regulation of DMSP Synthesis in the Diatom Thalassiosira pseudonana through APR Activity, Proteomics and Gene Expression Analyses on Cells Acclimating to Changes in Salinity, Light and Nitrogen. *PLoS ONE* **9**, e94795 (2014).

Kieber, D. J., J. Jiao, R. P. Kiene, and T. S. Bates. Impact of Dimethylsulfide Photochemistry on Methyl Sulfur Cycling in the Equatorial Pacific Ocean. *Journal of Geophysical Research: Oceans* **101** (C2): 3715–22 (1996).

Kiene, R. P. & Gerard, G. Determination of trace levels of dimethylsulphoxide (DMSO) in seawater and rainwater. *Marine Chemistry* **47,** 1–12 (1994).

Kiene, R. P. & Linn, L. J. The fate of dissolved dimethylsulfoniopropionate (DMSP) in seawater: tracer studies using 35S-DMSP. *Geochimica et Cosmochimica Acta* **64**, 2797–2810 (2000).

Kiene, R. P. & Slezak, D. Low dissolved DMSP concentrations in seawater revealed by small volume gravity filtration and dialysis sampling. *Limnol. Oceanogr. Methods* **4,** 80–95 (2006).

Kiene, R. P. & Taylor, B. F. Demethylation of Dimethylsulfoniopropionate and Production of Thiols in Anoxic Marine Sediments. *APPL. ENVIRON. MICROBIOL.* **54**, 5 (1988).

Kiene, R. P. Microbial Production and Consumption of Greenhouse Gases: Methane, Nitrogen Oxides, and Halomethanes (ASM, 1991).

Kiene, R. P., L. J. Linn, and J. A. Bruton. New and Important Roles for DMSP in Marine Microbial Communities. *Journal of Sea Research* **43** (3–4): 209–24 (2000).

Kiene, R. P., Linn, L. J., González, J., Moran, M. A. & Bruton, J. A. Dimethylsulfoniopropionate and Methanethiol Are Important Precursors of Methionine and Protein-Sulfur in Marine Bacterioplankton. *Appl. Environ. Microbiol.* **65**, 4549–4558 (1999).

Kiene, R.P. Microbiological Controls on Dimethylsulfide Emissions from Wetlands and the Ocean. in *Microbiology of Atmospheric Trace Gases* (eds. Murrell J.C. and Kelly D.P.) NATO ASI Series (I: Global Environmental Change), vol **39**. (Springer, Berlin, Heidelberg, 1996).

Kinsey, J. D. & Kieber, D. J. Microwave preservation method for DMSP, DMSO, and acrylate in unfiltered seawater and phytoplankton culture samples. *Limnology and Oceanography Methods* **14,** 196–209 (2016).

Kinsey, J.D., Kieber, D.J., Neale, P.J. Effects of iron limitation and UV radiation on Phaeocystis Antarctica growth and dimethylsulfoniopropionate, dimethylsulfoxide and acrylate concentrations. *Environ. Chem.* **13** (2), 195–211 (2016).

Kirst G. O. Osmotic adjustments in phytoplankton and macroalgae: the use of dimethylsulfoniopropionate (DMSP). In: Kiene RP, Visscher P, Keller M, Kirst GO (eds) Biological and environmental chemistry of DMSP and related sulfonium compounds. Plenum, New York, pp 121–129 (1996).

Kirst, G. O. *et al.* Dimethylsulfoniopropionate (DMSP) in icealgae and its possible biological role. *Marine Chemistry* **35,** 381–388 (1991).

Kirst, G. O. Salinity Tolerance of Eukaryotic Marine Algae. *Annual Review of Plant Molecular Biology* **40**, 21–53 (1989).

Kitaguchi, H., Uchida, A. & Ishida, Y. Purification and Characterization of L-Methionine Decarboxylase from Crypthecodinium cohnii. *Fisheries Science* **65** (4), 613–617 (1999).

Kloster, S. *et al.* Response of dimethylsulfide (DMS) in the ocean and atmosphere to global warming. *J. Geophys. Res.* **112**, (2007).

Korbee, N., Teresa Mata, M. & Figueroa, F. L. Photoprotection mechanisms against ultraviolet radiation in *Heterocapsa* sp. (Dinophyceae) are influenced by nitrogen availability: Mycosporine-like amino acids vs. xanthophyll cycle. *Limnol. Oceanogr.* **55**, 899–908 (2010).

Koroleff F. 1983a. Determination of ammonia. In: Methods of seawater analysis. Grasshoff K., Ehrhardt M., and K. Kremling (eds). Verlag Chemie. Basel: 150-157

Koroleff F. 1983b. Determination of silicon. In: Methods of seawater analysis. Grasshoff K., Ehrhardt M., and K. Kremling (eds). Verlag Chemie. Basel: 174-183

Koroleff F. 1983c. Determination of phosphorus. In: Methods of seawater analysis. Grasshoff K., Ehrhardt M., and K. Kremling (eds). Verlag Chemie. Basel: 125-139

Kovács, L. *et al.* Assessing the Applicability of Singlet Oxygen Photosensitizers in Leaf Studies. *Photochem Photobiol* **90**, 129–136 (2014).

Kraberg *et al*. Phytoplankton and microbial plankton of the North Sea and English Channel. In: *Marine and coastal ecosystem-based risk management handbook*. International Council for the Exploration of the Sea: Cooperative Research Report. n°313 Special Issue, 70 – 91 (2012).

Kramer, S. J. & Siegel, D. A. How Can Phytoplankton Pigments Be Best Used to Characterize Surface Ocean Phytoplankton Groups for Ocean Color Remote Sensing Algorithms? *J. Geophys. Res. Oceans* **124**, 7557–7574 (2019).

Kramer, S. J., Siegel, D. A. & Graff, J. R. Phytoplankton Community Composition Determined from Co-variability Among Phytoplankton Pigments from the NAAMES Field Campaign. *Front. Mar. Sci.* **7**, 215 (2020).

Krause, G.H. & Jahns, P. Non-photochemical energy dissipation determined by chlorophyll fluorescence quenching: characterization and function. In: *Chlorophyll a fluorescence: A signature of photosynthesis* (eds. Papageorgiou, G. & Govindjee) 463–495 (Springer, Dordrecht, 2004).

Krieger-Liszkay, A. Singlet oxygen production in photosynthesis. *Journal of Experimental Botany* **56**, 337–346 (2004).

Kulmala, M., Laaksonen, A. & Pirjola, L. Parameterizations for sulfuric acid/water nucleation rates. *J. Geophys. Res.* **103**, 8301–8307 (1998).

Kwint, R. & Kramer, K. Annual cycle of the production and fate of DMS and DMSP in a marine coastal system. *Mar. Ecol. Prog. Ser.* **134**, 217–224 (1996).

Kwint, R. L. J., X. Irigoien, and K. J. M. Kramer. Copepods and DMSP. In *Biological and Environmental Chemistry of DMSP and Related Sulfonium Compounds*, edited by R. P. Kiene, P. T. Visscher, M. D. Keller, and G. O. Kirst, 239–52. Springer US (1996).

Lana, A. *et al.* An Updated Climatology of Surface Dimethlysulfide Concentrations and Emission Fluxes in the Global Ocean (2011) https://core.ac.uk/display/30750319.

Lana, A., Simó, R., Vallina, S. M. et Dachs, J. Re-examination of global emerging patterns of ocean DMS concentration. *Biogeochemistry* **110,** 173–182 (2012).

Lancelot, C. *et al.* Modelling diatom and Phaeocystis blooms and nutrient cycles in the Southern Bight of the North Sea: the MIRO model. *Marine Ecology Progress Series* **289**, 63–78 (2005).

Lancelot, C., Keller, M.D., Rousseau, V., Smith Jr., W.O., Mathot, S. Autecology of the marine haptophyte *Phaeocystis* sp. In: Anderson, D.M., Cembella, A.D., Hallagraeff, G.M. (Eds.), Physiological Ecology of Harmful Algal blooms, vol. 41. Springer-Verlag, Berlin, pp. 209–224 (1998).

Laney, S. R. In situ Measurement of Variable Fluorescence Transients. in *Chlorophyll a Fluorescence in Aquatic Sciences: Methods and Applications* (eds. Suggett, D.J., Prásil, O. and Borowitzka, M. A.; Springer Netherlands, 2010).

Lavaud, J., Rousseau, B. & Etienne, A.-L. General features of photoprotection by energy dissipation in planktonic diatoms (Bacillariophyceae): photoprotection in diatoms. *Journal of Phycology* **40**, 130–137 (2004).

Lavoie, M. *et al.* Modelling dimethylsulfide diffusion in the algal external boundary layer: implications for mutualistic and signalling roles: DMS and phytoplankton phycosphere. *Environ Microbiol* **20**, 4157–4169 (2018).

Lavoie, M., Levasseur, M. & Babin, M. Testing the potential ballast role for dimethylsulfoniopropionate in marine phytoplankton: a modeling study. *J. Plankton Res.* **37**, 699–711 (2015).

Lavoie, M., Levasseur, M. & Sunda, W. G. A steady-state physiological model for intracellular dimethylsulfoxide in marine phytoplankton. *Environ. Chem.* **13**, 212 (2016).

Law, K. S. *et al.* Arctic Air Pollution: New Insights from POLARCAT-IPY. *Bulletin of the American Meteorological Society* **95**, 1873–1895 (2014).

Leaitch, W. R. *et al.* Dimethyl sulfide control of the clean summertime Arctic aerosol and cloud. *Elem. Sci. Anth.* **1**, 000017 (2013).

Lee, H., Park, K.-T., Lee, K., Jeong, H. J. & Yoo, Y. D. Prey-dependent retention of dimethylsulfoniopropionate (DMSP) by mixotrophic dinoflagellates: DMSP retention by mixotrophic dinoflagellates. *Environmental Microbiology* **14**, 605–616 (2012).

Lee, P. A. *et al.* Particulate dimethylsulfoxide in arctic sea-ice algal communities: the cryoprotectant hypothesis revisited. *J Phycol* **37**, 488–499 (2001).

Lee, P. A., & S. J. De Mora. Intracellular Dimethylsulfoxide (DMSO) in Unicellular Marine Algae: Speculations on Its Origin and Possible Biological Role. *Journal of Phycology* **35** (1): 8–18 (1999).

Lenhart, K. *et al.* Evidence for methane production by the marine algae Emiliania huxleyi. *Biogeosciences* **13**, 3163–3174 (2016).

Lesser, M. Acclimation of phytoplankton to UV-B radiation:oxidative stress and photoinhibition of photosynthesis are not prevented by UV-absorbing compounds in the dinoflagellate Prorocentrum micans. *Mar. Ecol. Prog. Ser.* **132**, 287–297 (1996).

Lesser, M. P. Oxidative stress in marine environments: Biochemistry and Physiological Ecology. *Annu. Rev. Physiol.* **68**, 253–278 (2006).

Levasseur, M. Impact of Arctic Meltdown on the Microbial Cycling of Sulphur. *Nature Geoscience* **6** (9): 691–700 (2013).

Levine, N. M. *et al.* Environmental, biochemical and genetic drivers of DMSP degradation and DMS production in the Sargasso Sea: Drivers of DMSP degradation and DMS production. *Environmental Microbiology* **14**, 1210–1223 (2012).

Li, G. *et al.* Increasing ocean stratification over the past half-century. *Nat. Clim. Chang.* **10**, 1116–1123 (2020).

Liss, P. S., Hatton, A. D., Malin, G., Nightingale, P. D. & Turner, S. M. Marine sulphur emissions. *Phil. Trans. R. Soc. Lond. B* **352**, 159–169 (1997).

Litchman, E. & Klausmeier, C. A. Competition of Phytoplankton under Fluctuating Light. *The American Naturalist* **157**, 170–187 (2001).

Liu, K. *et al.* Superoxide, Hydrogen Peroxide and Hydroxyl Radical in D1/D2/cytochrome b-559 Photosystem II Reaction Center Complex. *Photosynthesis Research* **81**, 41–47 (2004).

Liu, Y. & Whitman, W. B. Metabolic, Phylogenetic, and Ecological Diversity of the Methanogenic Archaea. *Annals of the New York Academy of Sciences* **1125**, 171–189 (2008).

Lizotte, M. *et al.* Macroscale patterns of the biological cycling of dimethylsulfoniopropionate (DMSP) and dimethylsulfide (DMS) in the Northwest Atlantic. *Biogeochemistry* **110**, 183–200 (2012).

Locarnini, S. J. P., Turner, S. M. & Liss, P. S. The distribution of dimethylsulfide, DMS, and dimethylsulfoniopropionate, DSMP, in waters off the Western Coast of Ireland. *Continental Shelf Research* **18**, 1455–1473 (1998).

Lovelock, J. E. & Margulis, L. Atmospheric homeostasis by and for the biosphere: the Gaia hypothesis. *Tellus* **26**, 2–10 (1974).

Lovelock, J. E., Maggs, R. J. & Rasmussen, R. A. Atmospheric Dimethyl Sulphide and the Natural Sulphur Cycle. *Nature* **237**, 452 – 453 (1972).

Lund, J.W.G., Kipling, C., Le Cren, E.D. The inverted microscope method of estimating algal numbers and the statistical basis of estimations by counting. *Hydrobiologia* **11** (2), 143–170 (1958).

Lyon, B. R., Lee, P. A., Bennett, J. M., DiTullio, G. R. & Janech, M. G. Proteomic Analysis of a Sea-Ice Diatom: Salinity Acclimation Provides New Insight into the Dimethylsulfoniopropionate Production Pathway. *Plant Physiol.* **157**, 1926–1941 (2011).

Lyons, M. G., Balls, P. W. & Turrell, W. R. A preliminary study of the relative importance of riverine nutrient inputs to the Scottish North Sea Coastal Zone. *Marine Pollution Bulletin* **26**, 620–628 (1993).

Mackey, M., Mackey, D., Higgins, H. & Wright, S. CHEMTAX - a program for estimating class abundances from chemical markers: application to HPLC measurements of phytoplankton. *Mar. Ecol. Prog. Ser.* **144**, 265–283 (1996).

Magnusson, L., Ferranti., L., Vamborg, F., 2018. Forecasting the 2018 European heatwave, ECMWF newsletter, 157, p. 4, https://www.ecmwf.int/en/newsletter/157/news/forecasting-2018-european-heatwave (accessed 07.03.19).

Malin, G., Turner, S., Liss, P., Holligan, P. & Harbour, D. Dimethylsulphide and dimethylsulphoniopropionate in the Northeast Atlantic during the summer coccolithophore bloom. *Deep Sea Research Part I: Oceanographic Research Papers* **40**, 1487–1508 (1993).

Mallick, N. & Mohn, F. H. Reactive oxygen species: response of algal cells. J. Plant Physiol. **157**:183-193 (2000).

Margalef, R. Life Forms of Phytoplankton as Survival Alternatives in an Unstable Environment. *Oceanology Acta* **1**, 493-509 (1978).

Masotti, I. *et al.* Spatial and temporal variability of the dimethylsulfide to Chlorophyll ratio in the surface ocean: an assessment in the light of phytoplankton composition determined from space. *Biogeosciences Discussions* **7**, 3605–3650 (2010).

Matrai, P. A. *et al.* Light-dependence of carbon and sulfur production by polar clones of the genus Phaeocystis. *Marine Biology* **124**, 157–167 (1995).

Mavi, H. S. & Tupper, G. J. Agrometeorology: principles and applications of climate studies in agriculture. CRC Press, 381p (2004).

Maxwell, K. & Johnson, G. N. Chlorophyll fluorescence—a practical guide. *Journal of Experimental Botany* **51**, 659 – 668 (2000).

McMurdie, P. J. & Holmes, S. phyloseq: An R Package for Reproducible Interactive Analysis and Graphics of Microbiome Census Data. *PLoS ONE* **8**, e61217 (2013).

McParland, E. L. & Levine, N. M. The role of differential DMSP production and community composition in predicting variability of global surface DMSP concentrations. *Limnology and Oceanography* **64**, 757–773 (2019).

Menden-Deuer, S. & Lessard, E. J. Carbon to volume relationships for dinoflagellates, diatoms, and other protist plankton. *Limnol. Oceanogr.* **45**, 569–579 (2000).

Menden-Deuer, S., Lessard, E. & Satterberg, J. Effect of preservation on dinoflagellate and diatom cell volume, and consequences for carbon biomass predictions. *Mar. Ecol. Prog. Ser.* **222**, 41–50 (2001).

Miles, C. J., Bell, T. G. & Lenton, T. M. Testing the relationship between the solar radiation dose and surface DMS concentrations using in situ data. *Biogeosciences* **6**, 1927–1934 (2009).

Mohapatra, B. R., Rellinger, A. N., Kieber, D. J. & Kiene, R. P. Kinetics of DMSP lyases in whole cell extracts of four Phaeocystis species: Response to temperature and DMSP analogs. *Journal of Sea Research* **86**, 110–115 (2014).

Møller, I. M., Jensen, P. E. & Hansson, A. Oxidative Modifications to Cellular Components in Plants. *Annu. Rev. Plant. Biol* **58** (2007);

Montagnes, D. J. S. & Franklin, M. Effect of temperature on diatom volume, growth rate, and carbon and nitrogen content: Reconsidering some paradigms. *Limnology and Oceanography* **46**, 2008–2018 (2001).

Montsant, A. *et al.* Identification and comparative genomic analysis of signaling and regulatory components in the diatom *Thalassiosira pseudonana*. *Journal of Phycology* **43**, 585–604 (2007).

Moran, M. A., C. R. Reisch, R. P. Kiene, and W. B. Whitman. Genomic Insights into Bacterial DMSP Transformations. *Annual Review of Marine Science* **4** (1): 523–4 (2012).

Mortelmans, J. *et al.* Nutrient, pigment, suspended matter and turbidity measurements in the Belgian part of the North Sea. *Scientific Data* **6**, 22 (2019).

Mouw, C. B. *et al.* A Consumer's Guide to Satellite Remote Sensing of Multiple Phytoplankton Groups in the Global Ocean. *Front. Mar. Sci.* **4**, (2017).

Müller, P., Li, X.-P. & Niyogi, K. K. Non-Photochemical Quenching. A Response to Excess Light Energy. *Plant Physiol.* **125**, 1558–1566 (2001).

Murata, N., Takahashi, S., Nishiyama, Y. & Allakhverdiev, S. I. Photoinhibition of photosystem II under environmental stress. Biochimica et Biophysica Acta (BBA) - Bioenergetics **1767**, 414–421 (2007).

Nair, A. *et al.* Remote sensing of phytoplankton functional types. *Remote Sensing of Environment* **112**, 3366–3375 (2008).

Neale, P. J., Banaszak, A. T. & Jarriel, C. R. Ultraviolet sunscreens in Gymnodinium sanguineum (Dinophyceae): mycosporine-like amino acids protect against inhibition of photosynthesis. *J Phycol* **34**, 928–938 (1998).

Neufeld, J. D., Boden, R., Moussard, H., Schäfer, H. & Murrell, J. C. Substrate-Specific Clades of Active Marine Methylotrophs Associated with a Phytoplankton Bloom in a Temperate Coastal Environment. *AEM* **74**, 7321–7328 (2008).

Nevitt, G. A. The Neuroecology of Dimethyl Sulfide: A Global-Climate Regulator Turned Marine Infochemical. *Integrative and Comparative Biology* **51**, 819–825 (2011).

Niki, T., Kunugi, M. & Otsuki, A. DMSP-lyase activity in five marine phytoplankton species: its potential importance in DMS production. *Marine Biology* **136**: 759–764 (2000).

Niyogi, K. K. Editorial overview: Physiology and metabolism: Light responses from photoreceptors to photosynthesis and photoprotection. *Current Opinion in Plant Biology* **37**, iv–vi (2017).

Nohe, A. *et al.* Marked changes in diatom and dinoflagellate biomass, composition and seasonality in the Belgian Part of the North Sea between the 1970s and 2000s. *Science of The Total Environment* **716**, 136316 (2020).

Nymark, M. *et al.* An Integrated Analysis of Molecular Acclimation to High Light in the Marine Diatom *Phaeodactylum tricornutum*. *PLoS ONE* **4**, e7743 (2009).

Nymark, M., Sharma, A. K., Sparstad, T., Bones, A. M. & Winge, P. A CRISPR/Cas9 system adapted for gene editing in marine algae. *Sci Rep* **6**, 24951 (2016).

Oduro, H., Van Alstyne, K. L. & Farquhar, J. Sulfur isotope variability of oceanic DMSP generation and its contributions to marine biogenic sulfur emissions. *Proceedings of the National Academy of Sciences* **109**, 9012–9016 (2012).

Olenina, I., Hajdu, S., Edler, L., Andersson, A., Wasmund, N., Busch, S., Göbel, J., Gromisz, S., Huseby, S., Huttunen, M., Jaanus, A., Kokkonen, P., Ledaine, I. and Niemkiewicz, E. Biovolumes and size-classes of phytoplankton in the Baltic Sea HELCOM Balt.Sea Environ. Proc. No. 106, 144pp (2006).

Olli, K. & Seppälä, J. Vertical niche separation of phytoplankton: large-scale mesocosm experiments. *Mar. Ecol. Prog. Ser.* **217**, 219–233 (2001).

Oremland, R. S., Kiene, R. P., Mathrani, I., Whiticar, M. J. & Boone, D. R. Description of an Estuarine Methylotrophic Methanogen Which Grows on Dimethyl Sulfide. *Applied and Environmental Microbiology* **55**, 994–1002 (1989).

Ou, B., Hampsch-Woodill, M. & Prior, R. L. Development and Validation of an Improved Oxygen Radical Absorbance Capacity Assay Using Fluorescein as the Fluorescent Probe. *J. Agric. Food Chem.* **49**, 4619–4626 (2001).

Paramor, *et al.* MEFEPO North Sea Atlas. University of Liverpool. ISBN 0 906370 60 4. (2009).

Peperzak, L. & Gäbler-Schwarz, S. Current knowledge of the life cycles of Phaeocystis globosa and Phaeocystis antarctica (prymnesiophyceae). *Journal of Phycology* **48**, 514–517 (2012).

Petrou, K. & Nielsen, D. A. Uptake of dimethylsulphoniopropionate (DMSP) by the diatom Thalassiosira weissflogii: a model to investigate the cellular function of DMSP. *Biogeochemistry* **141**, 265–271 (2018).

Pham, M., Müller, J.-F., Brasseur, G. P., Granier, C. & Mégie, G. A three-dimensional study of the tropospheric sulfur cycle. *J. Geophys. Res.* **100**, 26061 (1995).

Pietta, P.-G. Flavonoids as Antioxidants. *J. Nat. Prod.* **63**, 1035–1042 (2000).

Polovina, J. J., Howell, E. A. & Abecassis, M. Ocean's least productive waters are expanding. *Geophys. Res. Lett.* **35**, L03618 (2008).

Pospíšil, P. Production of Reactive Oxygen Species by Photosystem II as a Response to Light and Temperature Stress. *Front. Plant Sci.* **7**, (2016).

Pospíšil, P. The Role of Metals in Production and Scavenging of Reactive Oxygen Species in Photosystem II. *Plant and Cell Physiology* **55**, 1224–1232 (2014).

Prins, T. C., Desmit, X. & Baretta-Bekker, J. G. Phytoplankton composition in Dutch coastal waters responds to changes in riverine nutrient loads. *Journal of Sea Res*earch **73**: 49 –62. doi:10.1016/j.seares.2012.06.009 (2012).

Quante, M. *et al.* Introduction to the Assessment – Characteristics of the Region. In *North Sea Region Climate Change Assessment*. (Springer International Publishing, 2016).

Quinn, P. K. & Bates, T. S. The case against climate regulation via oceanic phytoplankton sulphur emissions. *Nature* **480**, 51–56 (2011).

Raina, J.-B. *et al.* DMSP biosynthesis by an animal and its role in coral thermal stress response. *Nature* **502**, 677–680 (2013).

Raina, J.-B. *et al.* Subcellular tracking reveals the location of dimethylsulfoniopropionate in microalgae and visualises its uptake by marine bacteria. *eLife* **6**, e23008 (2017).

Raven, J. A. & Waite, A. M. The evolution of silicification in diatoms: inescapable sinking and sinking as escape? *New Phytol* **162**, 45–61 (2004).

Raven, J.A. & Richardson, K. Dinophyte flagella - a cost-benefit-analysis. *New Phytologist* **98**, 259-276 (1984).

Reeburgh, W. S. Oceanic methane biogeochemistry. *Chem. Rev.* **107**, 486–513 (2007).

Reid, E., Lancelot, C., Gieskes, W. W. C., Hagmeier, E. & Weichart, G. Phytoplankton of the North Sea and its dynamics: a review. *Netherlands Journal of Sea Research* **26** (2-4), 295 – 331 (1990).

Reid, P.C., Borges, M.F. and Svendsen, E. A regime shift in the North Sea circa 1988 linked to changes in the North Sea horse mackerel fishery. Fisheries Research, 50: 163-171 (2001).

Reis, M. G. dos & Ribeiro, A. Conversion factors and general equations applied in agricultural and forest meteorology. *AgroM* **27**, (2020).

Repeta, D. J. *et al.* Marine methane paradox explained by bacterial degradation of dissolved organic matter. *Nature Geosci* **9**, 884–887 (2016).

Reynolds, C. S. The ecology of phytoplankton. Cambridge Univ. Press. (2006)

Richardson, A. J., & Schoeman, D. S. Climate impact on plankton ecosystems in the Northeast Atlantic. *Science* **305**: 1609–1612 (2004).

Richardson, K., Gissel Nielsen, T., Pedersen, F.Bo., Heilmann, J.P., Lokkegard, B. and Kass, H. Spatial heterogeneity in the structure of the planktonic food web in the North Sea. Marine Ecology Progress Series, 168: 197-211 (1998).

Riebesell, U., Kortzinger, A. & Oschlies, A. Sensitivities of marine carbon fluxes to ocean change. *Proceedings of the National Academy of Sciences* **106**, 20602–20609 (2009).

Riseman, S. F. & DiTullio, G. R. Particulate dimethylsulfoniopropionate and dimethylsulfoxide in relation to iron availability and algal community structure in the Peru Upwelling System. *Canadian journal of fisheries and aquatic sciences* **61**, 16 (2004).

Ritchie, R. J. Consistent Sets of Spectrophotometric Chlorophyll Equations for Acetone, Methanol and Ethanol Solvents. *Photosynth Res* **89**, 27–41 (2006).

Roberty, S., Béraud, E., Grover, R. & Ferrier-Pagès, C. Coral Productivity Is Co-Limited by Bicarbonate and Ammonium Availability. *Microorganisms* **8**, 640 (2020).

Roberty, S., Fransolet, D., Cardol, P., Plumier, J.-C. & Franck, F. Imbalance between oxygen photoreduction and antioxidant capacities in Symbiodinium cells exposed to combined heat and high light stress. *Coral Reefs* **34**, 1063–1073 (2015).

Roberty, S., Furla, P. & Plumier, J.-C. Differential antioxidant response between two *Symbiodinium* species from contrasting environments: Antioxidant responses of *Symbiodinium* sp. *Plant, Cell & Environment* **39**, 2713–2724 (2016).

Röttgers, R. & Wisotzki, A. Physical oceanography during HEINCKE cruise HE517. *Alfred Wegener Institute, Helmholtz Centre for Polar and Marine Research, Bremerhaven*, *PANGAEA*, (2018): https://doi.org/10.1594/PANGAEA.896214

Rousseau, V. Dynamics of *Phaeocystis* and diatom blooms in the eutrophicated coastal waters of the Southern Bight of the North Sea. Ph.D. thesis. Université Libre de Bruxelles. 205pp. (2000).

Rousseau, V., Chrétiennot-Dinet, M.-J., Jacobsen, A., Verity, P. & Whipple, S. The life cycle of Phaeocystis: state of knowledge and presumptive role in ecology. *Biogeochemistry* **87,** 29 – 47 (2007).

Rousseau, V., Leynaert, A., Daoud, N. & Lancelot, C. Diatom succession, silicification and silicic acid availability in Belgian coastal waters (Southern North Sea). *Marine Ecology Progress Series* **236**, 61–73 (2002).

Rousseau, V., Mathot, S. & Lancelot, C. Calculating carbon biomass of Phaeocystis sp. from microscopic observations. *Marine Biology* **107**, 305–314 (1990).

Royer, C., Borges, A. V., Lapeyra Martin, J. & Gypens, N. Drivers of the variability of dimethylsulfoniopropionate (DMSP) and dimethylsulfoxide (DMSO) in the Southern North Sea. *Continental Shelf Research* **216**, 104360 (2021).

Royer, S.-J. *et al.* A high-resolution time-depth view of dimethylsulphide cycling in the surface sea. *Sci Rep* **6**, 32325 (2016).

Ruban, A. V., Johnson, M. P. & Duffy, C. D. P. The photoprotective molecular switch in the photosystem II antenna. *Biochimica et Biophysica Acta (BBA) - Bioenergetics* **1817**, 167–181 (2012).

Ruddick, K. and Lacroix, G. Hydrodynamics, and meteorology of the Belgian Coastal Zone, 1 – 15 *in:* Current status of eutrophication in the Belgian Coastal Zone, edited by Rousseau, V., Lancelot, C. & Cox, D. (2006).

Ruiz-González, C. *et al.* Sunlight Effects on the Osmotrophic Uptake of DMSP-Sulfur and Leucine by Polar Phytoplankton. *PLoS ONE* **7**, e45545 (2012).

Russo, M. T., Aiese Cigliano, R., Sanseverino, W. & Ferrante, M. I. Assessment of genomic changes in a CRISPR/Cas9 *Phaeodactylum tricornutum* mutant through whole genome resequencing. *PeerJ* **6**, e5507 (2018).

Said-Ahmad, W. & Amrani, A. A sensitive method for the sulfur isotope analysis of dimethyl sulfide and dimethylsulfoniopropionate in seawater: Sulfur isotope analysis of dimethyl sulfide. *Rapid Commun. Mass Spectrom.* **27**, 2789–2796 (2013).

Salgado, P., Kiene, R., Wiebe, W. & Magalhães, C. Salinity as a regulator of DMSP degradation in Ruegeria pomeroyi DSS-3. *J Microbiol.* **52**, 948–954 (2014).

Santoferrara, L. F. Current practice in plankton metabarcoding: optimization and error management. *Journal of Plankton Research* fbz041 (2019).

Saragosti, E., Tchernov, D., Katsir, A. & Shaked, Y. Extracellular Production and Degradation of Superoxide in the Coral Stylophora pistillata and Cultured Symbiodinium. *PLoS ONE* **5**, e12508 (2010).

Sarthou, G., Timmermans, K. R., Blain, S. & Tréguer, P. Growth physiology and fate of diatoms in the ocean: a review. *Journal of Sea Research* **53**, 25–42 (2005).

Saunois, M. *et al.* The global methane budget 2000–2012. *Earth System Science Data* **8**, 697–751 (2016).

Savoca, M. S. & Nevitt, G. A. Evidence that dimethyl sulfide facilitates a tritrophic mutualism between marine primary producers and top predators. *Proceedings of the National Academy of Sciences* **111**, 4157–4161 (2014).

Scaduto, R. Oxidation of DMSO and methanesulfinic acid by the hydroxyl radical. *Free Radical Biology and Medicine* **18**, 271–277 (1995).

Scarratt, M. *et al.* Influence of phytoplankton taxonomic profile on the distribution of dimethylsulfide and dimethylsulfoniopropionate in the northwest Atlantic. *Mar. Ecol. Prog. Ser.* **244**, 49–61 (2002).

Schabhüttl, S. *et al.* Temperature and species richness effects in phytoplankton communities. *Oecologia* **171**, 527–536 (2013).

Schindler, D. W. Effects of Acid Rain on Freshwater Ecosystems. *Science* **239**, 149–157 (1988).

Seymour, J. R., Simo, R., Ahmed, T. & Stocker, R. Chemoattraction to Dimethylsulfoniopropionate Throughout the Marine Microbial Food Web. *Science* **329**, 342–345 (2010).

Sharma, P., Jha, A. B., Dubey, R. S. & Pessarakli, M. Reactive Oxygen Species, Oxidative Damage, and Antioxidative Defense Mechanism in Plants under Stressful Conditions. *Journal of Botany* **2012**, 1–26 (2012).

Shaw, G. E. Bio-controlled thermostasis involving the sulfur cycle. *Climate Change* **5**, 297–303 (1983).

Sheets, E. B., and D. Rhodes. Determination of DMSP and Other Onium Compounds in Tetraselmis Subcordiformis by Plasma Desorption Mass Spectrometry. In *Biological and Environmental Chemistry of DMSP and Related Sulfonium Compounds*, edited by R. P. Kiene, P. T. Visscher, M. D. Keller, and G. O. Kirst, 55–63. Boston, MA: Springer US (1996).

Shick, J. M. & Dunlap, W. C. Mycosporine-Like Amino Acids and Related Gadusols: Biosynthesis, Accumulation, and UV-Protective Functions in Aquatic Organisms. *Annu. Rev. Physiol.* **64**, 223–262 (2002).

Siaut, M. *et al.* Molecular toolbox for studying diatom biology in Phaeodactylum tricornutum. *Gene* **406**, 23–35 (2007).

Siegel, D. A., & Michaels. A. F. Quantification of nonalgal light attenuation in the Sargasso Sea: Implications for biogeochemistry and remote sensing. Deep-Sea Res. 43: 321– 345 (1996).

Simó, R. & Vila-Costa, M. Ubiquity of algal dimethylsulfoxide in the surface ocean: Geographic and temporal distribution patterns. *Mar. Chem.* **100,** 136–146 (2006).

Simó, R. *et al.* The quantitative role of microzooplankton grazing in dimethylsulfide (DMS) production in the NW Mediterranean. *Biogeochemistry* **141**, 125–142 (2018).

Simó, R. From cells to globe approaching the dynamics of DMS(P) in the ocean at multiple scales. *Can. J. Fish. Aquat. Sci.* **61**, 673–684 (2004).

Simó, R. Production of atmospheric sulfur by oceanic plankton: biogeochemical, ecological, and evolutionary links. *Trends in Ecology & Evolution* **16**, 287–294 (2001).

Simó, R., and C. Pedrós-Alió. Role of Vertical Mixing in Controlling the Oceanic Production of Dimethyl Sulphide. *Nature* **402** (6760): 396–99 (1999).

Simó, R., Archer, S. D., Pedrós-Alió, C., Gilpin, L. & Stelfox-Widdicombe, C. E. Coupled dynamics of dimethylsulfoniopropionate and dimethylsulfide cycling and the microbial food web in surface waters of the North Atlantic. *Limnol. Oceanogr.* **47**, 53–61 (2002).

Simó, R., Hatton, A., Malin, G. et Liss, P. Particulate dimethyl sulphoxide in seawater: production by microplankton. *Marine Ecology Progress Series* **167**, 291–296 (1998).

Simó, R., Pedrós-Alió, C., Malin, G. & Grimalt, J. Biological turnover of DMS, DMSP and DMSO in contrasting open-sea waters. *Mar. Ecol. Prog. Ser.* **203**, 1–11 (2000).

Slezak, D., Brugge, A. & Herndl, G. Impact of solar radiation on the biological removal of dimethylsulfoniopropionate and dimethylsulfide in marine surface waters. *Aquat. Microb. Ecol.* **25**, 87–97 (2001).

Slezak, D., Kiene, R. P., Toole, D. A., Simó, R. & Kieber, D. J. Effects of solar radiation on the fate of dissolved DMSP and conversion to DMS in seawater. *Aquat. Sci.* **69**, 377–393 (2007).

Small, J. D., Chuang, P. Y., Feingold, G. & Jiang, H. Can aerosol decrease cloud lifetime? *Geophys. Res. Lett.* **36**, L16806 (2009).

Smayda, T. J. & Reynolds, C.S. Community Assembly in Marine Phytoplankton: Application of Recent Models to Harmful Dinoflagellate Blooms. *Journal of Plankton Research* **23**, 447–461 (2001).

Smerilli, A. *et al.* Antioxidant and Photoprotection Networking in the Coastal Diatom Skeletonema marinoi. *Antioxidants* **8**, 154 (2019).

Sommer, U. & Lewandowska, A. Climate change and the phytoplankton spring bloom: warming and overwintering zooplankton have similar effects on phytoplankton. *Global Change Biology* **17**, 154–162 (2011).

Sommer, U. *et al.* Beyond the Plankton Ecology Group (PEG) Model: Mechanisms Driving Plankton Succession. *Annual Review of Ecology, Evolution, and Systematics* **43**, 429–448 (2012).

Sowers, K. R. & Ferry, J. G. Isolation and Characterization of a Methylotrophic Marine Methanogen, Methanococcoides methylutens gen. nov., sp. nov. *Applied and Environmental Microbiology* **45**, 684–690 (1983).

Speeckaert, G., Borges, A. V. & Gypens, N. Salinity and growth effects on dimethylsulfoniopropionate (DMSP) and dimethylsulfoxide (DMSO) cell quotas of Skeletonema costatum, Phaeocystis globosa and Heterocapsa triquetra. *Estuarine, Coastal and Shelf Science* **226**, 106275 (2019).

Speeckaert, G., Borges, A. V., Champenois, W., Royer, C. et Gypens, N. Annual cycle of dimethylsulfoniopropionate (DMSP) and dimethylsulfoxide (DMSO) related to phytoplankton succession in the Southern North Sea. *Science of The Total Environment* **622**–**623**, 362–372 (2018).

Spielmeyer, A. & Pohnert, G. Daytime, growth phase and nitrate availability dependent variations of dimethylsulfoniopropionate in batch cultures of the diatom Skeletonema marinoi. *Journal of Experimental Marine Biology and Ecology* **413**, 121–130 (2012).

Spielmeyer, A., Gebser, B. & Pohnert, G. Investigations of the Uptake of Dimethylsulfoniopropionate by Phytoplankton. *ChemBioChem* **12**, 2276–2279 (2011).

Spiese, C. E., Kieber, D. J., Nomura, C. T. & Kiene, R. P. Reduction of dimethylsulfoxide to dimethylsulfide by marine phytoplankton. *Limnol. Oceanogr.* **54**, 560–570 (2009).

Spiese, C. E., Le, T., Zimmer, R. L. & Kieber, D. J. Dimethylsulfide membrane permeability, cellular concentrations, and implications for physiological functions in marine algae. *J. Plankton Res.* **38**, 41–54 (2016).

Stawiarski, B. *et al.* Controls on zooplankton methane production in the central Baltic Sea. *Biogeosciences* **16**, 1 – 16 (2019).

Stefels, J. & Dijkhuizen, L. Characteristics of DMSP-lyase in Phaeocystis sp. (Prymnesiophyceae). *Mar. Ecol. Prog. Ser.* **131**, 307–313 (1996).

Stefels, J. & van Leeuwe, M. A. Effects of iron and light stress on the biochemical composition of Antarctic Phaeocystis sp. (Prymnesiophyceae). I. Intracellular DMSP concentrations. *Journal of Phycology* **34**, 486–495 (1998).

Stefels, J. Determination of DMS, DMSP, and DMSO in Seawater. Practical Guidelines for the Analysis of Seawater, 223 (2009).

Stefels, J. Physiological aspects of the production and conversion of DMSP in marine algae and higher plants. *Journal of Sea Research* **43,** 183–197 (2000).

Stefels, J., Steinke, M., Turner, S., Malin, G. et Belviso, S. Environmental constraints on the production and removal of the climatically active gas dimethylsulphide (DMS) and implications for ecosystem modelling. *Biogeochemistry* **83**, 245–275 (2007).

Steinke, M., Malin, G., Gibb, S. W. & Burkill, P. H. Vertical and temporal variability of DMSP lyase activity in a coccolithophorid bloom in the northern North Sea. *Deep Sea Research Part II: Topical Studies in Oceanography* **49**, 3001–3016 (2002).

Stevens, B. & Feingold, G. Untangling aerosol effects on clouds and precipitation in a buffered system. *Nature* **461**, 607–613 (2009).

Stocker, T., D. Qin, G. Plattner, M. Tignor, S. Allen, J. Boschung, A. Nauels, Y. Xia, B. Bex, B. Midgley (Eds), Climate Change 2013: The Physical Science Basis. Working Group I Contribution to the Fifth Assessment Report of the Intergovernmental Panel on Climate Change 2013 (Cambridge University Press: Cambridge, UK, and New York) (2013).

Ston, J., & Kosakowska, A. Qualitative and quantitative analysis of Baltic phytoplankton pigments. Oceanologia, **42**, 449-471 (2000).

Strickland, J. D. H. & Parsons, T. R. A Practical Handbook of Seawater Analysis. *A Pract. Handbook seawater Analysis* **167,** 185 (1972).

Striebel, M., Schabhüttl, S., Hodapp, D., Hingsamer, P. & Hillebrand, H. Phytoplankton responses to temperature increases are constrained by abiotic conditions and community composition. *Oecologia* **182**, 815–827 (2016).

Strom, S. *et al.* Chemical defense in the microplankton I: Feeding and growth rates of heterotrophic protists on the DMS-producing phytoplankter Emiliania huxleyi. *Limnology and Oceanography* **48**, 217–229 (2003)a.

Strom, S., Wolfe, G., Slajer, A., Lambert, S. & Clough, J. Chemical defense in the microplankton II: Inhibition of protist feeding by β-dimethylsulfoniopropionate (DMSP). *Limnol. Oceanogr.* **48**, 230–237 (2003)b.

Strychar, K. B. & Sammarco, P. W. Effects of Heat Stress on Phytopigments of Zooxanthellae (Symbiodinium spp.) Symbiotic with the Corals *Acropora hyacinthus*, *Porites solida*, and *Favites complanata*. *IJB* **4**, p3 (2011).

Suggett, D., Moore, C., Hickman, A. & Geider, R. Interpretation of fast repetition rate (FRR) fluorescence: signatures of phytoplankton community structure versus physiological state. *Mar. Ecol. Prog. Ser.* **376**, 1–19 (2009).

Suggett, D.J., Prásil, O. and Borowitzka, M. A. *Chlorophyll a Fluorescence in Aquatic Sciences: Methods and Applications*. (Springer Netherlands, 2010).

Suikkanen, S., Laamanen, M. & Huttunen, M. Long-term changes in summer phytoplankton communities of the open northern Baltic Sea. *Estuarine, Coastal and Shelf Science* **71**, 580–592 (2007).

Summers, P. S. *et al.* Identification and Stereospecificity of the First Three Enzymes of 3-Dimethylsulfoniopropionate Biosynthesis in a Chlorophyte Alga. *Plant Physiol.* **116**, 369–378 (1998).

Sun, Y.-L., Zhao, Y., Hong, X. & Zhai, Z.-H. Cytochrome *c* release and caspase activation during menadione-induced apoptosis in plants. *FEBS Letters* **462**, 317–321 (1999).

Sunda, W. G., Hardison, R., Kiene, R. P., Bucciarelli, E. & Harada, H. The effect of nitrogen limitation on cellular DMSP and DMS release in marine phytoplankton: climate feedback implications. *Aquat. Sci.* **69**, 341–351 (2007).

Sunda, W., Kieber, D. J., Kiene, R. P. et Huntsman, S. An antioxidant function for DMSP and DMS in marine algae. *Nature* **418,** 317–320 (2002).

Sunda, W., Litaker, R., Hardison, D. & Tester, P. Dimethylsulfoniopropionate (DMSP) and its relation to algal pigments in diverse waters of the Belize coastal lagoon and barrier reef system. *Mar. Ecol. Prog. Ser.* **287**, 11–22 (2005).

Takahashi, H., S. Kopriva, M. Giordano, K. Saito, and R. Hell. Sulfur Assimilation in Photosynthetic Organisms: Molecular Functions and Regulations of Transporters and Assimilatory Enzymes. *Annual Review of Plant Biology* **62**: 157–84 (2011).

Tang, K. & Simó, R. Trophic uptake and transfer of DMSP in simple planktonic food chains. *Aquat. Microb. Ecol.* **31**, 193–202 (2003).

Tapiolas, D. M., Raina, J.-B., Lutz, A., Willis, B. L. & Motti, C. A. Direct measurement of dimethylsulfoniopropionate (DMSP) in reef-building corals using quantitative nuclear magnetic resonance (qNMR) spectroscopy. *Journal of Experimental Marine Biology and Ecology* **443**, 85–89 (2013).

Taylor, B. F. & Visscher, P. T. Metabolic Pathways Involved in DMSP Degradation. in *Biological and Environmental Chemistry of DMSP and Related Sulfonium Compounds* (eds. Kiene, R. P., Visscher, P. T., Keller, M. D. & Kirst, G. O.) 265–276 (Springer US, 1996).

Telfer, A. What is β–carotene doing in the photosystem II reaction centre? *Phil. Trans. R. Soc. Lond. B* **357**, 1431–1440 (2002).

Tengs, T. *et al.* Phylogenetic Analyses Indicate that the 19′Hexanoyloxy-fucoxanthin-Containing Dinoflagellates Have Tertiary Plastids of Haptophyte Origin. *Molecular Biology and Evolution* **17**, 718–729 (2000).

Thauer, R. K., Kaster, A.-K., Seedorf, H., Buckel, W. & Hedderich, R. Methanogenic archaea: ecologically relevant differences in energy conservation. *Nat. Rev. Microbiol*. **6**, 579–591 (2008).

Thimijan, R. W. & Heins, R.D. Photometric, Radiometric, and Quantum Light Units of Measure A Review of Procedures for Interconversion. **18**, 6 (1983).

Thomas, A. C., Deagle, B. E., Eveson, J. P., Harsch, C. H., and Trites, A. W. Quantitative DNA metabarcoding: Improved estimates of species proportional biomass using correction factors derived from control material. Mol. Ecol. Resour. 16, 714–726 (2016).

Thume, K. *et al.* The metabolite dimethylsulfoxonium propionate extends the marine organosulfur cycle. *Nature* **563**, 412–415 (2018).

Todd, J. D., Curson, A. R. J., Dupont, C. L., Nicholson, P. & Johnston, A. W. B. The *dddP* gene, encoding a novel enzyme that converts dimethylsulfoniopropionate into dimethyl sulfide, is widespread in ocean metagenomes and marine bacteria and also occurs in some Ascomycete fungi. *Environmental Microbiology* **11**, 1376–1385 (2009).

Toole, D. A. et Siegel, D. A. Light-driven cycling of dimethylsulfide (DMS) in the Sargasso Sea: Closing the loop. *Geophys. Res. Lett.* **31** (2004).

Toole, D. A., Slezak, D., Kiene, R. P., Kieber, D. J. & Siegel, D. A. Effects of solar radiation on dimethylsulfide cycling in the western Atlantic Ocean. *Deep Sea Research Part I: Oceanographic Research Papers* **53**, 136–153 (2006).

Townsend, D. & Keller, M. Dimethylsulfide (DMS) and dimethylsulfoniopropionate (DMSP) in relation to phytoplankton in the Gulf of Maine. *Mar. Ecol. Prog. Ser.* **137**, 229–241 (1996).

Trevena, A. J., Jones, G. B. & Wright, S. W. Profiles of DMSP, algal pigments, nutrients and salinity in pack ice from eastern Antarctica. *Journal of Sea Research* **9** (2000).

Trossat, C. *et al.* Salinity Promotes Accumulation of 3-Dimethylsulfoniopropionate and Its Precursor *S* -Methylmethionine in Chloroplasts. *Plant Physiology* **116,** 165–171 (1998).

Turner, S. M., Nightingale, P. D., Broadgate, W. & Liss, P. S. The distribution of dimethyl sulphide and dimethylsulphoniopropionate in Antarctic waters and sea ice. *Deep Sea Research Part II: Topical Studies in Oceanography* **42**, 1059–1080 (1995).

Twomey, S. Pollution and the planetary albedo. *Atmospheric Environment* **8**, 1251–1256 (1974)

Tynes, C. Molecular Investigation of Candidate Genes for the Biosynthetic Pathway for Dimethylsulfoniopropionate (DMSP) in the Diatom Thalassiosira pseudonana. Department of Biology at the Norwegian University of Science and Technology (NTNU) (2013).

Vallina, S. M. & Simo, R. Strong Relationship Between DMS and the Solar Radiation Dose over the Global Surface Ocean. *Science* **315**, 506–508 (2007).

Van Alstyne, K. L. Ecological and physiological roles of dimethylsulfoniopropionate (DMSP) and its DMSP cleavage in marine macroalgae. *Algal Chem. Ecol.* 173–194 (2008).

van Bergeijk, S. A., Van der Zee, C. & Stal, L. J. Uptake and excretion of dimethylsulphoniopropionate is driven by salinity changes in the marine benthic diatom Cylindrotheca Closterium. *European Journal of Phycology* **38**, 341–349 (2003).

van Beusekom, J. E. E., Loebl, M. & Martens, P. Distant riverine nutrient supply and local temperature drive the long-term phytoplankton development in a temperate coastal basin. *Journal of Sea Research* **61**, 26–33 (2009).

van den Berg, A., Turner, S., van Duyl, F. & Ruardij, P. Model structure and analysis of dimethylsulphide (DMS) production in the southern North Sea, considering phytoplankton dimethylsulphoniopropionate- (DMSP) lyase and eutrophication effects. *Marine Ecology Progress Series* **145**, 233–244 (1996).

van Duyl, F. C., Gieskes, W. W. C., Kop, A. J. et Lewis, W. E. Biological control of short-term variations in the concentration of DMSP and DMS during a Phaeocystis spring bloom. *Journal of Sea Research* **40**, 221–231 (1998).

Van Rijssel, M., and W. W. C. Gieskes. 2002. Temperature, Light, and the Dimethylsulfoniopropionate (DMSP) Content of Emiliania Huxleyi (Prymnesiophyceae). *Journal of Sea Research* **48** (1): 17–27 (2002)

Vega de Luna, F., Dang, K.-V., Cardol, M., Roberty, S. & Cardol, P. Photosynthetic capacity of the endosymbiotic dinoflagellate Cladocopium sp. is preserved during digestion of its jellyfish host Mastigias papua by the anemone Entacmaea medusivora. *FEMS Microbiology Ecology* **95** (2019).

Vila-Costa, M. *et al.* Dimethylsulfoniopropionate Uptake by Marine Phytoplankton. *Science* **314**, 652–654 (2006).

Vila-Costa, M., Kiene, R. P. & Simó, R. Seasonal Variability of the Dynamics of Dimethylated Sulfur Compounds in a Coastal Northwest Mediterranean Site. *Limnology and Oceanography* **53**, 198–211 (2008).

von Glasow, R. & Crutzen, P. J. Model study of multiphase DMS oxidation with a focus on halogens. *Atmospheric Chemistry and Physics* **4**, 589–608 (2004).

Wang, P. *et al.* Mechanistic insight into acrylate metabolism and detoxification in marine dimethylsulfoniopropionate-catabolizing bacteria: Mechanistic insight into acrylate metabolism and detoxification. *Molecular Microbiology* **105**, 674–688 (2017).

Wang, S., Elliott, S., Maltrud, M. & Cameron-Smith, P. Influence of explicit *Phaeocystis* parameterizations on the global distribution of marine dimethyl sulfide. *J. Geophys. Res. Biogeosci.* **120**, 2158–2177 (2015).

Wang, S., Maltrud, M. E., Burrows, S. M., Elliott, S. M. & Cameron-Smith, P. Impacts of Shifts in Phytoplankton Community on Clouds and Climate via the Sulfur Cycle. *Global Biogeochem. Cycles* **32**, 1005–1026 (2018)a.

Wang, S., Maltrud, M., Elliott, S., Cameron-Smith, P. & Jonko, A. Influence of dimethyl sulfide on the carbon cycle and biological production. *Biogeochemistry* **138**, 49–68 (2018)b.

Wanninkhof, R. Relationship between wind speed and gas exchange over the ocean. *J. Geophys. Res.* **97**, 7373 (1992).

Webster, L. *et al.* Measurements of nutrients and contaminants in Scottish waters as part of the UK national marine monitoring programme. *Fisheries Research Services Internal Report* No **20/03** (2004).

Welsh, D. T. Ecological significance of compatible solute accumulation by micro-organisms: from single cells to global climate. *FEMS Microbiol Rev* **24**, 263–290 (2000).

Wilkinson, F., Helman, W. P. & Ross, A. B. Rate Constants for the Decay and Reactions of the Lowest Electronically Excited Singlet State of Molecular Oxygen in Solution. An Expanded and Revised Compilation. *Journal of Physical and Chemical Reference Data* **24**, 663–677 (1995).

Williams, B. T. *et al.* Bacteria are important dimethylsulfoniopropionate producers in coastal sediments. *Nat Microbiol* **4**, 1815–1825 (2019).

Wiltshire, K. H. *et al.* Control of phytoplankton in a shelf sea: Determination of the main drivers based on the Helgoland Roads Time Series. *Journal of Sea Research* **105**, 42–52 (2015).

Wiltshire, K. H. *et al.* Resilience of North Sea phytoplankton spring bloom dynamics: An analysis of long-term data at Helgoland Roads. *Limnology and Oceanography* **53**, 1294–1302 (2008).

Wittek, B. (2019). Temperature and Salinity changes as drivers of dimethylsulfoniopropionate (DMSP) and dimethylsulfoxide (DMSO) production in the sea ice brine habitat: an experimental approach (Unpublished doctoral dissertation). Université libre de Bruxelles, Faculté des Sciences – Ecole Interfacultaire des Bioingénieurs, Bruxelles.

Wittek, B., Carnat, G., Tison, J.-L. & Gypens, N. Response of dimethylsulfoniopropionate (DMSP) and dimethylsulfoxide (DMSO) cell quotas to salinity and temperature shifts in the sea-ice diatom Fragilariopsis cylindrus. *Polar Biol* **43**, 483–494 (2020).

Wolfe, G. V. & Sherr, B. F. Release and consumption of DMSP from Emiliania huxleyi during grazing by Oxyrrhis marina. *Marine Ecology Progress Series* **111**, 111 – 119 (1994).

Wolfe, G. V. & Steinke, M. Grazing-activated production of dimethyl sulfide (DMS) by two clones of *Emiliania huxleyi*. *Limnol. Oceanogr.* **41**, 1151–1160 (1996).

Wolfe, G. V., Steinke, M. & Kirst, G. O. Grazing-activated chemical defence in a unicellular marine alga. *Nature* **387**, 894–897 (1997).

Woodhouse, M. T. *et al.* Low sensitivity of cloud condensation nuclei to changes in the sea-air flux of dimethyl-sulphide. *Atmos. Chem. Phys.* **10**, 7545–7559 (2010).

Woodhouse, M. T., Mann, G. W., Carslaw, K. S. & Boucher, O. Sensitivity of cloud condensation nuclei to regional changes in dimethyl-sulphide emissions. *Atmos. Chem. Phys.* **13**, 2723–2733 (2013).

Wozniak, B., Dera, J., Ficek, D., Ostrowska, M. & Majchrowski, R. Dependence of the photosynthesis quantum yield in oceans on environmental factors. *Oceanologia* **44**, 439–459 (2002).

Wright, S. W. & Jeffrey, S. W. Pigment Markers for Phytoplankton Production. *Env. Chem.* **2**, 71 – 104 (2006).

Yadav, D. K. & Pospíšil, P. Evidence on the Formation of Singlet Oxygen in the Donor Side Photoinhibition of Photosystem II: EPR Spin-Trapping Study. *PLoS ONE* **7**, e45883 (2012).

Yang, G., C. Li, and J. Sun. Influence of Salinity and Nitrogen Content on Production of Dimethylsulfoniopropionate (DMSP) and Dimethylsulfide (DMS) by *Skeletonema Costatum*. *Chinese Journal of Oceanology and Limnology* **29** (2): 378–86 (2011).

Yoch, D. C. Dimethylsulfoniopropionate: Its Sources, Role in the Marine Food Web, and Biological Degradation to Dimethylsulfide. *AEM* **68**, 5804–5815 (2002).

Zapata, M., Rodriguez, F. et Garrido, J.L. Separation of chlorophylls and carotenoids from marine phytoplankton: a new HPLC method using reverse phase C_8 column and pyridine-containing mobile phase. *Mar Ecol Prog Ser* **195**: 29-45 (2000).

Zhang, H., Devred, E., Fujiwara, A., Qiu, Z. & Liu, X. Estimation of phytoplankton taxonomic groups in the Arctic Ocean using phytoplankton absorption properties: implication for ocean-color remote sensing. *Opt. Express* **26**, 32280 (2018).

Zhang, X.-H. *et al.* Biogenic production of DMSP and its degradation to DMS—their roles in the global sulfur cycle. *Sci. China Life Sci.* (2019)

Zhuang, G., G. Yang, J. Yu, and Y. Gao. Production of DMS and DMSP in Different Physiological Stages and Salinity Conditions in Two Marine Algae. *Chinese Journal of Oceanology and Limnology* 29 (2): 369–77 (2011).

Zindler, C. *et al.* Sulphur compounds, methane, and phytoplankton: interactions along a north–south transit in the western Pacific Ocean. *Biogeosciences* **10**, 3297–3311 (2013).

Zindler-Schlundt, C., Lutterbeck, H., Endres, S. & Bange, H. W. Environmental control of dimethylsulfoxide (DMSO) cycling under ocean acidification. *Environ. Chem.* **13**, 330 (2016).

Zuidema, P., Xue, H. & Feingold, G. Shortwave Radiative Impacts from Aerosol Effects on Marine Shallow Cumuli. *Journal of the Atmospheric Sciences* **65**, 1979–1990 (2008).